AFRPL-TR-70-6 VOL 3

UNCLASSIFIED

(UNCLASSIFIED TITLE)

C 85-0C 2580 C.2P
FRDC SUB-CONTROL STA. #2

AIR FORCE REUSABLE ROCKET ENGINE PROGRAM

XLR129-P-1

AD 508758

DEMONSTRATOR ENGINE DESIGN

AFRPL-TR-70-6

APRIL 1970

R. R. ATHERTON

PRATT & WHITNEY AIRCRAFT

DIVISION OF UNITED AIRCRAFT CORPORATION

FLORIDA RESEARCH AND DEVELOPMENT CENTER

In addition to securit[illegible]
document is subject to special export [illegible]
transmittal to foreign government[illegible]
be made only with prior approval of

TECHNICAL REPORT

AFRPL-TR-70-6 VOL 3

TO Unclassified
CITED IN DDC TAB
(Signature & Date)

GROUP 4 DOWNGRADED AT 3 YEAR INTERVALS; DECLASSIFIED AFTER 12 YEARS

PATENT SECRECY NOTICE

PORTIONS OF THIS DOCUMENT CONTAIN SUBJECT MATTER COVERED BY A U.S. PATENT OFFICE SECRECY ORDER WITH MODIFYING SECURITY REQUIREMENTS PERMIT. HANDLING SHALL BE IN ACCORDANCE WITH THE PERMIT AS DESCRIBED ON PAGE A AND INDICATED HEREIN. VIOLATORS MAY BE SUBJECT TO THE PENALTIES PRESCRIBED BY, TITLE 35, U. S. C. (1952), SECTIONS 182 AND 186.

THIS DOCUMENT CONTAINS INFORMATION AFFECTING THE NATIONAL DEFENSE OF THE UNITED STATES WITHIN THE MEANING OF THE ESPIONAGE LAWS, TITLE 18 U. S. C., SECTIONS 793 AND 794. ITS TRANSMISSION OR THE REVELATION OF ITS CONTENTS IN ANY MANNER TO AN UNAUTHORIZED PERSON IS PROHIBITED BY LAW.

AIR FORCE ROCKET PROPULSION LABORATORY (RPOR/STINFO)

AIR FORCE SYSTEMS COMMAND

EDWARDS AIR FORCE BASE

EDWARDS, CALIFORNIA 93523

UNCLASSIFIED

AFRPL-TR-70-6 VOL 3

(UNCLASSIFIED TITLE)

AIR FORCE REUSABLE ROCKET ENGINE PROGRAM

XLR129-P-1

DEMONSTRATOR ENGINE DESIGN

AFRPL-TR-70-6

APRIL 1970

AIR FORCE REUSABLE ROCKET ENGINE PROGRAM

XLR129-P-1

DEMONSTRATOR ENGINE DESIGN

VOLUME 3

PREFACE

(U) This volume contains data pertaining to the XLR129-P-1 Demonstrator Rocket Engine control system, demonstrator engine mockup, and plumbing system. Also included in this volume are appendixes containing structural design criteria and data. Refer to Volume 1 for introductory and summary information relating to program requirements and engine system characteristics. Detailed component descriptions are contained in Volume 2.

SECTION V
CONTROL SYSTEM

A. SYSTEM DESCRIPTION

SECTION V
CONTROL SYSTEM

A. SYSTEM DESCRIPTION

1. System Requirements - General

(U) A closed-loop control system is required to ensure safe, precise, responsive performance of the engine throughout its operating range. The planned system will accept vehicle or "man-in-the-loop" command signals at any rate and in any sequence, and will respond rapidly within the functional and structural limits of the engine. The system will be stable at any setting and will respond smoothly to command.

(U) Four discrete electric signals from the vehicle control engine starting and shutdown, and modulate the thrust and mixture ratio. The control signals may originate either in the vehicle guidance control or a pilot's command console in a manned vehicle. Response of the engine to these signals is governed by an electronic Engine Command Unit (ECU). The ECU in the demonstrator engine will be a solid-state electronic component incorporating all of the flight engine control logic. The valves, actuators, igniters, and plumbing will be constructed with lightweight, flight-type parts and will be contained within the engine envelope. (See figure 417.)

2. System Requirement - Specific

(C) The specific design requirements for the control system are as follows:

1. Schedule and execute the engine start sequence automatically when a discrete signal is input to the ECU

2. Schedule and execute the engine shutdown sequence automatically upon command

3. Use electric power and helium supply from the vehicle for starting, shutdown, and restarting the engine and use engine-supplied power to drive the control system and modulate the engine throughout the operating range.

4. Set any engine thrust level between 20 and 100% of rated thrust in response to a discrete signal to the ECU control rated thrust within $\pm 3\%$ accuracy

5. Set any engine mixture ratio between 5.0 and 7.0 in response to a discrete signal to the ECU and control the engine mixture ratio within $\pm 3\%$ of the requested mixture ratio at rated thrust

6. Change thrust and/or mixture ratio within the modulating range in less than 5 seconds

7. Perform all functions adequately when exposed to engine environmental conditions, which include ambient pressures from sea level to vacuum for 10 hours between overhauls, 100 reuses, 300 starts, 300 thermal cycles, and 10,000 valve cycles

3. Engine Description

(U) The XLR129-P-1 high-pressure rocket engine uses a staged combustion cycle in which most of the fuel is burned with a portion of the oxygen in a preburner to provide turbopump power before combustion with the remainder of the oxygen in the main burner chamber. A propellant flow schematic illustrating the principal flowpaths and functional component arrangement of this engine is shown in figure 18.

4. Control Component Description

a. Main Propellant Valves

(U) Analysis of the XLR129-P-1 rocket engine cycle has established that the following control points are required for satisfactory steady-state operation:

1. Preburner oxidizer valve
2. Preburner fuel valve
3. Main chamber oxidizer valve
4. Oxidizer low-speed inducer variable turbine actuator.

(U) The preburner oxidizer valve is a translating sleeve valve which regulates the total flow and flow split to the primary and secondary oxidizer elements of the preburner injector during engine operation. The resultant variation in primary and secondary flow split controls the effective ΔP of the oxidizer entering the preburner and ensures stable and efficient preburner combustion. This valve has a major influence on the available main turbine power and engine thrust, but only a minor influence on the overall engine mixture ratio. The preburner valve also shuts off the oxidizer flow to the preburner when the engine is not operating.

(U) The preburner fuel valve is a straight-shaft butterfly valve located downstream of the fuel pump in the line to the preburner supply heat exchanger. This valve regulates the hydrogen flow to the preburner, and provides a tapoff for the transpiration coolant flow for the main chamber. Because this valve regulates hydrogen flow, it has a major influence on pump discharge pressure, chamber mixture ratio, and available turbine power. It has only a minor influence on thrust, because fuel flow is a small part of the total propellant weight flow. Because the fuel valve influences pump discharge pressure, it affects the low-speed inducer drive power (i.e., main fuel pump NPSH) as well as transpiration cooling flow. Further, the fuel valve provides pressure loss to aid fuel system stability and provides the main fuel flow shutoff function.

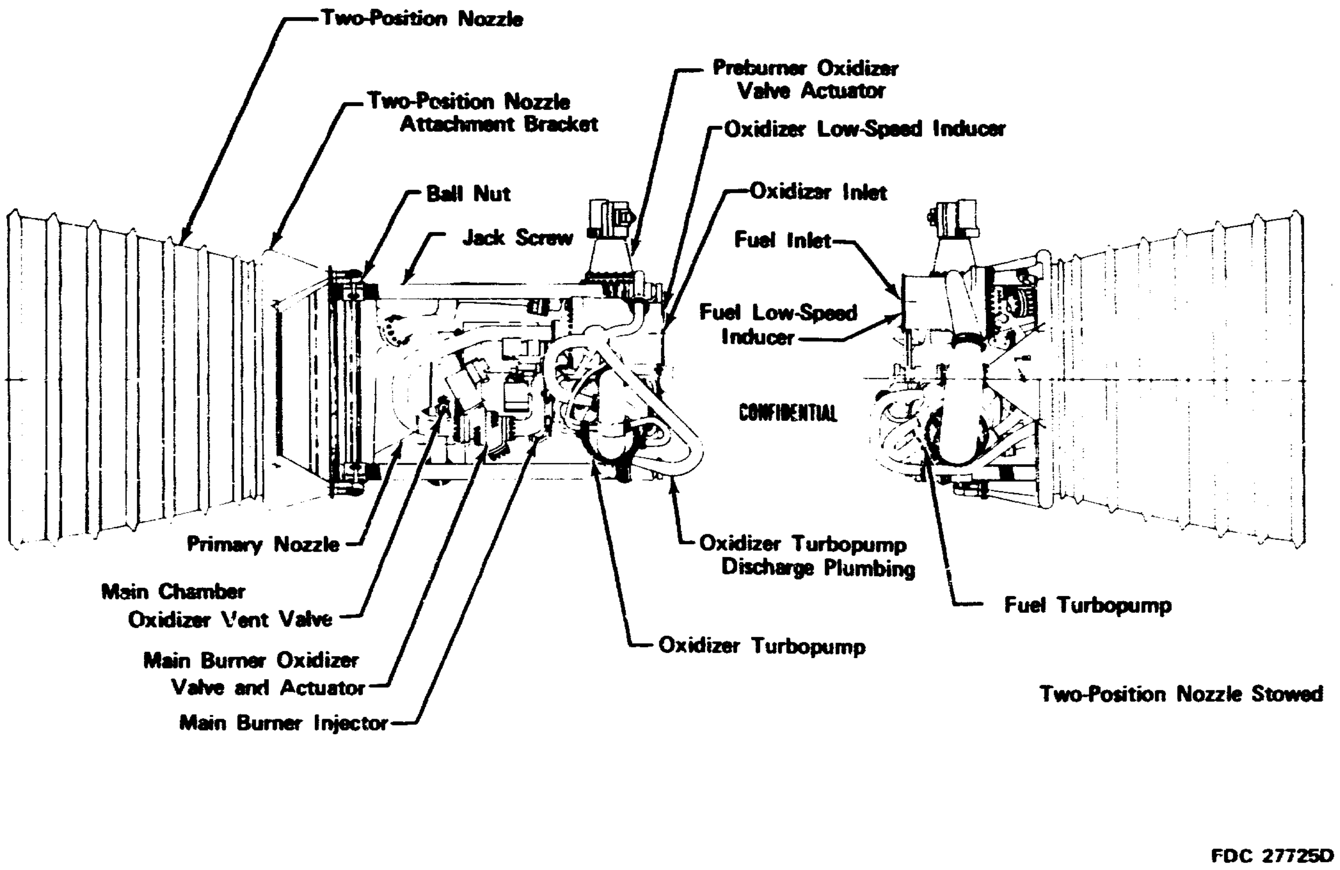

(U) Figure 417. Demonstrator Engine Layout

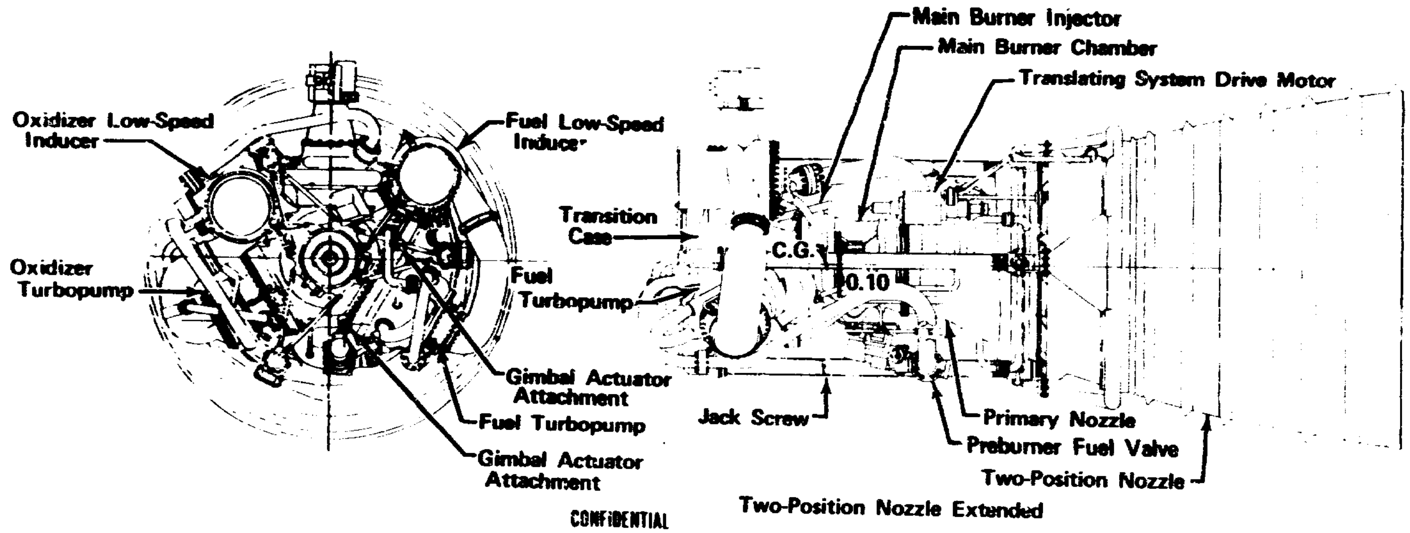

FDC 27725E

(U) Figure 417. Demonstrator Engine Layout (Continued)

(U) The main chamber oxidizer valve is a canted-shaft butterfly valve which is located in the oxidizer supply line to the main chamber. Because this control regulates the main chamber oxidizer flow, which is a major portion of the total propellant flow, it has a strong influence on both engine mixture ratio and thrust.

(U) The oxidizer low-speed inducer variable turbine actuator varies the turbine inlet area of the oxidizer low-speed inducer to regulate induced speed as a function of the oxidizer turbopump NPSH requirements.

b. Sequenced Valves

(U) Several sequenced "on-off" type valves utilized in the control system include:

1. Nozzle skirt coolant valve
2. Propellant vent valves
3. Helium system valves.

The nozzle skirt coolant valve is an on-off, two-way, solenoid-operated valve which shuts off the coolant flow to the translating nozzle when the nozzle is retracted.

(U) Vent valves for engine cooldown are located in the preburner fuel and oxidizer lines and in the main chamber oxidizer line. The main chamber oxidizer vent valve is also opened on shutdown to aid in decelerating the oxidizer turbopump. The vent valves are helium-actuated ball valves.

(U) The helium system consists of nine solenoid-actuated valves, five check valves, four flow-control orifices, and one relief valve. This system sequences helium to actuate the turbopump liftoff seals, provides preburner and main chamber purges, actuates the vent valves and provides a purge for the oxidizer turbopump.

c. Ignition System

(U) The ignition systems are integral spark igniter-exciter units that are mounted on the preburner and main chamber. Two systems are provided for the preburner and two for the main chamber to provide total spark redundancy. These units ignite oxygen/hydrogen torches, which in turn ignite the preburner and main burner chamber. The torch igniters are of the same basic design that has demonstrated vacuum ignition without failure in the P&WA RL10 engine used on the Centaur and Saturn programs.

5. Vendor Control System Effort

a. General

(U) A preliminary engine control system purchase performance specification was prepared and requests for proposal were forwarded to several prospective engine control system vendors with extensive backgrounds in turbojet and rocket engine control applications and electronic computer technology. The purchase specification (PPS T-7) outlined the requirements for flight-type actuators, flight-type sensors and a breadboard engine command unit. Competitive proposals were received and evaluated for the effort required for demonstrator engine control system synthesis, hardware delivery and flight engine control system definition.

(U) The basic control system incorporates scheduled valves and oxidizer low-speed inducer control, with limited-authority trim based on measured engine parameters. Various engine operating limits are protected by override authority. A complete control system consisting of a breadboard engine command unit, one set of all engine sensors, and actuators for the four main propellant valve will be supplied. A general description of the vendor-supplied components is as follows:

b. Engine Command Unit (ECU)

(1) General Description

(U) The ECU provides the starting and the shutdown sequences, on input signal, which includes command of the propellant flow control valves and the ignition system. The ECU controls and protects the engine during the transients and throughout the steady-state operating range in response to thrust and mixture ratio input signals. The ECU incorporates test features that allow bench-check and operational monitoring of the sequential and flow control schedules without engine operation.

(U) The ECU is required to respond to discrete electrical input signals of thrust and mixture ratio and to control the engine over the complete operating range. These input signals and the sensed parameters provide the information for transient and steady-state control system modulation. The required ECU input commands are:

1. Start
2. Thrust level
3. Desired mixture ratio
4. Shutdown.

(U) The ECU controls the engine by sequencing or modulating the following:

1. Ignition system
2. Helium solenoids
3. Preburner oxidizer valve area
4. Main chamber oxidizer valve area
5. Preburner fuel valve area
6. Oxidizer low-speed inducer control
7. Extendable nozzle coolant shutoff valve
8. Extendable nozzle actuator
9. Vent valves.

(U) The ECU incorporates a 16-bit, parallel, 2-MHz digital computer with a metal oxide semi-conductor permanent memory. It can compute 100 solutions per second, during which time extensive self-testing, input monitoring and system monitoring are performed. The digital section comprises ceramic Dual-In-Line Packages (DIP) for improved reliability, and extensive use is made of Medium Scale Integration (MSI) circuits.

(2) Starting and Shutdown Operation

(C) The engine starting sequence is initiated by a vehicle input signal to the ECU. The initial ECU starting sequence requirements are based on analytical engine starting studies. These studies have indicated that the engine can be started with safe operating conditions for all components with the control valve fixed in position during start. When thrust is above 90% of the idle thrust (20%) level, command of the engine transfers from the starting sequence to thrust and mixture ratio control, and the engine can accelerate to the selected thrust and mixture ratio setting. When the desired thrust signal is reduced below the idle level, the valves remain fixed in their starting positions. If the engine is started with the thrust input set at any level above the idle level, the control lock is removed only after the engine is above 90% of idle thrust.

(U) The shutdown sequence is initiated on signal. Shutdown control provides rapid engine shutdown within the engine structural limits from any combination of thrust and mixture ratio.

(3) ECU Logic

(U) The proposed ECU logic is outlined as follows. Definition of the ECU steady-state and transient logic was initiated in the Phase I, Contract AF04(611)-11401, dynamic analysis program. A nonlinear dynamic engine simulation was used which accurately described the engine parameters over the full transient range. These analog programs, with additional refinements, were used to establish the flight-type valve actuator requirements, transducer requirements, and precise engine command logic requirements to support the control design.

(U) The time-based gross control mode is the heart of the system that promotes both simplicity and reliability. This gross control utilizes known engine characteristics, but requires no external sensor information for safe operation. The independence of external sensor information significantly enhances system reliability.

(U) The gross mode for accelerations compensates for the principal engine dynamics that would otherwise prevent rapid accelerations, namely: time delay and lag in the fuel circuit and dynamic mismatch of the turbopumps. The operation of the gross mode during an acceleration is as follows. First, all control areas are advanced simultaneously along nominal timed schedules by the thrust velocity servo. Then oxidizer flow to the main burner chamber is retarded by reducing the main chamber oxidizer valve and low-speed inducer guide vane areas in proportion to each other as a function of the rate of change of thrust request. This results in a lower mixture ratio and gives more margin during acceleration. Finally, fuel flow is advanced by increasing the preburner fuel valve as a function of the rate of change of thrust request. This compensates for the inherent transport and accumulation delay in the fuel circuits.

(U) Engine characteristics permit fast and safe decelerations with a gross control mode without additional compensation. On decelerations, engine characteristics permit all control areas to be reduced along nominal schedules on a timed basis by the thrust velocity servo. Oxidizer flow reduces first because of normal deceleration of the pumps and the scheduled valve area changes. Fuel flow is maintained transiently by the inherent delay in the fuel circuit. Thus, mixture ratios in the main burner chamber and preburner are reduced and the engine decelerates safely.

(U) Control capability to protect the engine is critical to a man-rated system. Within the demonstrator engine operating envelope, the propellant schedule in the ECU prohibits operation beyond component limits. However, if abnormal conditions are experienced during either steady-state or transient operation, one of the engine limits could be exceeded. Direct measurements of the limiting parameters, such as turbopump speed, are monitored by the ECU. The limiter control function in the ECU (independent of the normal schedule function) has sufficient gain and response to override the normal function and limit engine operation. If the limit control is in command, a positive signal indicates that corrective pilot action is required.

(U) Ten closed-loop controllers support and back up the gross mode to provide the intelligence for control, limiting and trimming functions for:

1. Rapid engine transients with good safety margins
2. Accurate and stable steady-state operation
3. Protective controls to maintain system balance.

(U) The ten closed loops consist of four controllers, four limiters, and two trims. The engine parameters controlled by closed loops, in order of importance with respect to dynamic performance, are as follows:

1.	Main fuel pump speed	Controllers
2.	Transpiration cooling	
3.	LO_2 pump NPSH	
4.	Fuel pump NPSH	
5.	Maximum preburner temperature	Limiters
6.	Maximum LO_2 pump speed	
7.	Minimum preburner temperature	
8.	Maximum fuel pump speed	
9.	Engine thrust (total propellant flow)	Trims
10.	Engine mixture ratio	

c. Sensors

(U) The closed-loop control system uses flowmeters in both propellant lines to generate signals proportional to actual thrust and mixture ratio. These flowmeter signals are compared to the vehicle input signals in the ECU, which, in turn, automatically correct any difference between actual and desired values by modulating the engine propellant valves.

(U) Advanced versions of a lightweight force-screen, true-mass cryogenic flowmeter measure both the liquid oxygen and liquid hydrogen total flow-rates. This meter, with a low pressure drop, is insensitive to extraneous accelerations and can withstand high-velocity gases during engine cool-down. An experimental version has successfully operated at liquid hydrogen temperatures, and completely redundant sensing elements and electronics will provide the desired reliability.

(U) Twelve additional sensors are proposed for primary measurement and reference computation for ten closed loops to control and limit eight separate engine parameters. Four additional sensors (two pressure and two speed) provide separately computed oxidizer and fuel flow measurements from both low-speed inducer pump characteristics.

(U) Six pressure transducers, four temperature sensors, and four speed sensors monitor the oxidizer and fuel pumping as required by thrust demand. Signal conditioning electronics, developed from cryogenic amplifier circuits, are heat sinked to the liquid oxidizer lines for temperature stabilization. All temperature and speed sensors are triple-redundant and directly coupled to the input of the digital computer for selection and testing. Fail operating assurance is provided by a monitor in the computer that provides automatic cutout of a defective sensor.

d. Actuators

(U) Alternating current induction motors are proposed for the actuators because the lack of brushes completely eliminates commutation problems, and solid rotor construction eliminates the need for rotor coils. Alloy materials used for the cryogenically cooled rotors add rotor resistance and improve starting torque. However, the effect of the increased resistance on running conditions requires careful consideration to obtain optimum performance. An alloy of 95% copper and 5% zinc has been successfully used in cryogenic temperature development motors. Power for the valve actuators is supplied from an engine-driven electrical system.

(U) The basic approach chosen for packaging the electric servo-motor valve actuators is to close-couple the electronics and the actuator for a high-density package. The driving and shaping electronics, as well as the electronics required for redundancy, are packaged in the actuator housing. Triplicated electronic circuitry consists of active and standby channels as well as a model channel. In the event of a failure in an active channel, automatic switchover to the standby electronics is accomplished.

(U) To assure that controls are available for initial demonstrator engine tests and for the valve test programs, commercial actuators will also be provided. The propellant valves will be built to accept these commercial actuators as well as the flight-type actuators.

6. Reliability

(U) A high degree of reliability is attained through redundancy and self-testing. Temperature and pressure sensors are triple redundant. When all three elements are operative, the computer selects the middle signal. If one of the three signals is lost, the computer recognizes the signal that is closest to the previous median signal. Should that signal also become lost, then the signal from the third element will be accepted.

(U) Actuators are proposed with dual servo motors using master and standby concepts, and the flowmeters utilize dual redundancy throughout for the maximum reliability factor.

(U) In addition to the monitoring schemes applied to the sensor systems, the computer includes self-testing of the arithmetic section and the permanent memory. The arithmetic unit is programmed to test each instruction that the unit can execute. Automatic, programmed testing of the permanent memory data is performed continuously by a "check sum" test. The test adds up all the words in the memory and compares the total against a previously stored sum.

(U) Dual electronic computers are used. One is designated the master unit and controls the engine unit unless self-test proves it defective. A switching circuit then changes control over the standby unit.

(U) Continuing and systematic failure analyses of all control system components will be conducted and design improvements incorporated to:

1. Provide a proven and dependable control to ensure demonstrator engine testing to meet the performance and operational objectives.

2. Provide assurance that the flight control designs can be implemented and ultimately developed to the standards of a man-rated flight system.

B. PREBURNER OXIDIZER VALVE

B. PREBURNER OXIDIZER VALVE

1. Introduction

a. Function

(U) The function of the preburner oxidizer valve is to divide the oxidizer supply into two separate flows as required by the preburner injector. The valve is designed with fixed primary passages and variable area secondary ports. Control of the preburner oxidizer flow over the engine operating range is accomplished by modulating the area of the secondary ports. The valve will allow primary flow without secondary flow for engine ignition during the start transient. The preburner oxidizer valve also provides a positive shutoff for the total preburner oxidizer supply.

b. Location

(U) The valve is located in the preburner dome on the engine as shown in figure 418. The servoactuator is mounted external to the dome.

2. Design Requirements

(C) Design requirements for the preburner oxidizer valve are:

1. External leakage from the actuator shaft shall not exceed 10 sccs of GN2 at operating pressure
2. Provide a positive shutoff with a shutoff leakage not to exceed 10 sccs of GN_2
3. Component shall be capable of 10,000 valve cycles, 500 pressure cycles, 300 starts, and 10 hours time between overhauls
4. Flange leakage shall not exceed 10^{-4} sccs of GN_2 per inch of seal at operating pressure
5. Operate in a liquid oxygen environment
6. The valve shall operate over the range of secondary effective area, ΔP and flow as shown in figure 419. These requirements are generated by the engine cycle balance.

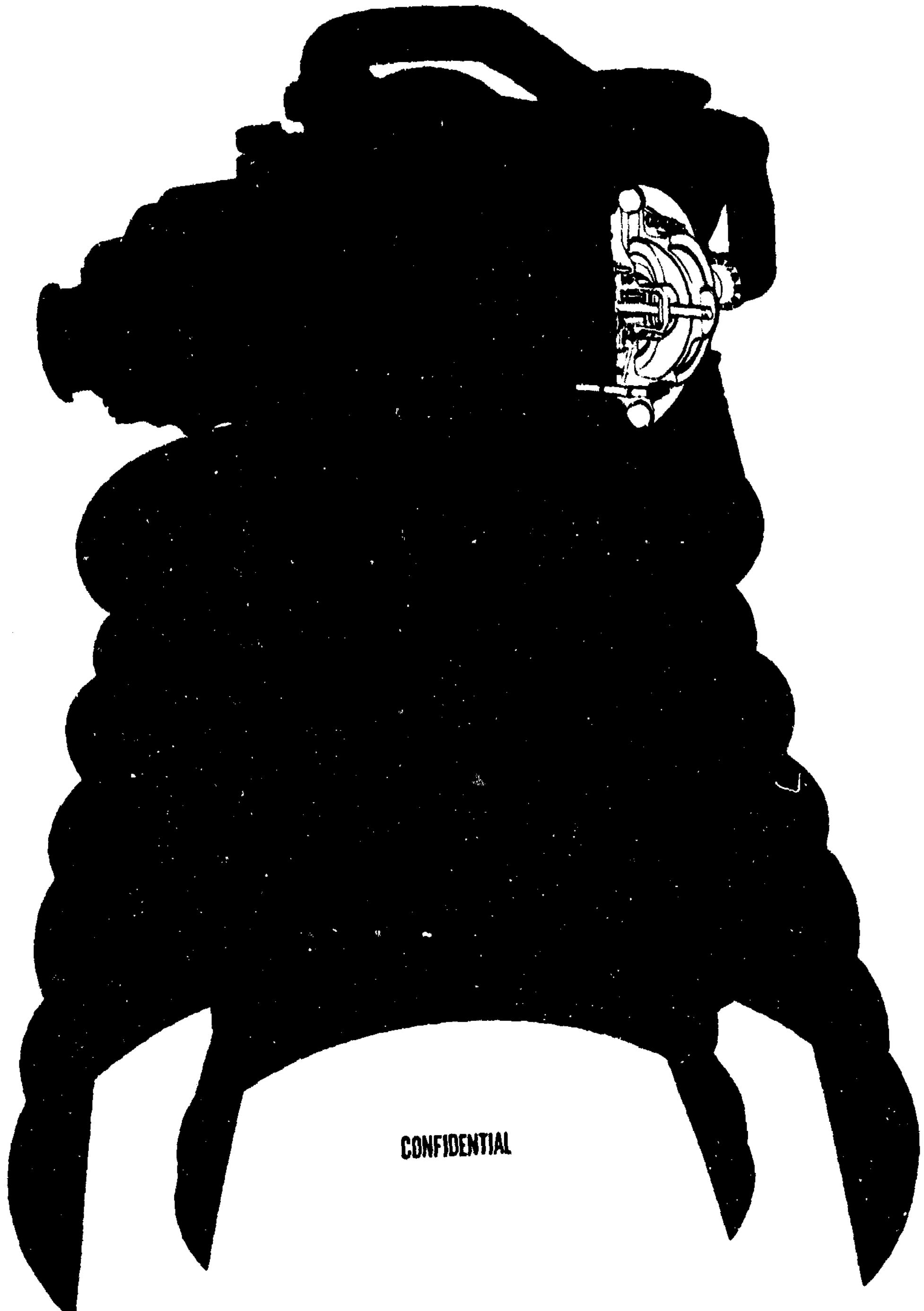

FDC 31422

(U) Figure 418. Preburner Oxidizer Valve Location

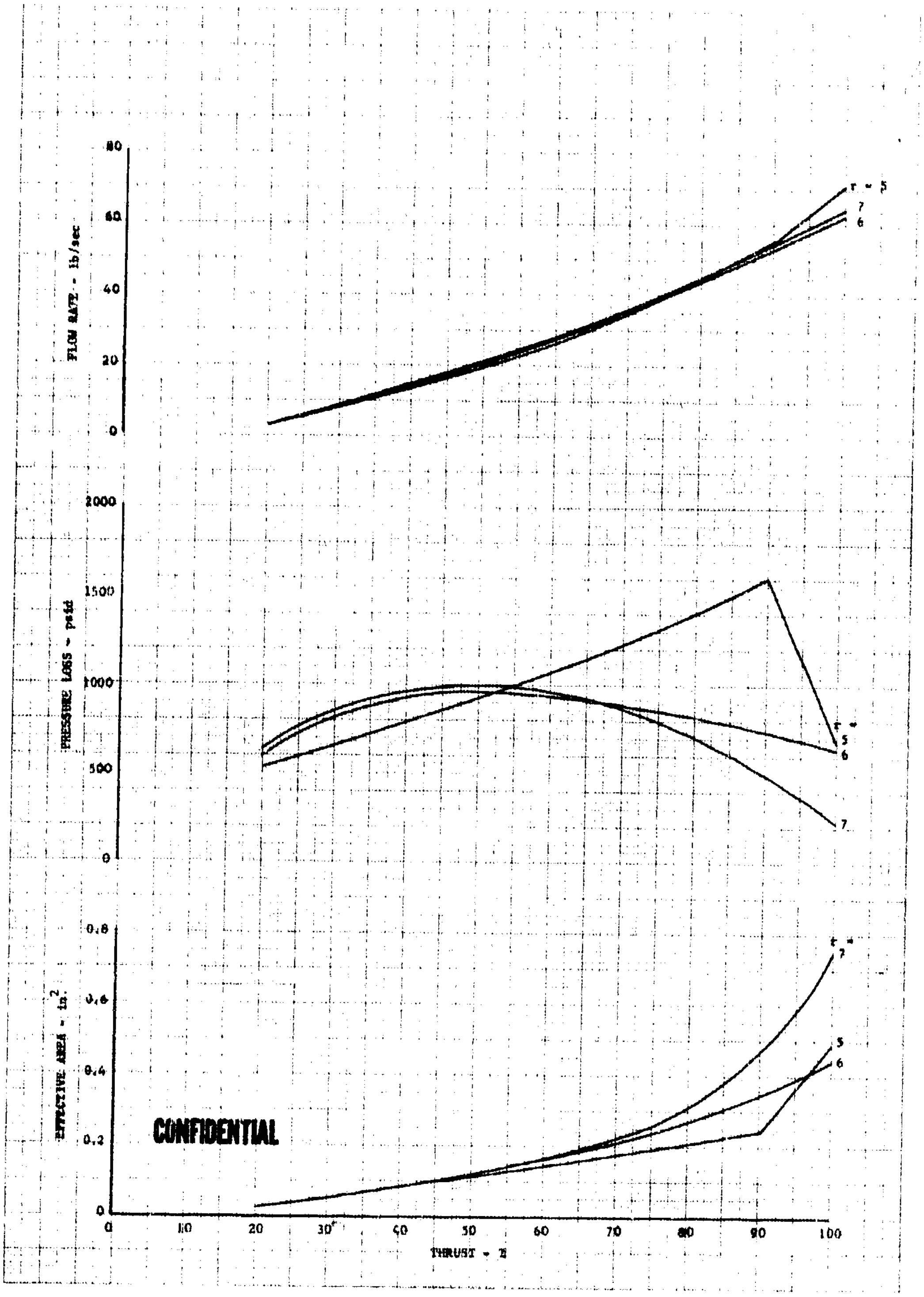

DFC 69951

(U) Figure 419. Preburner Oxidizer Valve Control Characteristics

3. Design Criteria

(U) Design criteria for the preburner oxidizer valve are:

1. Minimize overall length, including consideration of the actuation system

2. Lightweight configuration that is representative of a flight design but with safety factors sufficient for confident operation

3. Maintain the Phase I flow divider valve approach of the sleeve-type valve and contoured secondary ports, but eliminate the primary metering function

4. Provide primary flow without secondary flow for engine starting

5. Utilize a minimum-length commercial hydraulic actuator

6. Minimize secondary volume

7. Minimize actual forces

8. Provide a vent between the primary and secondary shaft seals.

4. Mechanical Description

(U) The preburner oxidizer valve, shown disassembled in figure 420 and in cross section in figure 421, consists of a translating sleeve and a fixed housing that incorporates six contoured ports as shown in figure 422 for secondary flow and six equally spaced radial holes for distribution of the primary flow. The valve assembly is bolted to the lower flange of the preburner dome.

(U) The preburner dome, illustrated in figure 423, has a 180-degree ring manifold with a flanged inlet located centrally relative to the manifold. The ring manifold also has a mounting flange at one end for the vent valve. The manifold is divided by a baffle plate that separates the oxidizer inlet flow from the vent flow. After entering the ring manifold, the oxidizer flows into the dome cavity through 12 radial ports located between studs. There are three additional radial ports for oxidizer to flow from the dome through the vent valve prior to engine starting. The 12 oxidizer inlet ports permit the oxidizer to be well distributed as it enters the dome cavity so that hydraulic side force on the translating sleeve is minimized. The dome housing contains drilled passages for the primary oxidizer supply to the injector, provisions for temperature and pressure instrumentation, purges, and seal leakage connections. A precision surface for mounting the actuation system is low on the dome for minimum deflection. Tapered shims can be used during assembly to align the actuation system and dome-valve housing assembly.

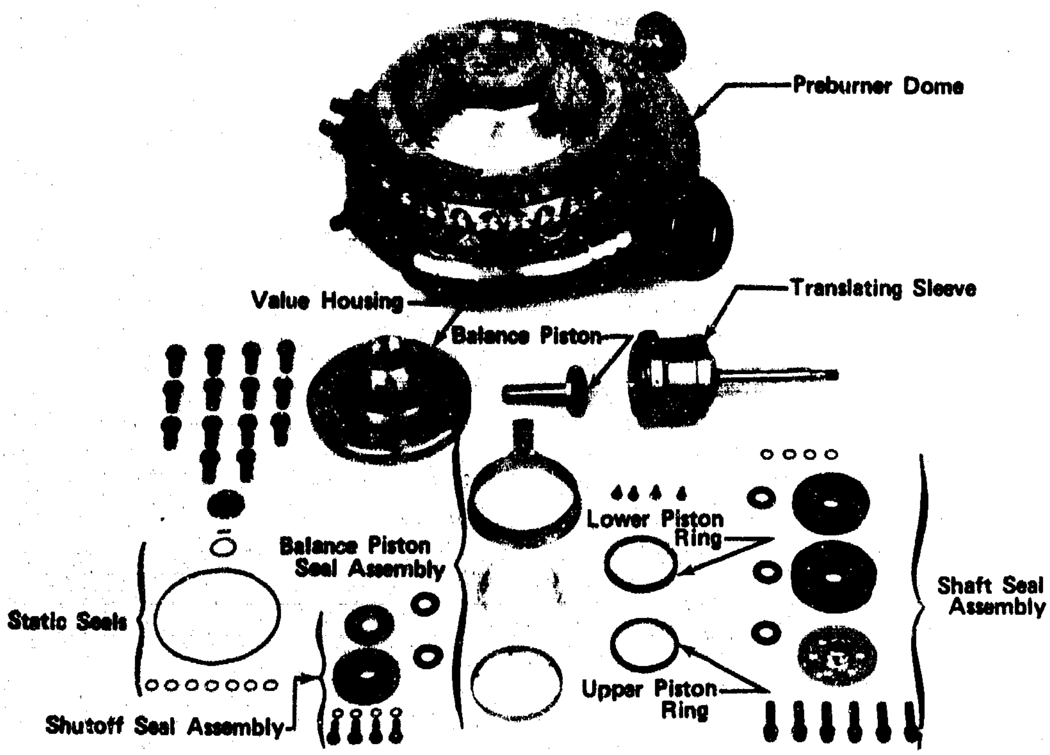

FE 88807
FD 35633

(U) Figure 420. Preburner Oxidizer Valve Disassembled

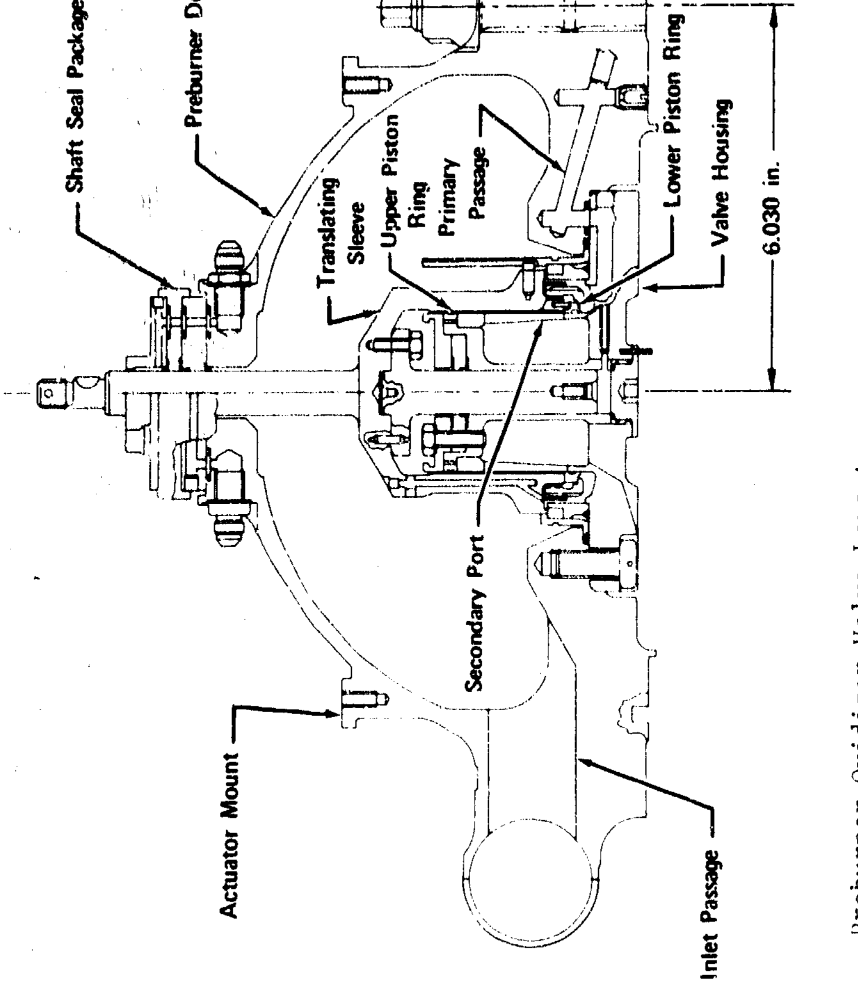

(U) Figure 421. Preburner Oxidizer Valve Layout

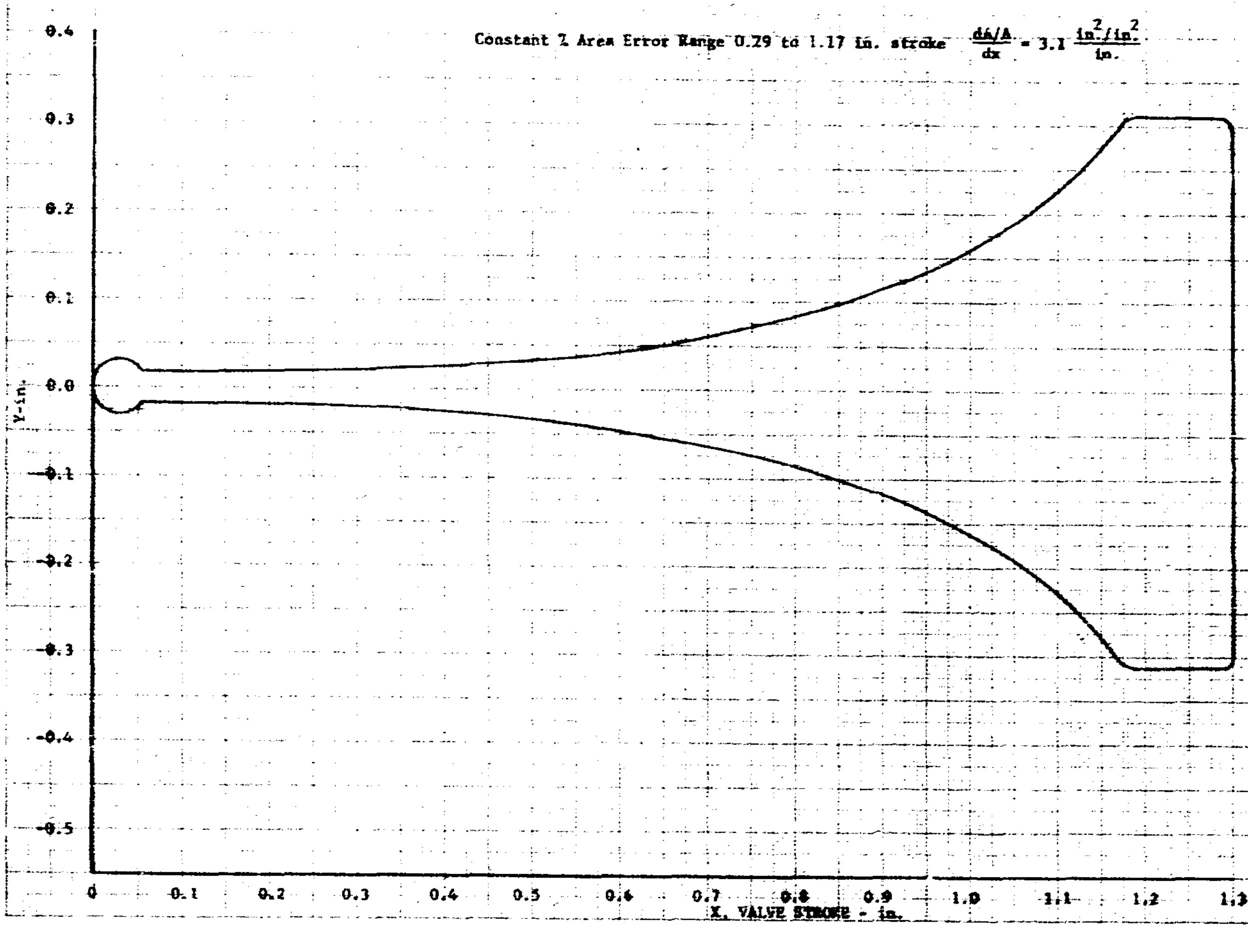

X	± Y
0 - in.	0 - in.
0.03	0.03
0.05	0.0175
0.29	0.0175
0.33	0.020
0.38	0.023
0.48	0.0316
0.58	0.0428
0.68	0.0587
0.78	0.0797
0.88	0.1046
0.98	0.1400
1.03	0.1750
1.08	0.216
1.13	0.252
1.17	0.300
1.19	0.310
1.29	0.316
1.30	0.300

(U) Figure 422. Preburner Oxidizer Valve Port Contour

DF 69952

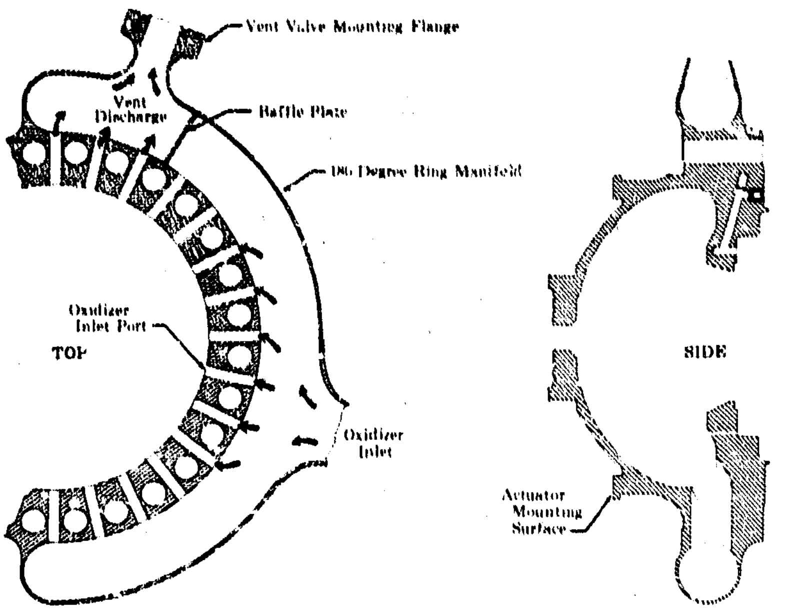

(U) Figure 423. Preburner Dome Cross Section FD 25979A

(C) Engine thrust modulation requires variation of the preburner oxidizer flow by modulating the secondary port effective area. The desired preburner injector performance is maintained by the fixed area of the primary passages which increase the ratio of primary to secondary flow as thrust level is decreased. The primary oxidizer flow is provided to the preburner injector through six equally spaced radial holes. The primary flow passages are designed to flow at 10% of preburner oxidizer flow at a mixture ratio of 7 and 100% thrust. The primary flow orifices are 0.080 inch in diameter; however, the orifice is provided as a removable plug to permit experimental adjustment of the flow split at design point. The secondary oxidizer flow is metered by the six contoured ports and flows through the valve housing to the preburner injector as shown in figure 424. The valve is designed with 25% excess secondary area, accomplished with 0.070 inch of additional valve stroke.

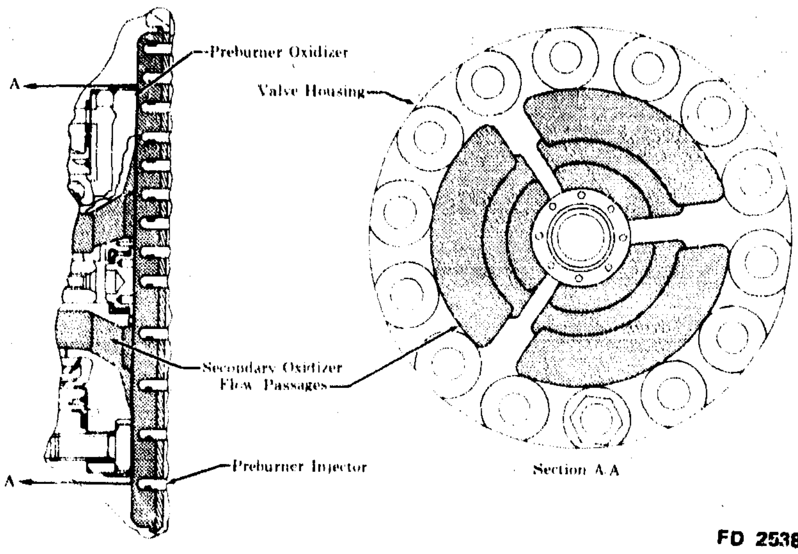

FD 25388

(U) Figure 424. Secondary Oxidizer Flow Passage

5. Operating Characteristics

(C) The preburner oxidizer valve operates in a liquid oxygen environment with a maximum pressure of approximately 6000 psia. The valve modulates an orifice upstream of the preburner injector secondary elements with a maximum area of 0.751 square inch and a minimum area of 0.024 square inch. The valve provides a passage upstream of the preburner primary elements with a constant area and shuts off the oxidizer flow to the preburner. The valve incorporates a dynamic seal where the actuator shaft passes through the dome. This seal is designed to withstand liquid oxygen at approximately 6000 psia pressure differential for 10,000 cycles.

(U) The preburner oxidizer valve is designed to meet the requirements of the XLR129-P-1 demonstrator engine. The volumes and the effective areas of the primary and secondary flowpaths at the valve and injector passages are shown in figure 425.

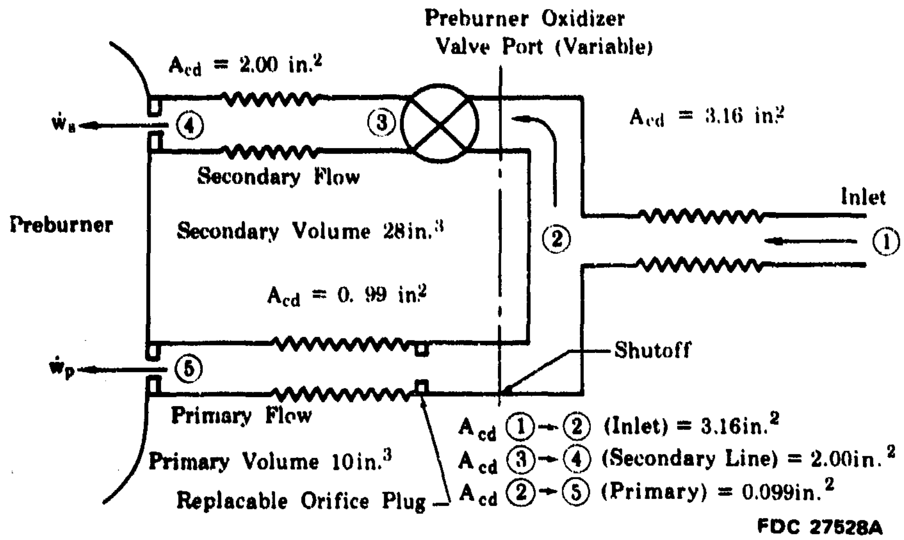

(U) Figure 425. Preburner Oxidizer Valve and Injector Flow Passage Schematic

(U) The valve's contoured secondary metering ports provide constant percent area error. The predicted 3.1% flow area error will remain constant over 87% of the operating range (a valve stroke of 0.29 inch to 1.17 inches), with the error increasing at the low area end and diminishing near the full-open end as shown in figure 426. The width of the secondary metering port is constant (0.62 inch) from 1.14 inches to the maximum stroke of 1.3 inches. This was done to minimize the unsupported length of the valve piston ring and to reduce stresses on the valve wall. As a result, the valve positioning error decreases above a 1.17-inch stroke. Minimum port width was set at 0.035 inch, which increases the positioning error below a 0.29-inch stroke.

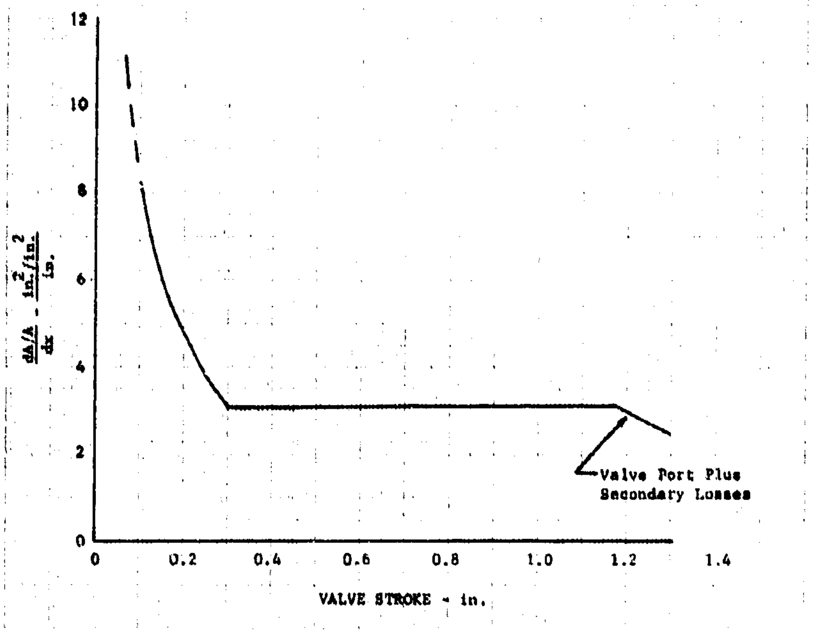

(U) Figure 426. Preburner Oxidizer Valve Area Error/ Positional Error vs Valve Stroke

(U) A discharge coefficient (C_d) of 0.6 was assumed for the total range of secondary port metering. When the valve is operating at low flow areas, the narrow port width relative to the wall thickness tends to reduce the expansion loss and may increase the C_d. Even with an increase in C_d at low flow areas, it is within the capability of the valve to achieve minimum flow area by decreasing the minimum stroke.

(U) Figure 427 shows the preburner oxidizer valve port contour. Minimum port width is 0.035 inch; maximum port width is 0.62 inch; and overall valve stroke is 1.3 inches.

(U) The primary valve and injector volume is 9.9 cubic inches. The secondary valve and injector volume downstream of the metering port is 28 cubic inches. The characteristic of the valves secondary effective area from port inlet to valve discharge is shown in figure 427. The design goal of effective area exceeded the cycle requirement by 7%. Without the actuator, the valve weighs 102 lb.

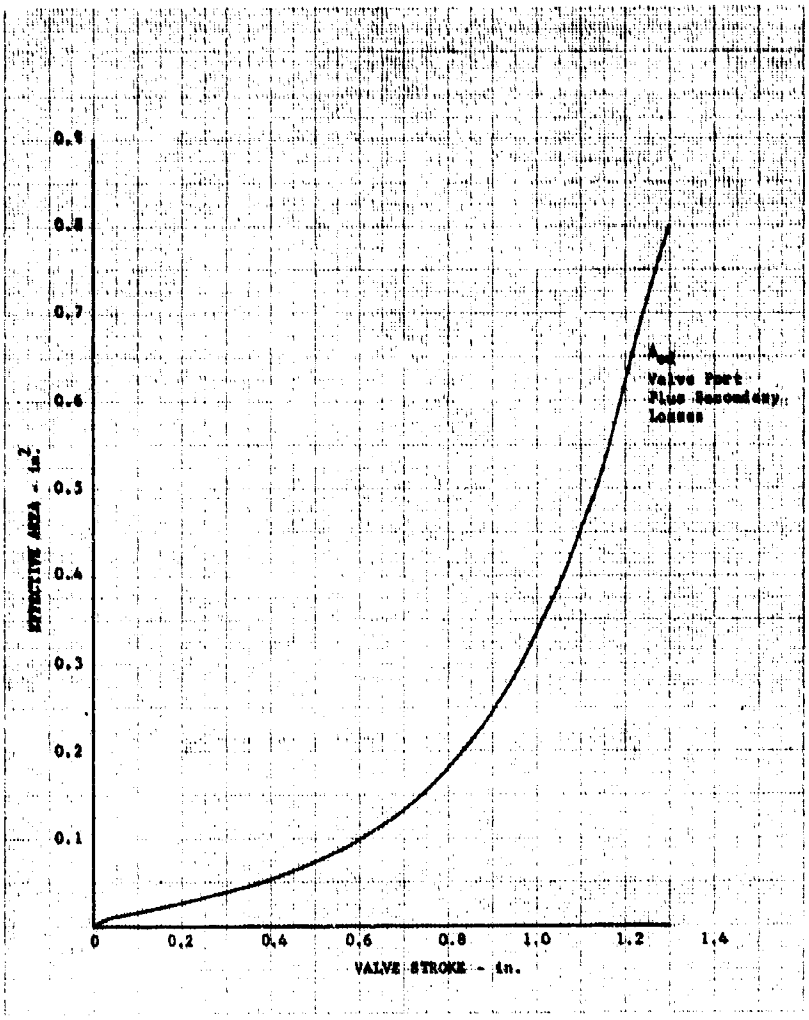

DF 69953

(U) Figure 427. Preburner Oxidizer Valve Effective Area vs Stroke

6. Design Approach

a. Background

(U) The preburner oxidizer valve design is based on the Phase I flow divider valve configuration. The Phase I flow divider valve, illustrated assembled on the preburner injector in figure 428, divides the oxidizer supply into two separate flows to the dual-orifice oxidizer system for the preburner. This valve also provided an oxidizer supply to the igniters for both the preburner and main chamber, and incorporated a positive shutoff for the total preburner oxidizer supply. The flow divider valve was located in the preburner dome with the servoactuator mounted outside the dome. To permit more flexibility in the valve operating schedule, the flow divider valve was longer than the current demonstrator engine design and did not include the thrust control function.

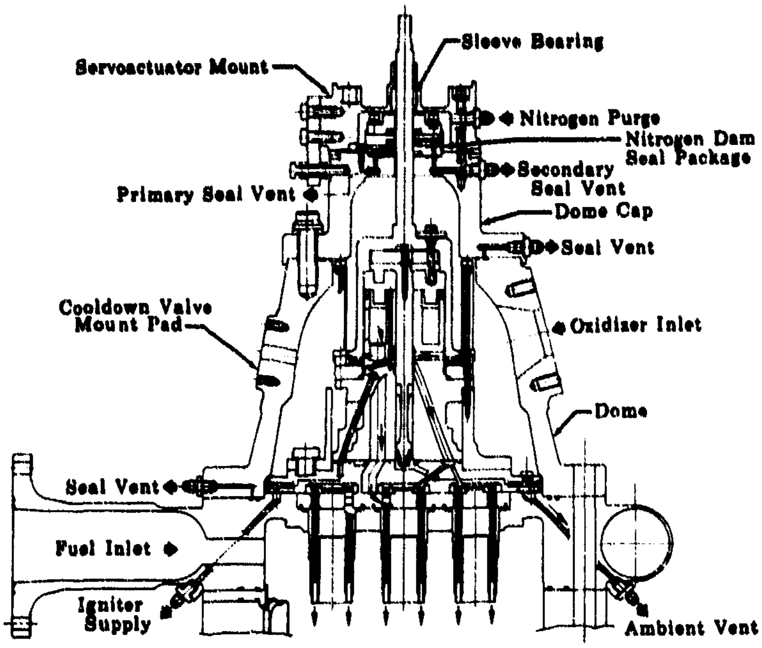

(U) Figure 428. Flow Divider Valve

(U) Basic design features differing from the preburner oxidizer valve tested previously include incorporating the preburner dome cover as part of the valve housing, removable orifices in the primary flow passages, shaft lip seals, pressure balanced piston rings, an improved lower piston ring retainer, and reduced overall length.

(U) The valve actuation stroke of approximately 1.600 inches includes an initial 0.070-inch travel to move from shutoff position to the primary open, secondary closed position. This action relates to the engine starting sequence. An additional motion of 0.100 to 0.130 inch will initiate secondary flow, with a subsequent travel of 1.300 inches required to move the valve fully open to the secondary port limit. The valve is then capable of approximately 0.050-inch over-travel.

b. Design Evolution

(U) A design analysis task for the valve piston rings, to reduce the valve actuation drag load that was experienced during the tests conducted under the supporting data and analysis subtask was completed. The valve has two piston rings as shown in figure 420: an upper ring attached to the valve housing which seals the secondary sleeve ID and a lower ring attached to the secondary sleeve which seals the valve housing OD. Figure 429 compares the four upper rings that were analyzed in this design study and figure 430 compares the lower rings. All rings were made of Berylco 25, either AMS 4650 or AMS 4532.

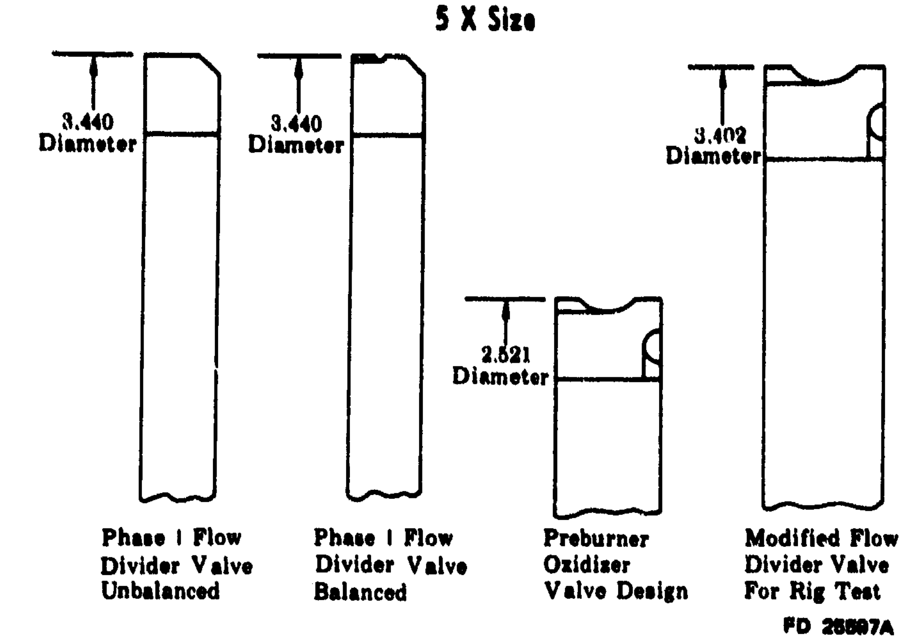

(U) Figure 429. Upper Piston Rings Analyzed

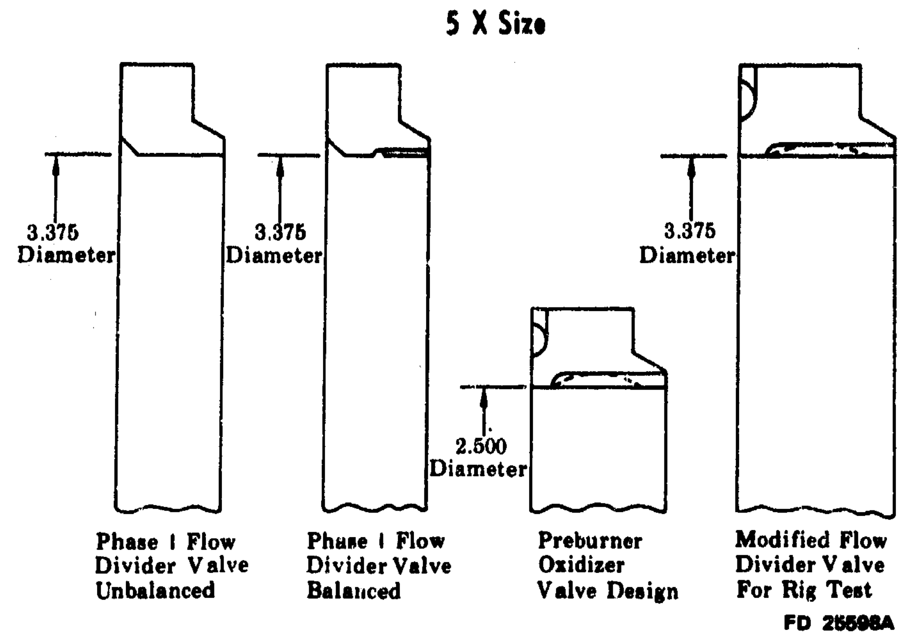

(U) Figure 430. Lower Piston Rings Analyzed

(C) Two sets of data were available from previous flow divider valve tests. At a pressure differential of 2000 psi, the unbalanced rings had a drag force of 1480 pounds when opening and 4560 pounds when closing. Under the same conditions, the pressure balanced rings had a drag of 755 pounds when opening and 1890 pounds when closing. The difference between the opening and closing drag loads and the wear patterns on the previously tested piston rings indicated that the rings were twisting and that the corners were possibly digging into the sliding surfaces. These conditions would, therefore, cause the friction factor to vary. The unbalanced and balanced rings were analyzed to determine if the drag loads experienced could be found analytically. Ten different loading cases could be found for each ring when they were allowed to twist. Of these, only three of each could be solved and they gave scattered results, none of which were usable. The unsolvable cases were redundant or impossible loadings. The lower ring solutions even indicated the ring should twist opposite to the direction that the wear indicated. The analytical solution for an absolute value of drag was abandoned at this point.

(C) The next method of analysis was to use the data of the two previous tests to estimate the changes in loading required to reduce the drag sufficiently. It was desired to reduce the piston ring drag of the preburner oxidizer valve to less than 300 pounds in either direction with a pressure differential of 1500 psi. The percentage changes of several quantities (figure 431) were found between the balanced and unbalanced rings as shown in table LXII. A definition of all terms used is provided in table LXIII. The new ring required a reduction of 88% in drag (H_A) over the unbalanced ring for the desired reduction in the actuation force. Comparing this to the balanced ring change, the percentage changes required in the other properties were found. This determined the design criteria for the new ring loads.

(U) Table LXII. Percentage Change from Unbalanced Ring

Quantity		Phase I Balanced	Required for New Ring	New Ring as Designed
Combined Upper and Lower H_A	Open	-49.0%	-88.0%	--
	Close	-58.5%		
Combined Upper and Lower G_R		-42.0%	-63.2%	-78.0%
Combined Upper and Lower F_R		-55.0%	-82.7%	-82.3%
Average Upper and Lower UP^R		-48.2%	-72.5%	-76.6%

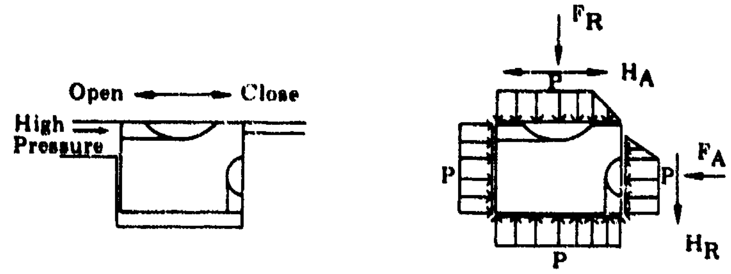

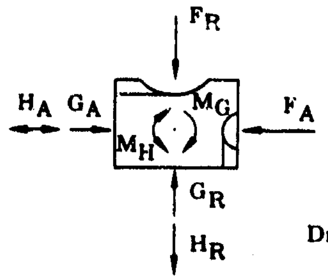

$$F_A = G_A \pm H_A$$
$$F_R = G_R - H_R$$
$$H_A = \mu F_R$$
$$|H_R| \leq \mu F_A$$
$$UP = \frac{F_R}{A_R}$$

$$\frac{F_A}{F_R} \leq 3 \qquad \frac{G_A}{G_R} \leq 3$$

$$\text{Drag} = 2\pi r \mu (F_R \text{ upper} + F_R \text{ lower})$$
$$= 2\pi r (H_A \text{ upper} + H_A \text{ lower})$$

Approximations: $H_A = \mu G_R$, $H_R = \mu G_A$

FD 25509

(U) Figure 431. Nomenclature Explanation and Definition

(U) The radial load per inch of circumference because of pressure unbalance (G_R) was chosen because it could be calculated and its change should be proportional to the change in drag. The radial load per inch of circumference because of wall reaction (F_R) used was found with an appropriate value for the radial load per inch of circumference caused by friction forces (H_R) derived from a friction coefficient of 0.25. The change in F_R should also be proportional to changes in drag. The unit pressure was also approximate because it is derived from F_R; however, it could contribute to drag as well as leakage. It was kept as high as possible to prevent leakage but low enough to reduce drag.

(U) The results for the unbalanced ring show that the closing drag was reduced more than any of the other quantities. The only explanation found is that the balanced ring had smaller moments because of pressure and friction and thus had less tendency to twist.

(U) Besides the restrictions put on G_R, F_R, and unit pressure on the rubbing surface of the ring (UP), the new rings were designed so that the pressure moment per inch of circumference caused by pressure unbalance (M_G) was negligible. The moment of inertia was increased to reduce the ability to twist. In the new designs the upper ring was 6.1 times stiffer than the balanced ring and the lower ring was 4.2 times stiffer. The moment caused by friction was decreased about 35%.

The combination of the reduced moments and increased stiffness was expected to provide an 88% reduction in twist of the rings.

(C) Other results from the new designs are shown in the last column of table LXII and the first column of table LXIV. If it can be assumed that the percentage of change method is a good analysis, then the piston ring drag will be less than 300 pounds in either direction at a 1500 psi pressure differential. Because most of the twisting was taken out of the ring, it can be assumed to remain flat against the rubbing surface. The drag may be estimated using the drag forumulas shown in figure 431. With a coefficient of friction of 0.35 and a pressure differential of 1500 psi, the total drag will be 188 pounds using G_R, and 112 pounds using F_R. The unit pressure will be 248 psi on the upper ring and 172 psi on the lower ring. The unit pressure on the balanced rings was (upper) 752 psi and (lower) 560 psi.

(U) Table LXIII. Nomenclature Definition

ΔP	Differential Pressure Across Ring
G_A	Axial Load Per Inch of Circumference Because of Pressure Unbalance
G_R	Radial Load Per Inch of Circumference Because of Pressure Unbalance
H_A	Axial Load Per Inch of Circumference Because of Friction Forces
H_R	Radial Load Per Inch of Circumference Because of Friction Forces
F_A	Axial Load Per Inch of Circumference Because of Wall Reaction
F_R	Radial Load Per Inch of Circumference Because of Wall Reaction
M_G	Moment Per Inch of Circumference Because of Pressure Unbalance
M_H	Moment Per Inch of Circumference Because of Friction Forces
r	Average Radius of Rubbing Surfaces of Both Rings
μ	Coefficient of Friction
UP	Unit Pressure on Rubbing Surface of Ring
A_R	Rubbing Area Per Inch of Circumference

(U) Table LXIV. Comparison of New and Tested Piston Rings

	New	Test	Scale Factor
Combined G_R	0.0450 P	0.0525 P	1.168
Combined F_R	0.0274 P	0.0320 P	1.168
UP Upper	0.1655 P	0.1625 P	
UP Lower	0.1145 P	0.1025 P	
Average Circumference	7.85	10.65	1.358

(U) The balancing grooves on the lower ring were designed so that a minimum amount of leakage would occur through the grooves and into the metering port of the valve. This leakage is kept below 5% of the total minimum metered flow.

(U) The test rig used for piston ring evaluation was the Phase I flow divider valve which had a 3.375 in. diameter valve housing as compared to a 2.5 in. diameter housing used on the present preburner oxidizer valve.

(U) The test rings were designed with the same twisting characteristics as the new design so that twisting would not have to be scaled. By scaling up the ring, the GR and F_R terms were 16.8% too high. The circumference of the test ring was also 35.8% higher than the new design. Because of the scaling, the measured drag from the test rings had to be multiplied by a factor of 0.63 to obtain the estimated drag of the rings for the preburner oxidizer valve and the measured leakage had to be multiplied by a factor of 0.74 to obtain a leakage estimate.

(U) A piston ring actuation force test program was conducted to evaluate the actuator force requirements for balanced piston rings. These piston rings were scaled from the design planned for the preburner oxidizer valve. The valve sleeve was nickel plated to reduce the original clearances to provide a 0.0115-inch clearance between the housing and sleeve. The sleeve was then precision chrome coated 0.001-inch thick with no subsequent machining.

(C) The upper ring was pressure balanced to a unit bearing load of 325 psi at 2000 psi ΔP, and the lower ring was pressure balanced to a unit bearing load of 205 psi at 2000 psi ΔP. The rig was subjected to 200 cycles at LN_2 temperatures. The valve was cycled at pressure differentials of 1000, 1500, 1750, and 2000 psi. Strain gage force measurements were used to indicate piston ring drag. The force versus inlet pressure is shown in figure 432. As shown, the forces recorded on the oscillograph compared favorably with the predicted values. Very little wear of the piston rings or moving surfaces was noted. The redesigned secondary piston rings were found suitable for use in the preburner oxidizer valve. As shown in figure 432, the force loading was close to the predicted results and gave a decidedly advantageous reduction in force loading.

(C) A structural analysis of the preburner dome is provided in figure 433. The analysis was conducted at 120% of the maximum operating pressure at 100% thrust and a mixture ratio of 5 (8,400 psi). The stress levels in the dome are well below the 85% yield strength (141,000 psi) allowed for the Inconel 718 (AMS 5662) material. The highest stress, 72% of the allowable, is near the top of the dome. The bolts and flanges are fabricated of Inconel 718 (AMS 5663) material and the inlet and vent flanges are undercut to achieve cantilever action. Flange deflections of 0.001 inch, together with the bolt bending associated with flange preload bending, was used to establish thickness. Bolts that hold the flanged portion of the valve housing to the dome have a factor of safety of 2.0 to minimize deflection at the static seal where leakage of liquid oxygen into the preburner (in parallel with the shutoff seal) could occur, and to provide enough bolt preload to avoid failure in the event of an abort shutdown from 100% thrust. Analysis shows that compressive stresses are maintained at the bolted interface to approximately 2200 psi and that the 14 Inconel 718 (AMS 5662) bolts would withstand a malfunction where the valve is failed closed at the maximum dome pressure. At this malfunction condition an instantaneous maximum dome pressure and a zero chamber pressure was considered. This structural analysis also shows that the actuator mounting surface has a negligible axial movement under 120% of maximum operating pressure. Because the lower valve housing deflection is only 0.0035 inch with the overpressure, the relative motion between the actuator cylinder and the valve housing (ports) will be well within the 0.005 inch desired. The actuator mount is a flexible (slotted cone) design to eliminate radial deflection problems.

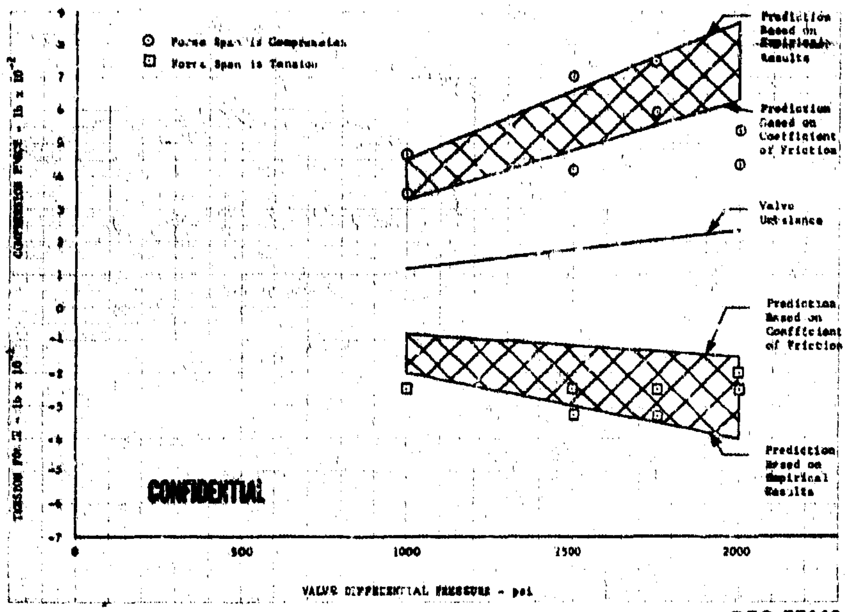

(U) Figure 432. Actuation Force vs Inlet Pressure

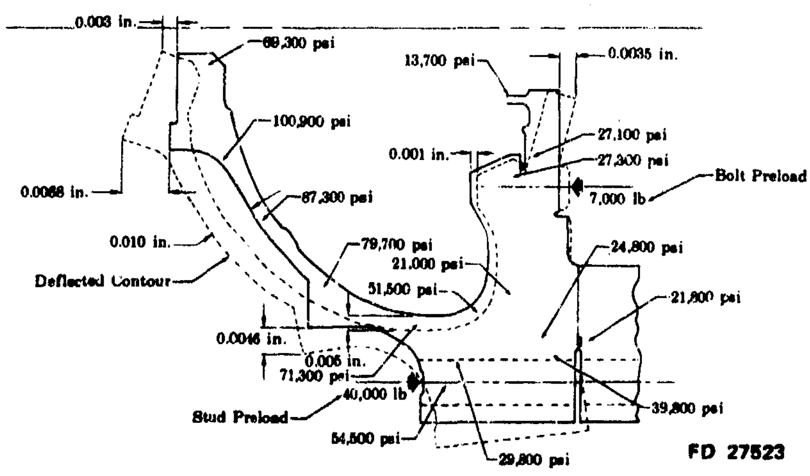

(U) Figure 433. Preburner Dome Structural Analysis

(U) The lip seal package fastens to the top of the dome to prevent leakage where the shaft of the translating sleeve protrudes from the dome as shown in figure 421. Another lip seal group on the secondary sleeve balance piston excessive oxidizer leakage overboard where the balance piston passes through the core of the valve housing. The translating shaft lip seal package is illustrated in figure 434, and the balance piston lip seal package is illustrated in figure 435. The lip seals are a five-ply laminate of TFE Teflon and Kapton. The translating shaft seal package can be shifted laterally 0.021 to 0.031 inch to accommodate overall misalignment between the sleeve and the main housing.

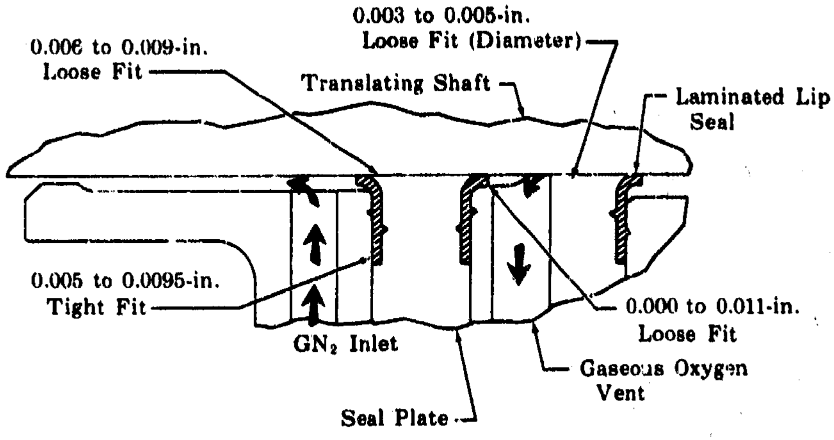

(U) Figure 434. Translating Shaft Lip Seal Package

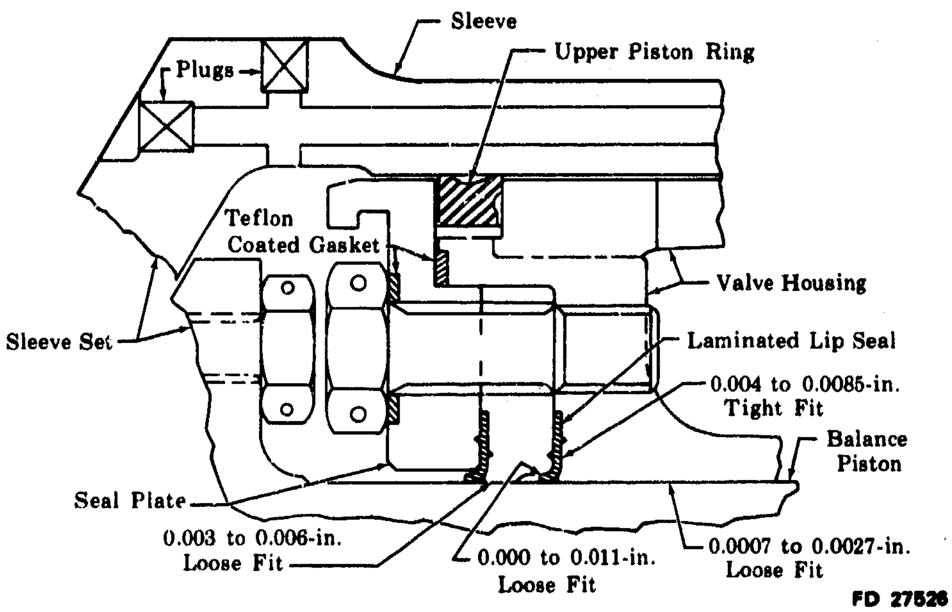

(U) Figure 435. Balance Piston Lip Seal Package and Upper Piston Ring

(C) The valve housing diameter was sized basically to minimize the pressure losses downstream of the secondary metering port to maximize the pressure drop available for thrust modulation. Stress analysis of the structure between ports shows a possible inward radial deflection of 0.005 inch under a pressure differential of 1750 psi, with the sleeve positioned 60% of full stroke from the shutoff position. The maximum combined stress is 70,000 psi, while the pressure differential limit for housing buckling is predicted at 3500 psi at operating temperature. The wall of the inner balance piston cylinder is stressed to only 30,000 psi under the maximum externally applied differential pressure of 5200 psi. Inward radial deflection of this wall is then 0.0003 inch, which is acceptable since the radial bearing clearances established for the balance piston on the inside of this cylinder are 0.0007 to 0.0027 inch loose.

(U) The outside diameter of the valve housing determines the diameters of the piston rings. The preburner oxidizer valve has two pressure-balanced piston rings, an upper ring attached to the valve housing as shown in figure 435 and a lower ring attached to the sleeve as shown in figure 436. Both rings are made of Berylco 25 (AMS 4650 or 4532).

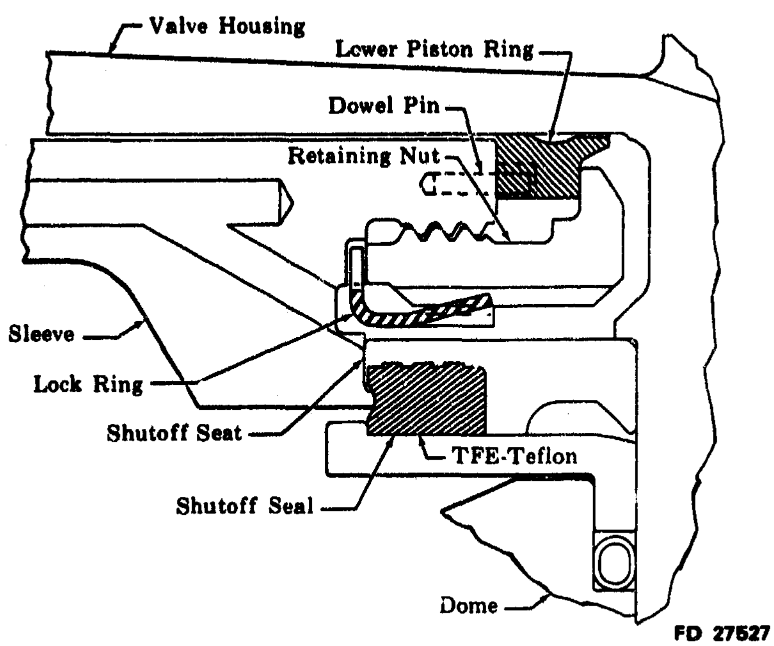

(U) Figure 436. Lower Piston Ring Installation

(C) The preburner oxidizer valve piston rings have a nominal sealing diameter of 2.50 inches. The pressure loading method used for design was that described in Koppers piston ring design handbook; however, the friction loads were also included in the axial and radial loads. The piston rings were designed so that the pressure moments are negligible. The piston ring drag is predicted to be less than 350 pounds in either direction at a differential pressure of 1750 psi. The unit pressure is 290 psi on the upper ring and 200 psi on the lower ring at a pressure differential of 1750 psi.

(U) The balancing grooves on the lower ring were designed so that a minimum amount of leakage would occur through the grooves and into the metering port of the valve. This leakage is kept below 5% of the total flow.

(U) The sleeve and balance piston were established as a matched set to achieve the necessary precision between the shaft sections that must be parallel to avoid adverse bearing conditions relative to the translation movement. The lower piston ring, retained at the end of this sleeve set, is maintained in a fixed angular relationship to the ports in the valve housing by dowel pin control as shown in figure 436. Study of the tolerances involved for the pins, holes, slots, and port location errors shows a possible misalignment, however, of plus or minus 0.033 inch between the balance groove cuts of the piston ring and their related ports.

(U) The sleeve incorporates eleven 0.110-inch diameter holes to vent the cavity between the sleeve and valve housing. During the maximum translation rate, the fluid velocity increases to 56 feet per second. This velocity is less than prior experience has shown, and no objectionable back pressure and associated drag force should be experienced. Calculations are based on 15 inches per second maximum sleeve velocity during actuation.

(C) A differential area exists on the secondary sleeve that tends to open the valve as a function of ΔP when the valve is off the shutoff seat. An opening force of 144 pounds is calculated at a ΔP of 1750 psi; however, there is a counteracting closing force on the base of the valve sleeve caused by high-velocity flow in the vicinity of the metering ports, which locally reduces the static pressure. This closing force can be adjusted by chamfering the piston ring retainer in the vicinity of the metering ports to reduce the local velocity. The closing force with no relief is estimated at 635 pounds and at 218 pounds with full relief. The unbalanced forces will be measured experimentally and the net unbalance minimized.

(U) Teflon-coated metallic O-rings are used for static seal, and Teflon-coated flat gaskets are used for external fitting seals. Both ID and OD vented rings are used, as required, where pressure difference is expected to exceed 100 psi. A Parker 8814 Series Inconel X750 Teflon-coated V-seal is used for the valve housing-to-injector overboard static seal.

C. PREBURNER FUEL VALVE

C. PREBURNER FUEL VALVE

1. Introduction

a. Function

(C) The preburner fuel valve shown in figure 437 operates in a liquid hydrogen environment with a maximum inlet pressure of approximately 5600 psig. The valve is driven by a rotary actuator bolted to the drive cover and coupled to the shaft of the valve assembly. The valve also acts as a modulating orifice upstream of the preburner heat exchanger as well as providing positive fuel shutoff. A secondary function is to provide a tapoff port, downstream of the shutoff seal, for main chamber transpiration cooling flow.

b. Location

(U) The preburner fuel valve is located in the main flowpath between the fuel turbopump and the preburner supply heat exchanger as shown in figure 417.

2. Design Requirements

(C) Design requirements for the preburner fuel valve are:

1. Preburner fuel valve operating requirements are as shown in figure 438. These requirements are generated by the engine cycle balance.
2. Shutoff Seal Leakage: Positive shutoff with leakage less than 10 sccs gaseous nitrogen at tank head pressure
3. External Valve Leakage: Less than 10 sccs of gaseous nitrogen at operating pressure.
4. Flange Static Seal Leakage (Per Inch): Less than 10^{-4} sccs of gaseous nitrogen at operating pressure
5. Durability: 10,000 valve cycles and 500 pressure cycles, (300 starts, 10 hours time between overhauls)
6. Supply transpiration chamber coolant flow with a low loss tapoff downstream of the shutoff seal.

3. Design Criteria

(U) Design criteria for the preburner fuel valve are:

1. Regulate preburner flow with a maximum effective area of 4.8 square inches (including margin) and a maximum turndown ratio of 14.8 to 1
2. Maintain an approximately "equal percentage" characteristic over the regulating range (The equal percentage characteristic is commonly used for control valve applications).

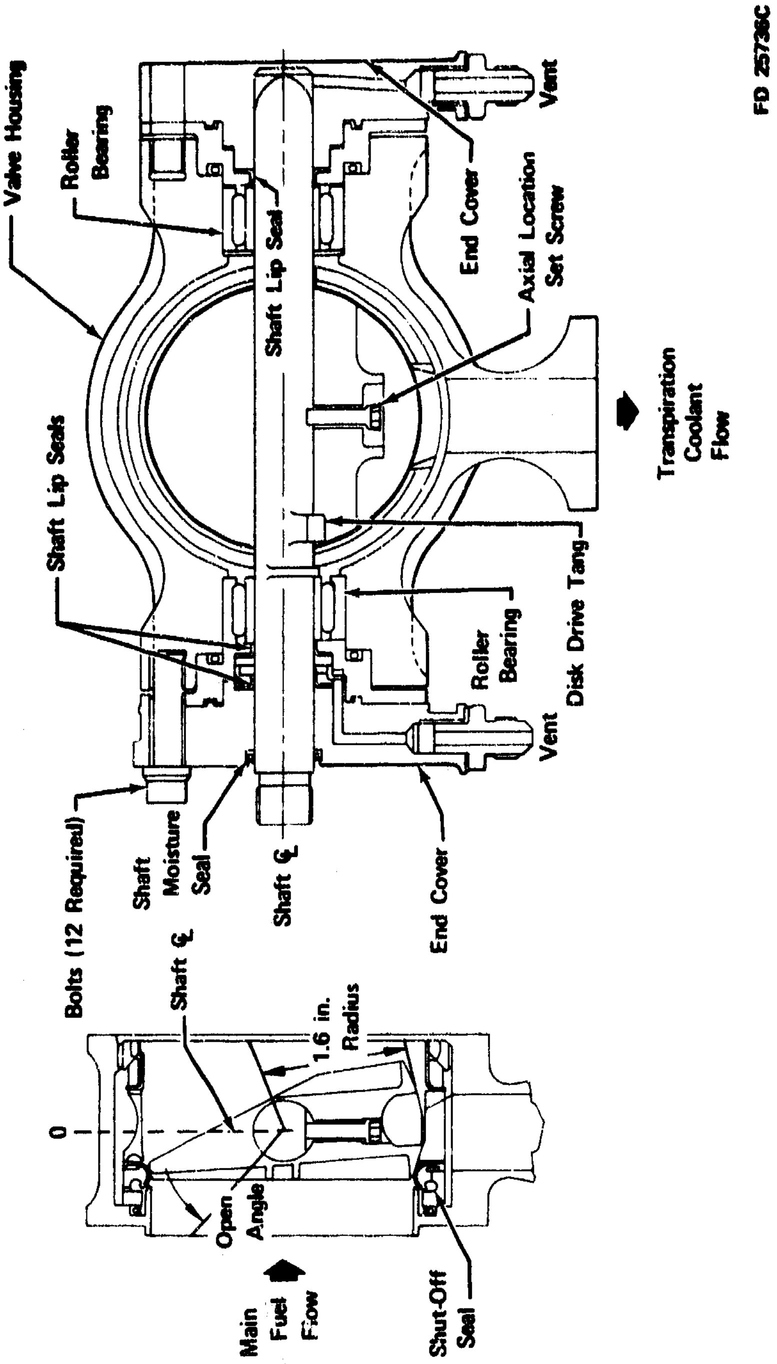

(U) Figure 437. Preburner Fuel Valve

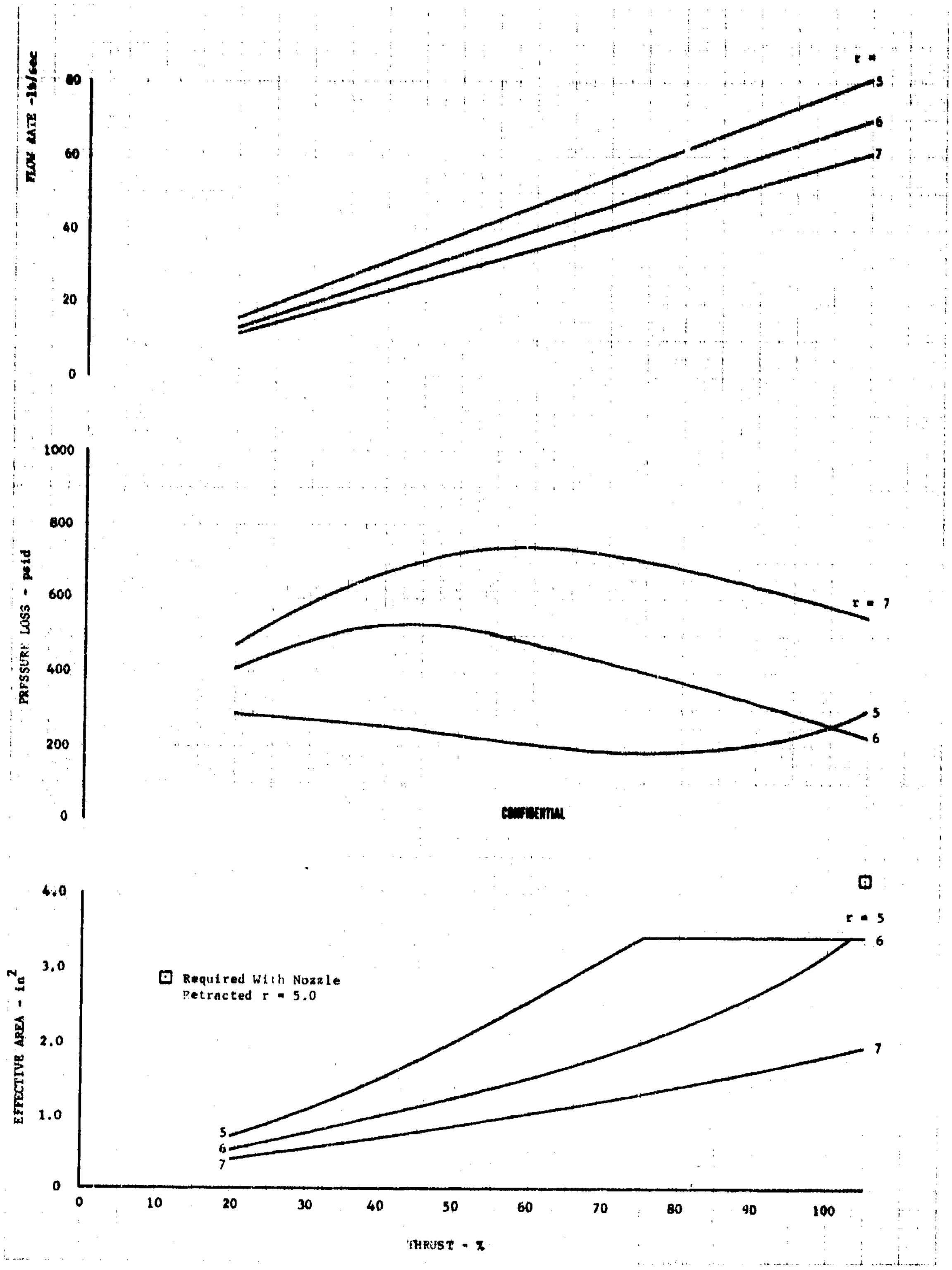

(U) Figure 438. Preburner Fuel Valve Operating Requirement

4. **Mechanical Description**

(C) The preburner fuel valve is a truncated ball type butterfly valve with a straight shaft. The valve has a regulating range of 0.42 to 3.42 square inches effective area with a maximum design effective area of 4.8 square inches and an approximately constant ratio of percentage of effective area to percentage of stroke (rotation) over the design range of preburner fuel flow shown in figure 464. The pressure drop across the valve at the maximum flow design point (100% thrust and r = 5) is 300 psid. A tapoff port for the main burner transpiration coolant flow is also provided to meet the design requirement.

(U) Positive fuel shutoff is provided when the spherical surface of the valve disk is seated against a pressure-energized, hoop-type shutoff seal. Figure 439 shows a cross section of the hoop seal. The valve disk and shaft are constructed of Inconel 718, and the seal element consists of a thin, silver-plated, hydroformed Inconel X-750 (AMS 5598) hoop. When viewed from the spline end of the valve shaft, the valve disk opens counterclockwise as shown in figure 437. As the valve is opened, the transpiration coolant port exposure starts at 3 degrees and is fully uncovered at 28 degrees. The design control range extends from 20 to 52 degrees.

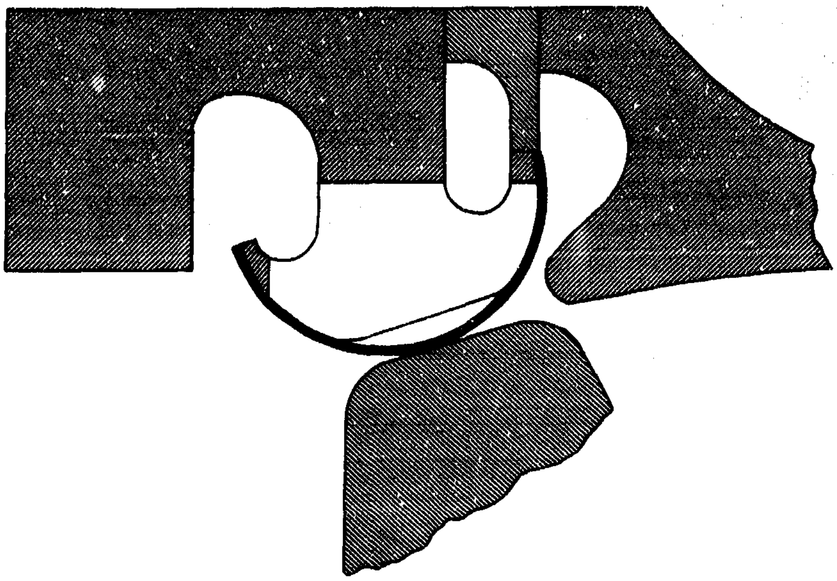

FD27537

(U) Figure 439. Hoop Seal Cross Section

(U) Approximately two-thirds of the valve shaft load is supported by the inner roller bearings close to the disk as shown in figure 437. The bearings are made of 440C stainless steel (AMS 5630) and their size permits the use of tie bolts through the housing without excessive gaps in the bolt pattern. The remainder of the valve shaft load is supported by silver-plated, load-bearing surfaces in the end covers.

(U) Shaft lip seals of Kapton/FEP Teflon laminate are located between the roller bearings and the outer load-bearing surfaces. As illustrated in figure 440, a double lip seal is used at the spline end of the shaft, and a single lip seal is used at the blind end of the shaft. At the spline end of the shaft, the double lip seals are separated by a seal plate that has drilled ports. High-pressure gas that leaks past the primary lip seal passes through the seal plate and is vented overboard. A double lip seal is not required at the blind end of the shaft because the cover collects all of the leakage and vents it overboard. The use of a vent at the blind end of the shaft prevents unbalanced shaft loads caused by internal pressure and eliminates the need for a thrust bearing.

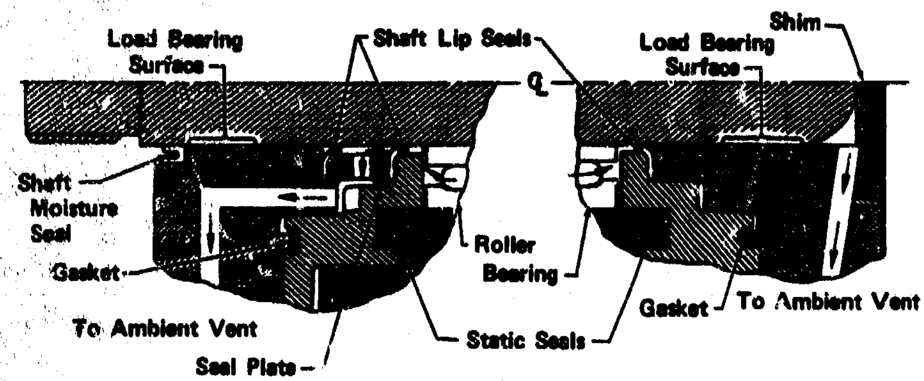

(U) Figure 440. Shaft Lip Seal

(U) The high-pressure static seals are formed and silver plated Inconel 718 (AMS 5598) metal rings, and the low-pressure static seals are fluorocarbon gaskets of TFE Teflon film. A reversed Bal-Seal is used at the drive end of the shaft to prevent external dirt or moisture from entering the valve.

(U) The preburner fuel valve housing, covers, and bolts are made of Inconel 718. Each end cover is bolted to the valve housing by six 0.375 inch x 24 bolts.

(U) The housing, valve disk, shaft, covers, and bolts are machined from Inconel 718 nickel alloy. This alloy was chosen for its high strength and good ductility at cryogenic temperatures. The bearings are fabricated from 440C corrosion resistant steel alloy (AMS 5630). Silver plating is used on rubbing surfaces (outer bushings, the shutoff seal, thrust faces, and bolts) to prevent galling. Devices that require material deformation for locking are constructed of soft stainless steel (300 series) because of its ductility.

5. Operating Characteristics

(U) The predicted preburner fuel valve operating characteristics are illustrated in figures 441 through 444. Figures 441 and 442 show the main flow effective area schedule and the coolant port area, respectively, as a function of disk angle.

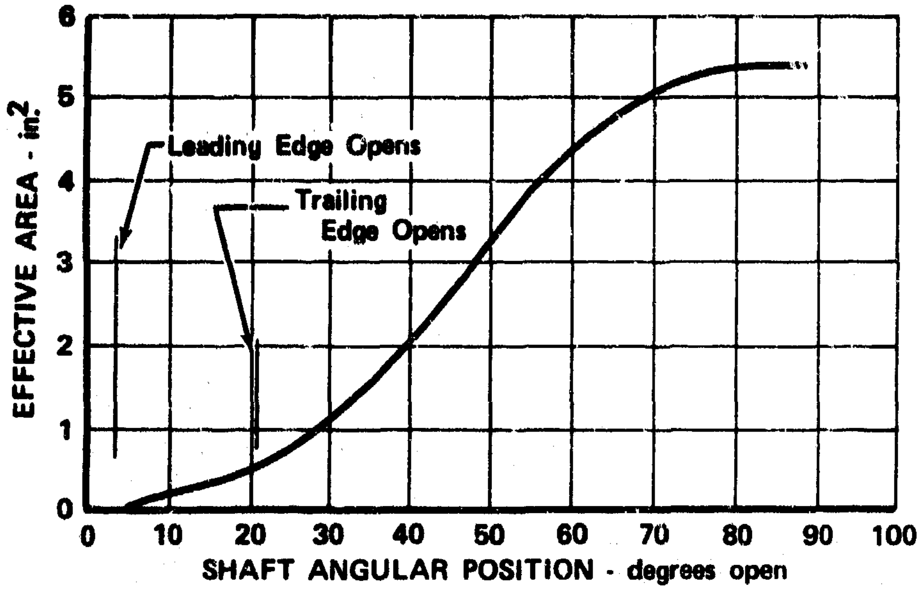

(U) Figure 441. Main Flow Effective Area
Schedule

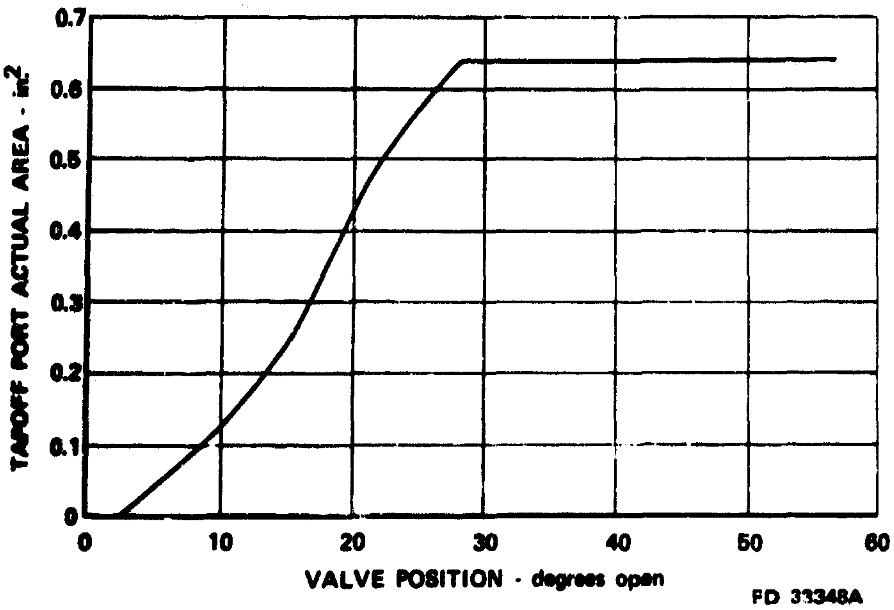

(U) Figure 442. Coolant Tapoff Area Schedule

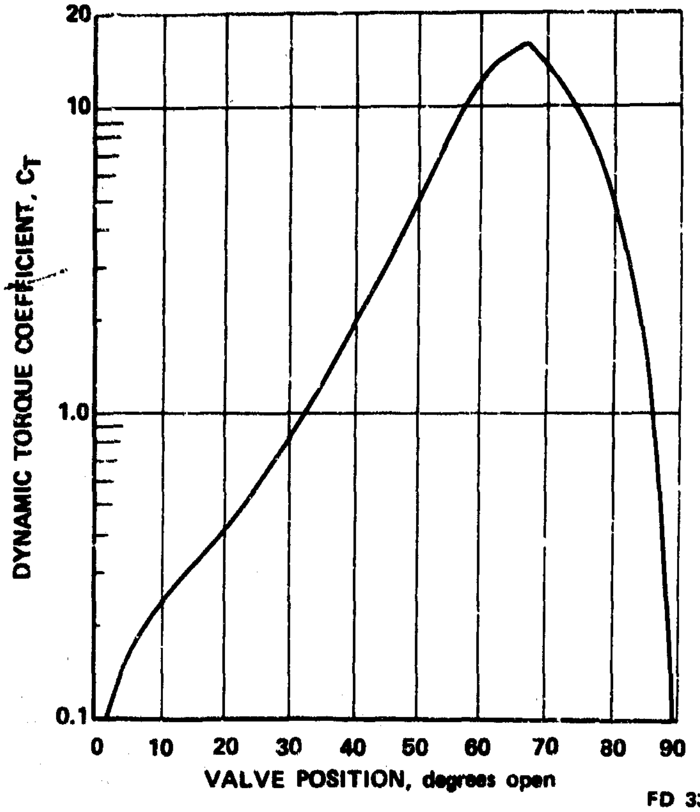

FD 33367A

(U) Figure 443. Dynamic Torque Coefficient vs Shaft Angular Position

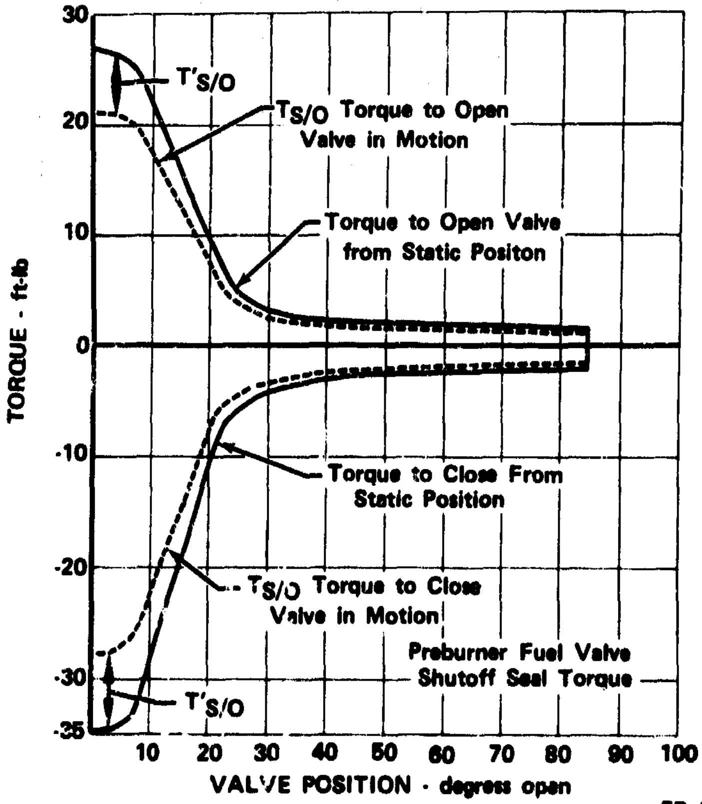

FD 33368

(U) Figure 444. Shutoff Seal Torque

(U) The total torque throughout the operating range may be calculated by adding dynamic torque, coulomb torque, stiction torque, and viscous torque. Shutoff seal torque in the operating range should not exceed the values shown in figure 444.

(U) The torque caused by flow forces on the valve disk tending to close the valve can be calculated from the formula:

$$T_{DYN} = C_T D^3 \Delta P$$

where $$\Delta P = \frac{2.238\ \dot{w}^2\ \text{psi}}{\rho A^2}$$

T_{DYN} = Dynamic torque in pound-feet
C_T = Torque coefficient
D = Disk diameter in feet
ΔP = Pressure drop across valve in psi
$\dot{w}$ = Flowrate in pounds per second
ρ = Density in pounds per cubic foot
A = Effective area in square inches

(U) Valve effective area, A, and torque coefficient, C_T, are plotted in figures 441 and 443, respectively. Flow and density variables can be obtained from the engine design cycle. D^3 is equal to 0.0189 ft^3. The constant 2.238 is used to obtain ΔP in psi.

(U) Torque caused by sliding dry friction can be calculated from the formula:

$$T_{COULOMB} = 0.0184\ \Delta P + 0.0025\ P + T_{s/o}$$

(U) The three terms of the equation represent shaft bearing torque, shaft seal torque, and disk shutoff seal torque, respectively. The ΔP may be obtained from the engine design cycle. P represents upstream pressure which may be obtained from the design cycle. P and ΔP are in psi. $T_{s/o}$ is plotted in figure 444 with a dashed line. $T_{COULOMB}$ is in pound-feet.

(U) Torque in excess of coulomb torque required to break away from a static valve position can be calculated from the equation:

$$T_{STICTION} = 0.0046\ \Delta P + T'_{s/o}$$

The two terms represent shaft bearing torque and disk shutoff seal torque, respectively. ΔP in psi is obtained from the design cycle. $T'_{s/o}$ is obtained from figure 444 as indicated. Torque is in pound-feet.

(U) Resisting fluid torque due to the opening or closing rate is small and can be neglected since valve rate is slow.

6. Design Approach

a. Background

(U) Predevelopment work was not conducted or investigations made in Phase I (Contract AF 04(611)-11401) for the preburner fuel valve.

b. Design Evolution

(1) Valve Type Selection

(U) A selection study was conducted to evaluate various valve types and to select one for use in this engine application. The evaluation included definition of the actuation power requirements, weight, and packaging studies and general performance characteristics. The various candidates are discussed in the following paragraphs. As a result of this selection study, the butterfly valve candidate was selected for the preburner fuel valve.

(2) Translating Sleeve Valve Candidates

(U) The four translating sleeve valve candidates are illustrated in figures 445 through 448. Parametric curves for sizing these valves are provided in figure 449 in which valve diameter is plotted as a function of stroke for various ratios of maximum port width to valve circumference. Experience and minimum envelope requirements dictated the point selection shown.

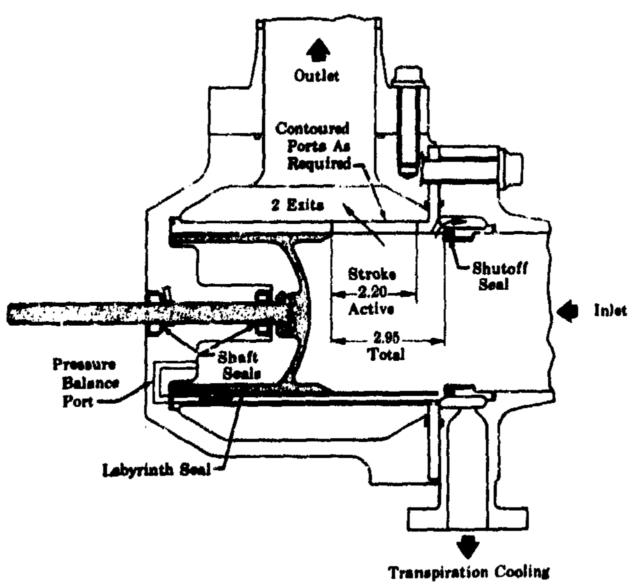

FD 25346

(U) Figure 445. Internal Sleeve Valve (Out Flow) Candidate

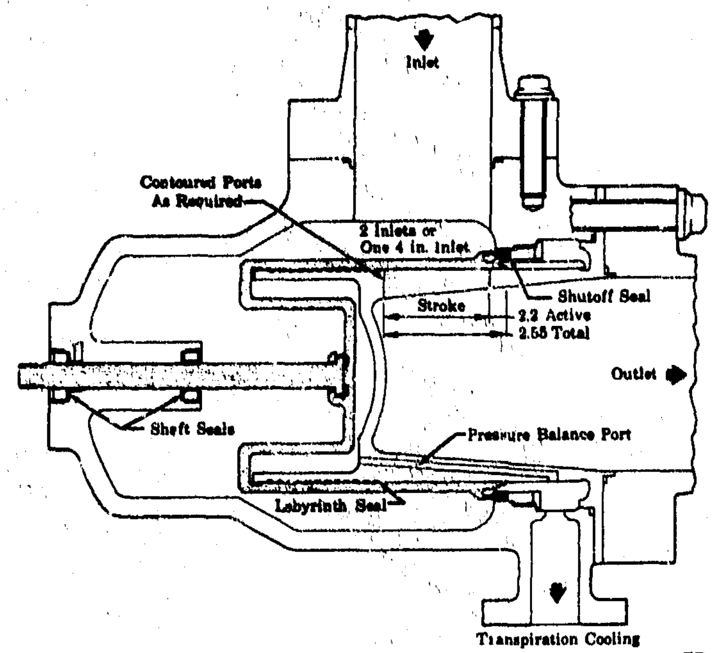

(U) Figure 446. External Sleeve Valve Candidate

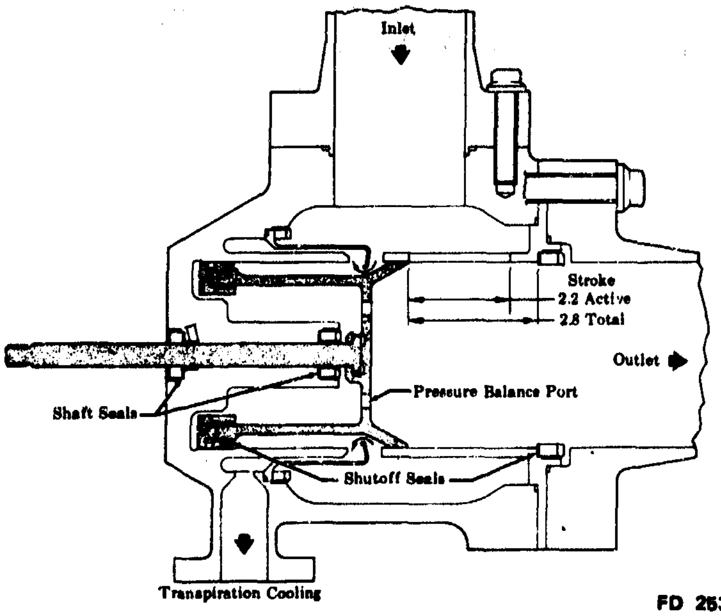

(U) Figure 447. Internal Sleeve Valve (Fixed Ports) Candidate

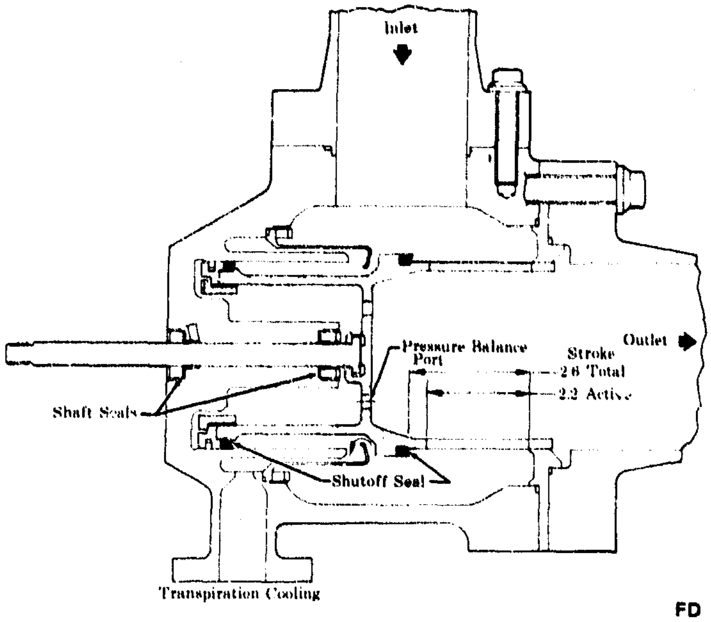

(U) Figure 448. Internal Sleeve Valve (Movable Ports) Candidate

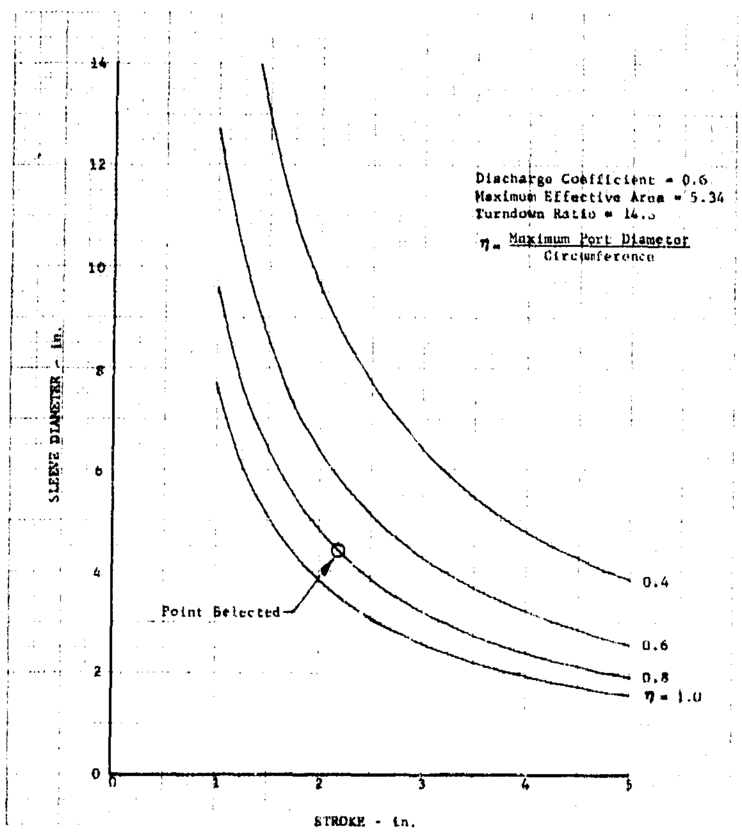

(U) Figure 449. Sleeve Valve Diameter vs Stroke

(U) The sleeve valve candidates illustrated in figures 444 and 445 only on shutoff seal. These candidates also have a relatively long clearance path with a labyrinth type of seal between the sleeve and the housing that is intended to eliminate the requirement for a piston ring secondary seal.

(U) The sleeve valve candidates illustrated in figures 447 and 448 have two shutoff seals. The second seal shuts off the transpiration chamber coolant flow as well as the secondary leak path around the sleeve. This configuration requires a flexible housing member that deflects and permits both seals to attain adequate sealing pressure. The preburner oxidizer valve program has shown that the face type of seal is durable and has low leakage.

(U) The axial flow forces acting on the sleeve valve candidates are shown in figures 450 through 453. A comparison plot of the maximum force curves for these valves is shown in figure 454.

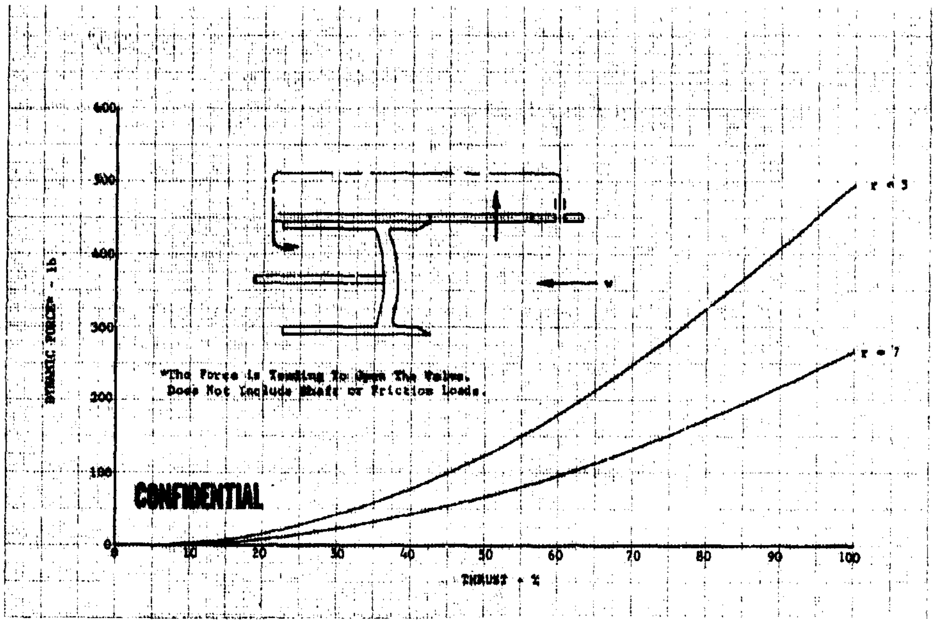

DF 68373

(U) Figure 450. Dynamic Force vs Thrust (Internal Sleeve Valve - Reverse Flow)

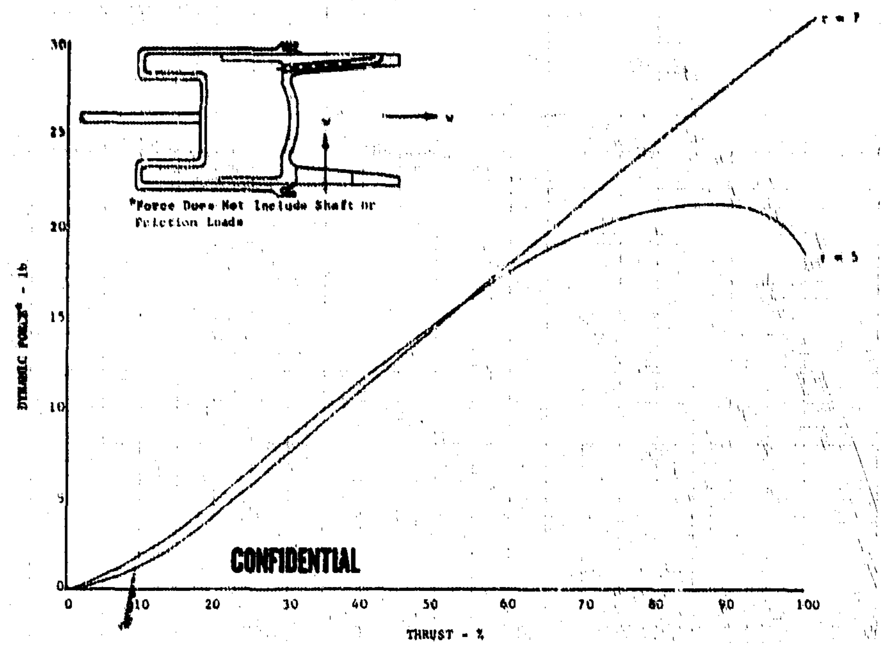

DF 68374

(U) Figure 451. Dynamic Force vs Thrust (External Sleeve Valve)

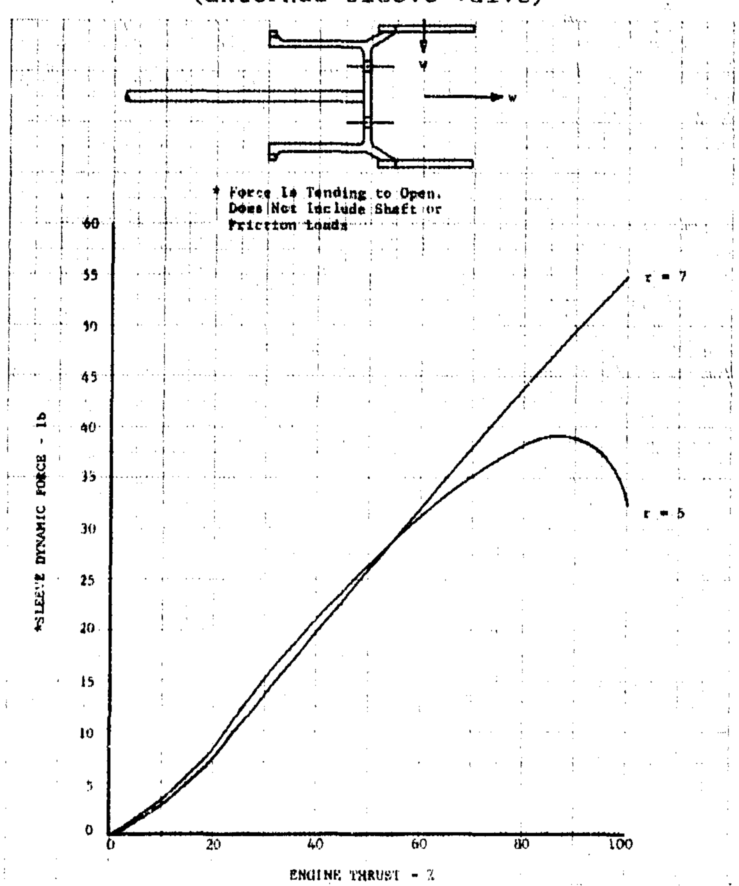

DF 68375

(U) Figure 452. Dynamic Force vs Thrust (Internal Sleeve Valve - Fixed Ports)

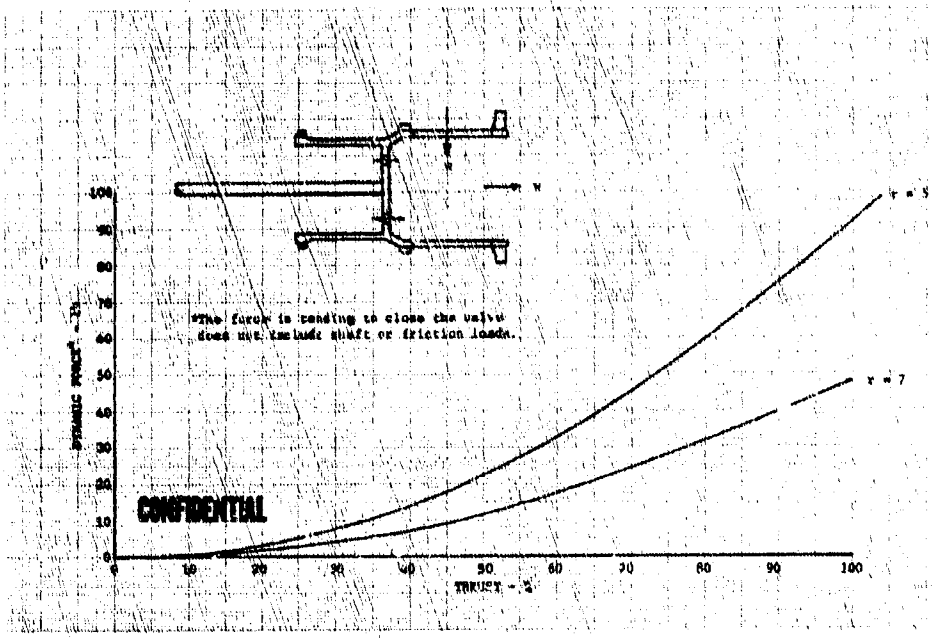

DFC 68376

(U) Figure 453. Dynamic Force vs Thrust (Internal Sleeve Valve - Movable Ports)

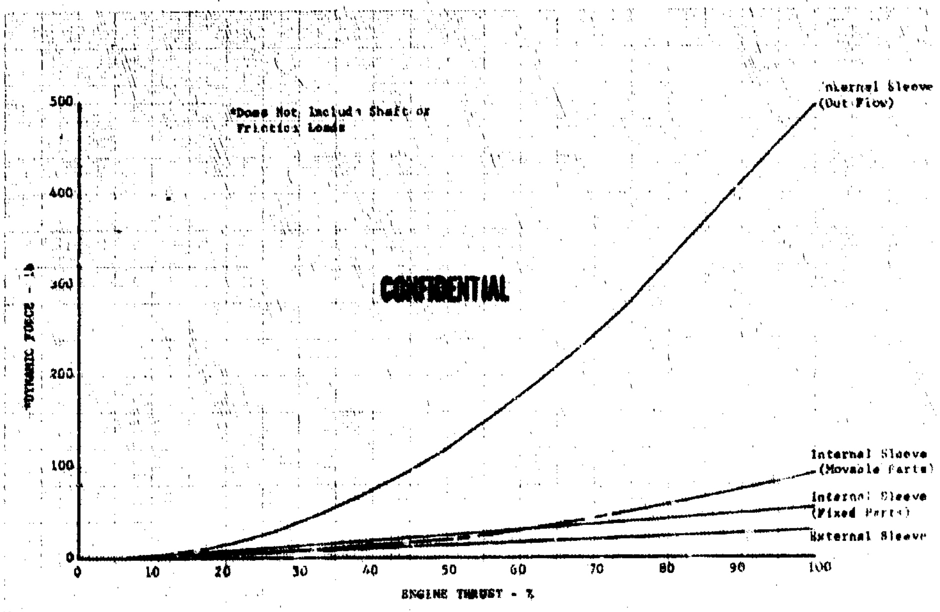

DFC 68637

(U) Figure 454. Dynamic Force Comparison of Sleeve Valve Candidates

(3) Pintle Valve Candidate

(U) The pintle valve candidate is illustrated in figure 455. The valve is similar in construction to the sleeve type valve candidate except that a contoured pintle is utilized for flow control instead of a sleeve and contoured ports. The inlet port is 90 degress from the axis of the valve. The pintle valve candidate also has two shutoff seals; one for primary fuel flow and one for transpiration coolant flow. The pintle valve candidate parametric sizing is shown in figure 456. The point selected provides the shortest stroke compatible with a reasonable orifice diameter and pintle contour angle. The axial dynamic force acting on the pintle as a function of engine thrust is shown in figure 457.

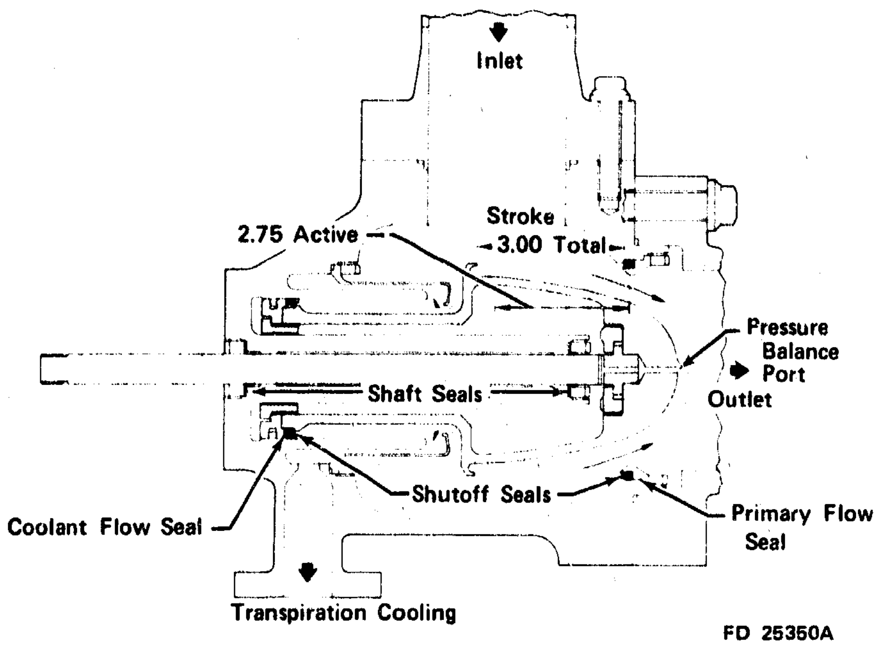

(U) Figure 455. Pintle Valve Candidate

(U) Operational and mechanical problems previously experienced with respect to force reversals, parts concentricities, and contamination sensitivity also apply to this application.

(4) Inverted Pintle Valve Candidate

(U) The inverted pintle valve candidate is illustrated in figure 458. The inverted pintle is similar to the pintle valve candidate except that the housing is contoured to produce the effective area versus stroke relationship. This causes the area with a variable pressure profile to be on the housing instead of being on the moving part. Two shutoff seals are also required for this candidate.

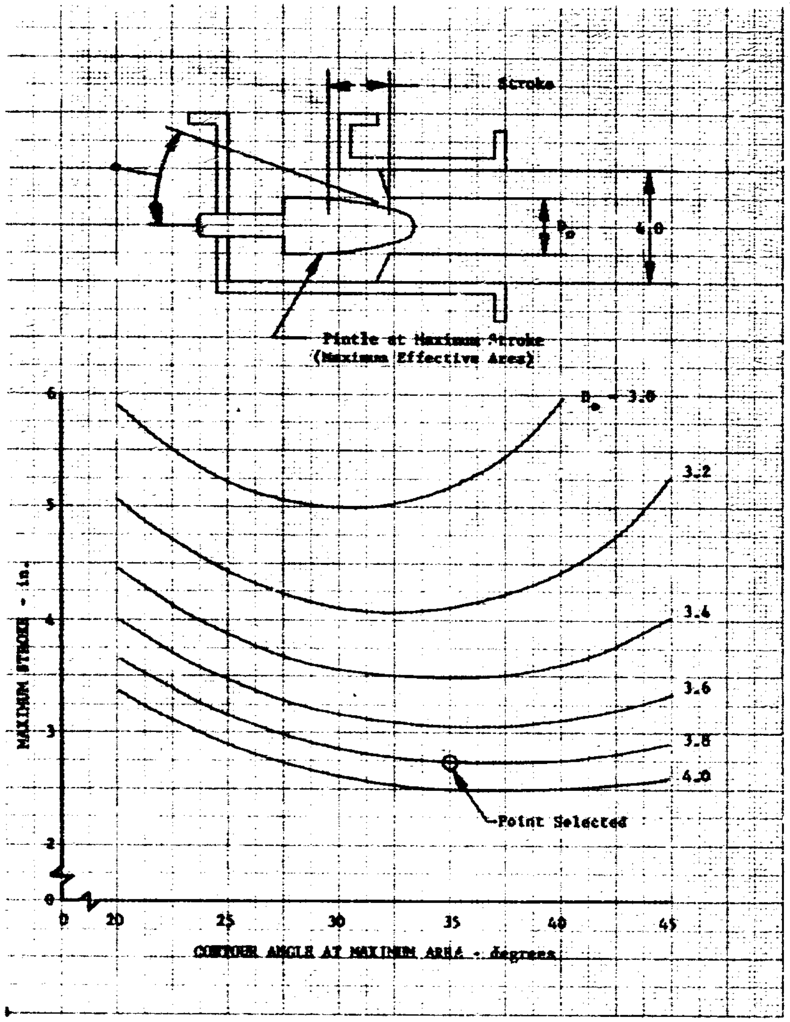

DF 68377

(U) Figure 456. Maximum Stroke vs Contour Angle (Pintle Valve)

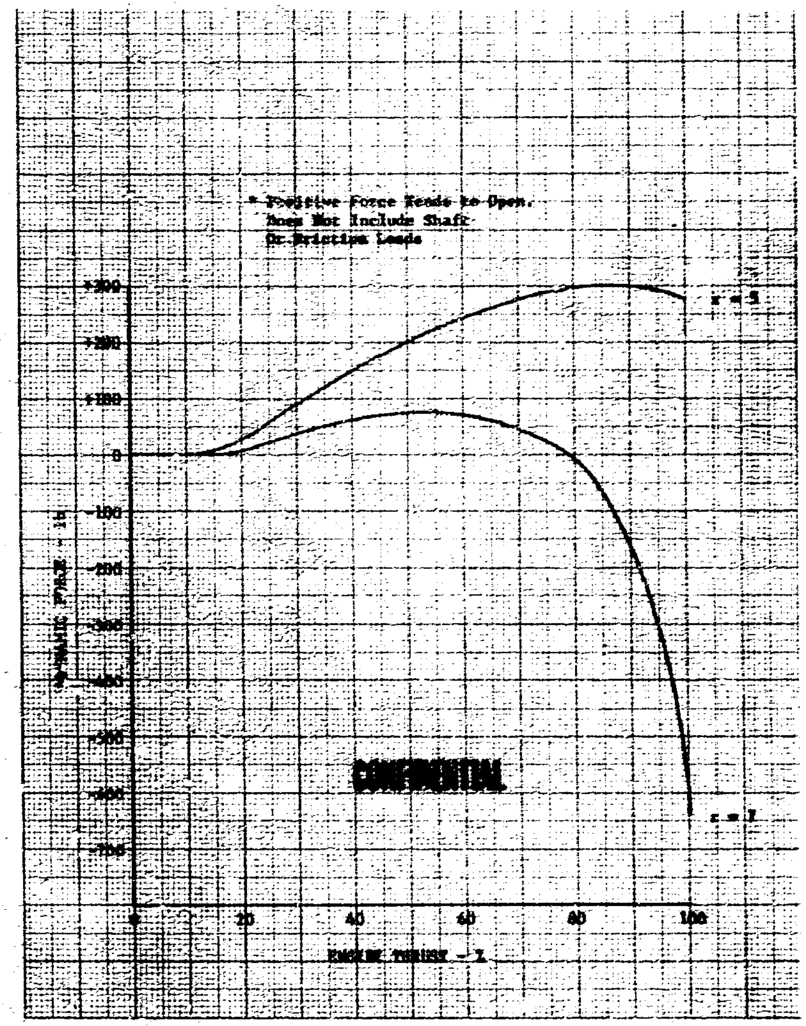

DF 68378

(U) Figure 457. Dynamic Force vs Thrust (Pintle Valve)

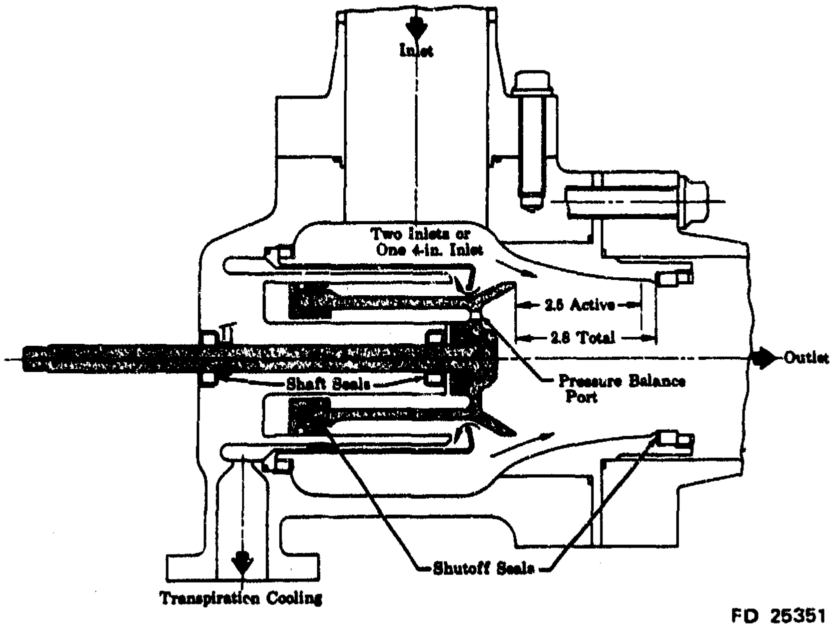

FD 25351

(U) Figure 458. Inverted Pintle Valve Candidate

(U) The throat sizing is illustrated in figure 459 and the parametric valve sizing curves are illustrated in figure 460. The points selected allow reasonable package size and low parasitic losses.

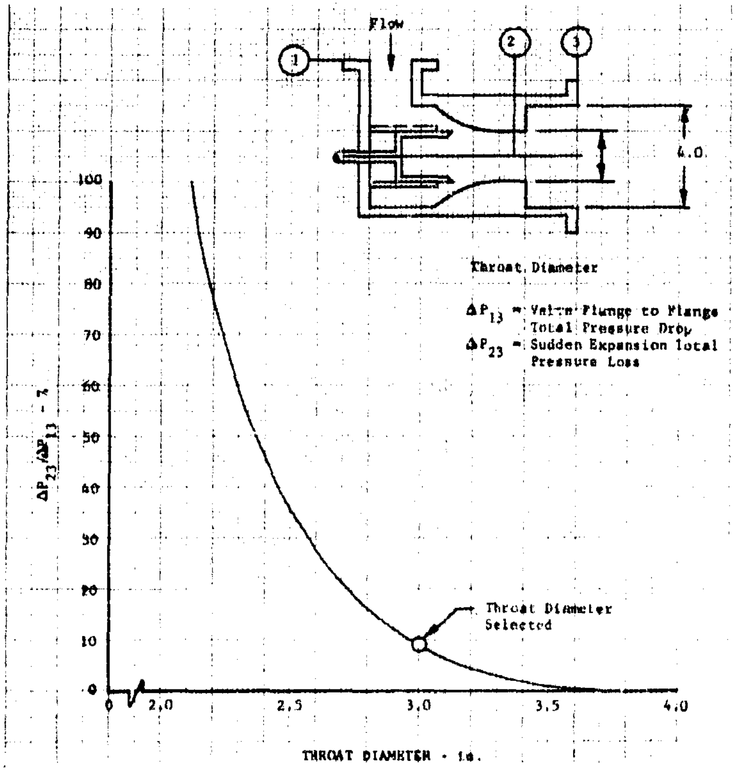

DF 68379

(U) Figure 459. Throat Size Selection (Inverted Pintle)

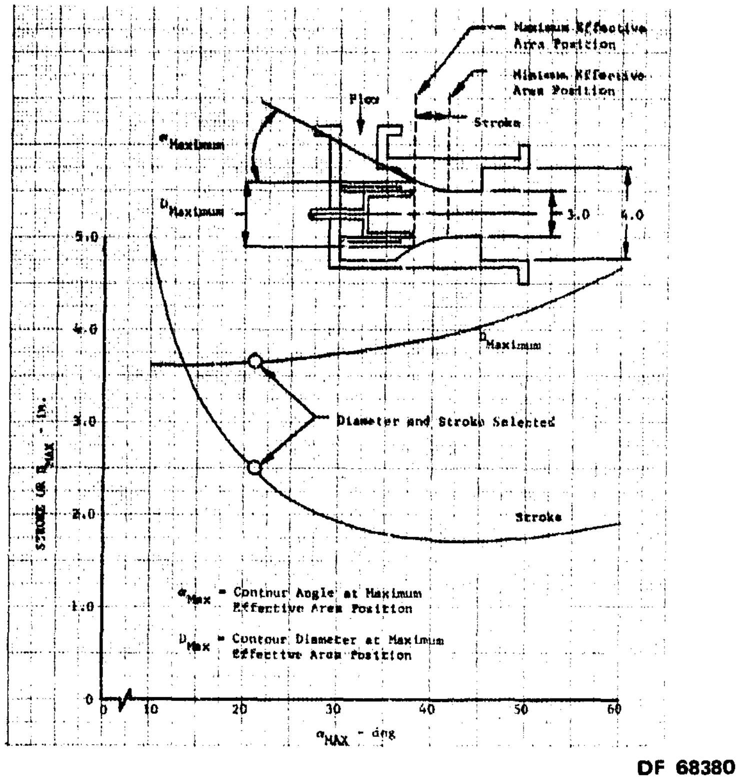

(U) Figure 460. Parametric Sizing for Inverted Pintle

(5) Butterfly Valve Candidate

(U) The butterfly valve candidate is illustrated in figure 461. The trailing edge of this butterfly valve, instead of being streamlined, is rather broad and shaped to cause the flow coefficient to remain low on the trailing edge, as it normally does for the leading edge, over the entire stroke. The throat sizing point illustrated in figure 462 was selected to provide optimum percentage area characteristics with reasonable area margin.

(U) The flow velocity across the face of the disk is lower than for a standard disk shape, resulting in low dynamic torque as shown in figure 463. The design also allows a spherical zone on the disk, offset from the shaft centerline, that may be used as the sealing surface. This eliminates the necessity for an inclined shaft and the resulting unbalanced thrust load.

(U) The configuration shown allows an angular travel of 18 degrees from the shutoff position to the position where the trailing edge starts regulating. This travel deadband provides a convenient location to tap off transpiration chamber coolant flow upstream of the regulated area. Figures 464 and 465 show effective area versus stroke and percent error characteristics for this valve with a cylindrical flowpath. The housing contour may be modified as shown in figure 461 to optimize the percentage error characteristics.

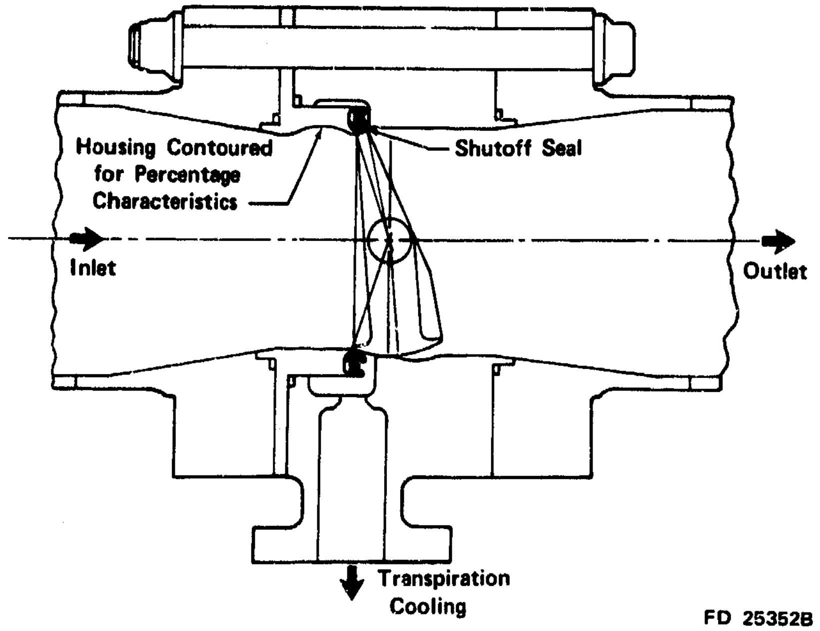

(U) Figure 461. Butterfly Valve Candidate

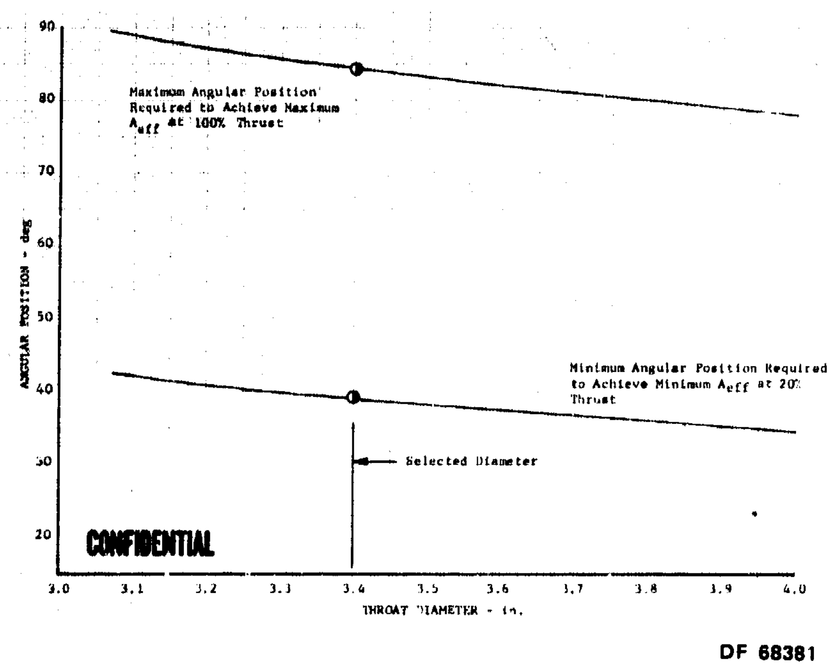

(U) Figure 462. Angular Position vs Throat Diameter (Butterfly Valve)

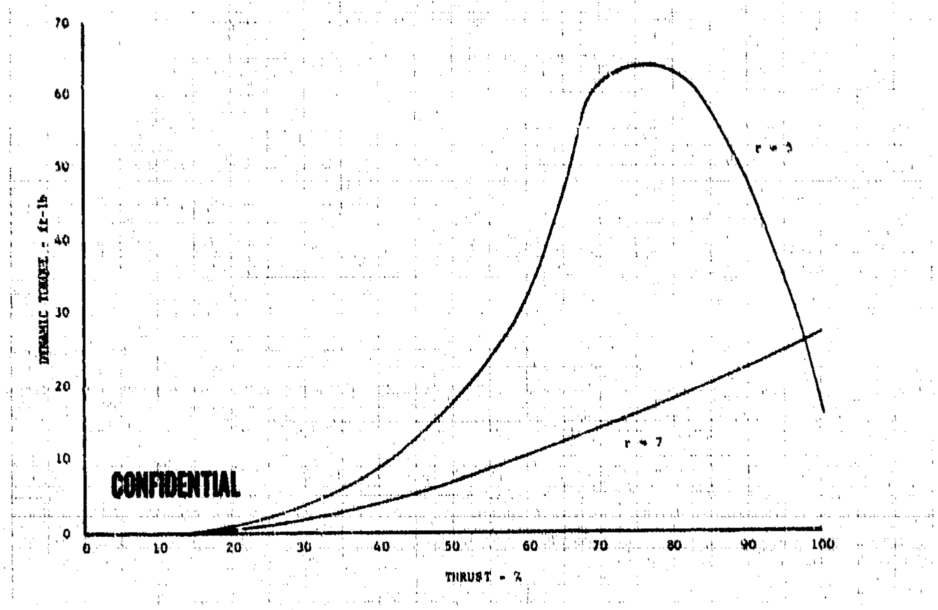

DF 68382

(U) Figure 463. Dynamic Torque vs Thrust (Butterfly Valve)

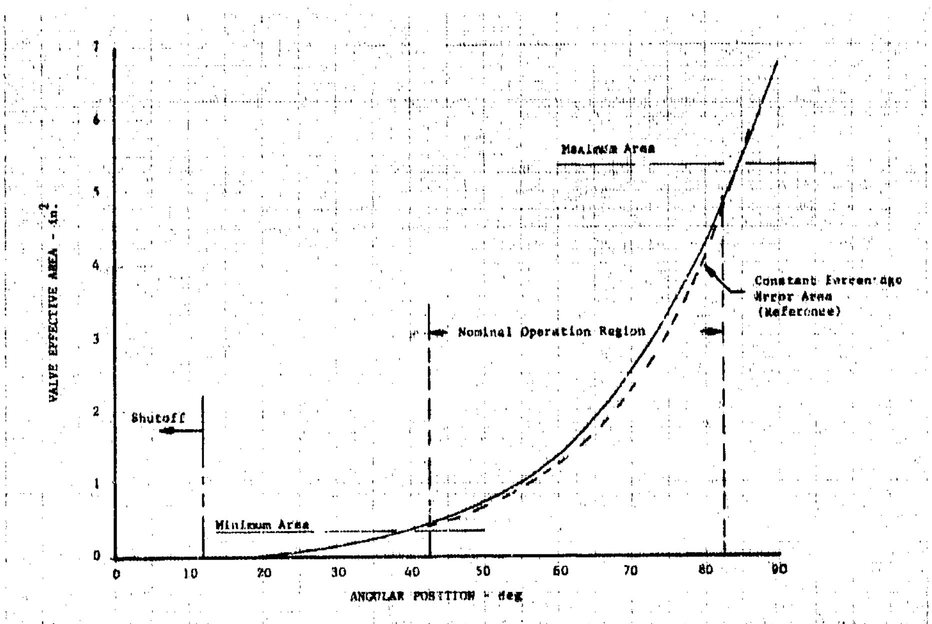

DF 68383

(U) Figure 464. Effective Area vs Angular Position (Butterfly Valve)

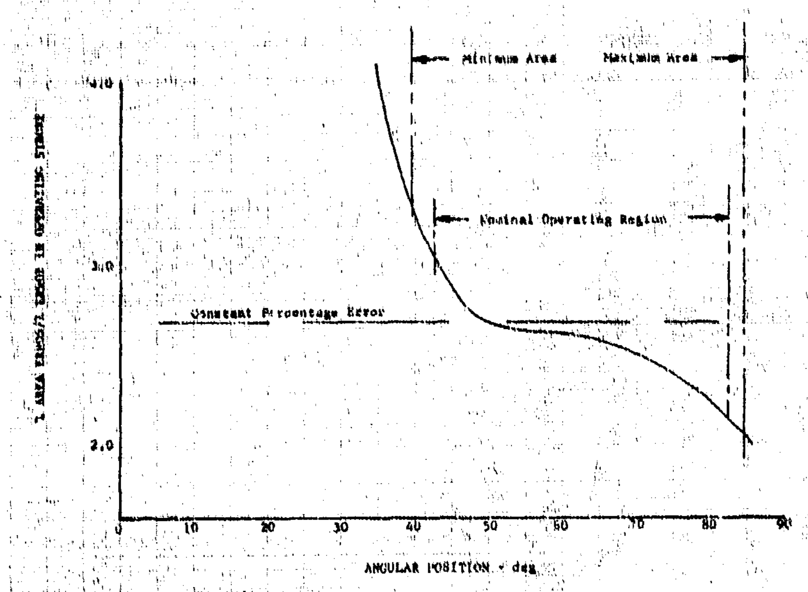

DF 68384

(U) Figure 465. Area Error vs Angular Position (Butterfly Valve)

(6) Comparison Summary

(U) Valve and associated system weight for each of the candidates is provided in table LXV, which also includes the power required for each candidate. The ratings for all were made in the same manner. The dynamic power value is based on a 10 cps frequency at the maximum force required for each candidate. The total power includes that required for shaft lip seals and piston ringe secondary seals if applicable. The ratings for valve weight are based on the total installation requirements and include the attaching flanges shown shaded in figure 466.

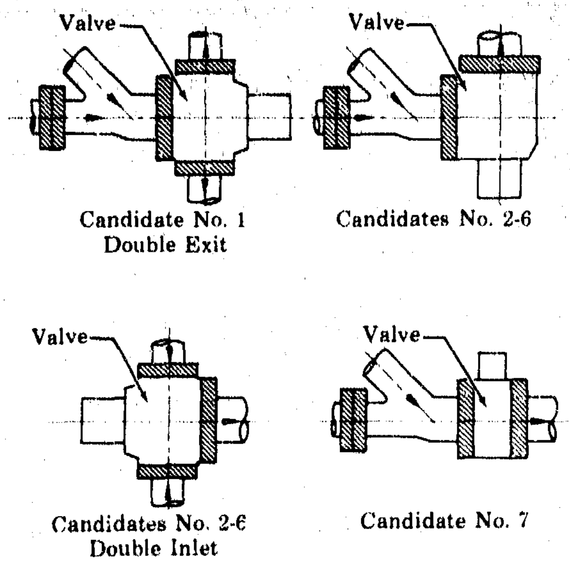

Candidate No.

1. Internal Sleeve Valve (Out Flow)
2. External Sleeve Valve
3. Internal Sleeve Valve (Fixed Ports)
4. Internal Sleeve Valve (Movable Ports)
5. Pintle Valve
6. Inverted Pintle Valve
7. Butterfly Valve

FD 25359

(U) Figure 466. Preburner Fuel Valve Installation Schematic

(U) The relative values of the selection criteria are shown in the first column of tables LXVI, LXVII, and LXVIII. The highest rated candidate received the greatest number of points. The ratings in table LXVI consider single pipe inlets and unbalanced actuation shafts as shown in the valve configuration sketches. Those in table LXVII assume that the actuator shaft has been fully balanced by the addition of opposing pressure areas. Table LXVIII shows the added advantage gained through the use of two inlet lines for those valve types that would benefit from such an arrangement. The butterfly valve received the highest number of points in each rating. The external sleeve valve received the next highest number of points for two of the three ratings.

(U) Table LXV. Weight and Power

		Internal Sleeve Valve (Out Flow)	External Sleeve Valve	Internal Sleeve Valve (Fixed Ports)	Internal Sleeve Valve (Movable Ports)	Pintle Valve	Inverted Pintle Valve	Butterfly Valve
Valve Weight (lb)		52.9	54.7	52.9	52.9	47.0	51.2	33.3
Valve and Associated Flange Weight (lb)* Single Inlet		92.5	100.9	99.1	99.1	93.2	97.4	69.5
Valve and Associated Flange Weight (lb)* Double Inlet		92.5	81.1	79.3	79.3	73.4	77.6	69.5
Horsepower ** Unbalanced Actuator Rod	Dynamic	43.0	22.4	23.1	17.9	16.6	27.4	5.6
	Shaft Seal	2.2	2.2	2.2	2.2	2.2	2.2	5.9
	Piston Ring			3.2	3.2	3.6	0.4	
Dynamic Includes Pressure on Rod	Total	45.2	24.6	28.5	23.3	22.4	30.0	6.5
Horsepower ** Pressure Balanced Actuator Rod	Dynamic	10.0	0.6	1.1	1.1	17.0	0.0	5.6
	Shaft Seal	4.0	4.0	4.0	4.0	4.0	4.0	0.9
	Piston Ring			3.2	3.2	3.6	2.6	
	Total	14.0	4.6	8.3	8.3	24.6	6.6	6.5

*This weight includes flanges shown shaded in figure 465.
**Horsepower is based on an arbitrarily selected frequency of 10 cycles per second because the actual required frequency has not been determined.

(U) Table LXVI. Valve Rating Based on Single Inlets
Unbalanced Actuation Shafts

Selection Criteria	Maximum No. of Points For Each Category	Internal Sleeve Valve (Out Flow)	External Sleeve Valve	Internal Sleeve Valve (Fixed Ports)	Internal Sleeve Valve (Movable Ports)	Pintle Valve	Inverted Pintle Valve	Butterfly Valve
Weight (Valve and Flanges)	100	75	69	70	70	70	71	100
Shutoff Seal Development Req'd	100	100	100	80	80	80	80	50
Actuator Power	95	14	25	22	28	28	20	95
Reliability	90	70	70	50	50	50	50	70
Low Parasite Pressure Loss	70	50	35	35	35	40	40	70
No. of Dynamic Seals Req'd.	65	65	65	65	65	65	65	65
Packaging	60	60	45	45	45	45	45	55
Percent Error Characteristics	60	60	60	60	60	55	55	60
Manufacturing Ease	55	45	40	35	35	30	30	55
Flexibility	50	40	40	40	40	50	50	35
Complexity	45	40	40	35	35	30	35	45
Total Points	790	619	589	537	543	548	541	700

(U) Table LXVII. Valve Rating Based on Single Inlets and Balanced Actuation Shafts

Selection Criteria	Maximum No. of Points For Each Criteria	Internal Sleeve Valve (Out Flow)	External Sleeve Valve	Internal Sleeve Valve (Fixed Ports)	Internal Sleeve Valve (Movable Ports)	Pintle Valve	Inverted Pintle Valve	Butterfly Valve
Weight (Valve and Flanges)	100	75	86	88	88	95	90	100
Shutoff Seal Development Req'd.	100	100	100	80	80	80	80	50
Actuator Power	95	31	95	53	53	18	66	67
Reliability	90	65	65	45	45	45	55	70
Low Parasite Pressure Loss	70	50	35	35	35	40	40	70
No. of Dynamic Seals Req'd.	65	50	50	50	50	50	50	65
Packaging	60	60	45	45	45	45	45	55
Percent Error Characteristics	60	60	60	60	60	55	55	60
Manufacturing Ease	55	40	35	30	30	25	25	55
Flexibility	50	40	40	40	40	50	50	35
Complexity	45	35	35	30	30	25	30	45
Total Points	790	606	646	556	556	528	586	672

(U) Table LXVIII. Valve Rating on Double Inlets (Where Applicable) and Balanced Actuation Shafts

Selection Criteria	Maximum No. of Points For Each Category	Internal Sleeve Valve (Out Flow)	External Sleeve Valve	Internal Sleeve Valve (Fixed Ports)	Internal Sleeve Valve (Movable Ports)	Pintle Valve	Inverted Pintle Valve	Butterfly Valve
Weight (Valve and Flanges)	100	75	69	70	70	75	71	100
Shutoff Seal Development Req'd.	100	100	100	80	80	80	80	50
Actuator Power	95	31	95	53	53	18	66	67
Reliability	90	65	65	45	45	45	55	70
Low Parasite Pressure Loss	70	50	35	35	35	40	40	70
No. of Dynamic Seals Req'd.	65	50	50	50	50	50	50	65
Packaging	60	60	45	45	45	45	45	55
Percent Error Characteristics	60	60	60	60	60	55	55	60
Manufacturing Ease	55	40	35	30	30	25	25	55
Flexibility	50	40	40	40	40	50	50	35
Complexity	45	35	35	30	30	25	30	45
Total Points	790	606	629	538	538	508	567	672

D. MAIN CHAMBER OXIDIZER VALVE

D. MAIN CHAMBER OXIDIZER VALVE

1. Introduction

a. Function

(U) The functions of the main chamber oxidizer valve (figure 467) are to control the overall engine oxidizer-to-fuel weight ratio by regulating the flow of oxidizer to the main burner injector, and to provide positive oxidizer shutoff to the main burner injector. The valve area is modulated as a function of the engine thrust level and the scheduled mixture ratio. The position is controlled by an error signal from the control system, which compares the actual engine mixture ratio as a function of oxidizer flow with the desired mixture ratio.

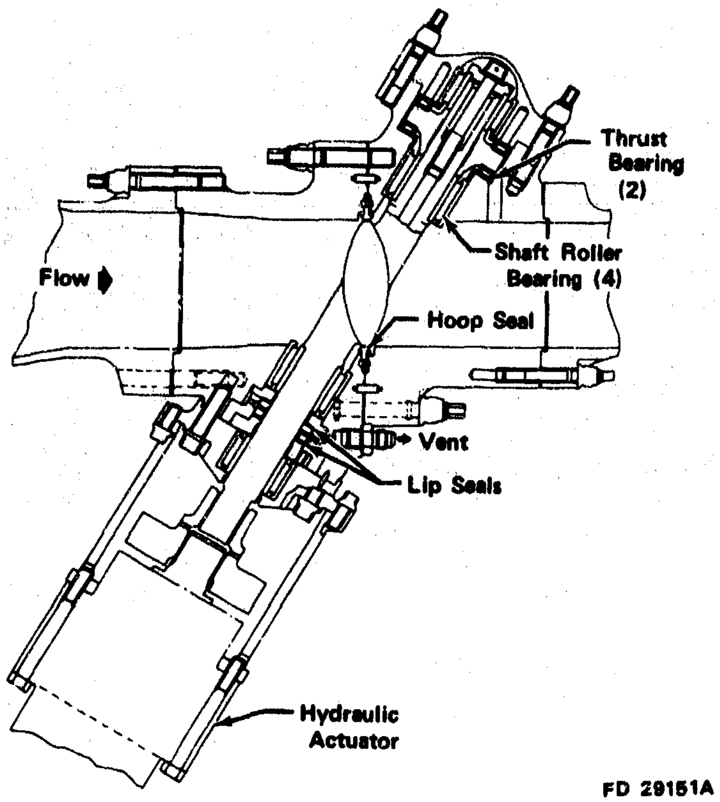

(U) Figure 467. Main Chamber Oxidizer Valve

b. Location

(U) The main chamber oxidizer valve is located in the main oxidizer line upstream of the main burner injector as shown in figure 417.

2. Design Requirements

(C) Design requirements for the main chamber oxidizer valve are:

1. Control Accuracy: ±3% in thrust and mixture ratio at nominal thrust
2. Control Dynamics: Excursion from extreme to extreme in thrust and mixture ratio within 5 seconds
3. Shutoff Seal: Positive shutoff with leakage less than 10 sccs of gaseous nitrogen at tank head pressure
4. External Valve Leakage: Less than 10 sccs of gaseous nitrogen at operating pressure
5. Flange Leakage: Less than 10^{-4} sccs per inch of gaseous nitrogen at operating pressure
6. Durability: 10,000 valve cycles and 500 pressure cycles, (300 starts, 10 hours time between overhauls)
7. Pressure drop, flow, and area requirements as a function of engine thrust are shown in figure 468. These requirements are generated by the engine cycle balance.

3. Design Criteria

(U) Design criteria for the main chamber oxidizer valve are:

1. Retain the Phase I, Contract AF04(611)-11401, angle shaft design concept
2. Incorporate the flexible hoop shutoff seal and laminated FEP Teflon shaft seal designs
3. Design for minimum weight consistent with design requirements
4. Employ the cantilever, bolted-flange design concept
5. Valve pressure and flow requirements based on oxidizer pump "recirculation"
6. Support the servo-actuator assembly
7. Provide sufficient space for alternative static seals at each overboard leakage interface
8. Maintain a disk diameter of 3.00 inches, but decrease the outlet diameter from 4.210 to 3.000 inches to match the main injector oxidizer inlet design

9. Eliminate the double static seal scheme used in Phase I, Contract AF04(611)-11401

10. Eliminate the Phase I, Contract AF04(611)-11401, valve shaft gaseous nitrogen purge fitting because moisture problems were not encountered

11. Provide a main injector helium purge boss just downstream of valve disk

12. Provide an actuator coupling that is tight on the actuator spline with a sliding fit on the valve spline.

(C) Shutoff seal requirements are:

1. Maximum leakage: 10 sccs at 50 psid nitrogen
2. Maximum static differential pressure: 1500 psi
3. Maximum flowing differential pressure: 1580 psid.

4. Mechanical Description

(C) The main chamber oxidizer valve is a canted-shaft butterfly valve as shown in figure 467. The maximum effective area of 4.65 square inches is approximately 38% greater than required. The maximum pressure drop across the valve is 1580 psid. The canted-shaft, integral disk arrangement allows an unbroken shutoff sealing surface, but results in a higher ratio of shaft diameter to throat diameter than would occur in a 90-degree design and requires a two-piece main housing so that the valve can be assembled. The shaft angle also results in axial (shaft) thrust that varies in direction and magnitude with engine operating conditions. The shaft is supported by four roller bearings and is positioned by two thrust roller bearings that ensure low operating friction and minimum wear. Oxidizer leakage at the actuator end of the shaft is held to the minimum by laminated lip seals. Leakage at the blind end of the shaft is prevented by the thrust cover and a static seal.

(U) Positive oxidizer shutoff is provided by the pressure-assisted, hoop-type shutoff seal. The valve disk and shaft material is Inconel 718 (AMS 5663), and the seal element is a hydroformed, silver-plated, Inconel X-750 (AMS 5598) hoop. Figure 469 shows a cross section of the seal.

(C) The shaft size was established by the minimum acceptable size of radial roller bearings required to withstand the maximum pressure loading on the butterfly disk. This condition occurs at 100% thrust and a mixture ratio of 5. The resulting disk force and bearing reaction loads as well as a stress analysis summary are presented in figure 470.

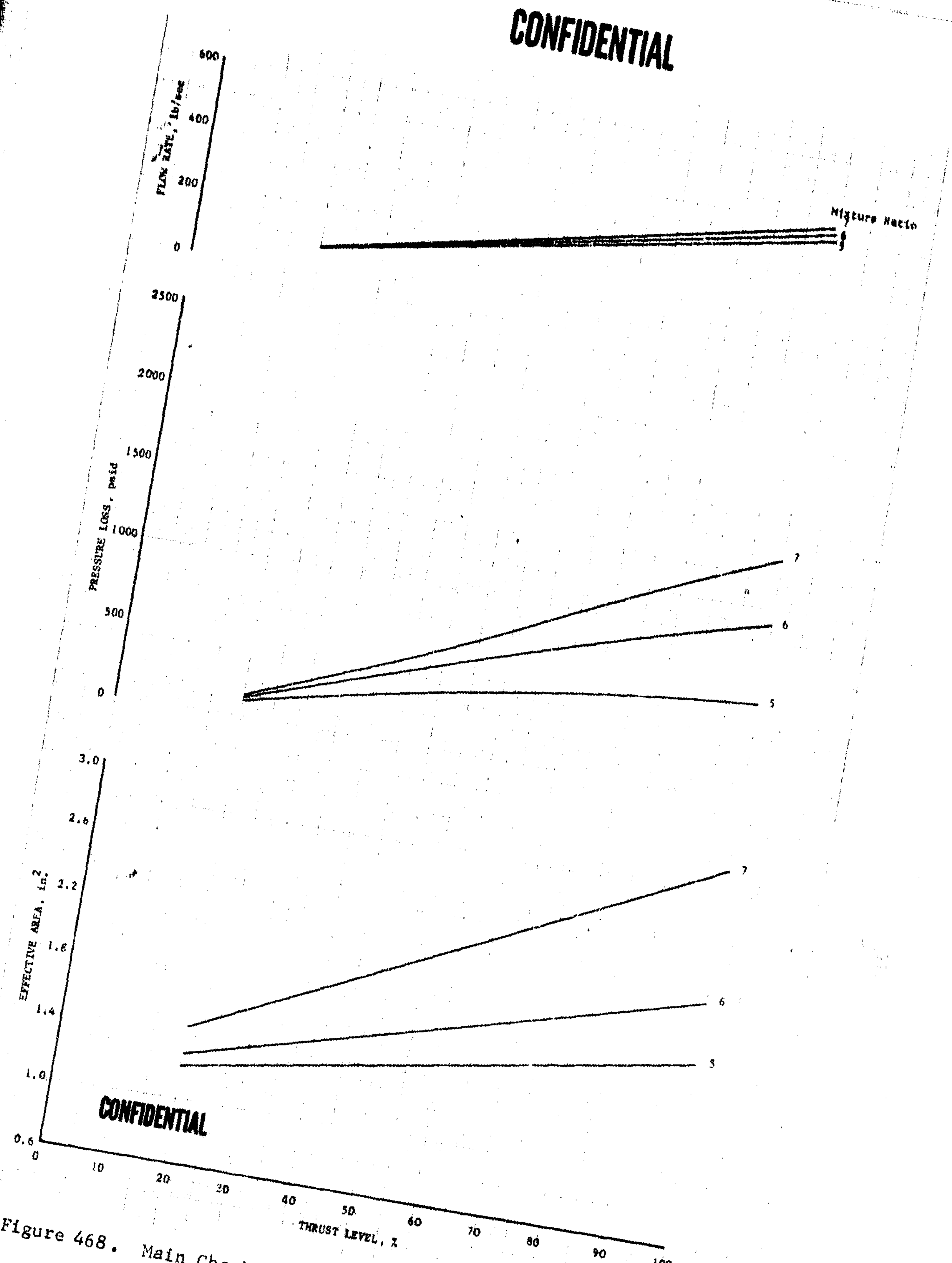

(U) Figure 468. Main Chamber Oxidizer Control Valve Operating Requirements

DF 75611

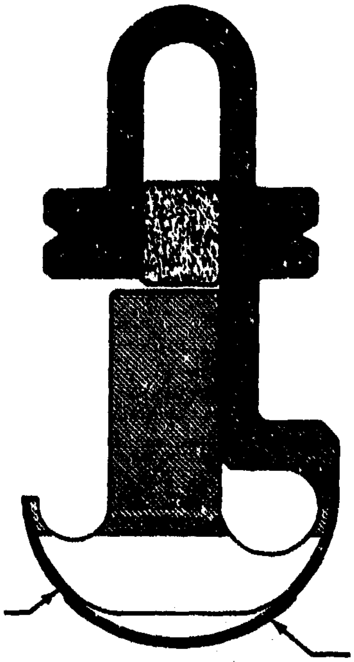

(U) Figure 469. Hoop Seal Assembly Cross Section

(C) The maximum deflection at the disk centerline is about 0.006 inch, and the corresponding disk bending stress is 50,000 psi. The maximum reaction load on the inboard bearings is 6500 pounds, or about 40% of the quoted capacity. The corresponding value for the outboard bearings is approximately 10%. The calculated shear stress at the splined neck diameter is 43,000 psi at an assumed torque of 2400 pound-inches. This torque consists of 1400 pound-inches of hydraulic unbalance and a conservative estimate of 1000 pound-inches caused by seal and bearing friction loads. The maximum thrust load expected for the outboard thrust bearing is 2300 pounds at 100% thrust and a mixture ratio of 5. The maximum thrust load expected for the inboard thrust bearing is 700 pounds at 100% thrust and mixture ratio of 7. The bearing loads expected for the outboard thrust bearing during the engine shutdown transient are 2000 pounds at 20% thrust and mixture ratio of 7 and 2150 pounds at 20% thrust and a mixture ratio of 5. The bearing load capacity quoted by the vendor is 11,900 pounds.

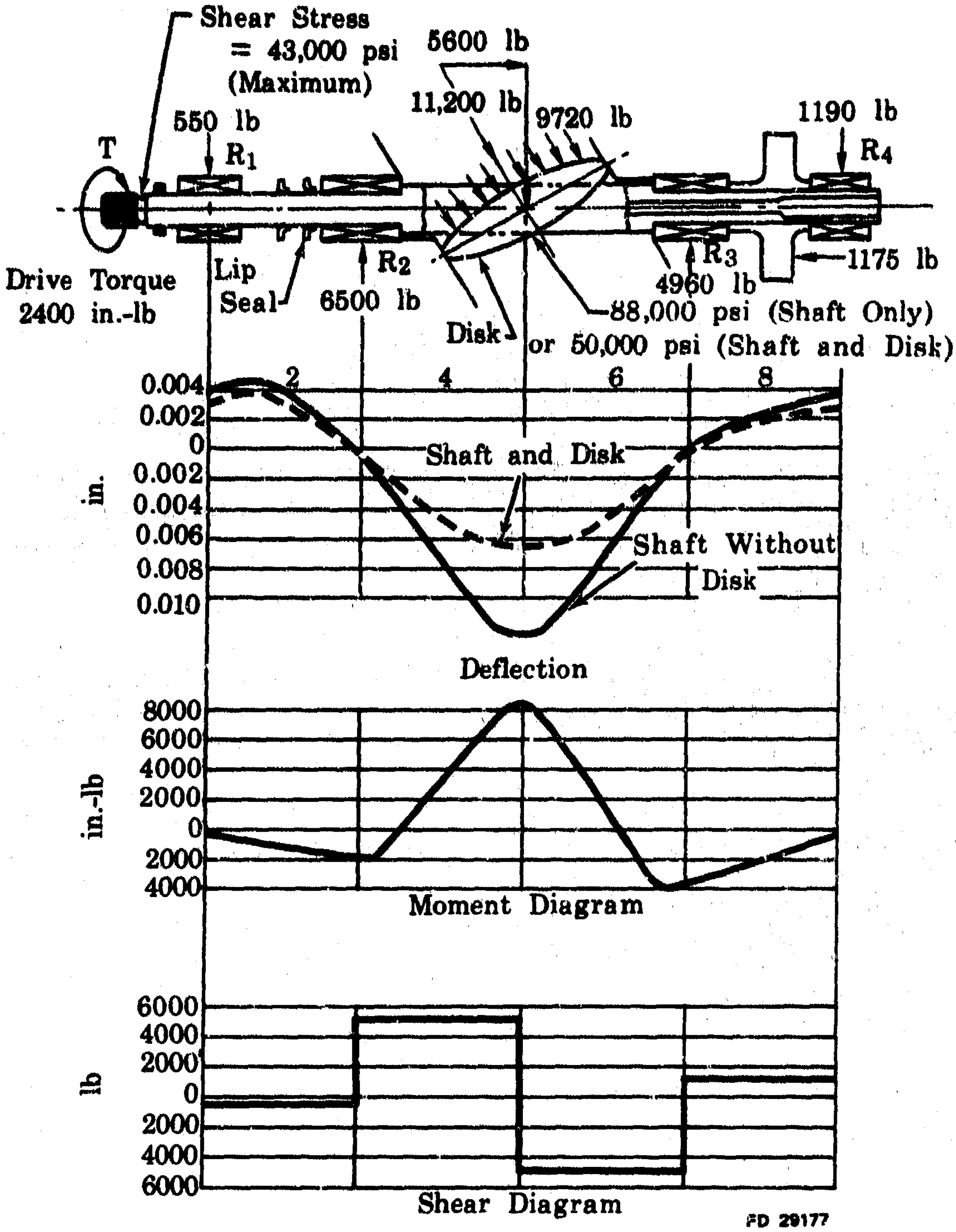

(U) Figure 470. Force, Load and Stress Analysis Summary

(U) Double lip seals, consisting of an innner layer of FEP Teflon and three layers of Kapton F, are used at the actuator end of the valve shaft between the inboard and outboard roller bearings. The nominal thickness of the seals is 0.0195 inch. As shown in figure 471, a fitting is provided to vent leakage past the primary lip seal overboard.

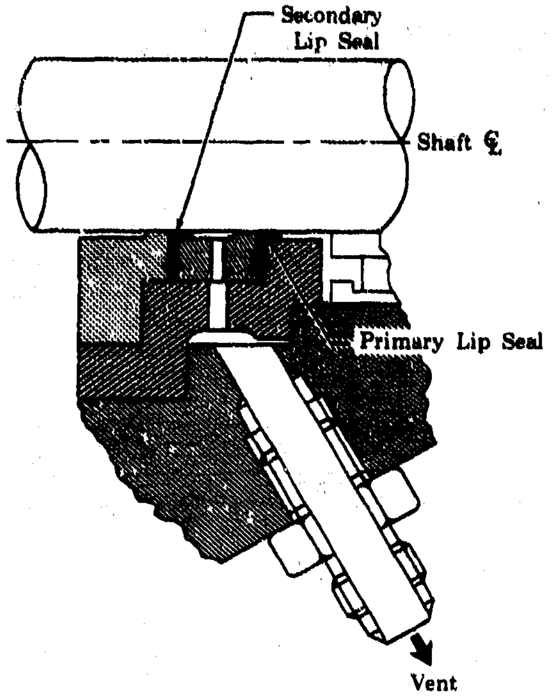

(U) Figure 471. Shaft Lip Seals

(U) A helium purge fitting is in the split flange just downstream of the butterfly disk. This location will provide injector purge capability at engine shutdown.

(U) The main housing components are designed as a matched set to achieve the required dimensional precision for bearing and shutoff seal alignment. Bolts and flanges are designed for a proof pressure factor of 1.5 times the maximum local operating pressures. Studs are used where necessary to minimize the torsional stresses inherent in bolt torquing. Flange thicknesses are designed for 0.002-inch maximum deflection at the seal mean diameter. Results of a complete analysis of the flange configuration assumptions are summarized in figure 472. Simplified geometry was employed in the analysis as shown to overcome the complications of the actual housing design shapes. The results of the inlet and outlet flanges are also valid for the mating flanges.

F_B - Maximum Stud Load
F_S - Seal Load
F_{BL} - Blowoff Load
F_{TB} - Thrust Bearing Load
F_{LS} - Lip Seal Load

Flange Identification	Inlet (A)	Split (B)	Outlet (C)	Thrust (D)	Drive (E)
Stud Thread Size	0.375-24	0.4375-20	0.3125-24	0.375-24	0.375-24
No. of Studs	15	14	15	10	11
Stud Preload, lb	7300-9100	9300-11,600	4300-5300	4600-5800	5600-7000
Stud Tensile Stress, lb	123,000	123,000	110,000	82,500	108,000
Stud Bending Stress, lb	18,700	25,600	24,500	55,000	39,000
Seal Load, lb	4100	16,000 ◪	3700	6700 ⊗	25,600 △
Total Preload Minimum	110,000	130,000	64,500	46,000	61,600 ◐
*Face Contact Stress	37,000	24,000	27,000	29,500	21,000
*Flange Stress Maximum	65,300	44,000	45,700	62,500	55,000

* At 120% Maximum Cycle Pressure

◪ Laminated Plastic Seal (2-Ply Kapton)
⊗ Includes 3700 lb Thrust Bearing Load Allowance
△ Consists of 18,600 lb for Lip Seal Preload, Plus 7000 lb for Primary and Secondary Static Seals
◐ Includes 7700 lb for External Moment Due to Weight of Actuator at 50 g's Acceleration

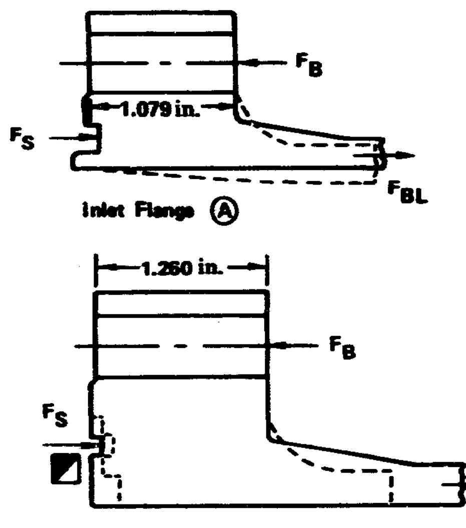

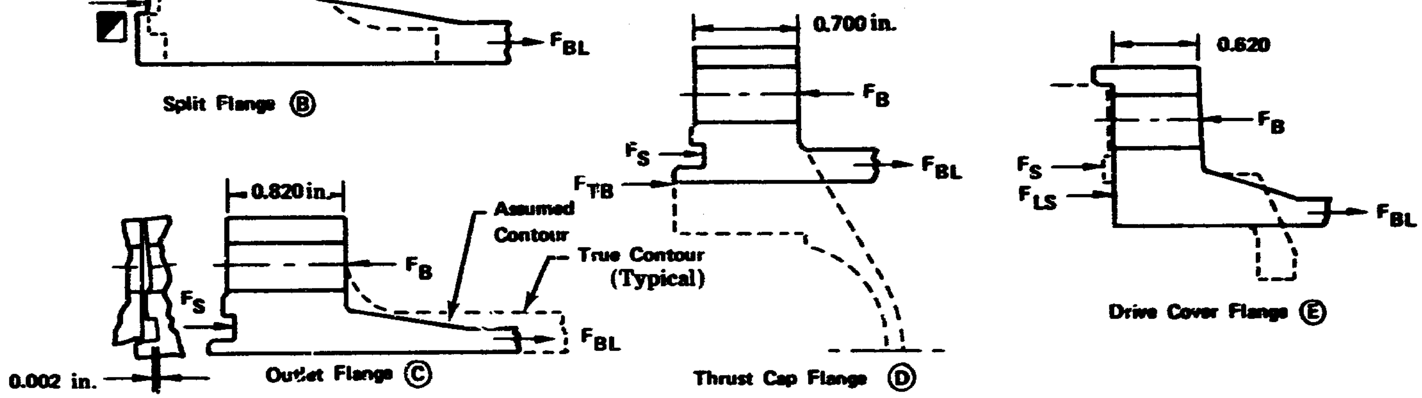

FD 29178

(U) Figure 472. Flange Stress Analysis Summary

(U) The split-flange bolt circle has two pairs of holes located 0.500 inch outside the remainder of the circle to avoid the bearing cavities. An appropriate ridge is left to increase wall thickness locally to keep flange deflection within the established limits. The overall length of the housing is minimized and external contouring is employed to save weight. The main chamber oxidizer valve is designed for cryogenic temperature operation. The flanges and studs must be cooled to operating temperature before maximum cyclic pressures are applied if design stress margins are to be maintained. The calculated weight of the main chamber oxidizer valve assembly (less actuator and coupling) is 52 pounds, 37 pounds less than the valve used in the Phase I program.

5. Operating Characteristics

(U) The predicted main chamber oxidizer valve operating characteristics are illustrated in figures 473, 474, and 475. Figure 473 illustrates the pressure drop across the valve throughout the throttling range at the three mixture ratios, figure 474 shows the predicted effective area as a function of shaft angle, and figure 475 illustrates the percentage of area error as a function of shaft angle.

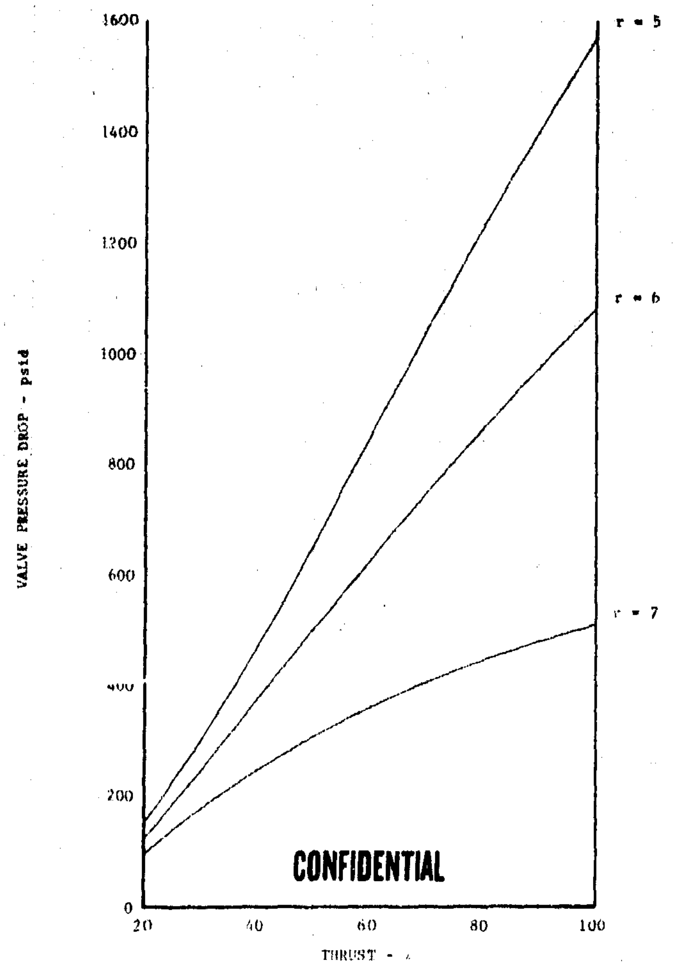

DFC 71085

(U) Figure 473. Valve Pressure Drop vs Thrust

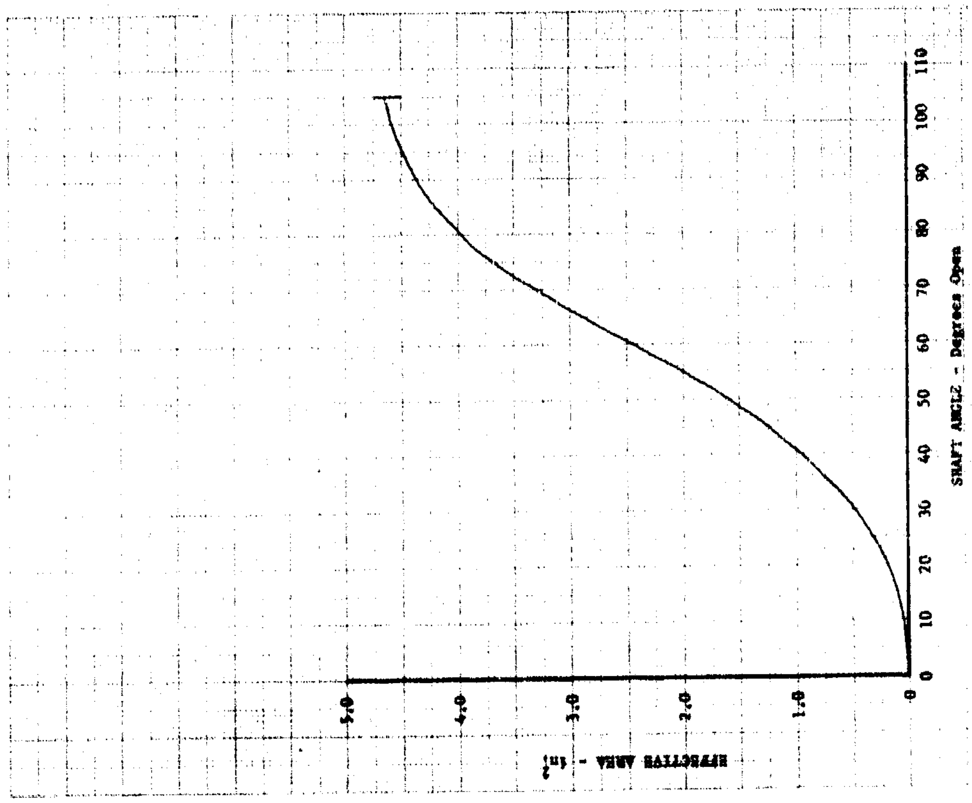

DF 71066

(U) Figure 474. Valve Effective Area vs Shaft Angle

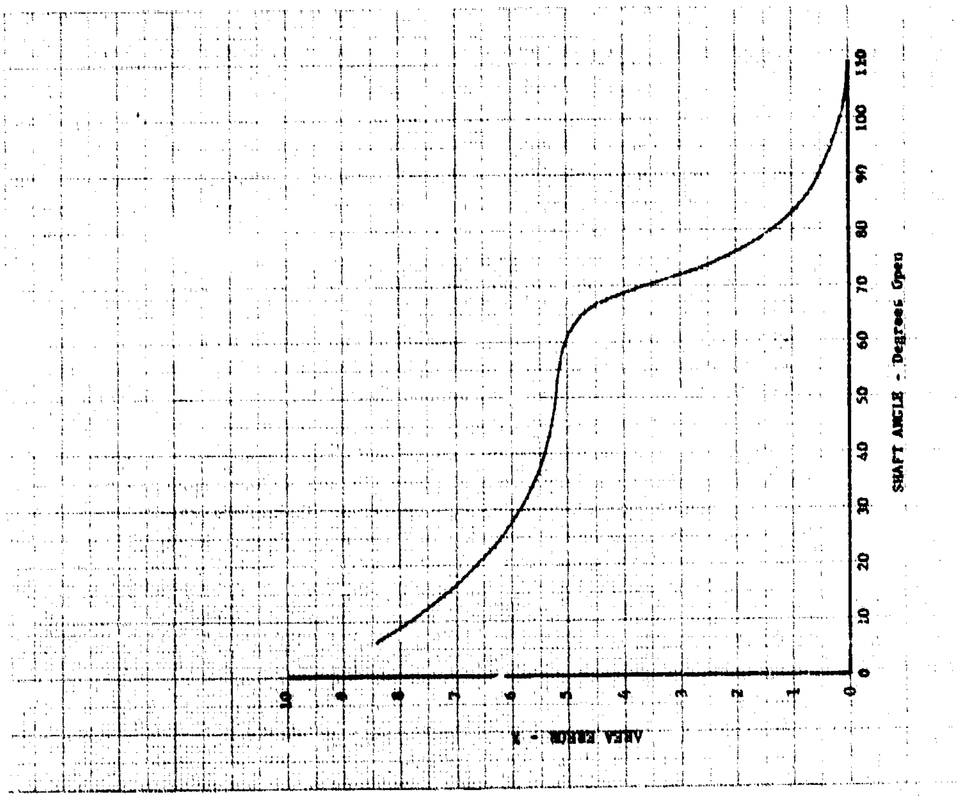

DF 71067

(U) Figure 475. Valve Area Error per Degree Shaft Angle

6. Design Approach

a. Background

(U) The basic valve is a canted-shaft butterfly type of valve designed during Phase I, Contract AF04(611)11401. The canted-shaft butterfly valve configuration was selected as a result of an evaluation including both external and internal sleeve valves, two types of pintle valves, a ball valve, and a butterfly valve. The butterfly valve was selected on the basis of a superior overall rating (700 out of a possible 790 points) on factors listed for the preburner fuel valve in table LXVI.

(U) The Phase I, Contract AF04(611)-11401, main chamber oxidizer valve was used to develop the hoop-type shutoff seal and the laminated Kapton F/FEP Teflon shaft lipseals during the supporting data and analysis phase of the current contract (Section VJ5, AFRPL-TR-69-3). The revised design shaft lip seal configuration performed satisfactorily during the endurance tests conducted for shutoff seal development. Four shutoff seal designs were fabricated and tested for endurance and leakage. Of the four, the silver-plated hoop-type shutoff seal provided the most consistent endurance testing results, met all of the testing goals, and was still serviceable after all tests were completed. The silver-plated hoop seal was therefore selected for the main chamber oxidizer valve design for the demonstrator engine.

b. Shutoff Seal Design Evolution

(U) Two builds (Rig F-33466-11 and Rig F-35106-8) of the main chamber oxidizer valve were subjected to extended endurance tests under the component development subtask (Section V, AFRPL-TR-69-3). The primary objectives of these tests were to test the shutoff cycle endurance of hoop and cam-actuated shutoff seals at cryogenic and ambient temperatures. Secondary objectives were to leak check the seals hydrostatically at 1300 psid, perform valve position versus effective area waterflow calibrations, and test the seals at high flow conditions. A description of these builds, test conditions, and test results leading to the selection of the silver-plated, hoop-type seal configuration is as follows.

(1) Hardware Description

(a) Rig F-33466-11

(U) Rig F-33466-11 of the main chamber oxidizer valve used a rotary hydraulic servoactuator and incorporated the following features:

1. A shutoff seal consisting of a silver-plated hoop with a 0.010-inch tight fit on the disk. Improved silver plating and more access area for cleaning inside the hoop was incorporated. The seal was installed on the disk by heating the seal to approximately 250°F and cooling the disk in LN_2. Figure 476 shows a cross section of the seal as installed. Figure 477 shows an overall view of the seal, and figure 478 is a closeup of the seal element.

2. An integral shaft and butterfly Inconel 718 spherical seal surface which is chrome-plated with an 18 microfinish.

3. Revised shaft lip seal design (figure 479).

4. Shaft lip seals of laminated Kapton F (three layers) and FEP Teflon (one layer next to shaft). Total thickness was 0.019 inch.

5. Tufram thrust bearing and silver-plated thrust washers.

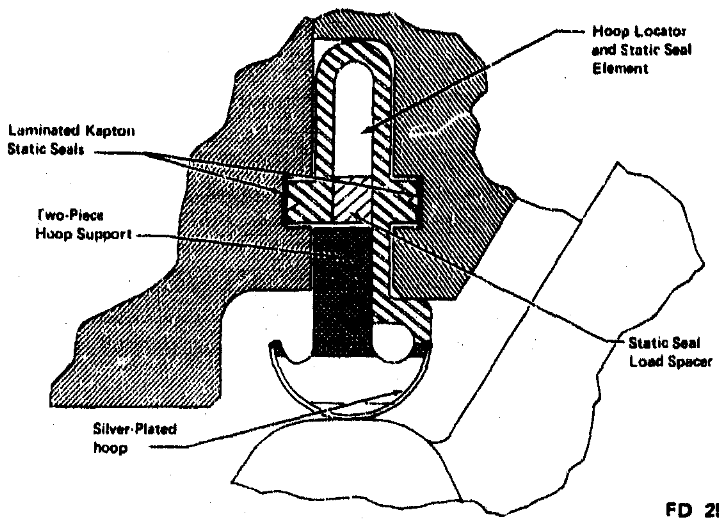

FD 25572A

(U) Figure 476. Main Chamber Oxidizer Valve Shutoff Seal Cross Section Rig F-33466-11

FE 80066

(U) Figure 477. Main Chamber Oxidizer Valve Shutoff Seal Overall View Rig F-33466-11

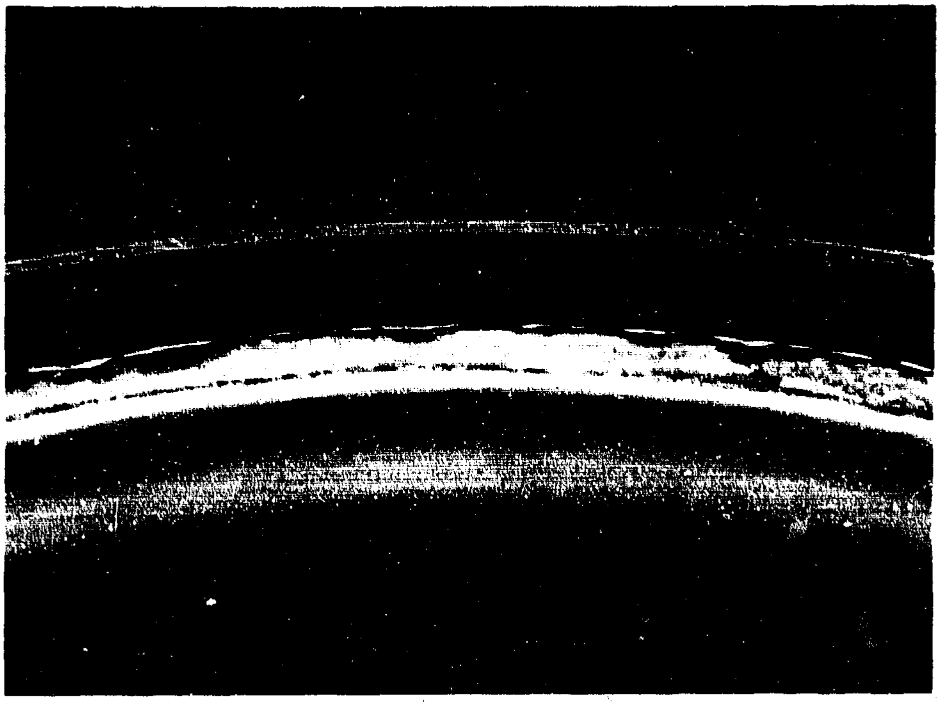

FE 80067

(U) Figure 478. Main Chamber Oxidizer Valve Shutoff Seal Element, Rig F-33466-11

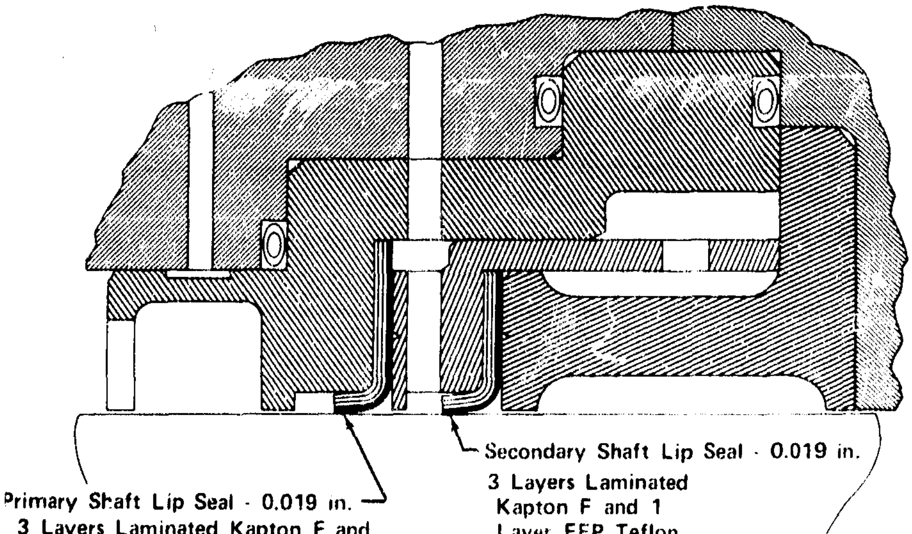

(U) Figure 479. Revised Shaft Lip Seal Design

(b) Rig F-35106-8

(U) Rig F-35106-8 of the main chamber oxidizer valve used a cam-actuated shutoff seal and incorporated the following features:

1. An FEP Teflon seal element contracted against the disk surface by a cam-actuated tapered slipring. The assembly also included a 0.010-inch thick Inconel X (AMS 5667) seal support. Figure 474 shows a cross section of the seal, and figure 481 shows the layout of the seal assembly.

2. The disk was chrome-plated Inconel 718 with a spherical seal surface and a 9.5 microfinish. The shaft actuating lug was modified from the original configuration to return the drive cam to the open position during the first few degrees of valve opening.

3. Revised shaft lip seal design (figure 479)

4. Shaft lip seals of laminated Kapton (three layers) and FEP Teflon (one layer next to the shaft). Total thickness was 0.019 inch.

5. Rotary hydraulic servoactuator.

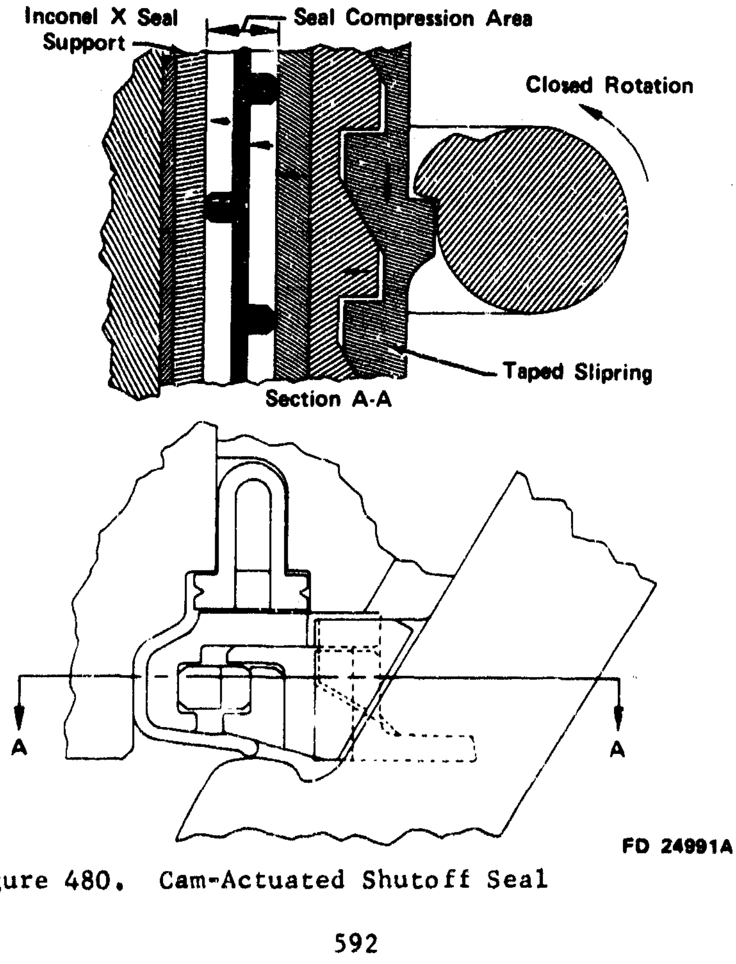

(U) Figure 480. Cam-Actuated Shutoff Seal

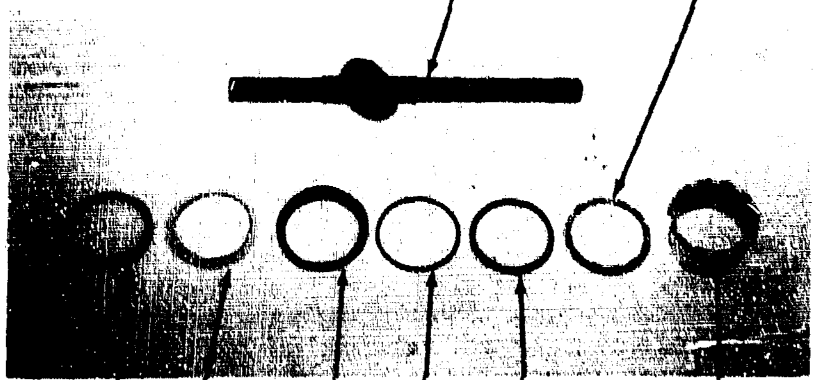

(U) Figure 481. Cam-Actuated Seal Parts Layout

(2) Testing

(a) Rig F-33466-11

(C) The valve was installed and tested on B-22 stand. No mechanical malfunctions were observed during the tests. Ambient temperature shutoff seal leakage was undetectable prior to cycling the valve at 50-psid nitrogen. The torque required to open the valve at liquid argon temperatures prior to cycling was approximately 400 pound-inches.

(C) The first 2500 of the required shutoff cycles were performed with the valve submerged in liquid argon. The valve was then allowed to warm to ambient temperature, and the remaining 7500 of the programmed shutoff cycles were completed at ambient temperature. The valve was again submerged in liquid argon and 100 additional shutoff cycles were completed. All cycles were performed at one cycle per second with 50-psid nitrogen pressure across the closed valve disk seal. Shutoff seal leakage measurements at 50 psid were taken periodically during the test.

(C) Shutoff seal leakage during the endurance test is shown in figure 482. Stable disk seal leakage during the cryogenic testing was observed approximately 15 minutes after the valve was closed. Figure 483 shows typical indicated leakage decay due to boiloff in the discharge housing. The cryogenic leakage values shown in figure 482 were recorded at least 15 minutes after the valve was closed. Disk seal leakage versus shaft position is shown in figure 484. Post-test leakage at liquid argon temperatures at 50 psid nitrogen is shown in figure 485.

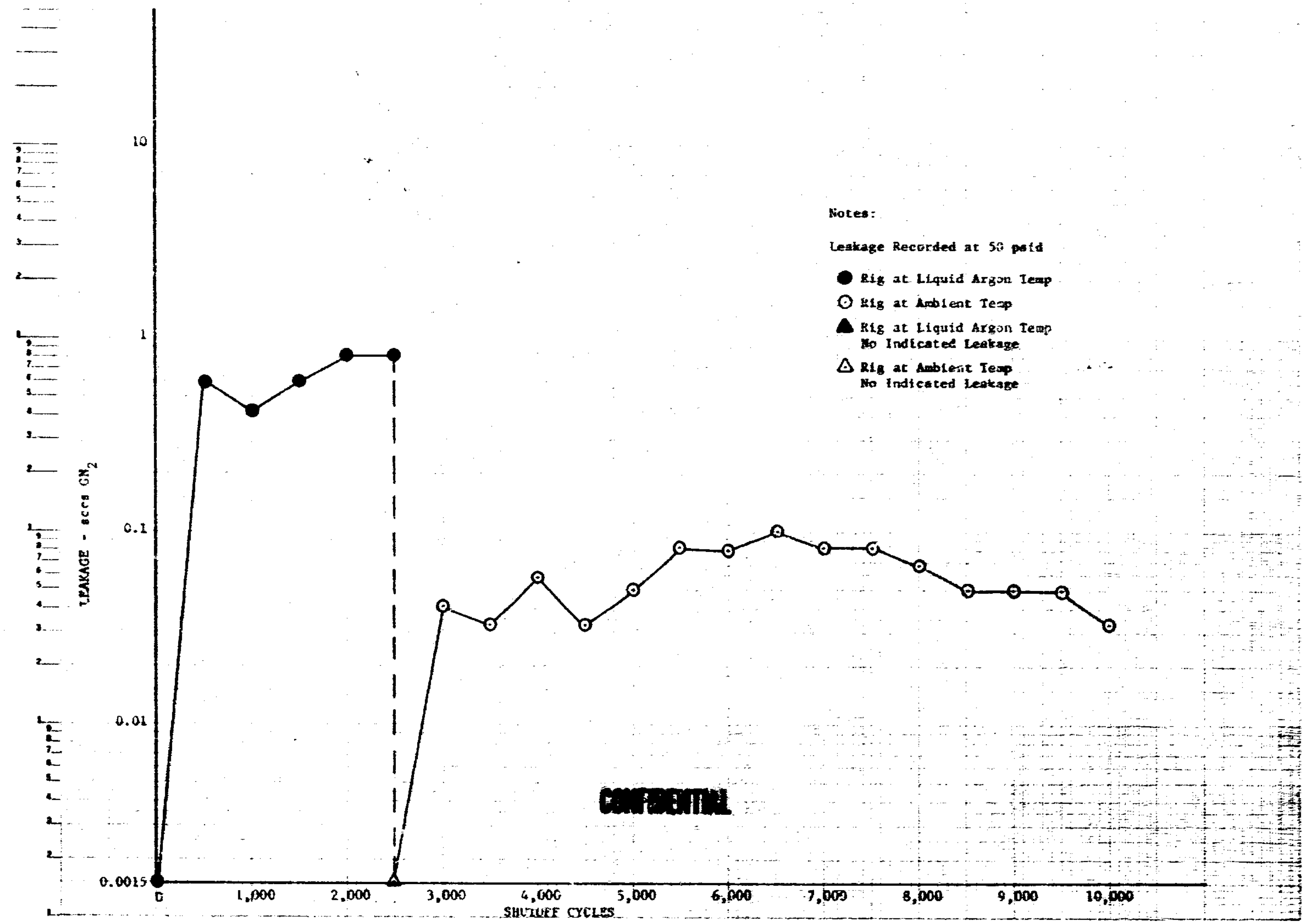

DFC 68892

(U) Figure 482. Shutoff Seal Leakage vs Shutoff Cycles, Rig F-33466-11 Recorded 15 Minutes After Valve Closed

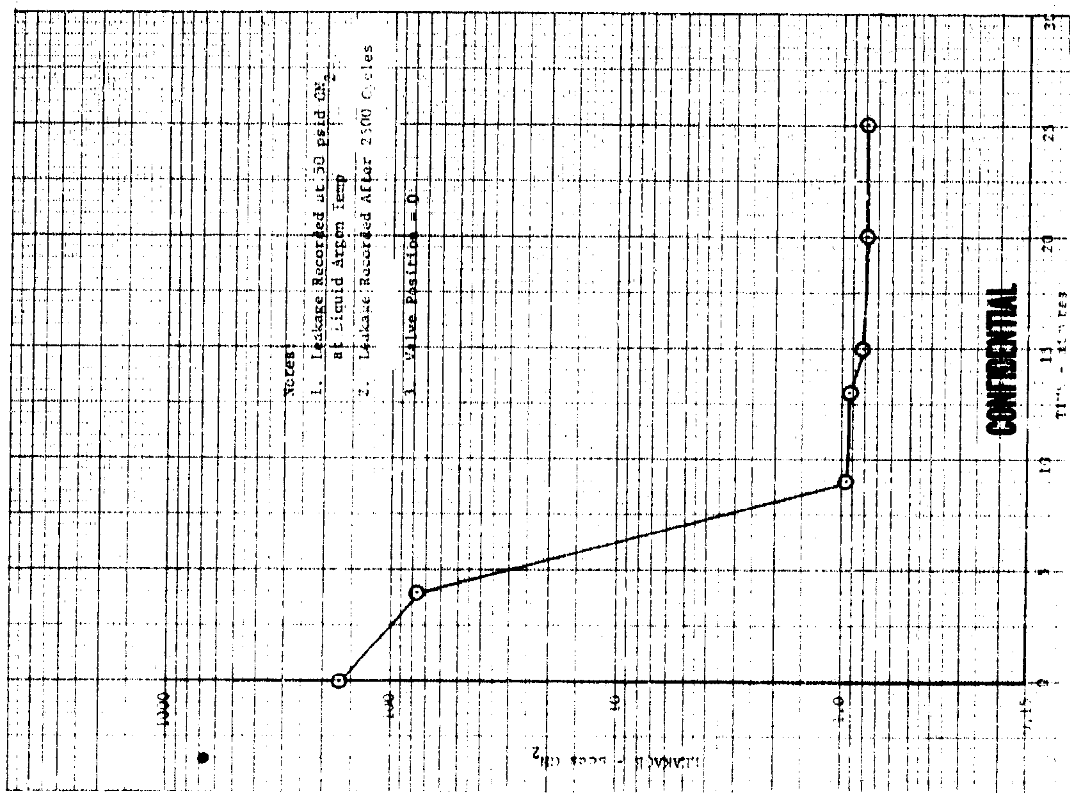

(U) Figure 483. Seal Leakage vs Time, Rig F-33466-11

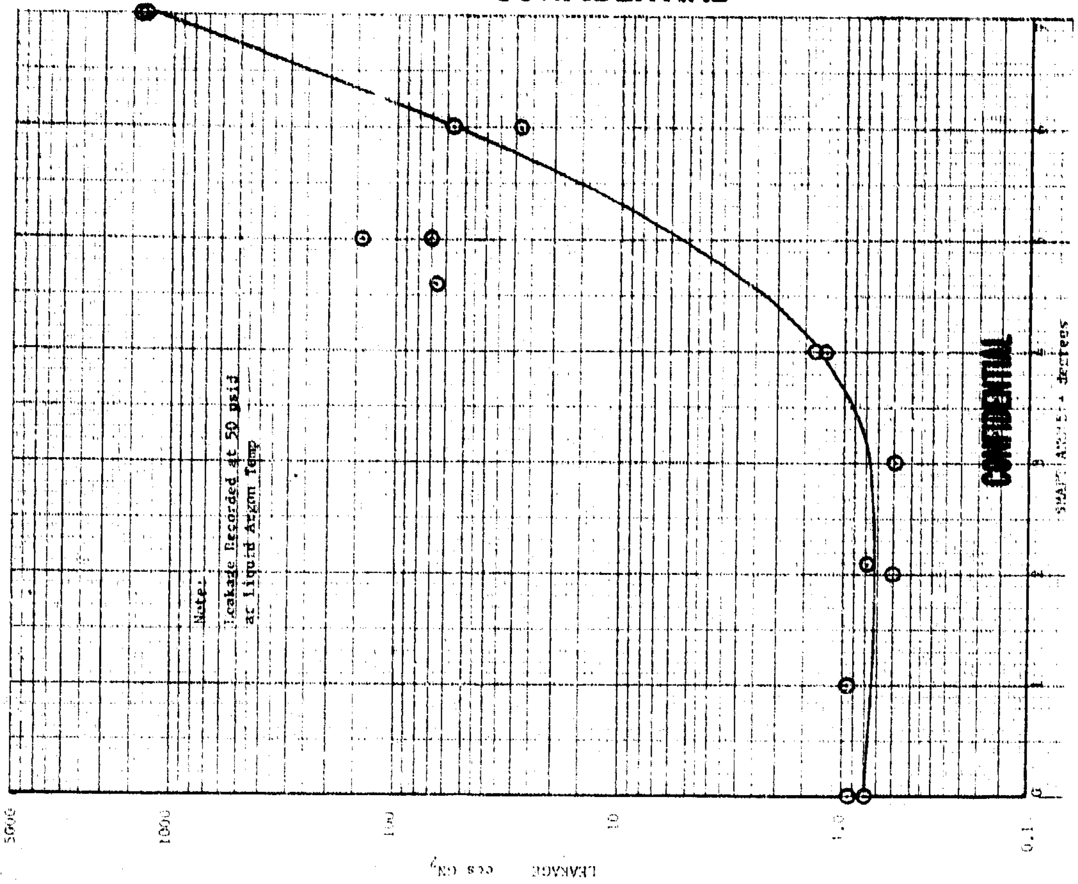

(U) Figure 484. Disk Seal Leakage vs Shaft Angle, Rig F-33466-11

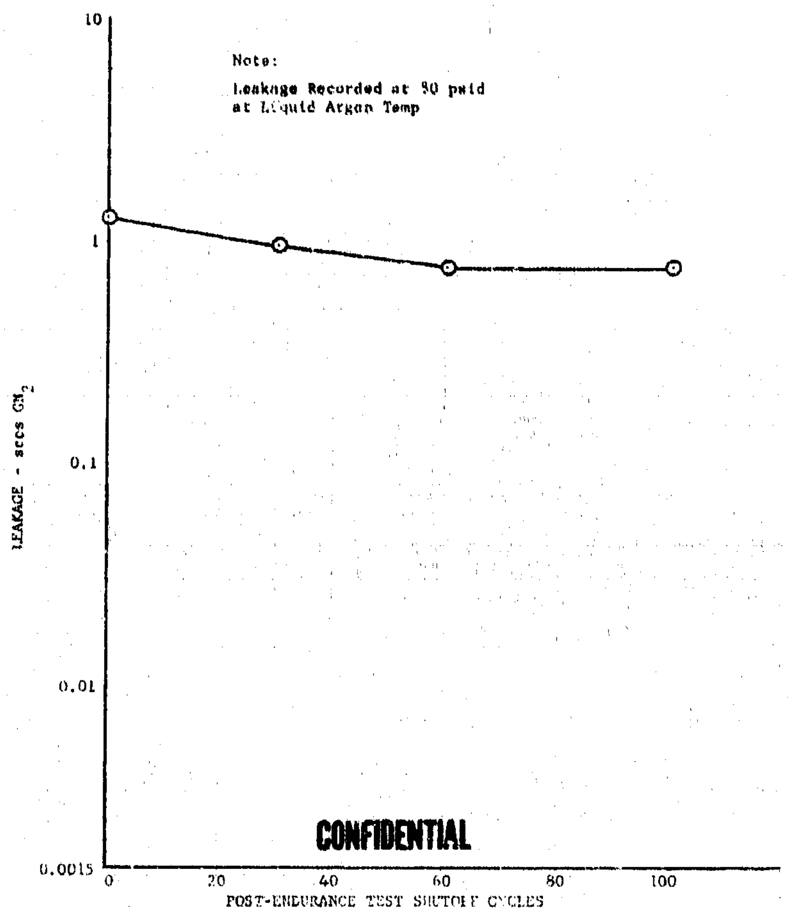

(U) Figure 485. Post-Test Leakage, Rig F-33466-11

(C) Post-test ambient disk seal leakage at 50 psid nitrogen was 0.03 sccs with the valve at zero degrees. Inspection revealed that the hoop seal wear area was approximately 0.100-inch wide as shown in figure 486. The disk seal surface was in good condition as shown in figure 487.

(U) Moisture was found in the inlet housing and on the upstream side of the disk at teardown. No moisture was found elsewhere in the valve. The origin of this contamination was not determined.

(C) The valve was hydrostatically leak checked and flow calibrated with water. A shutoff seal test at 1300-psid water pressure resulted in no visible leakage prior to the water-flow calibration. The water calibration results are shown in figure 488. Post-test shutoff seal leakage at ambient temperature and 1300-psid water pressure was 0.3 sccs and was undetectable with 50-psid nitrogen.

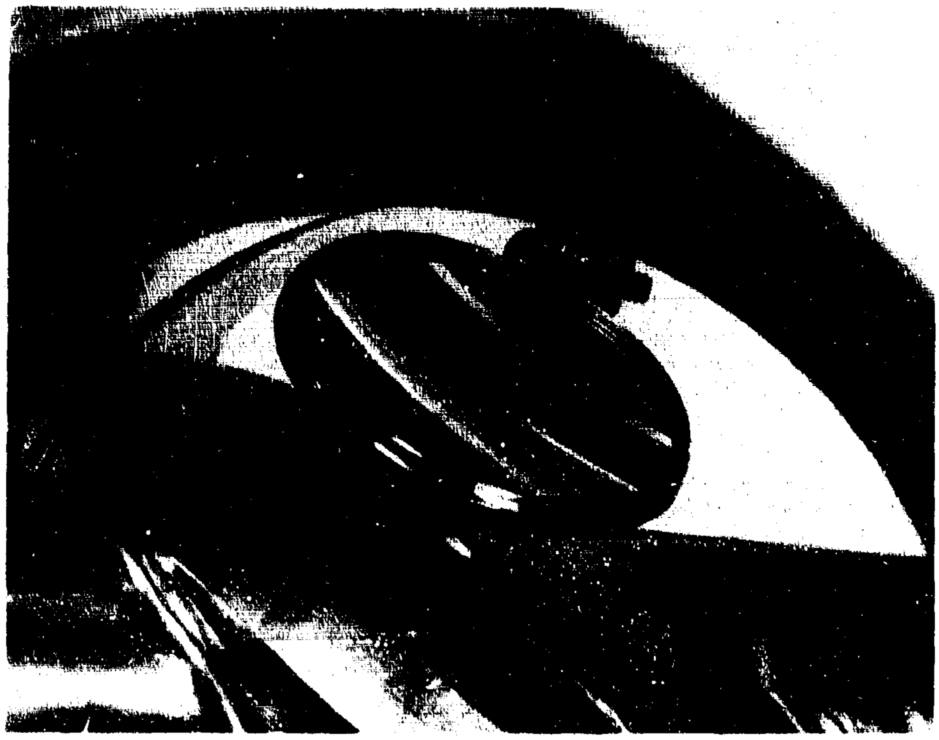

FE 80567

(U) Figure 486. Hoop Seal Wear, Rig F-33466-11

FE 80566

(U) Figure 487. Disk Seal Post-Test Condition, Rig F-33466-11

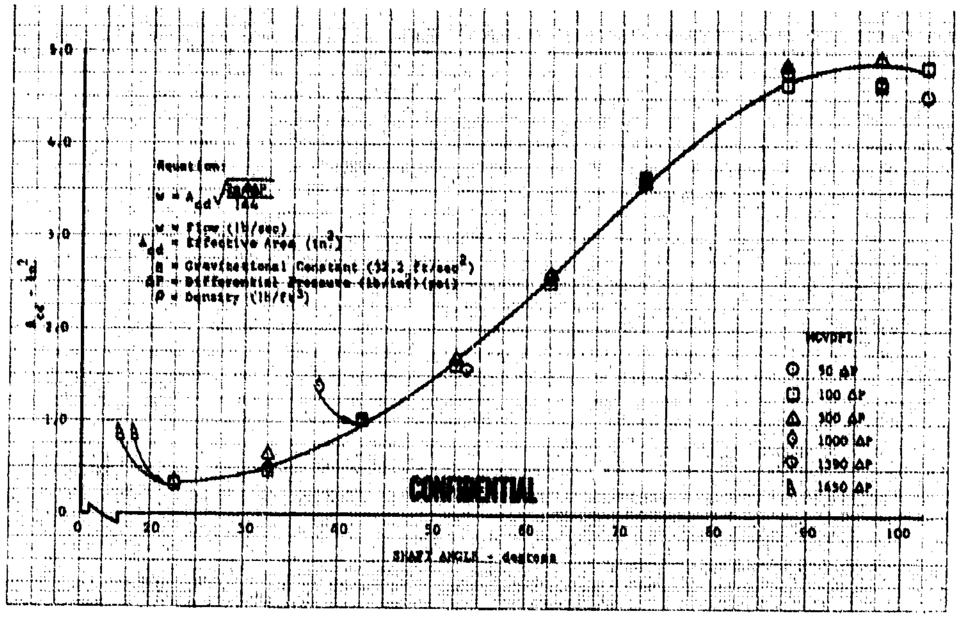

DFC 68888

(U) Figure 488. Water Calibration Results, Rig F-33466-11

(C) Teardown inspection revealed that the hoop sealing surface was in good condition with some minor scratches in the contact area (figure 489). The seal fit on the disk measured 0.005-inch tight. The seal element had failed for approximately 0.75 inch along the upstream lipweld (figure 490). Seal surface roughness at this point (figure 491) indicated possible flow cavitation damage. This area and a similar rough area on the seal surface approximately 120 degrees from this point indicated that the valve was open when this occurred. The index of cavitation $(P_{in} - P_{out})/(P_{in} - P_{vapor})$ was greater than 0.90 at 20-degree shaft angle and 1450 psid and at several additional points during the water calibration. The general index of incipient cavitation for a butterfly valve is 0.37. Engine operating conditions result in less than the incipient cavitation index of 0.37.

(U) The disk sealing surface was in excellent condition as shown in figure 492. All other parts were in excellent condition as shown in figure 493.

(b) Rig F-35106-8

(C) Testing revealed that ambient disk seal leakage at 50-psid nitrogen prior to cycling was undetectable with 700 pound-inches of torque applied to the shaft in the closed direction.

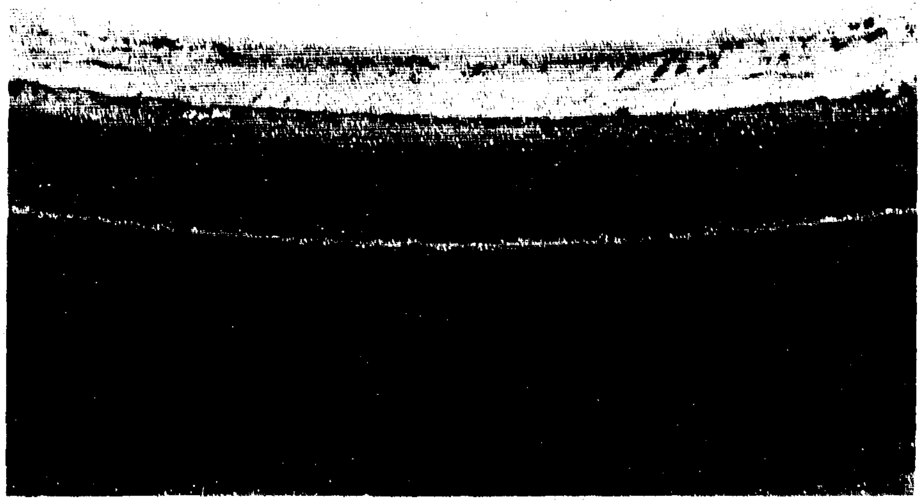

FE 80770

(U) Figure 489. Hoop Seal Condition, Post-Test, Rig F-33466-11

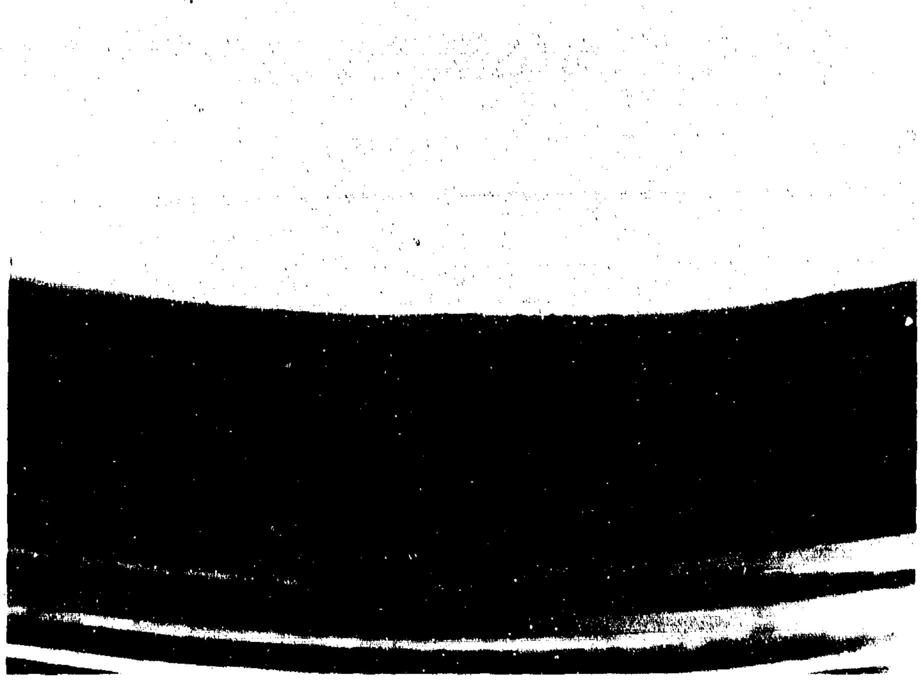

FE 80771

(U) Figure 490. Hoop Seal Element Failure, Rig F-33466-11

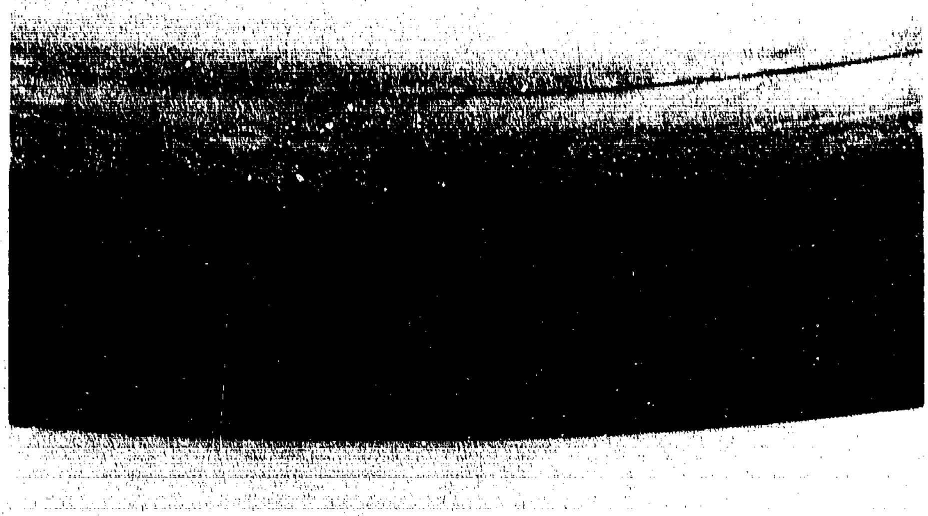

FE 80978

(U) Figure 491. Possible Cavitation Damage to Hoop Seal, Rig F-33466-11

FE 80772

(U) Figure 492. Post-Test, Disk Sealing Surface Common Rig F-33466-11

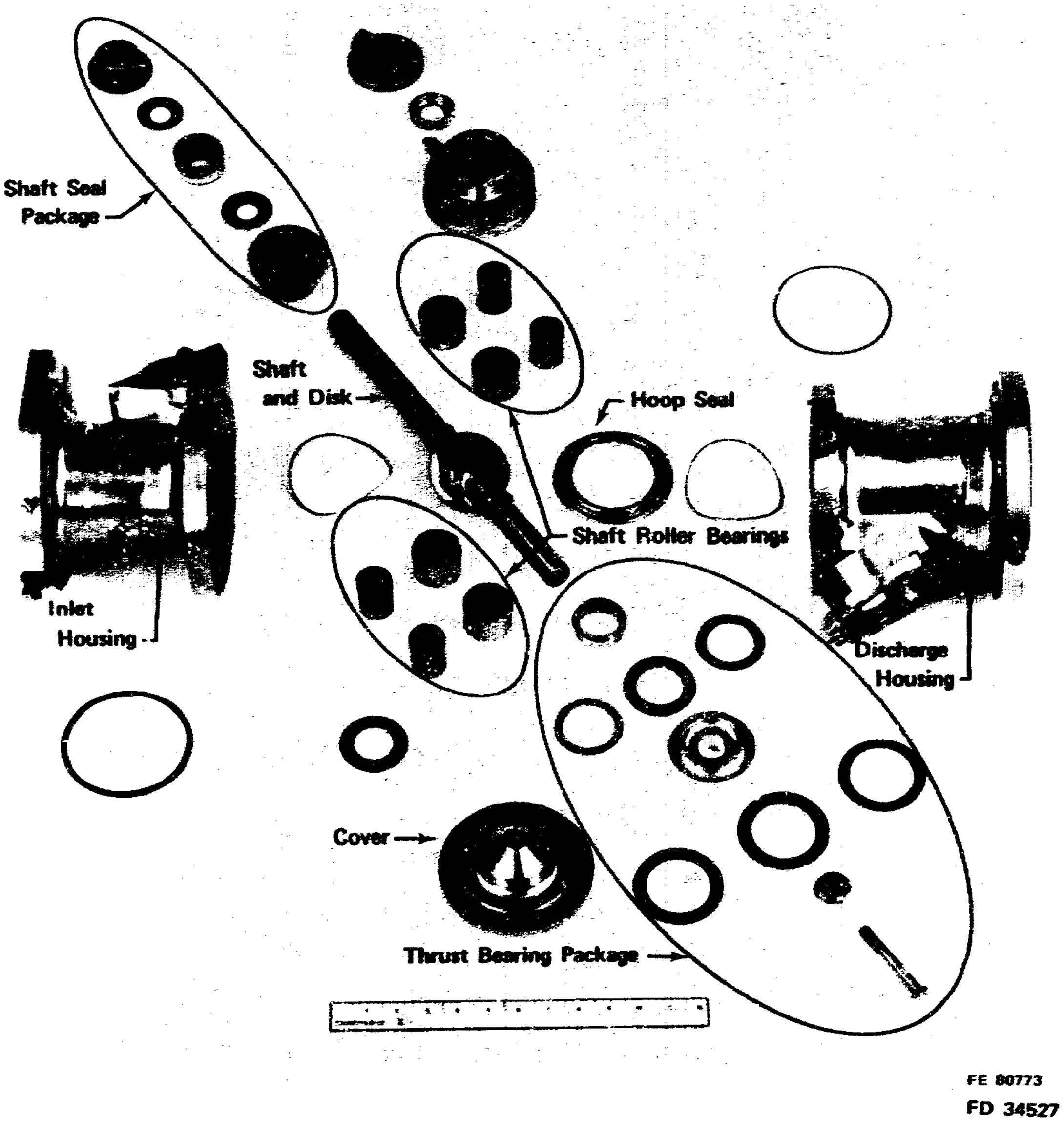

(U) Figure 493. Post-Test Teardown of Main Chamber Oxidizer Valve, Rig F-33466-11

(C) The first 2500 shutoff cycles were performed with the valve submerged in liquid argon. The valve was then allowed to warm to ambient temperature and the remaining 7500 shutoff cycles were completed at ambient temperature. The valve was again submerged in liquid argon and 100 shutoff cycles were completed. All cycles were performed at one cycle per second and with 50-psid nitrogen pressure across the closed valve shutoff seal. Shutoff seal leakage measurements at 50 psid were taken periodically during the test.

(U) Shutoff seal leakage during the endurance test is shown in figure 488. Stable disk seal leakage during the cryogenic testing was observed approximately 15 minutes after the valve was closed. Figure 495 shows typical indicated leakage decay due to boil off in the discharge housing. Cryogenic leakage, shown in figure 494, was measured approximately 15 minutes after the valve was closed.

(C) Disk seal leakage versus shaft angle is shown in figure 496. Post-test leakage at liquid argon temperature and 40-psid nitrogen is shown in figure 497. Post-test ambient disk seal leakage at 50-psid nitrogen was 0.008 sccs with the valve at zero degrees. Inspection revealed that both the cam-actuated seal element and the shaft seal surface were in excellent condition as shown in figures 498 and 499, respectively. Physical measurement of the disk angle with the valve in the closed position indicated the disk to be one degree from fully closed. Post-test visual inspection was completed and photographs were taken prior to hydrostatic leak checks and water calibration. A shutoff seal leakage test at 1300-psid water pressure indicated 13-sccs leakage prior to waterflow calibration. The water calibration results are shown in figure 500. Post-test shutoff seal leakage was greater than 80 sccs at 25-psid water pressure. Post-test inspection revealed seal damage as shown in figure 501. An enlarged view of the damaged seal area is shown in figure 502. The 10-micron filter just upstream of the valve inlet was inspected and no deterioration was found. All seal damage was on the portion of the seal that is down stream of the disk edge as shown in figure 503.

(C) The appearance of the seal element indicates flow cavitation at the butterfly disk as the cause of the seal damage. The index of cavitation $(P_{in} - P_{out})/(P_{in} - P_{vapor})$ was greater than 0.85 at all flow points of 1000 psid or more. Engine operating conditions produce less than the general index of incipient cavitation for a butterfly valve of 0.37.

(U) Inspection of the seal support revealed cracks as shown in figure 504. All slots on the damaged side of the seal were cracked, but no cracks were apparent on the other side. The disk sealing surface was in good condition (figure 505), but the drive cam was cracked adjacent to the lug contact point as shown in figure 506. Figure 507 shows the post-test layout.

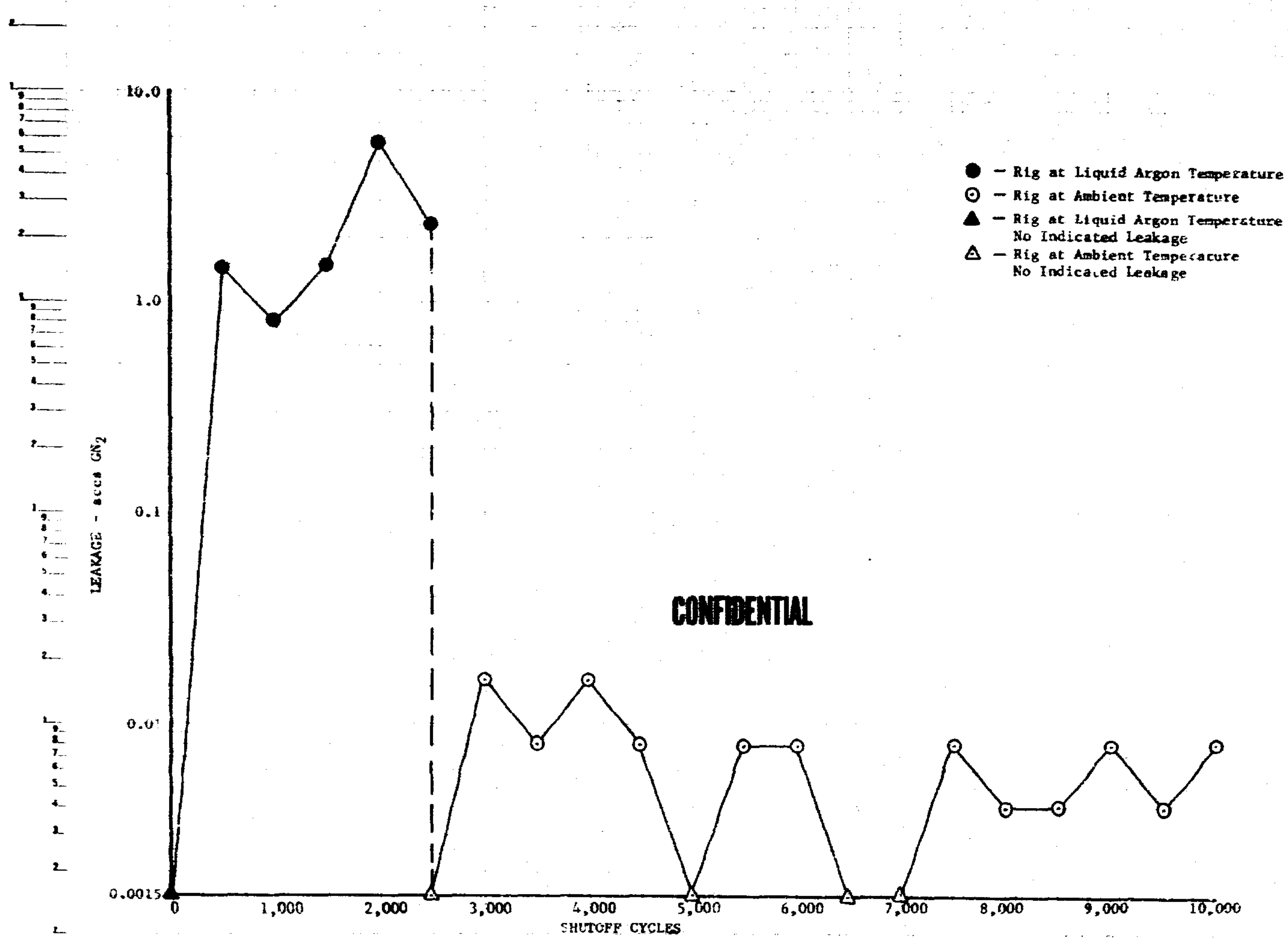

(U) Figure 494. Shutoff Seal Leakage vs Percent of Test Goal, Rig F-35106-8

DFC 68914

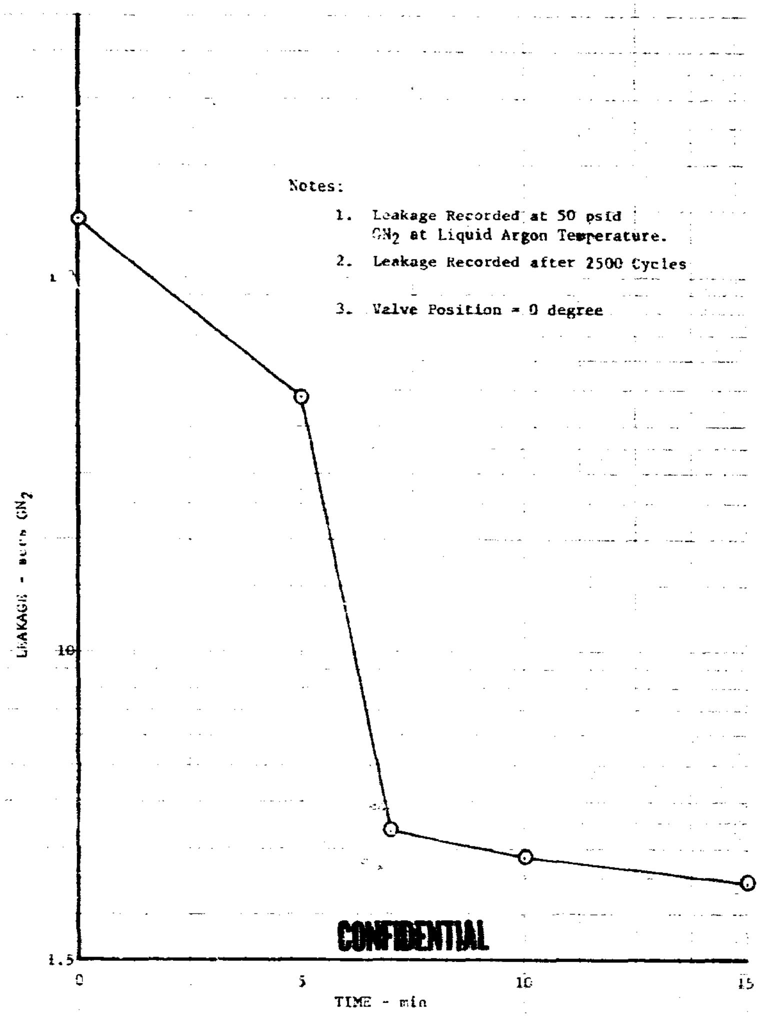

DFC 68915

(U) Figure 495. Shutoff Seal Leakage vs Time, Rig F-35106-8

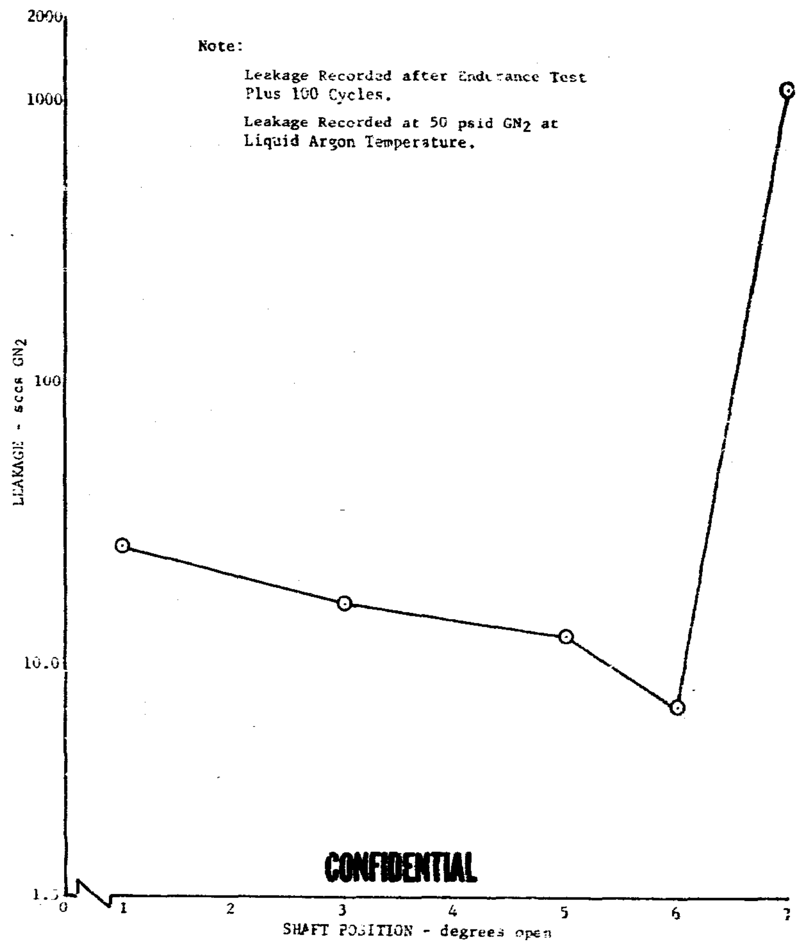

DFC 68916

(U) Figure 496. Shutoff Seal Leakage vs Shaft Position, Rig F-35106-8

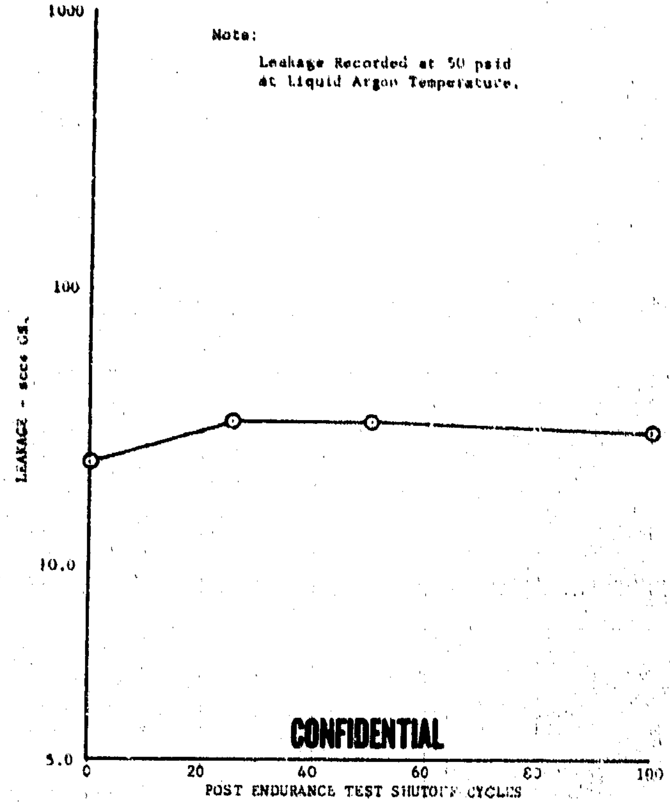

DFC 68917

(U) Figure 497. Shutoff Seal Leakage vs Shutoff Cycles, Rig F-35106-8

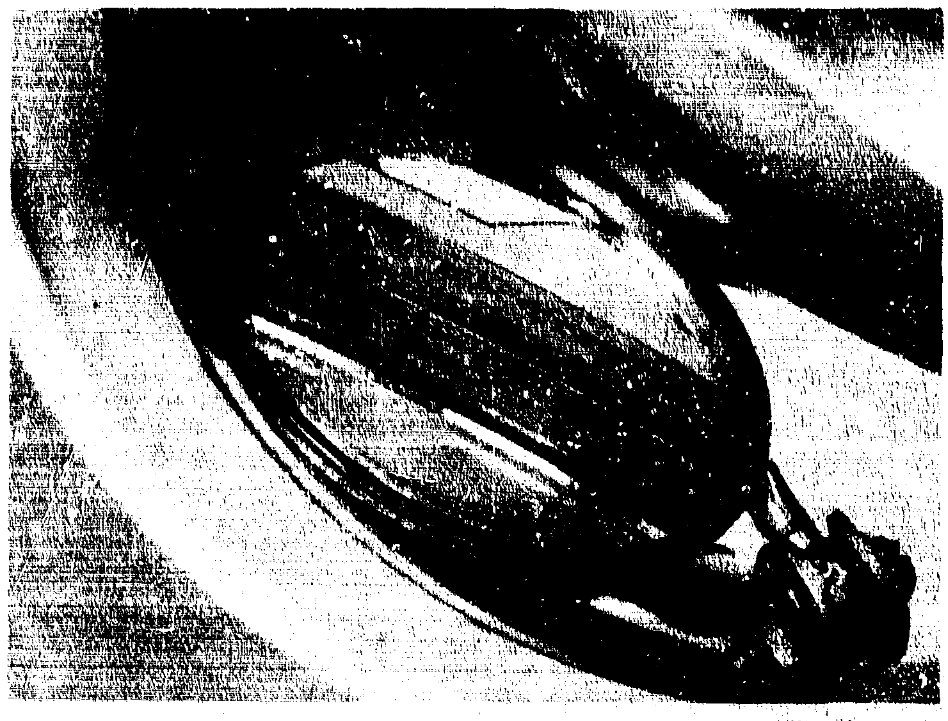

FE 80692

(U) Figure 498. Shutoff Seal Wear, Rig F-35106-8

FE 80694

(U) Figure 499. Disk Surface Post-Test Condition, Rig F-35106-8

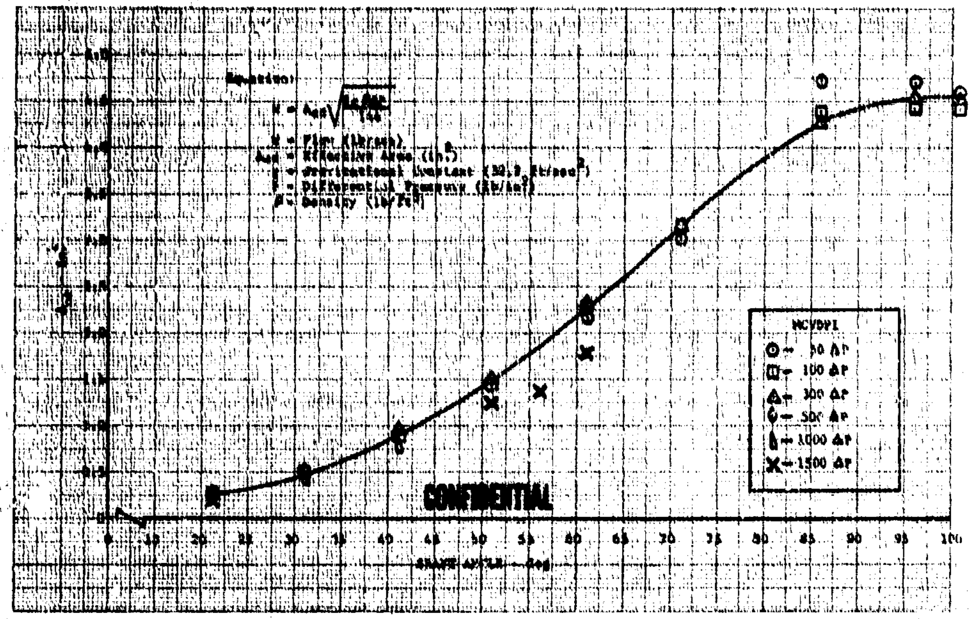

DFC 68918

(U) Figure 500. Water Calibration Results, Rig F-35106-8

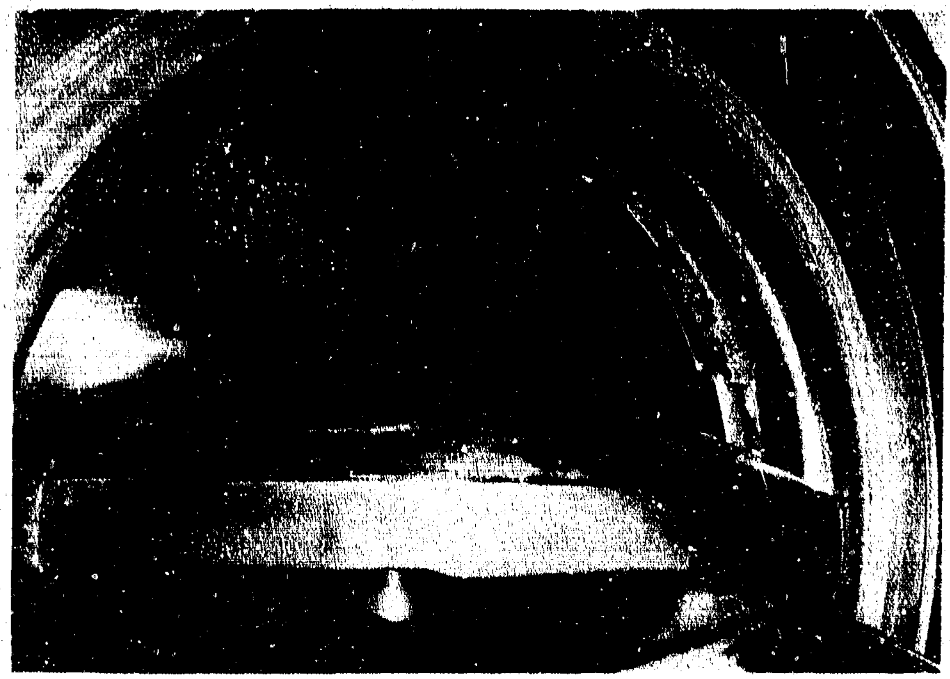

FE 80838

(U) Figure 501. Seal Element Damage After Water Calibration, Rig F-35106-8

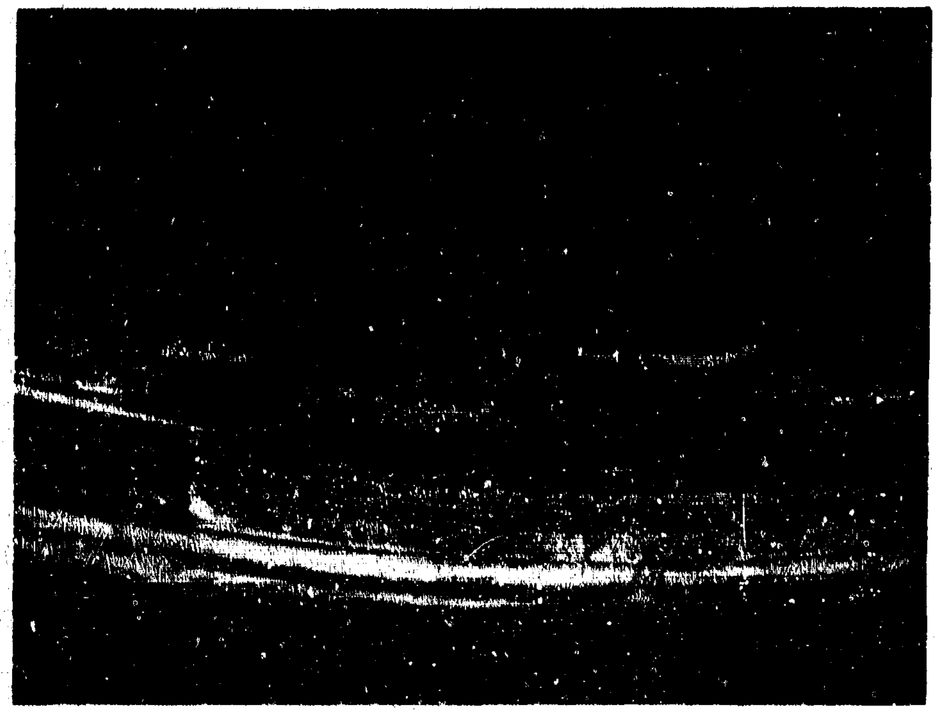

FE 80846

(U) Figure 502. Damaged Seal Element, Rig F-35106-8

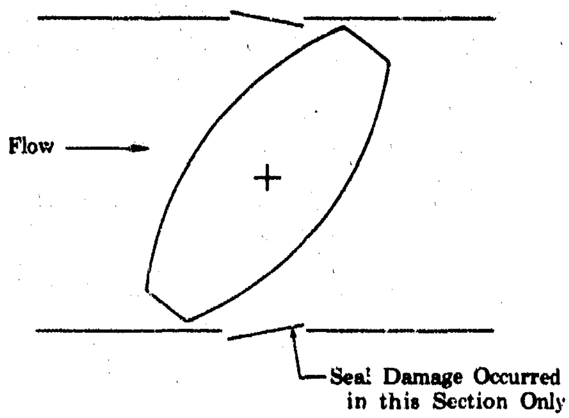

FD 25708

(U) Figure 503. Location of Seal Damage Area

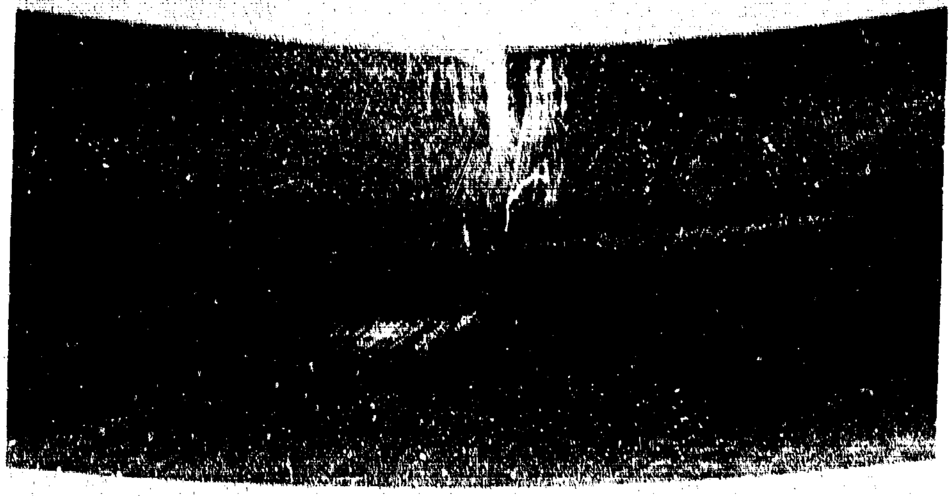

FE 80842

(U) Figure 504. Support Area Crack, Rig F-35106-8

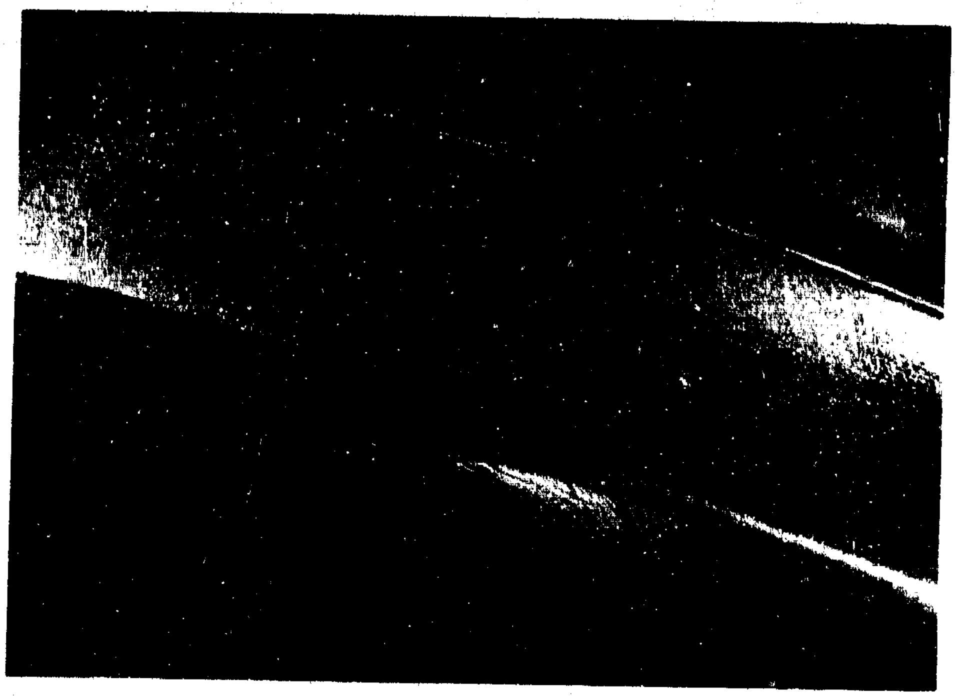

FE 80851

(U) Figure 505. Disk Seal Surface, Rig F-35106-8

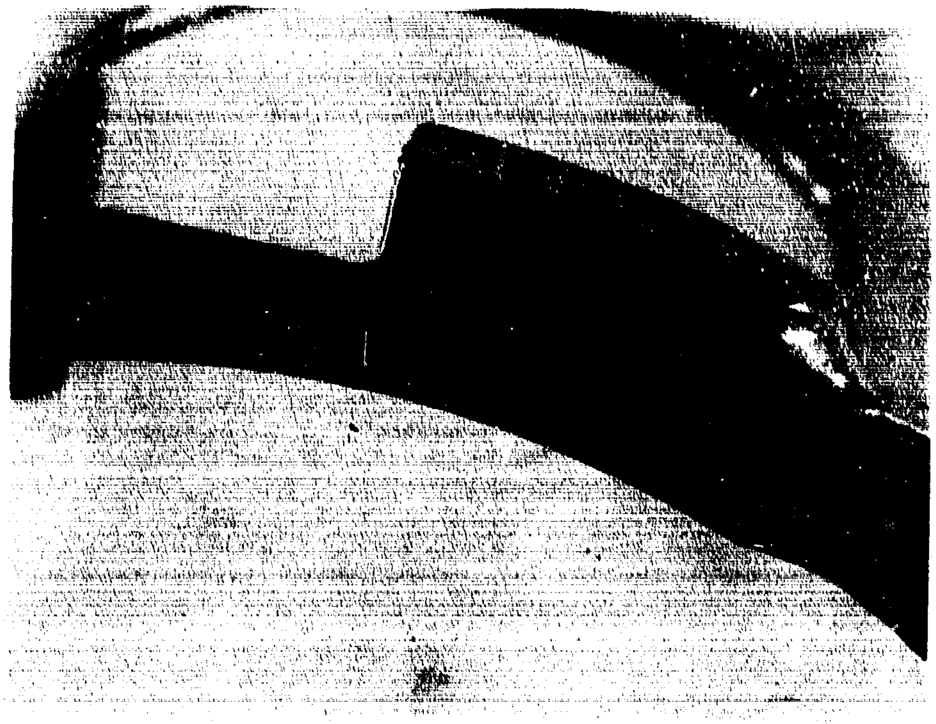

(U) Figure 506. Crack in Cam Drive, Rig F-35106-8

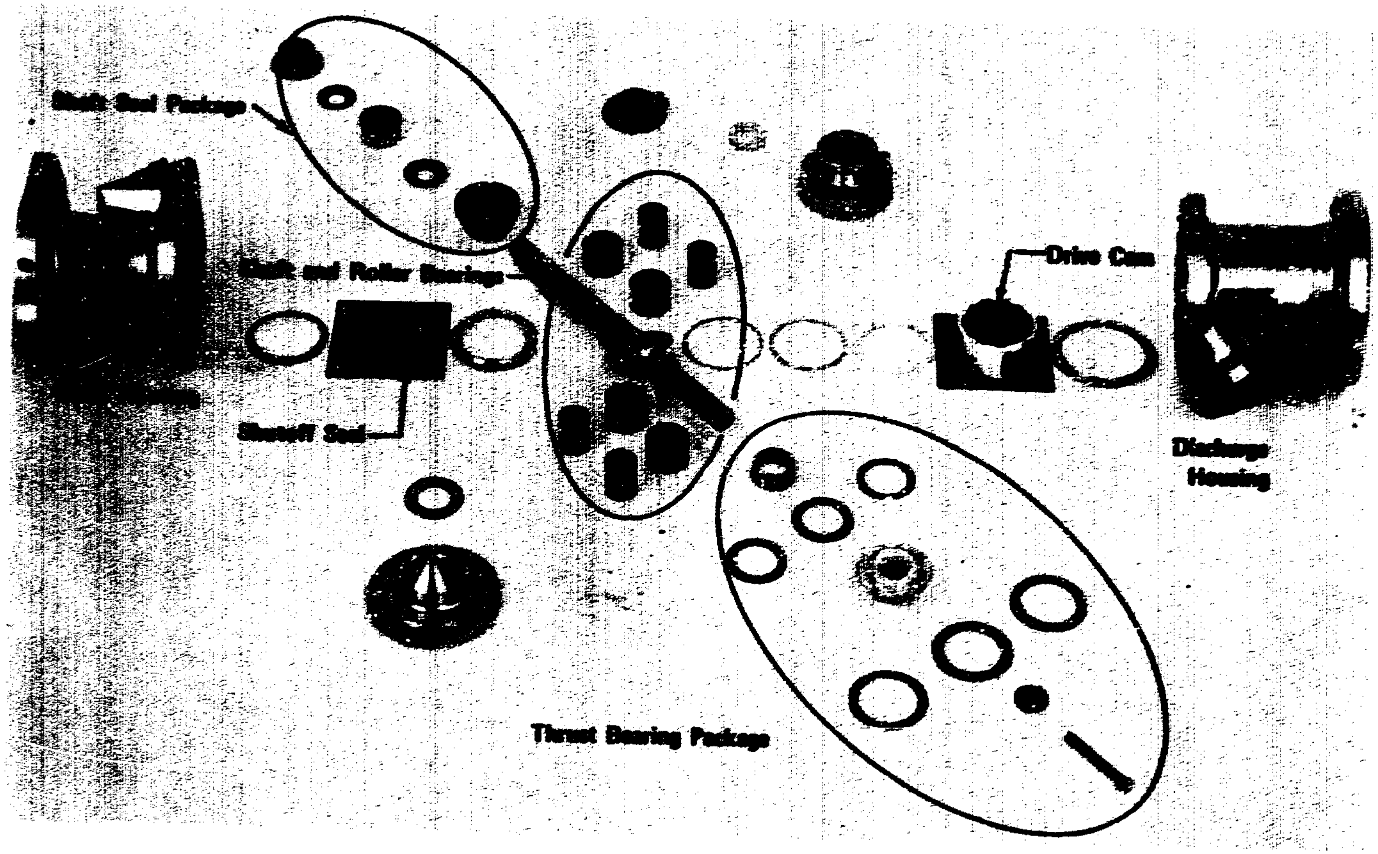

FE 80899

(U) Figure 507. Post-Test Parts Layout, Rig F-35106-8

E. TWO-POSITION NOZZLE COOLANT SUPPLY SYSTEM

E. TWO-POSITION NOZZLE COOLANT SUPPLY SYSTEM

1. Introduction

a. Function

(U) The function of the two-position nozzle coolant supply system is to provide liquid hydrogen coolant to the two-position nozzle from a fixed coolant source at the flow rate necessary to cool the nozzle throughout the engine operating regime, and to provide shutoff of the coolant flow when the nozzle is retracted.

b. Location

(U) The two-position nozzle coolant supply system linkage consists of a two-piece tubular assembly and is attached at one end to a bracket on the preburner heat exchanger (primary nozzle). From this point it extends toward and attaches to a manifold inlet on the two-position nozzle as shown in figure 508. Coolant is obtained through a coolant supply tube, as controlled by a solenoid valve, from the fuel pump interstage line, as shown in figure 509, and flows through the linkage to the two-position nozzle inlet. As the two-position nozzle is extended, the two-piece tubular linkage also is extended as shown in figure 508, and conversely is retracted when the two-position nozzle is retracted.

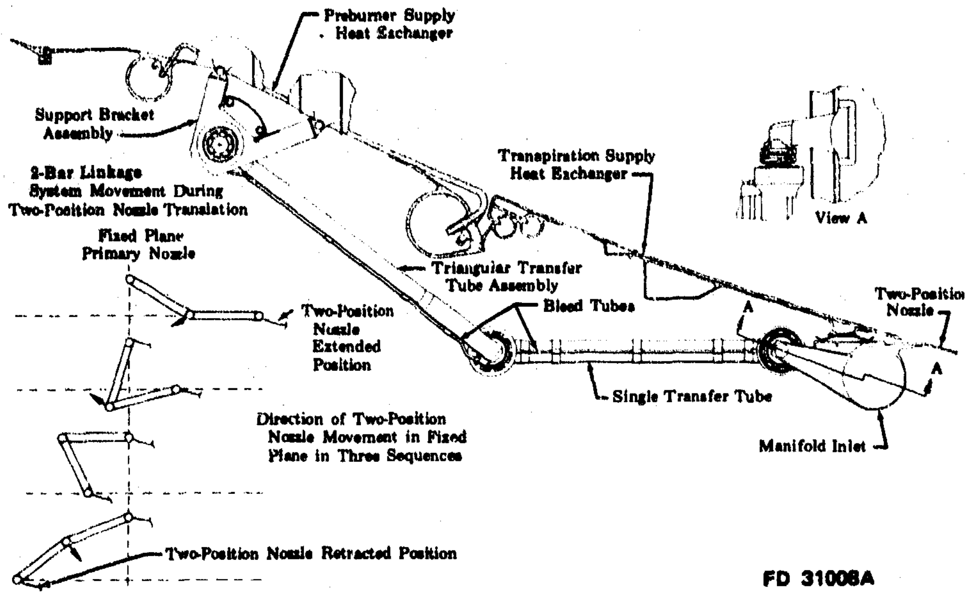

(U) Figure 508. Two-Position Nozzle Coolant Supply System, Extended Position

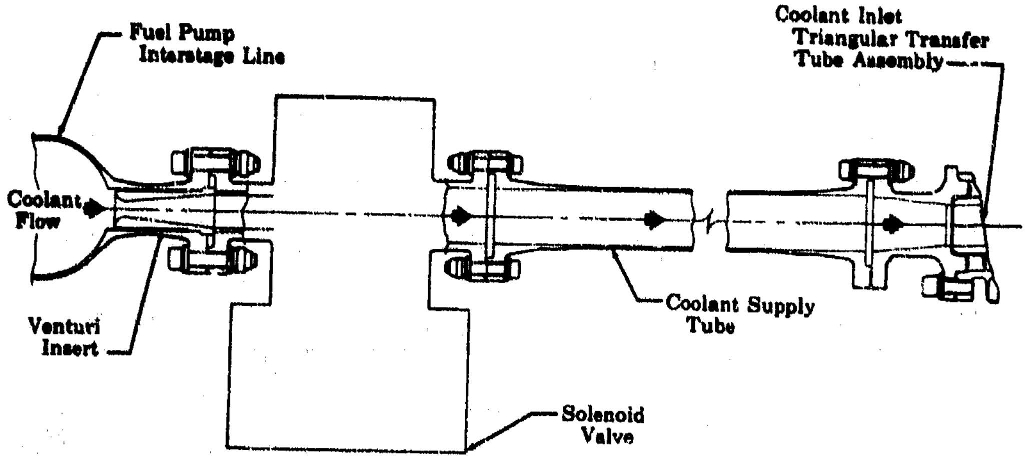

(U) Figure 509. Two-Position Nozzle Coolant Supply System, Control Valve and Venturi

2. Design Requirements

(C) Design requirements for the two-position nozzle coolant supply system are:

1. External leakage shall not exceed 10 sccs of GN_2 at operating pressure per rotary seal.
2. The system shall provide positive shutoff, and shutoff leakage shall not exceed 10 sccs of GN_2.
3. The assembly shall be capable of 10,000 cycles, 500 pressure cycles, 300 starts and 10 hours time between overhauls.
4. Flange leakage shall not exceed 10^{-4} sccs of GN_2 per inch of seal at operating pressure.
5. The desired coolant flow rates are 2.8 lb/sec at 100% thrust, v = 7.0 and 1.4 lb/sec at 20% thrust, and r = 7.0.

3. Design Criteria

(C) Design criteria for the two-position nozzle are:

1. Coolant supply should be obtained from the fuel pump interstage pressure region
2. Coolant flow shall be fully established before the nozzle skirt enters the primary nozzle exhaust plume
3. A coolant flow rate shall always be delivered at or above the minimum flow rate required for cooling the nozzle skirt

4. The shutoff valve shall be mounted as close to the interstage supply flange as possible to reduce dynamic coupling of the fuel pump flow circuit and to reduce the static fluid volume upstream of the valve during flow shutoff.

5. Most advantageous apportionment of the required pressure drop between the shutoff valve and the coolant transfer system to minimize weight

6. Common collection and venting of seal leakage shall be provided.

7. The system shall be capable of withstanding approximate pressure at 1.5 times the maximum operating pressure without permanent deformation or yield.

4. Mechanical Description

(U) The two-position nozzle coolant supply system consists of three basic components: (1) a venturi to establish the required coolant flow rate, (2) a solenoid-operated, two-way valve to provide coolant shutoff, and (3) a two-part tubular linkage with ball joints that incorporates dynamic lip seals and provides a flowpath for the coolant supply to the translating nozzle.

(U) The liquid hydrogen enters the coolant supply system, and immediately passes through a venturi, which sets the coolant flow rate and dynamically decouples the fuel pump flow system from the nozzle coolant supply system. The venturi is sonic-choked at the higher thrust levels and acts as a cavitating venturi at the lower thrust levels. Before the two-position nozzle is extended, the solenoid-operated valve opens allowing coolant to flow through the two-piece tubular linkage (as shown in figure 510) into the nozzle manifold inlet. The nozzle manifold distributes the coolant to the 360 nozzle coolant passages, and the coolant exits into the exhaust stream. The two-position nozzle is extended 52.61 inches to place the two-position inlet in the same plane as the primary nozzle exhaust plane. During translation of the two-piece tubular linkage the triangular segment of the two-part linkage system swings through an arc with a 16-inch radius.

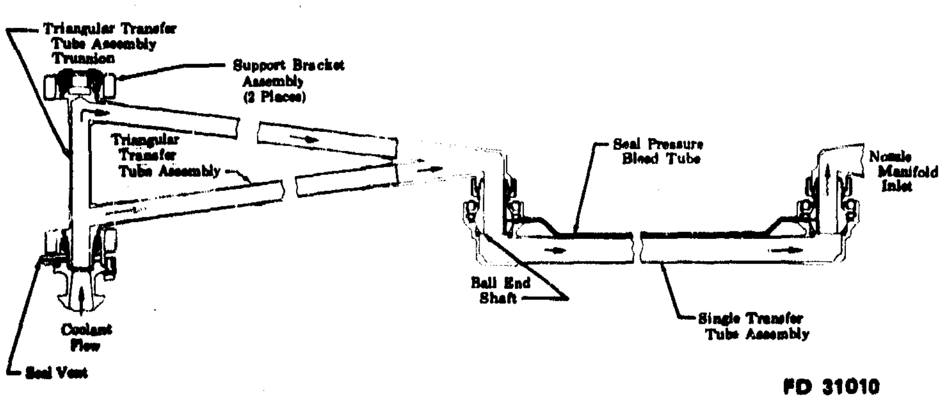

(U) Figure 510. Two-Position Nozzle Coolant Supply System, Coolant Flow

(U) The venturi insert is mounted and held between the fuel pump interstage supply flange and the mating flange on the shutoff valve as shown in figure 509. The venturi geometry is as shown in figure 511.

Venturi Classes	
Coolant Flow At r = 7.0, 100%	Throat Diameter
2.8 lb/sec	0.282 in.
2.5	0.266
2.23	0.252
2.1	0.244

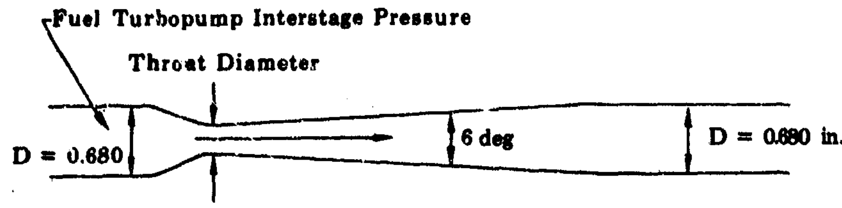

(U) Figure 511. Two-Position Nozzle Choked Venturi Configuration

(C) The cooling system shutoff valve is a solenoid-operated, two-way valve with a minimum design effective area (A_{cd}) of 0.074 in.^{2} The valve will be procured from a vendor per requirements of the purchase Specification PPST-9. Valve specifications include full open to fully closed response of 50 milliseconds and a maximum shutoff leakage of 10 sccs of gaseous nitrogen at the maximum steady-state operating pressure of 2048 psia. A voltage of 28 volts with a maximum current limitation of 1.0 amp defines the electrical characteristics. The maximum allowable valve envelope is a box 4-1/2 x 4 x 6 inches. A weight limit of 4.0 lb for the solenoid valve is imposed. The ambient exterior environment for the valve is -65°F to + 165°F and 14.7 psia to space vacuum.

(U) A 1.000-in. OD tube with a 0.035 in. wall carries the coolant flow from the valve to the first arm of the translating linkage. The tube is the smallest in conjunction with the remaining system pressure drop that may be used without causing the system back pressure to exceed 80% of the venturi inlet pressure and unchoke the venturi, thereby reducing the coolant flow rate from its desired level.

(U) The flow proceeds from the 1.00 OD tube on the engine to the movable nozzle via a two-part tubular linkage. The first bar is a triangular-shaped tubular assembly. Extensions on the base of the triangle attach through two ball bearings, as shown in figures 512 and 513, to a bracket, thereby allowing movement in a fixed plane about its base. The structure has sufficient wheel base along the line of rotation to hold itself rigidly in the rotation plane, despite vibrational or dynamic loading normal to this plane. A second bar is fixed to the apex of the triangular assembly and to the movable nozzle by ball joints at each end, as shown in figures 514 and 515. During nozzle translation, this arm articulates in a vertical plane producing rotary motion at each joint. The ball joint feature allows the arm to readily "rock" out of its articulating plane to accommodate motion of the nozzle attachment joint or the apex joint of the first arm from this plane. Sealing is effected in each ball joint by double Kapton-Teflon laminated lip seals bearing on the spherical ball surface (as shown in figure 514. An interstage vent passage is supplied between seals to reduce the overboard leakage at each joint to acceptable levels. A series of passages in each joint ducts the leakage back to a fitting fixed on the engine. The vent leakage port is fabricated integral with the two-position nozzle manifold, thereby completing the flow passage.

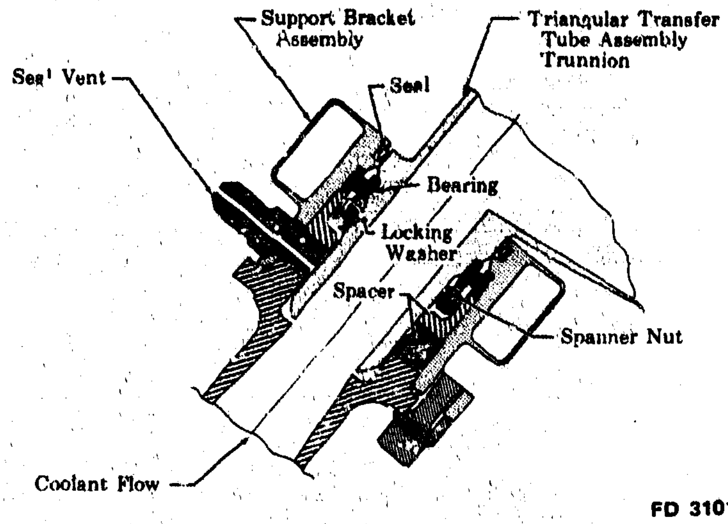

(U) Figure 512. Triangular Transfer Tube Assembly Coolant Inlet Trunnion

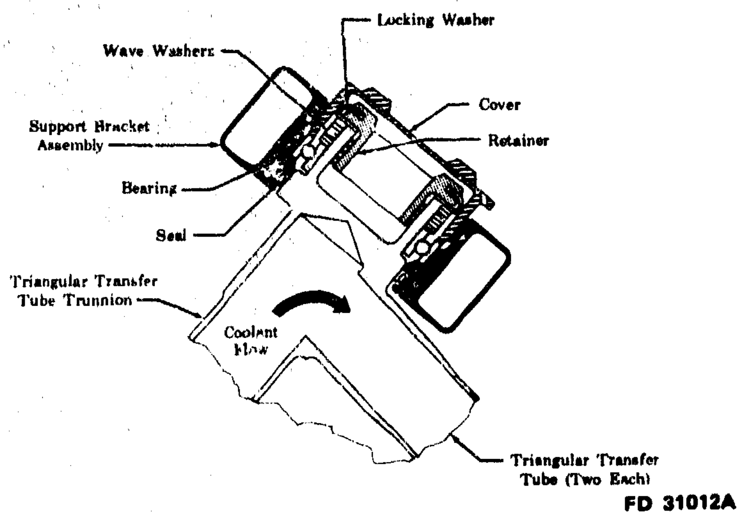

(U) Figure 513. Triangular Transfer Tube Assembly Closed-End Trunnion

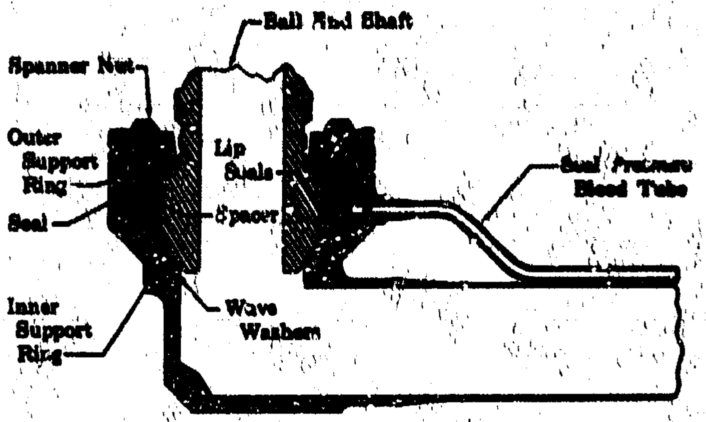

(U) Figure 514. Single Transfer Tube Assembly Ball Joint

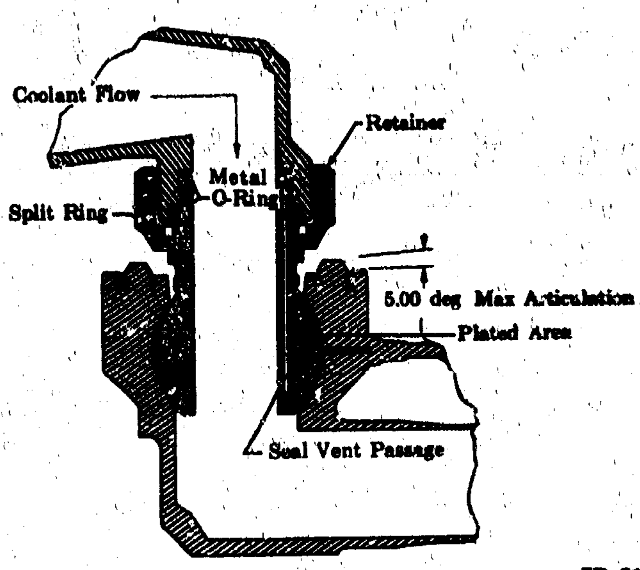

(U) Figure 515. Single Transfer Tube Assembly Ball Joint Passages and Shaft Retention

(U) The mounting bracket that retains the triangular shaped tubular arm is mounted to lugs provided on the upper segment of the primary nozzle, as shown in figure 508. Ball bearings are used to attach each end of the rotating arm to sealed housings at each end of the bracket. The housing, shown in figure 512, contains a bearing, a rotory seal to prevent water vapor from entering the housing and freezing on the bearing, and two lip seals to seal the rotating joint. A vent passage is supplied between the lip seals. The opposite housing, shown in figure 513, contains an identical ball bearing and rotary seal plus a stack of wave washers which: (1) preload the bearing races axially within the housing, and (2) allow the tubular arm to thermally contract independently of the support bracket.

5. Operating Characteristics

(C) The shutoff valve and fuel system were sized to ensure that the venturi discharge pressure does not exceed 80% of the venturi inlet pressure. This design consideration will ensure a choked venturi at all operating conditions. This available pressure drop is distributed between the shutoff valve and feed system to minimize the size of those components. A 1-in. line size was selected because of the relatively low line pressure desired at the dynamic seals. This line size also allowed a large shutoff valve pressure drop, when flowing, which minimized the valve effective area without exceeding the requirements for a choked venturi. The predicted flow characteristics of the system are shown in Figure 516. A maximum flow design point of 2.8 lb/sec was used. A series of venturi sizes are provided to allow overcooling of the nozzle flow during initial development testing. Inlet pressure to the fuel system will vary with a maximum pressure of 2048 psia (100% thrust, r = 7.0). Actuation forces are minimized by the use of ball bearings and ball sockets in the rotary joints. Seal friction will also be minimal due to the low operating pressure.

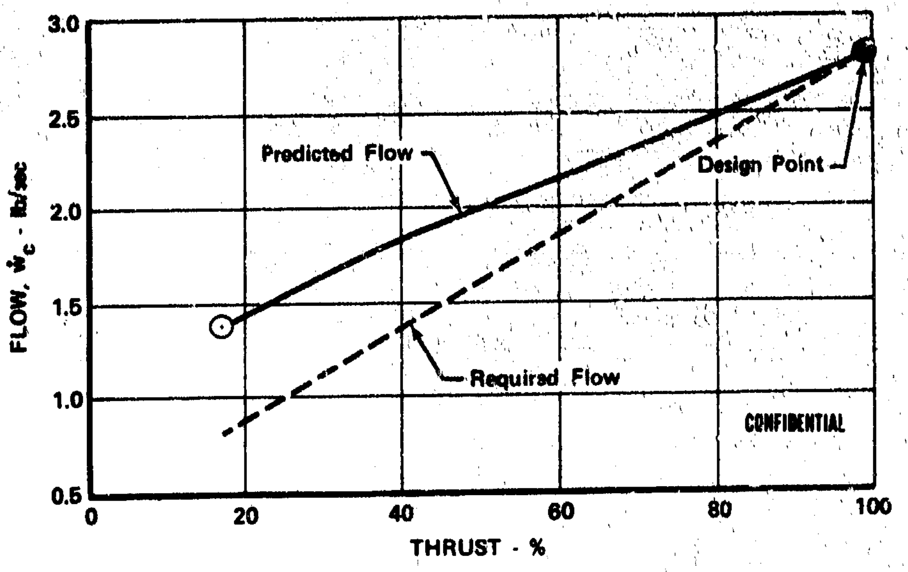

FD 31019

(C) Figure 516. Two-Position Nozzle Venturi Flow, r = 7

8. Design Approach

a. Background

(U) Prior to starting the feed system design, a selection study was conducted for the translating nozzle feed system and included an evaluation of the following configurations:

1. Telescoping Tube - Collapses when nozzle is retracted
2. Telescoping Tube - Extends when nozzle is retracted
3. Flexible Tube
4. Two-part linkage with three rotary joints
5. Two-part linkage with two rotary and one sliding joint.

(U) The telescoping tube approaches were discounted because of the multiplicity of segments and dynamic seals. The flexible tube approach required excessive tube deflection, and would have necessitated rotary joints. Accordingly, the two-part linkage was selected as the simplest approach. The linkage with three rotary joints was finally selected over the linkage with two rotary joints and one sliding joint, because common seal designs could be used, and a rotary seal is less subject to contamination than a translating seal.

b. Design Evolution

(1) Materials

(C) Because of the relatively low pressure involved downstream of the solenoid shutoff valve (400 psia), a high strength plumbing material is not used, to minimize weight. All flanges are deflection, not strength, limited in their configuration. The pressure carrying members are designed to be cylindrical segments, thereby eliminating bending stresses. Other components are sized by geometry rather than by strength requirements, such as use of standard seal sizes, thread sizes, clearance and assembly features. AISI type 347 stainless steel (AMS 5512) is used in fabricating most assemblies. The ball joint shaft is fabricated of austenitic stainless steel type A-286 (AMS 5735). The two-position nozzle manifold inlet neck is fabricated of Inconel 625, the same material as the manifold, to ensure thermal compatibility. All wave washers are fabricated of Inconel 718.

(2) Coolant Supply Tube

(C) The 1.00-in. OD tube with a 0.035-in. wall thickness from the valve outlet to the linkage inlet is subjected to a maximum pressure of 432 psi (1.2 x 360 psi) for a hoop stress of 5750 psi. The 0.035-in. wall thickness was selected over thinner wall section for ease of fabrication and resistance to handling damage.

(3) Tubular Linkage

(U) Similarly, the ID of the tubular linkage arms is limited by flow area requirements and a 0.035-in. wall thickness for fabrication and handling considerations. Because of dynamic loading during nozzle translation, the linkages are subjected to axial loads, end moments, and torsion. Small torsional loads during translation are imposed due to bearing friction and seal drag. These dynamic loads were determined at each instant of translation by graphical differentiation of a position versus time plot for each tubular link. By plotting the direction and magnitude of the loads on each end of a link, the magnitude of the axial and torsional loads was determined. The stresses produced in the link were compared to the available yield stress of 30 ksi and found to be negligible. The critical stress required for axial and torsional buckling was determined to be well in excess of the actual stresses. In the articulating link, the maximum axial stress is 100 psi, the maximum bending stress is 6210 psi and the maximum torsion stress (shear) is 2040 psi. The lowest margin of safety for failure from (1) local buckling of the thin walled tube under axial load, (2) column buckling under a bending load, and (3) buckling caused by a torsion load was found to be 8.6:1.

(4) Ball Joints

(U) The loads acting on the articulating link are transferred through a spherical ball joint that allows rotary motion during translation of the two-position nozzle plus 5 degrees of out-of-plane rotation because of link misalignment from the vertical plane. The spherical surface of the ball joint bears between two mating rings. A stack of wave washers loads one ring against the other via the ball with a governed force of 105 lb to 355 lb depending on stackup tolerances. Pressure blow-off load applies an additional 620 lb of axial load on the fixed bearing ring for a total of 975 lb axial load with a direct bearing stress of 3890 psi or a bearing-stress to yield-stress ratio of 0.046 (A-286 material). To reduce wear between the sliding surfaces, the ball is polished and flash chrome plated. The mating rings are polished and nickel plated. An alternative solution for reducing wear on the ball is to shape the mating rings from a molydisulfide filled polimide plastic. This material has a coefficient of friction against steel of 0.15 to 0.21, a compressive strength of 16,000 psi before permanent distortion, and is inert to cryogenic liquids. Very low wear rates at temperatures to -420°F and in a hard vacuum without lubrication have been observed.

(C) Sealing is accomplished in the ball joint by use of double-lip seals. Each lip seal is a laminate of FEP Teflon and Kapton, sized, bonded and compressed during installation to provide a static seal across each sealing cavity. The compressive unit load is controlled by the depth of its mounting cavity and will be between 8000 to 12,000 psi depending on seal and cavity tolerances. Higher unit loads have been necessary for previous higher pressure applications; however, the above unit load will be adequate because the maximum internal pressure to which the lip seals will be exposed is 400 psi. The same is true for the lip seal assembly used at the rotary joint on the rotating link.

(U) Axial loads on the rotating link are carried by two ball bearings. An axial preload of 40 to 135 lb (depending on tolerance stackup and differential thermal contraction) is applied via a wave washer stack to each bearing. One bearing carries an additional 290 lb axial load because of pressure blow-off. The bearings carry maximum axial loads of 425 lb and 135 lb, respectively, as compared to a recommended axial load limit of 2200 lb. These ball bearings were chosen, however, for their bore size of 1.065 in., which was the minimum size to conveniently clear the 0.750-in. ID flow passage. Radial loads during translation are approximately 25 lb maximum. The anti-friction feature of the ball bearing was desirable in order to reduce the applied load through the linkage structure.

(U) The 25-lb radial load on the bearings is transferred via the support bracket to the primary nozzle structure. The bracket has a pin joint mounting, which ensures that all radial loads are transferred to each of the four legs. All the axial load is transmitted through two legs while the other two legs may slide axially to allow independent thermal contraction of the bracket and the primary nozzle structure. This axial load may be created by inertial motion of the bracket and linkage because of maneuver and gimbaling acceleration and has a value of 92 lb for a 10_g axial acceleration. Simultaneously, the bracket may be subjected to translation, maneuver and gimbaling loads of varying magnitude and direction in its radial plane. In the worst instance, the primary nozzle incurs a concentrated load at one lug of 45 lb axially (shear) and a 32-lb radial ("punch") load . Each lug has an area of 3.1 in^2, (neglecting transfer of load to the supporting nozzle shell) which spreads the concentrated load to a maximum local pressure load of 10 psi.

(5) Inlet Neck

(C) At the opposite end of the tubular linkage, the inlet neck for the two-position nozzle manifold becomes the supporting structure. In addition to its internal pressure, the neck must support loads transmitted to it by the articulating arm of the linkage. The exit area of the inlet neck was sized to be as large as practicable to reduce the local pressure perturbation in the nozzle manifold. It is desirable to have each nozzle coolant passage receive the same total pressure at the inlet from the nozzle manifold and thereby provide symmetrical coolant flow distribution. The local velocity head at the inlet is 3.4 psi(approximately 2% of manifold static pressure) and well within reasonable limits for unsymmetrical pressure distribution. The low local internal pressure of 140 psi maximum allows the walls of the cone-shaped inlet structure to be fabrication limited rather than stress limited. Consequently, the imposed bending, twisting and axial loads were found to be small compared to those required to buckle or overstress the resulting inlet neck.

F. PROPELLANT VENT VALVES

Page

F. PROPELLANT VENT VALVES

1. Introduction

a. Function

(U) The functions of the vent valves are: (1) to vent to overboard the gaseous propellants that boil-off during tanking and chilldown, and (2) to reduce the possibility of propellant pump stall during engine shutdown. The spring-loaded valves are opened by helium pressure and are returned to the normally closed position by the actuator spring when the pressure is removed. A common valve design is used for the three propellant vent valve applications.

b. Location

(U) The propellant vent valves are located: (1) on the preburner injector oxidizer supply manifold, (2) upstream of the preburner fuel valve, and (3) upstream of the main chamber oxidizer valve.

2. Design Requirements

(C) Design requirements for the propellant vent valve are:

1. Leakage Limits: Shutoff seal leakage of liquid nitrogen less than 10 sccs of gaseous nitrogen at operating pressure

2. External valve leakage less than 10 sccs of gaseous nitrogen at operating pressure

3. Flange seal leakage less than 10^{-4} sccs/inch of gaseous nitrogen at operating pressure

4. Durability: 10,000 valve cycles and 500 pressure cycles.

3. Design Criteria

(C) Design criteria for the propellant vent valves are:

1. Based on the design selection study results, the valve is a single acting, two-position, normally-closed ball type valve

2. Maximum effective area is 0.75 square inch, including entrance losses

3. An integral actuator shall cause the valve to open by application of 1500 psig helium pressure and the valve shall close by spring force

4. The valve shall actuate open and remain open, and close and remain closed, with 100 psi maximum upstream pressure

5. Maximum upstream static pressure for valve actuation closed to open is to be 1300 psia

6. The valve shall be capable of opening and remaining open with 250 psi maximum downstream pressure

7. Maximum closed valve static pressure at the inlet is to be 6000 psia.

4. Mechanical Description

(U) The propellant vent valve, shown in figure 517, incorporates an integral ball and shaft that is actuated open by helium pressure and closed by spring force. The valve is sized to provide a maximum effective area of 0.75 in^2 including entrance losses. Provision for installing a flow restriction orifice is incorporated in the inlet seal housing so that the valve effective area may be varied as required for particular applications. A metal-to-metal shutoff seal is incorporated at the valve inlet.

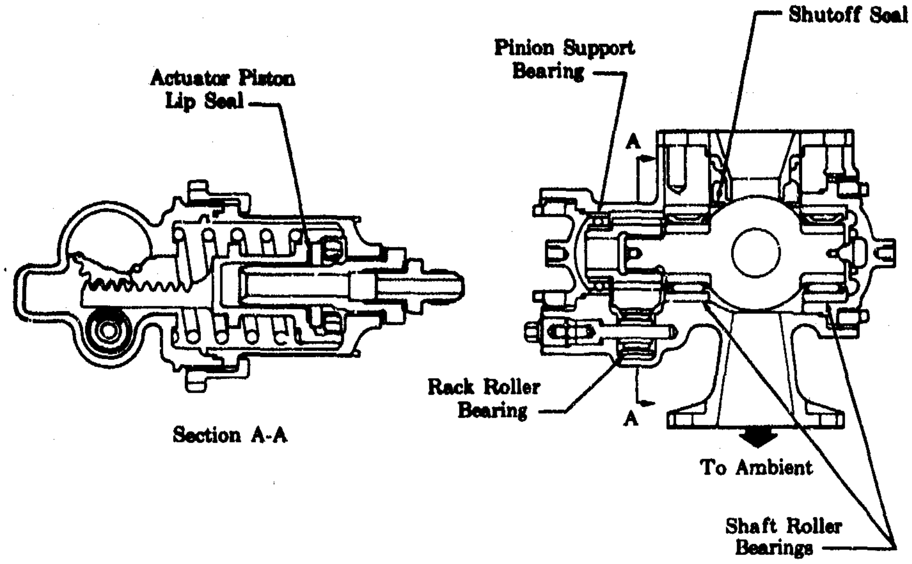

(U) Figure 517. Propellant Vent Valve

(U) The shutoff seal (figure 518) uses a deflecting seal plate supported by a thin metal cylinder that allows the silver-plated lip to center on the spherical surface of the ball and provides support when the lip is deflected by contact with the ball surface. The seal carrier radially supports the thin cylinder at high valve inlet pressures. Propellant leakage is minimized by limiting the valve assembly high pressure sealing requirements to the shutoff seal. All shutoff seal material is Inconel 718 (AMS 5663).

(U) All static seals in the valve are required to seal only when the valve is open and are therefore exposed to static pressures of less than 900 psia. The valve internal static seals are compressed, trapped TFE Teflon. The seal recesses are double-piloted with a maximum loose fit of 0.0015 inch to prevent Teflon extrusion. One high-pressure static seal will be required in the flange to which the valve is mounted.

(C) The ball shaft is supported by two caged needle roller bearings. The maximum roller bearing static load per bearing is 1815 pounds and the maximum dynamic load is 570 pounds per bearing. A full complement ball bearing is used to support the pinion. This bearing is lightly loaded and serves also to axially position the pinion and ball shaft. The rollers, balls, and races of these bearings are made of AISI 440C stainless steel (AMS 5630).

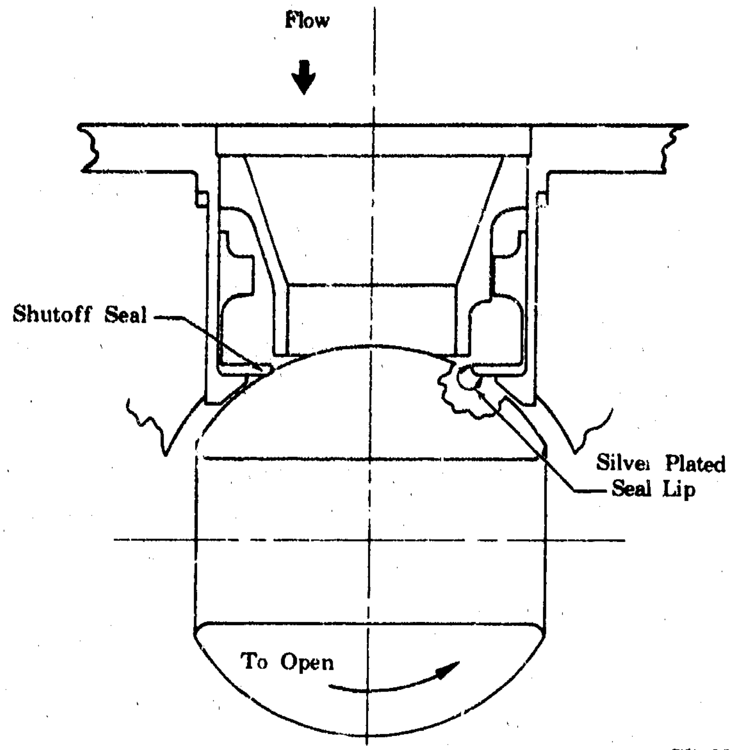

FD 29202

(U) Figure 518. Shutoff Seal

(U) The propellant vent valve is actuated to the open position by a pneumatically operated rack acting on the pinion, which is splined to the valve shaft. The rack is supported by a lightly loaded roller bearing selected for its compactness and availability. The backlash between the rack and pinion is adjusted by selecting the appropriate size classified rack support bearing sleeve. The maximum contact stress between the rack and pinion involute surfaces is 100,000 psi. A-286 stainless steel (AMS 5737) was selected for the rack and pinion because of its good tensile strength and excellent impact strength at cryogenic temperatures. The involute surfaces of the rack and pinion are coated with MOS_2 dry film lubricant to minimize wear. A combination of 17 gear teeth and 18 splines was selected for the pinion to facilitate alignment of the valve ball. Included in the actuator design is the provision for incorporating a helium flow control orifice to adjust valve response time required by limiting the rate of actuator pressure rise.

(U) Helium leakage into the actuator assembly is prevented by a single lip seal. This seal is laminated Kapton-F and FEP Teflon.

(U) A 17-7PH stainless steel (AMS 5673) spring is used to return the valve to its normally closed position when actuator pressure is vented. This material was selected because of its high strength. It has a spring fatigue life five times greater than required. The calculated weight of the valve assembly is 5.6 lb.

5. Operating Characteristics

(U) The actuator is designed to provide satisfactory valve actuation at 1300 psia inlet pressure with 1200 psi helium pressure. Provision is included for a helium flow control orifice to adjust valve response time by limiting the rate of actuator pressure change.

6. Design Approach

a. Background

(U) Pre-development work was not conducted nor investigations made in Phase I (Contract AF04(611)-11401) for the propellant vent valves.

b. Design Evolution

(U) The demonstrator engine requires fuel and oxidizer vent valves for engine conditioning prior to start and/or pump discharge bleed during shutdown. A common valve design is satisfactory for the three required locations. A vent valve selection study was conducted to evaluate valve candidates that would satisfy the vent valve requirements and to select the most suitable design.

(U) The basic requirements for this valve were:

1. A positive shutoff seal
2. Two-position actuation (off-on)
3. Normally closed position requiring actuation pressure to remain open
4. A maximum effective area of 0.75 sq. in.

(U) A preliminary investigation revealed three valve types capable of fulfilling these requirements. These valve candidates; a poppet valve (figure 519), a ball valve (figure 520), and a blade valve (figure 521), were then subjected to detailed studies to determine their relative rank with respect to seal development requirements, weight, reliability, contamination tolerance and other selection criteria.

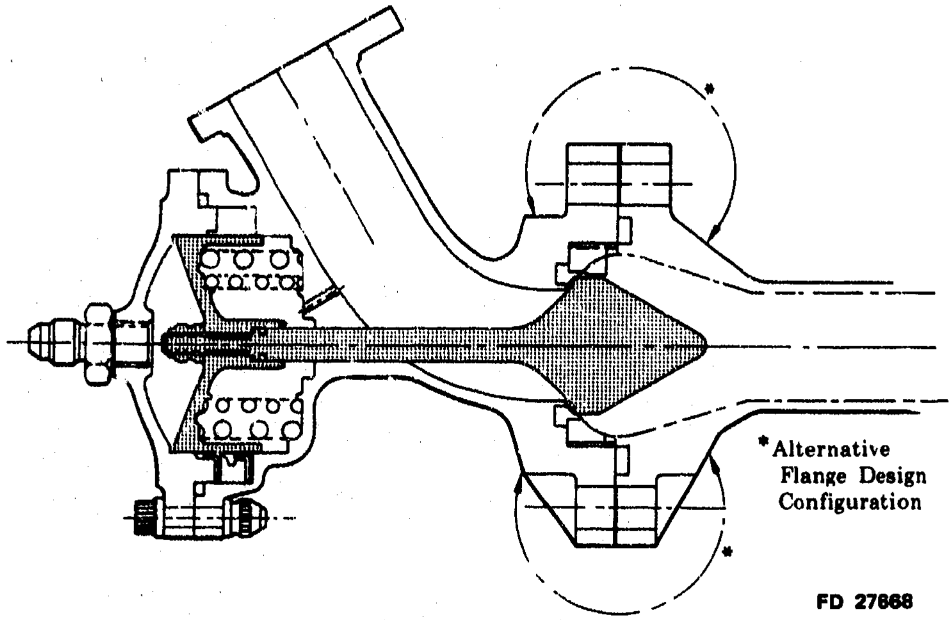

(U) Figure 519. Poppet Valve

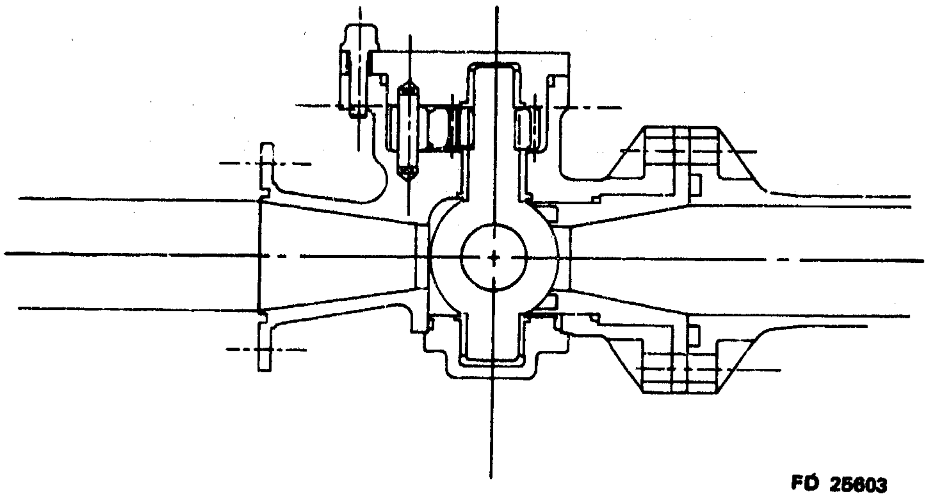

(U) Figure 520. Ball Valve

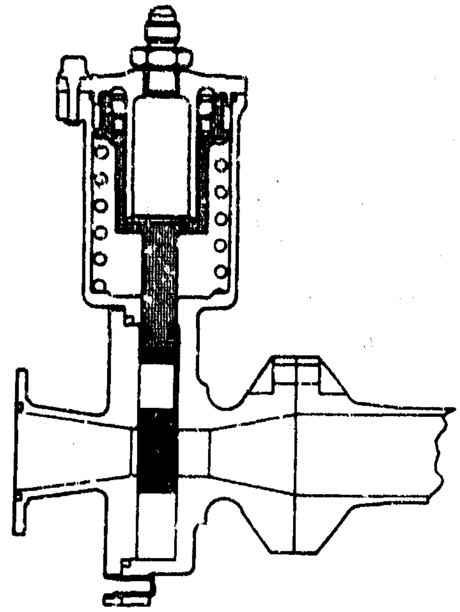

(U) Figure 521. Blade Valve

(U) At the conclusion of the study, a point rating system and weighting scale were established as shown on table LXIX. The weighting scale resulted from averaging four similar independent scales from Design and Project Engineering. Each valve type was rated for each selection criterion. The valve type most satisfactorily meeting the requirements of each criterion was assigned the maximum number of points for that criterion, the other types receiving proportionately less. Based on the total point system, the ball valve design shown in figure 520 received the highest rating from all evaluators and was selected for the fuel and oxidizer vent valves.

(U) The ball valve offers an excellent combination of the following features:

1. Light weight
2. Compact - excellent packaging flexibility
3. Small seal diameters for both static and dynamic seals
4. Low actuator requirements
5. Excellent resistance to dynamic seal contamination due to seal wiping action.

(U) Table LXIX. Relative Development Ranking

Selection Criteria	Weighting Factor (Maximum Number of Points)	Poppet Valve	Ball Valve	Blade Valve
Weight (Valve and High Pressure Flanges)	90	75	85	90
		75	85	90
		75	85	90
Shutoff Seal Development Required	100	100	50	30
		100	70	70
		50	100	80
Actuator Volume	50	11	50	14
		11	50	14
		10	50	15
Actuator Leakage Circumference	50	14	50	34
		14	50	34
		15	50	35
Reliability	85	85	60	75
		85	70	50
		65	85	65
Packaging	50	20	50	40
		30	50	50
		50	35	40
Ability to Combine with Adjacent Components	60	40	60	60
		30	60	60
		40	60	60
High Pressure Seal Diameter	55	37	55	55
		37	55	55
		35	55	55
Manufacturing Ease	45	45	25	35
		45	40	40
		36	14	45
Complexity	35	35	15	25
		35	20	20
		35	7	25
Contamination Tolerance	70	30	70	50
		30	50	40
		21	56	35
Total Points Possible	690	492	570	508
		492	600	523
		432	599	551

"PRECEDING PAGE BLANK-NOT FILMED".

G. HELIUM SYSTEM

G. HELIUM SYSTEM

1. Introduction

a. Function

(U) The function of this system is to supply helium to the engine at 1500 ±50 psia and 500°R for valve and seal actuation and engine purges. The system consists of solenoid actuated valves, check valves, a relief valve and the flow control orifices required for helium management. Figure 522 schematically depicts the pneumatic system.

(U) Helium is used to actuate the three engine vent valves and the three turbopump liftoff seals. Helium purges are provided for the preburner primary and secondary injector manifolds and for the main chamber oxidizer manifold. A purge is also provided for the oxidizer turbopump shaft seal package.

b. Location

(U) The helium system will consist of a modular package that will include the required solenoids, check values and flow control orifices. The package will be attached to the transition case flange and located between the fuel and oxidizer turbopumps.

2. Design Requirements

(C) Design requirements for the helium system are:

1. External leakage shall not exceed 10 sccs of GN_2 at operating pressure
2. Shutoff leakage shall not exceed 10 sccs of GN_2
3. Components shall be capable of 10,000 valve cycles, 500 pressure cycles, 300 starts and 10 hours operating time between overhauls
4. Flange leakage shall not exceed 10^{-4} sccs of GN_2 at operating pressure
5. Material used must be compatible with contacting fluids and for mating with stainless steel lines
6. Components shall operate in an ambient environment ranging from space vacuum to 15 psia over temperature range from -65°F to +165°F
7. Electrical power is available at 28 vdc with a maximum current per solenoid of 1.0 amp at average operating condition.

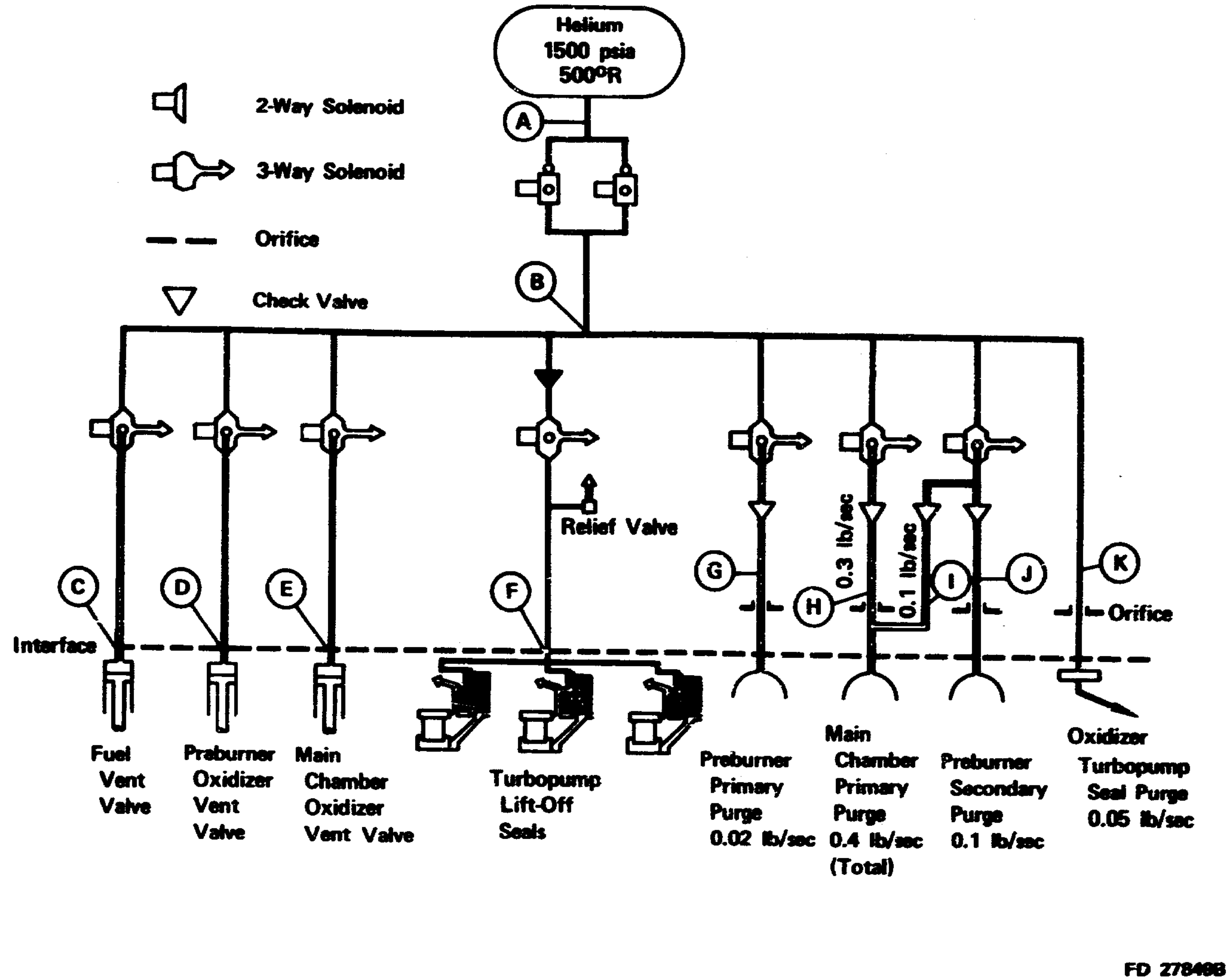

(U) Figure 522. XLR129-P-1 Helium System

3. Design Criteria

(U) Design criteria for the pneumatic system are:

1. Redundant (2 parallel) supply shutoff valves for the helium system.

2. Separate solenoid valves to actuate the three engine vent valves.

3. A single solenoid valve to actuate the three turbopump liftoff seals. A check valve and relief valve to prevent backflow and overpressure of helium system in the event of a turbopump bellows failure.

4. Three solenoid valves to control the preburner injector primary purge, secondary purge, and main chamber injector purges; the main chamber injector purge requires two levels of flowrate. Four flow control orifices to meter the purge flowrates. Five check valves to prevent backflow into the helium system.

5. A metered purge flow is required for the oxidizer turbopump seal package.

6. The system shall not require electrical power during coast periods.

7. The system shall be mounted on the engine as a unit.

8. Failure modes for the solenoids shall be consistent with safe engine operation.

9. System weight shall not exceed 30 pounds.

10. The components shall not be damaged or permanently deformed nor shall the original calibration be affected by any inlet pressures up to 1.5 maximum operating pressure over the range of operating temperatures.

11. The components shall withstand the following flight loads

    6g transverse
    11g axial
    10g axial with 2g transverse
    6.5g axial with 3g transverse
    3g axial with 6g transverse.

12. The solenoid valves shall have a full stroke actuation time of 50 milliseconds.

13. The overall system shall be sized in accordance with the following table (Ref. figure 522).

Designation	Location	ΔP_{max} at Flow	Minimum Effective Area (AC_d)	Remarks
A-B (1-S, & 2-S)	Main Helium Supply	62.5 psid at 0.54 lb/sec		Consider equal flow through 1-S and 2S
B-C (3-S)	Fuel Vent		0.004 $in.^2$	
B-D (4-S)	Preburner Oxidizer Vent		0.004 $in.^2$	
B-E (5-S)	Mainburner Oxidizer Vent		0.004 $in.^2$	
B-F (1-C, 6-S, 1-R)	Turbopump Shaft Seal		0.004 $in.^2$	
B-G (7-S, 2-C)	Preburner Primary Purge	200 psid at 0.02 lb/sec		
B-H (8-S, 3-C)	Mainburner Purge	300 psid at 0.3 lb/sec		
B-I (9-S, 4-C)	Mainburner Purge	300 psid at 0.2 lb/sec 0.1 lb/sec		Through solenoid Through check valve
B-J (9-S, 5-C)	Preburner Secondary Purge	150 psid at 0.2 lb/sec 0.1 lb/sec		Through solenoid Through check valve
B-K (10-S)	Turbopump Dynamic Seal Purge	100 psid at 0.02 lb/sec		

4. Mechanical Description

(U) Nine solenoid-operated valves are required for the engine system. Two types are used: (1) direct-lift-operated and (2) pilot-piston pressure-actuated. Of these two types, both two-way and three-way valves are used. In the direct-lift type, the pull of the solenoid coil opens the valve port directly by lifting the plunger and stem assembly off the valve seat. These valves depend solely on the power of the solenoid for operation.

(U) For the valves requiring higher flow and higher operating pressure drops, pilot-operated valves are used. In these valves, the plunger and stem assembly does not open the main port directly, but opens the pilot orifice and the source pressure forces the piston off the seat, opening the valve and keeping it open.

(U) Valve solenoids are energized with 28 (±1) vdc and have response times of 50 milliseconds. Maximum current drain for each energized solenoid is 1.0 ampere.

(U) A description of the valves selected for this system is provided in table LXX.

(U) Table LXX. Solenoid Valve Description

Valve Description	Valve Type	Energized Position
Fuel and oxidizer vent solenoid valves (3)	Three-way direct-operated	Open
Preburner primary injector purge solenoid valve	Three-way direct-operated	Closed
Turbopump liftoff seal solenoid valve	Three-way direct-operated	Open
Main supply shutoff solenoid valves (2)	Two-way pilot-operated	Open
Main burner injector purge solenoid valve	Three-way pilot-operated	Closed
Preburner secondary purge solenoid valve	Three-way pilot-operated	Closed

(U) A total of five check valves are required to prevent backflow and contamination of the helium system. They are utilized as follows: four valves to isolate the engine purge system, and one valve to isolate the turbopump shaft seal actuation system.

(U) A relief valve is required for the turbopump liftoff seal actuation system. This valve is included as a fail-safe feature in the event of a shaft seal bellows failure.

(U) Replaceable orifices are required to establish the helium flowrates as required. Four orifices are in the engine purge flow lines.

(U) Since the helium system is a vendor supplied item, a hardware mechanical description will be provided when the system design is complete. The envelope allowed for the helium system is shown on figure 523.

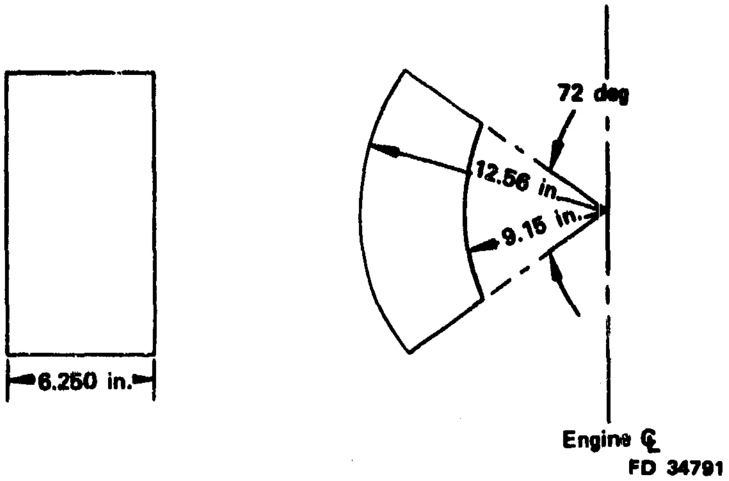

(U) Figure 523. Helium System Envelope

5. Operating Characteristics

(U) An engine cycle is described as follows:

1. COOLDOWN - The two supply solenoid valves are opened and remain open until shutdown. The oxidizer and fuel vent valves are sequenced open and closed to facilitate engine cooldown. All other solenoid valves are closed.

2. START - The turbopump liftoff seal solenoid valve is opened, allowing helium to actuate the liftoff seals in the turbopumps. The preburner secondary and the main chamber injector purge solenoid valves are initially opened and then closed during the start transient. The preburner primary purge solenoid valves remains closed.

3. STEADY-STATE OPERATION - The two supply solenoid valves and the turbopump liftoff solenoid valves are opened, all other valves are closed.

4. SHUTDOWN - The three purge solenoid valves and the main burner oxidizer vent valve are opened during deceleration.

5. COAST - All solenoid valves are de-energized. The helium remaining in the system downstream of the shutoff solenoid valves is vented overboard.

(U) Figure 524 represents this typical mission. The system is designed to operate with helium supplied at 1500 psi and 500°R.

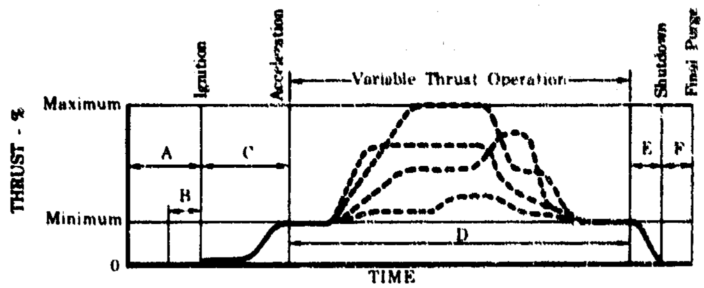

⊕ Ground Supplied

	Cycle - Seconds		
	1st	2nd	3rd
A Fuel Vent	⊕	120	120
B Oxidizer Vent	⊕	60	60
C Accelerate to Minimum Thrust	2.0	1.5	1.5
D Typical Mission	600	600	600
E Shutdown	1.0	1.0	1.0
F Final Purge	1.0	1.0	1.0

	Energized/Cycle
Supply Shutoff Solenoids (2)	A Through F
Fuel Vent Valve Solenoid	A
Main Chamber Oxidizer Vent Valve Solenoid	A and E
Preburner Oxidizer Vent Valve Solenoid	A
Turbopumps Liftoff Seal Solenoid	C Through E
Preburner Oxidizer Primary Injector Purge Solenoid	E and F
Preburner Oxidizer Secondary Injector Purge Solenoid	C, E and F
Main Chamber Injector Purge Solenoid	C, E and F

FD 27850

(U) Figure 524. Helium System Mission Definition

(U) Failure modes for the system valves were evaluated regarding their effect on engine operation location. The results of this evaluation are shown in table LXXI.

6. Design Approach

(U) Because the helium system is a vendor supplied item, and will be purchased in accordance with P&WA preliminary purchase specification T-8 the hardware design approach will be provided when the system design is complete. Neither pre-development investigations or studies were conducted because they were not considered necessary for this system.

(U) Table LXXI. XLR129 Helium System Solenoid Valve Failure Analysis

Location	Failure Mode	Failure Effect During Engine Operation: Coast	Cooldown	Start	Operate	Shutdown
Supply valve	Closed	No effects because of redundant valve	No effects because of redundant valve	No effects because of redundant valve	No effects because of redundant valve	No effects because of redundant valve
Fuel vent valve	Closed	None	Normally open - prevents normal cooldown	None	None	None
Preburner oxidizer vent valve	Closed	None	Normally open - prevents normal cooldown	None	None	None
Main burner oxidizer vent valve	Closed	None	Normally open - prevents normal cooldown	None	None	Possible oxidizer pump cavitation and piston malfunction
Turbopump liftoff seal valve	Open	None - helium shut off at supply	Normally closed - bearing coolant flow leakage through labyrinth seal	None	None	None
Preburner primary purge valve	Open	None - helium shut off at supply	Normally closed depletes helium supply at 0.02 lb/sec	Normally closed - depletes helium supply at 0.02 lb/sec	Normally closed depletes helium supply at 0.02 lb/sec at part thrust	None
Preburner secondary purge valve	Open	None-Helium shut-off at supply	Normally closed depletes helium supply at 0.20 lb/sec	None	Normally closed depletes helium supply at 0.20 lb/sec at part thrust	None
Main chamber oxidizer purge valve	Open	None-Helium shut-off at supply	Normally closed depletes Helium supply at 0.30 lb/sec	None	Normally closed depletes helium supply at 0.30 lb/sec at part thrust	None

H. STATIC SEALS

H. STATIC SEALS

1. Introduction

(U) During seal rig, component, and staged combustion rig testing conducted in Phase I (Contract AF04(611)11401), excessive overboard static seal leakage was experienced. Dual static seals were incorporated in the rig couplings. The measured primary static seal leakage at maximum thrust during the staged combustion rig test firings was equivalent to an impulse loss of approximately 2 seconds, and additional uncontrolled overboard leakage was visible. Static pressure tests with the main chamber oxidizer valve indicated the leakage problem was aggravated by excessive flange separation and inadequate static seals.

(U) Under the current demonstrator engine program, extensive high pressure coupling rig design analysis was conducted. Conventional analysis methods proved inadequate for lightweight high pressure coupling deflection and weight optimization predictions, so computer analysis programs were developed to assist the designer. A 6-in. aluminum hydrostatic coupling rig was designed and tested for stress and deflection at XLR129 operating pressures. A finite element disk analysis computer program was then modified to provide satisfactory deflection prediction correlation with the test results. Continued analysis indicated that "zero deflection" coupling flanges would not meet the "lightweight" engine requirement, but that allowing deflection of 0.002 in. total at the sealing diameter would significantly reduce coupling weight, especially if the raised face configuration was utilized. The 0.002 in. deflection allowance and raised face configuration were adopted for the seal test rig design and specified for the demonstrator engine coupling designs. A simplified finite element computer program was written and utilized for the engine flange designs.

(C) A 5-inch Inco 718 seal test rig was designed, using the finite element computer program. It was to have 0.002 in. (total) deflection at the sealing diameter at 7000 psig internal pressure at LN_2 temperature. Six commercial cryogenic seals with "zero leakage" and 0.002 in. claimed deflection capability were selected for test in the rig. Twenty-nine cryogenic pressure-cycle endurance and seal leakage tests were completed. Nineteen configurations of 8 basic seal designs were tested. The toroidal-segment seal configuration was selected for the demonstrator engine couplings, and a design-standard configuration was established, as shown in figure 525.

(U) Deflection tests conducted during the seal pressure cycle endurance and leakage test program confirmed the validity of the finite element computer analysis technique. The computer program model was kept current during the tests to provide a good stress and deflection analysis capability for the demonstrator engine flanges.

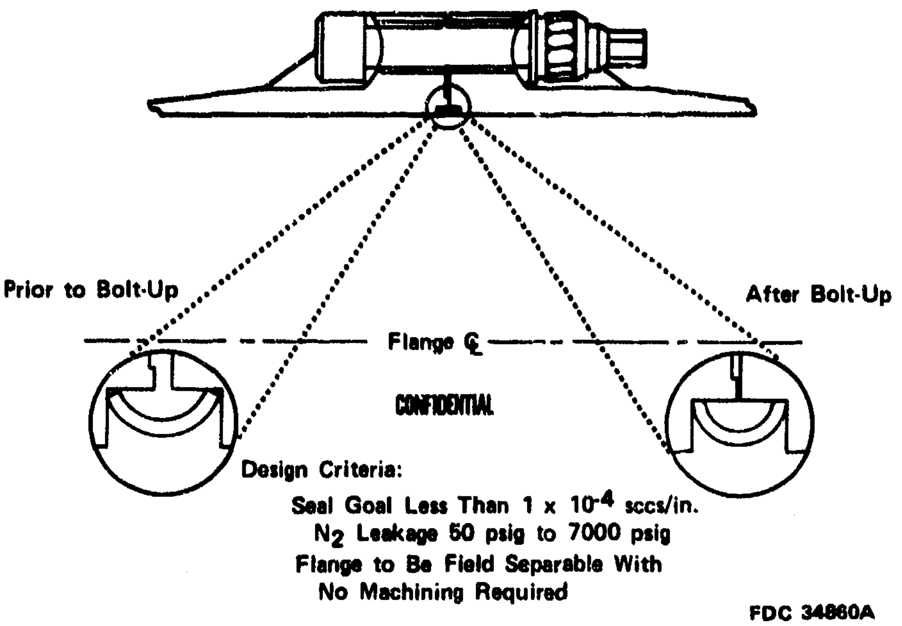

(U) Figure 525. Inverted C-Ring Detail Part, Fit and Installed Shape

2. Design Requirements

(C) The general structural design requirements for the XLR129-P-1 engine, as listed in Section II, were also used for the seal rig design. In addition, the following requirements were specified:

1. Maximum leakage: 10^{-4} standard cc/sec N_2 per inch of seal circumference

2. Durability: 500 pressure cycles (300 starts, 10 hours between overhaul).

3. Design Criteria

(C) Design criteria for the seal test rig are:

1. Size: Five inch inside diameter pressure vessel

2. Material: Inconel 718 (PWA 1010)

3. Maximum temperature for test: Ambient (+70°F)

4. Minimum temperature for test: -320°F (LN_2)

5. Maximum pressure at -320°F: 7000 psig

6. Minimum pressure at both minimum and maximum temperatures: 0 psig

7. Vibration: Seal rig will not be used for vibration tests. Flanges must be designed to meet contract vibration requirements.

8. Pressure Cycles: Seal rig will be designed and tested for 500 pressure cycles (from zero-to maximum-to zero) at -320°F (test rig will not be allowed to warm between pressure cycles)

9. Thermal Cycles: Thermal cycles will be run on seals that meet the pressure cycle test leakage goal

10. Coupling Deflection: 0.002-in. total at sealing diameter (both flanges) with 7000 psig internal pressure and temperature of -320°F

11. The rig design must allow progressive reoperation so a minimum of 5 different seals may be tested.

4. Mechanical Description

(U) The seal test rig, as shown in figure 526, consists of a cylindrical pressure vessel approximately 20.0-in. long with a 5.00-in. ID made in halves and joined together centrally by 15 tie bolts. The pressure vessel, flanges and tie bolts are made of Inconel 718. Ports are provided to attach the vessel to a nitrogen pressure source and to allow access for internal instrumentation. The pressure vessel is surrounded by a cylinder that is sealed at both ends and acts as a collector for seal leakage. Schemes for reworking the seal gland to provide the proper gland configuration for each seal to be tested were included in the design. A flange rework scheme for moving the raised face pivot point inside the sealing diameter was also included as shown in figure 527.

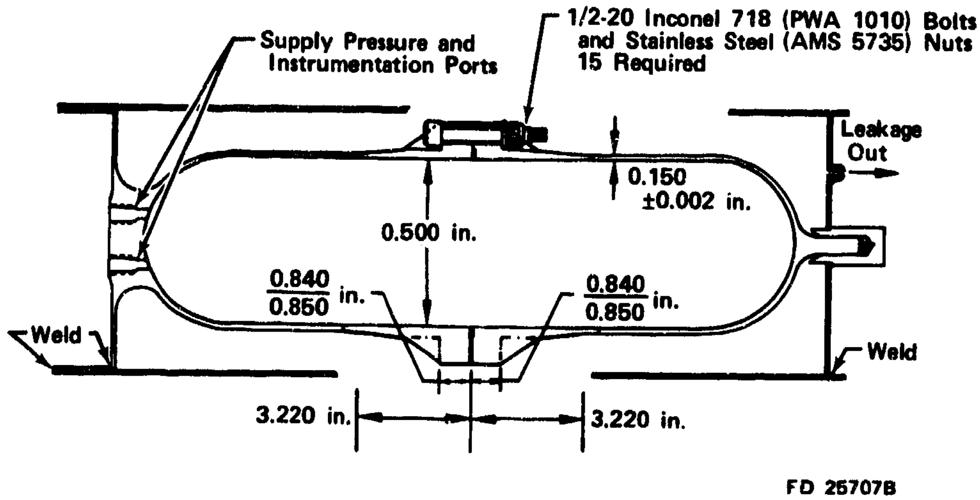

(U) Figure 526. Static Seal Rig

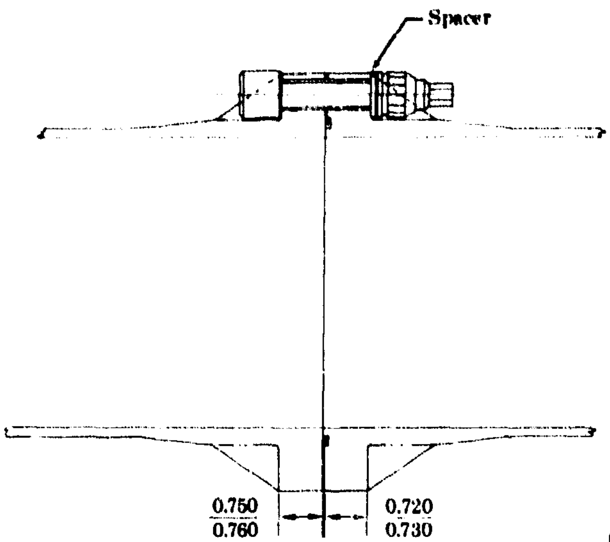

FD 25706A

(U) Figure 527. Flange Rework, Static Seal Test Rig

(C) Two hydrostatic pressure/deflection and twenty-nine cryogenic pressure cycle endurance tests were completed with the seal test rig. Nineteen configurations of eight basic seal designs were tested, including the particular configuration recommended for inclusion in the XLR129-P-1 demonstrator engine design. None of the configurations tested met the test objectives at all test points. The seal design shown in figure 528 consistently performed well at pressures to 6000 psia and failed to meet the test objective at only one point during one of the endurance tests. (See figure 529.) However, the characteristic leakage at maximum pressures made this configuration less attractive than one with sealing assisted by pressure.

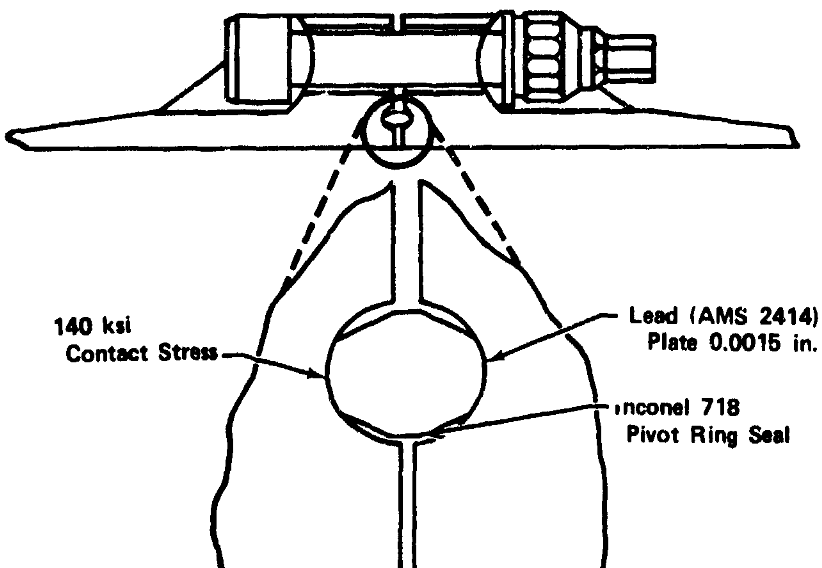

FD 37244

(U) Figure 528. Pivot Ring Seal Configuration

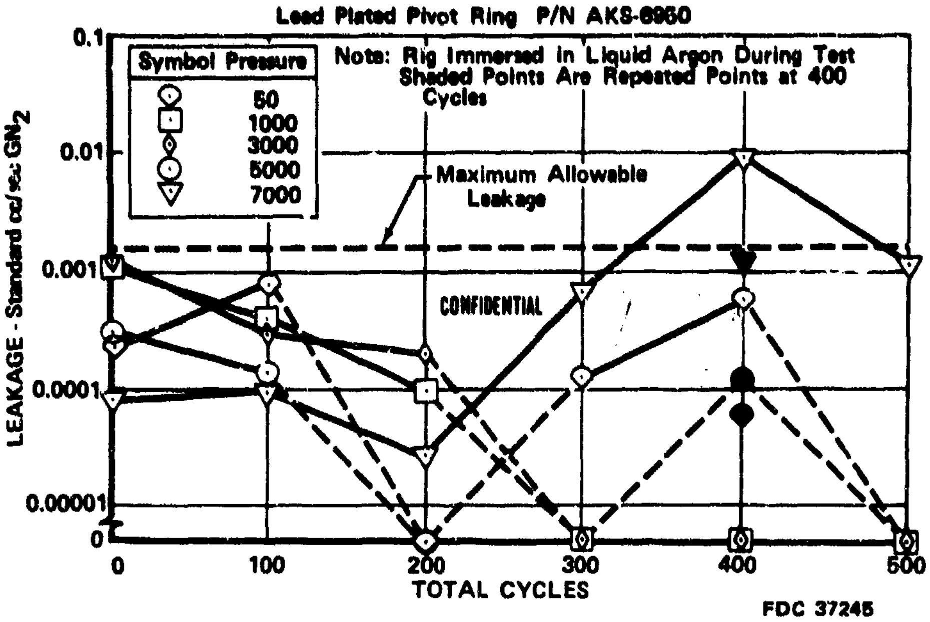

(U) Figure 529. Lead Plated Pivot Ring Static Seal Rig Test Results, Rig 35120-33

(C) The toroidal-segment seal configuration, shown in figure 519, provided reasonably consistent performance throughout the entire 0 to 7000 psig pressure range (see figure 530). Most samples of this configuration tended to leak excessively at intermediate pressures, so the seal was redesigned to improve low and intermediate pressure performance. The toroidal-segment static seal design (figure 531) selected for the XLR129-P-1 demonstrator engine, utilizes axial compression to produce the radial deflection and high unit loads necessary for effective sealing at low operating pressures. The installed radial load of 20 lb/in. minimum produces 2,000 psi minimum sealing surface stress for the lead plated Inconel-X seals. The seal groove depth, cross-section size, and thickness are varied as required to meet the load requirements over a large range of coupling diameters. Complete seal size information is given in figure 531. Testing will be used to establish the actual minimum load required, and the seal cross section and groove design will be changed as necessary to meet the sealing goal of 10^{-4} standard cc/sec/in. maximum leakage.

5. Operating Characteristics

(U) Primary sealing is accomplished by a radial sealing force developed at installation. (See figure 532.) By keeping the radial contact width of the sealing legs equal to 0.010 inch or less, a minimum value of radial sealing stress can be set at 2000 psi. This value of radial stress is sufficient to yield the lead plating on the seal. The addition of pressure increases this force, thus maintaining a sealing pressure greater than the internal pressure.

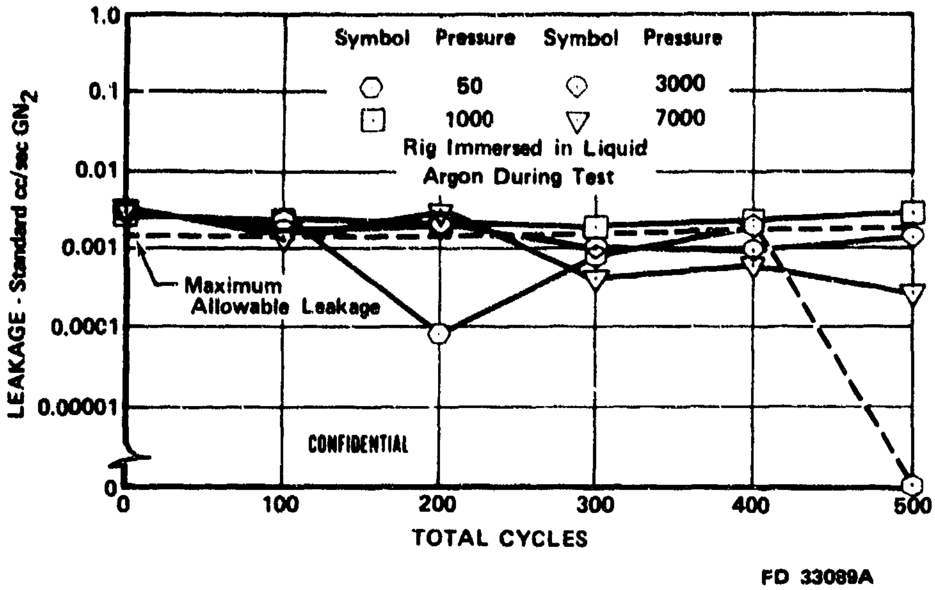

(U) Figure 530. Toroidal-Segment Seal Test Results, Rig 35120-28

a. Determine Sealing Forces

(1) Radial Sealing Force

(U) As the seal is installed, it is axially compressed by an amount ΔV which causes a radial growth of the seal, ΔR_o. If ΔR_o is greater than the radial clearance between the seal OD and the seal groove OD, then the seal is in effect subjected to a hoop compression by the groove wall. (See figure 533.)

Summing forces in the x direction:

$$P_o R_o R \sin \Phi \, d\theta + \sigma_c R \Phi t \frac{2d\ell}{2} = H R_o d\theta$$

$$\text{Let } \sigma_c = F \frac{\Delta R_o'}{R_o} \text{ and } \Delta R_o' = (\Delta R_o - \text{clearance})$$

$$\therefore H = P_o R \sin\Phi + E \frac{\Delta R_o'}{R_o^2} R \Phi t$$

at installation $P_o = 0$

$$\therefore H = E \frac{\Delta R_o'}{R_o^2} R \Phi t$$

(2) Axial Force

$$\sum M_o = 0$$

$$VR(1 - \cos\Phi) + P_oR^2(1 - \cos\Phi) = HR\sin\Phi + M_o$$

$$\therefore \quad V = \frac{H\sin\Phi + M_o/R}{1 - \cos\Phi} - P_oR$$

Definition of terms

$$P_oR_oR\sin\Phi \quad d\theta + \sigma_c R\Phi t\frac{2d\theta}{2} = HR_o d\theta$$

R_o = radius to radial sealing face, in.

P_o = internal pressure, psi

R = seal cross section radius, in.

Φ = half segment angle of seal cross section

$d\theta$ = seal segment

σ_c = hoop stress in seal, lb/in.^{2}

t = seal thickness, in.

H = radial force per inch on seal leg, lb/in.

$$\sigma_c = E\frac{\Delta R_o'}{R_o}$$

E = modulus of elasticity, lb/in.^{2}

$\Delta R_o' = (\Delta R_o$ - clearance)

Clearance = initial radial clearance between seal and groove prior to installation, in.

ΔR_o = unrestrained radial growth of seal due to ΔV, in.

$$VR(1 - \cos\Phi) + P_oR^2(1 - \cos\Phi) = HR\sin\Phi + M_o$$

V = axial force on seal leg, lb/in.

M_o = distributed moment at point 0, in-lb/in.

ΔV = axial deflection of seal, in.

(U) The radial deflection of each point along the seal cross section is plotted for various values of free seal angle, Φ. Since the seal forms a closed ring, the deflection plots are equivalent to hoop stress plots across the seal cross section. To maintain equilibrium, the hoop compression must equal the hoop tension on the seal cross section. The plots are thus used to relate the radial deflection ΔR_o to ΔV. (See figure 533.)

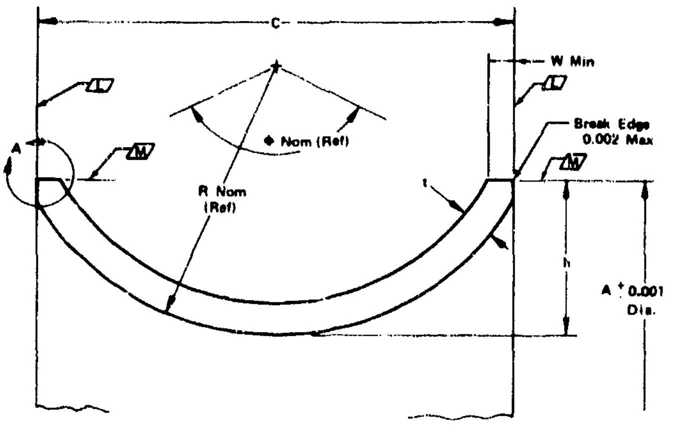

	Nom. Seal Size, in.	A Dia Max and Min, in.	C, in.	h, in.	t, in.	ΦNom (Ref) deg	R Nom (Ref) in.	W Min in.	Groove Dimensions (Ref)					
									J in.	K in.	R' in.	θ	x ± 0.001	Y
1	3/32 x 0.012	1.000 to 2.000	0.082 0.080	0.028 0.026	0.013 0.011	123	0.049	0.010	0.045	0.069 0.066	0.022			
2	1/8 x 0.012	2.000 to 3.000	0.109 0.107	0.036 0.034	0.013 0.011	121	0.067	0.008	0.056	0.093 0.089	0.028			
3	3/16 x 0.015	3.000 to 4.000	0.164 0.160	0.056 0.052	0.016 0.014	127	0.096	0.010	0.078	0.144 0.140	0.040			
4	1/4 x 0.015	4.000 to 8.500	0.217 0.211	0.074 0.070	0.016 0.014	125	0.123	0.010	0.108	0.181 0.177	0.078			
5	1/4 x 0.015	8.500 to 10.750	0.217 0.215	0.074 0.070	0.016 0.014	124	0.124	0.010	0.108	0.181 0.177	0.078			
6	5/16 x 0.020	8.500 to 14.500	0.271 0.265	0.090 0.084	0.022 0.019	127	0.155	0.016	0.130	0.223 0.219	0.094			
7	5/16 x 0.020	8.500 to 17 000	0.271 0.269	0.090 0.084	0.022 0.019	127	0.156	0.016	0.130	0.223 0.219	0.094			
8	5/16 x 0.025	14.500 to 16.500	0.271 0.265	0.090 0.084	0.027 0.024	127	0.156	0.021	0.130	0.223 0.219	0.094			
9	5/16 x 0.030	16.500 to 18.000	0.271 0.265	0.090 0.084	0.032 0.028	125	0.158	0.026	0.130	0.223 0.219	0.094			
10	5/16 x 0.030	16.500 to 19.000	0.271 0.277	0.090 0.084	0.032 0.028	126	0.158	0.026	0.130	0.223 0.219	0.094			

FD 37246

(U) Figure 531. Toroidal-Segment Static Seal

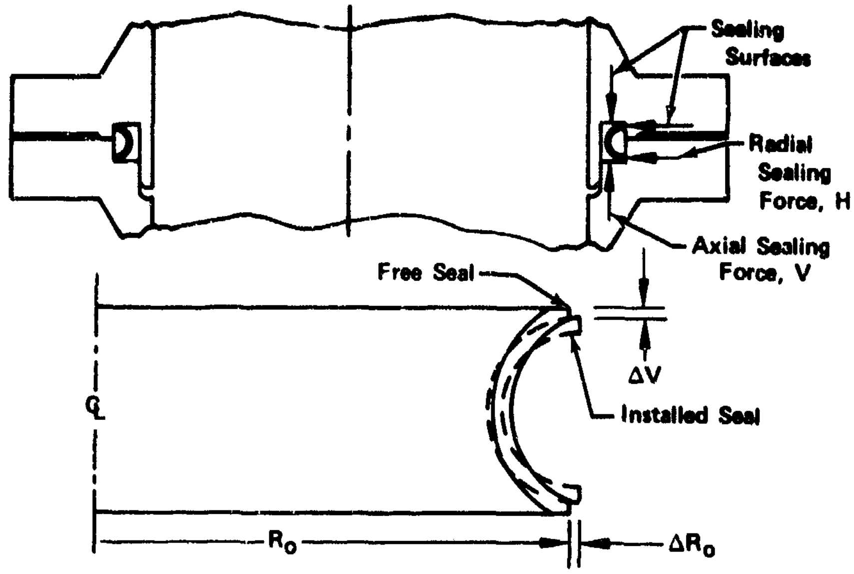

(U) Figure 532. Sealing Surfaces on Typical Installation

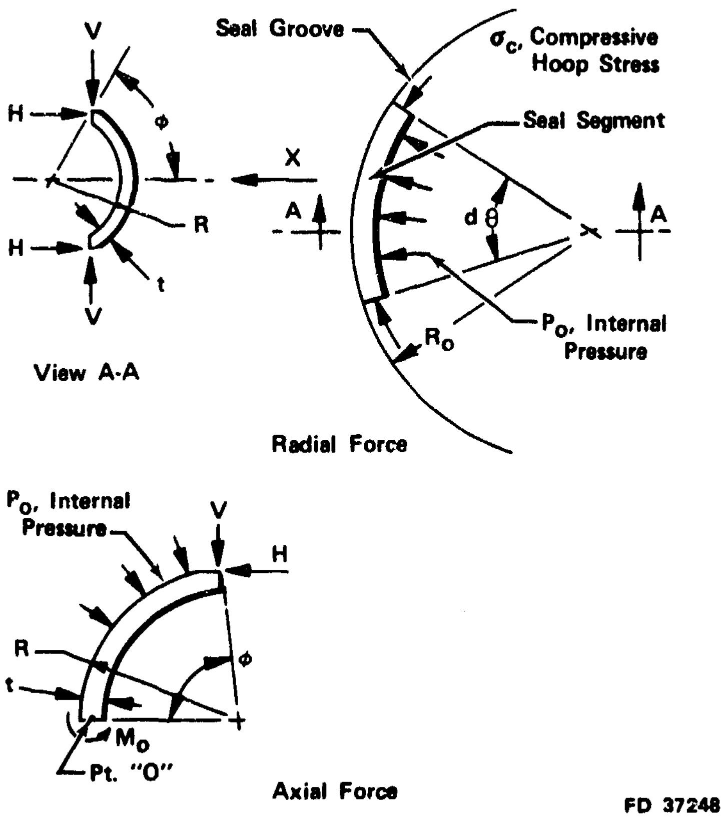

(U) Figure 533. Radial and Axial Force Computation

(U) Using this relation, radial sealing force can be expressed as:

$$H = \frac{ER\phi t}{R_o^2}\left[\Delta V\frac{\Delta F(\phi)}{F_2(\phi)} - \text{clearance}\right]$$

6. Design Approach

a. Background

(U) Major design effort was required to define the coupling configuration for a high-pressure static seal rig design. Several configurations were sketched for specialized flange and seal combinations before calculation difficulties indicated the design effort should be concentrated on basic coupling configurations with analysis directed toward minimum weight and deflection with demonstrator engine materials.

(U) A 6-inch diameter aluminum (AMS 4127) pipe coupling was chosen for initial analysis because of its relatively poor (high) deflection characteristics when compared to those of the same-diameter steel or smaller-diameter aluminum or steel couplings. A high-pressure coupling design analysis of five basic coupling types was completed. The configurations considered are shown in figure 534 A through E.

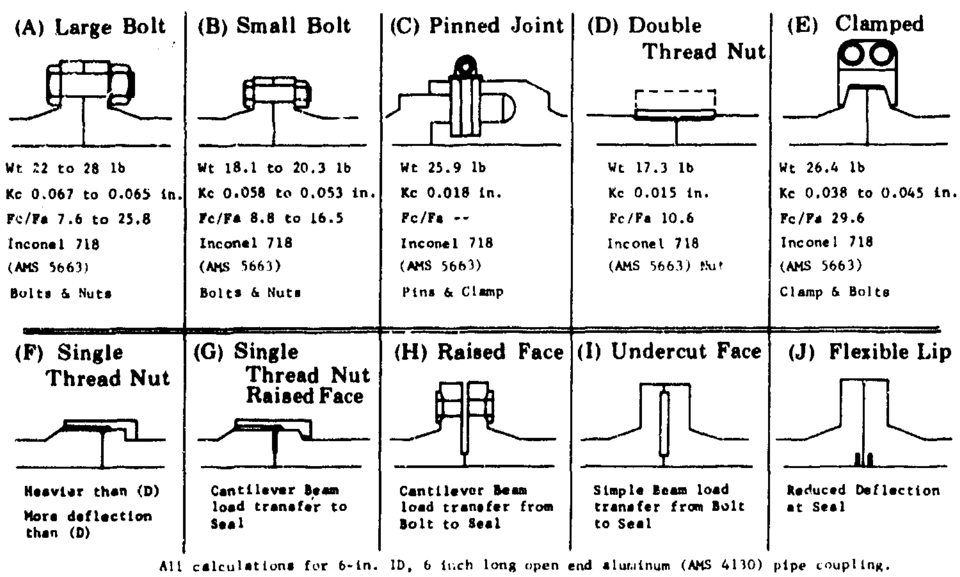

FD 25605A

(U) Figure 534. Coupling Configuration

(C) Results of the coupling-spring rate deflection calculations, as shown in figure 535, indicated that increasing the number of bolts had a minor effect on bolted-coupling overall spring rate, whereas weight increase was significant. Calculation to determine the initial clamping load required for each of the couplings to provide a minimum of 460 lb/in. seal load at 7500 psia resulted in the clamping load to blow-off load ratio (F_C/F_A) values shown in figure 534 A through E. Aside from the impracticality of attempting to obtain such high clamping loads, the numbers indicated some method of improving the clamping load transfer to the seal area was required.

(U) Figure 534 F through I shows some methods of providing this seal force, while figure 534J shows a pressure assisted coupling intended to maintain seal load when flange deflection is present. Another method of providing more effective seal loading, not shown, is to move the seal closer to the clamping load circle. In this case, part of the improved load transfer advantage is lost because of the increased blowoff load. The obvious advantages and disadvantages of each coupling for engine application were considered, and the small bolt-flanged coupling was selected for detailed analysis and initial hydrostatic test rig design. Analysis necessary for optimizing the flange configuration or seal location to provide satisfactory seal load characteristics over the full pressure range was undertaken as a primary effort.

(U) A study computer program was developed to analyze proposed coupling rig designs for stress and deflection characteristics. Initial rig designs were predicted by computer analysis to be unsuitable for the intended application. A 6-inch aluminum hydrostatic coupling stress and deflection test rig was designed to evaluate the computer program predictions. Concurrently, a finite element computer program originally developed for disk analysis was modified for use in coupling deflection and stress analysis.

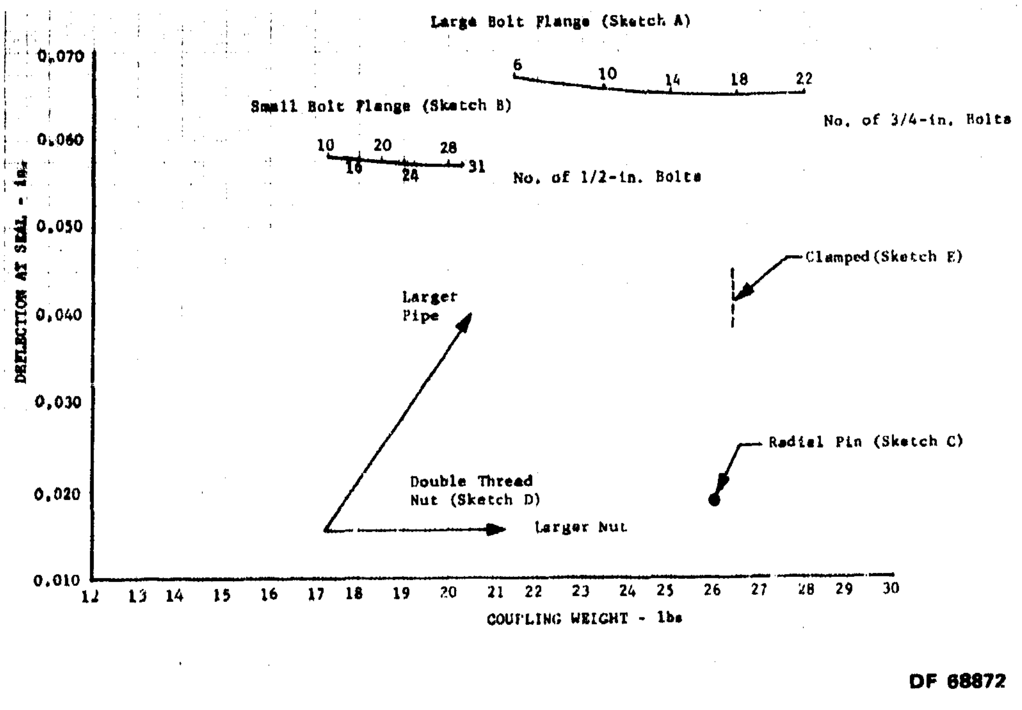

(U) Figure 535. Predicted Coupling Deflection of Seal vs Weight

(U) A reanalysis of the hydrostatic aluminum coupling layout using the finite element deck on the IBM 360 computer resulted in somewhat lower predicted maximum flange stresses and higher deflections than had been predicted by the previous study computer program.

(U) Additional flange design analysis based on shear center theory was completed. The application of this theory is that the load must pass through the shear center, or center of flexure, to prevent twisting. Preliminary calculations indicated the shear center design would improve flange stiffness slightly, but would probably be more bulky than a conventional flange design. Further analysis of the shear center flange design calculations indicated that effective coupling weight reduction by removing flange material not highly stressed may be possible without significantly affecting flange stiffness.

(U) The flat-faced aluminum hydrostatic test rig data showed reasonably good agreement with the finite element computer program predictions for both stress and deflection as shown in figure 536. The program was revised to improve matching by expansion to include both coupling members, multipoint bolt loading, and consideration of the effects of the bolt holes. The revised model was used to predict stress and deflection of the cantilevered or raised face coupling.

(U) The aluminum test rig flanges were reworked to the raised-face design configuration. Hydrostatic pressure testing was again conducted at ambient temperature.

(U) The flanges did not separate under the maximum internal pressure, but pivoted at the raised-face outer diameter so that deflection at the seal diameter reached a value of approximately 0.004 inch. Maximum flange separation at the inside diameter wall was 0.008 inch at this pressure.

(U) Review of the deflection and stress curves (figures 537 and 538) for the raised-face flange hydrostatic pressure test rig revealed that maximum surface stresses (below yield) near the flange were still somewhat below the finite element program predictions, but agreement was improved as shown in figure 538. Both bolt loads and proximity proves indicated flange separation was imminent at the maximum pressure applied, but bolt load was nearly constant up to that point.

b. Static Seal Rig Design Evolution

(U) The finite element computer program for analysis of flange deflection and stress was used to investigate bolted-flange coupling designs suitable for use in the XLR129-P-1 engine.

(C) Four basic bolted flange configurations, chosen for the investigation (figure 539) were analyzed using the finite element technique. All were sized to provide zero deflection at the seal on a 5.00-inch inside diameter Inconel 718 fluid coupling under 7000 psig fluid pressure. This represented the maximum conditions of fluid pressure and fluid line inside diameter foreseen for the XLR129-P-1 engine. Inconel 718 was chosen as the flange material because of its high strength-to-weight ratio, its good ductility at cryogenic temperature, and its compatibility with other major rocket engine components.

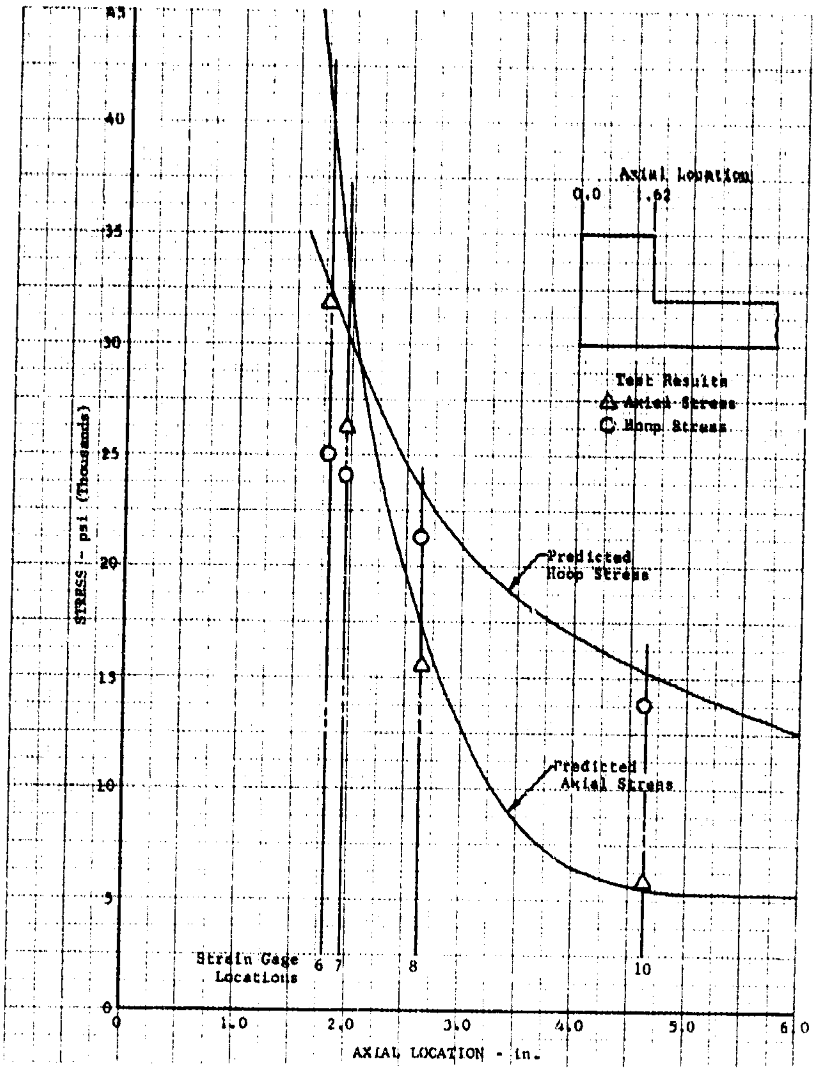

DF 68871

(U) Figure 536. Finite Element Computer Program Predictions

(U) The variables affecting flange weight for any given seal deflection are bolt circle diameter, flange thickness, bolt load, seal point diameter, taper height, taper length, and webs between bolt holes. Flange thickness, bolt circle diameter, and required bolt load have the greatest influence on flange weight and the study concentrated on these factors. All the factors except flange thickness and total bolt load were held constant during the analysis.

(U) The minimum bolt-circle diameter was determined by the minimum requirement for wrench clearance and was used for all but the loose-ring design where the bolt circle was limited by other geometric considerations such as minimum bearing surface and a taper height consistent with other flanges. A bolt load of 15,000 lb/bolt was used throughout the analysis while the maximum permissible bolt load was 17,750 lb/bolt. The difference was used as an allowance for bolt bending.

(U) Cantilever (raised face) and simple beam flange seal loading schemes were then analyzed using the computer program. This analysis indicated the raised face design would be lighter than the simple beam designs for the same deflection limit. A raised-face flange rework of the initial flat-faced flange test rig was designed and added to the test rig layout.

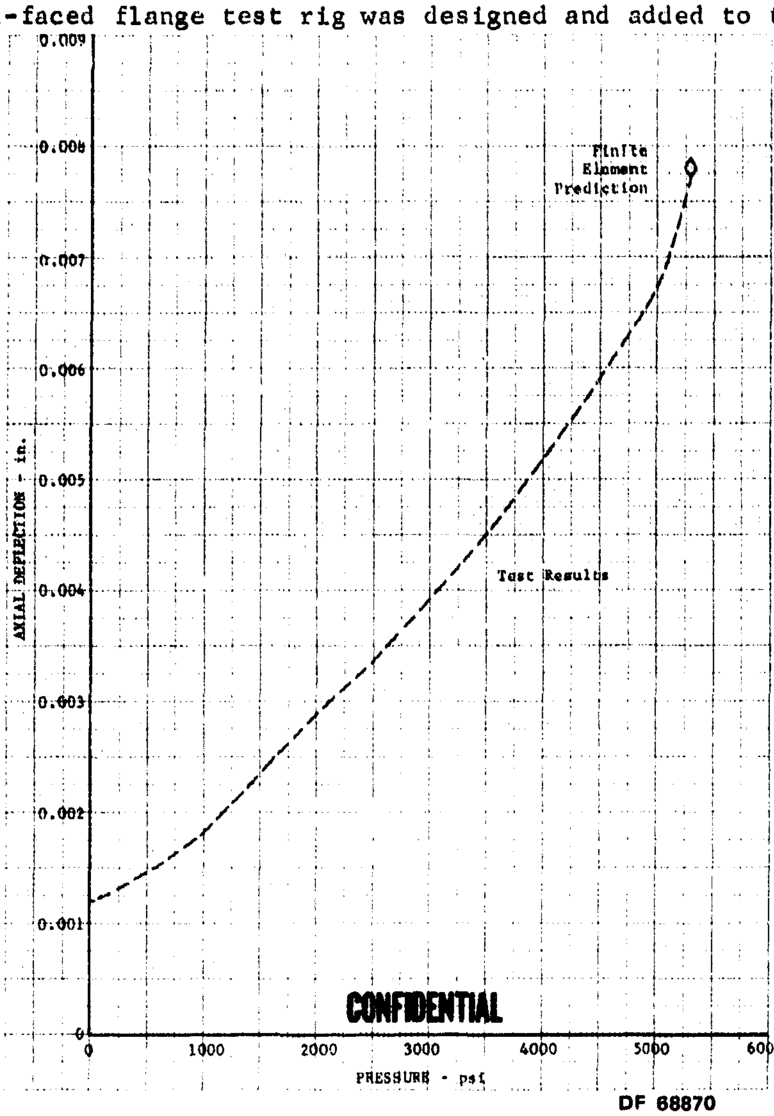

(U) Figure 537. Axial Deflection at ID of Flange, Rig 35120-3

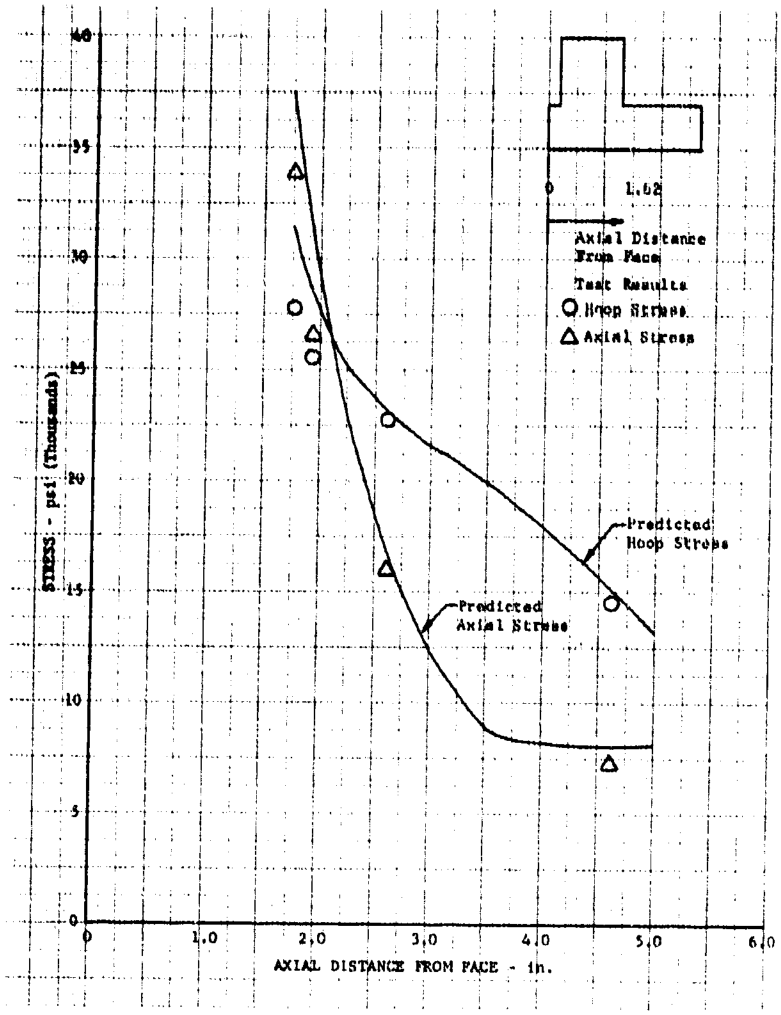

(U) Figure 538. Comparison of Predicted and Measured Stresses on OD Wall, Rig 35120-3

(U) Stresses in the flange designs for zero deflection are not limiting and the size of the flanges shown in figure 533 result from the deflection requirement. The rings for the loose-ring flange design are stress limited and constitute about 50% of the flange weight. A trade-off study of bolt load versus flange thickness was made for the loose-ring but flange weight was hardly affected by decreasing the bolt load. The loose-ring configuration shown in figure 539 represents the smallest envelope that can be used zero deflection.

(U) Flange weights shown in figure 539 account for all the weight outboard of a straight tube of 0.15-inch wall for a complete flange connection (two halves) including the weight of nuts and bolts. As indicated, all flanges have essentially the same weight, because for zero deflection the rotation of the flange hub must be approximately zero and the type of flange was found to have very little effect on the required hub size for zero rotation.

(U) The size and weight of these couplings was considered to be prohibitive for engine application, so a limited deflection (0.002 inch) analysis was initiated to take advantage of the claimed deflection capability of commercial seals. The flanges were revised to produce a 0.002 inch deflection at the seal gland for the operating conditions.

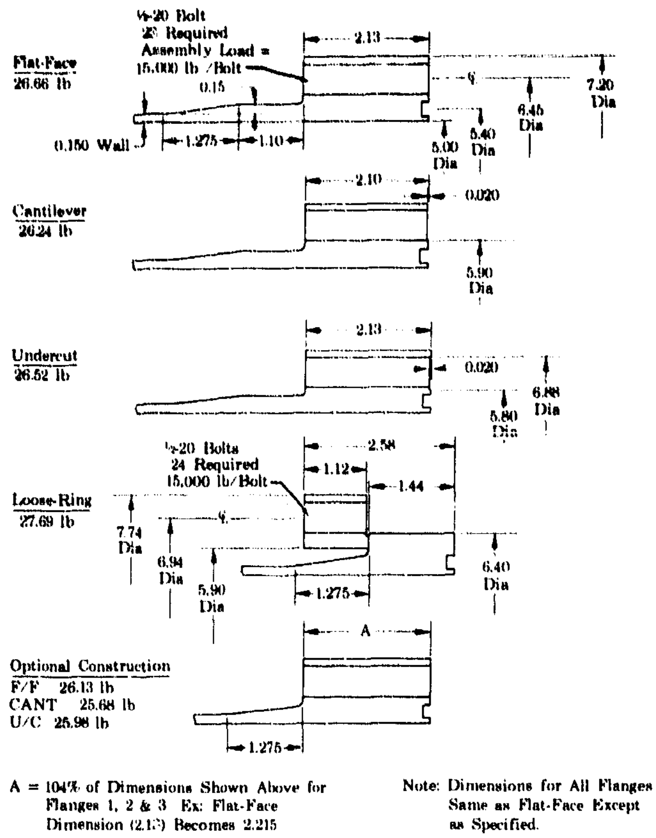

FD 25771A

(U) Figure 539. Static Seal Rig Zero Deflection Flanges

(U) A weight and size comparison for four couplings having total axial deflection at the seal point of 0.002 inch is shown in figure 540. The raised-face flange proved to be lightest while the undercut flange is heaviest. The flat-face flange was eliminated because it had no advantage over the undercut flange. The distance from the theoretical pivot point to the sealing point was found to be a major influence on flange size because very little bending occurs in the flange.

(U) An effort was made to further reduce flange weight by moving the pivot point as close to the sealing point as possible. This was accomplished on the raised-face flange by moving the bearing surface inboard of the seal cavity. The resultant additional weight reduction was 1 lb over the conventional raised-face flange shown in figure 540.

(U) Figure 541 shows the variation in weight of raised-face, undercut, and loose-ring flange couplings with increasing axial deflection. The raised-face flange shows the sharpest weight decline as the allowable deflection is increased.

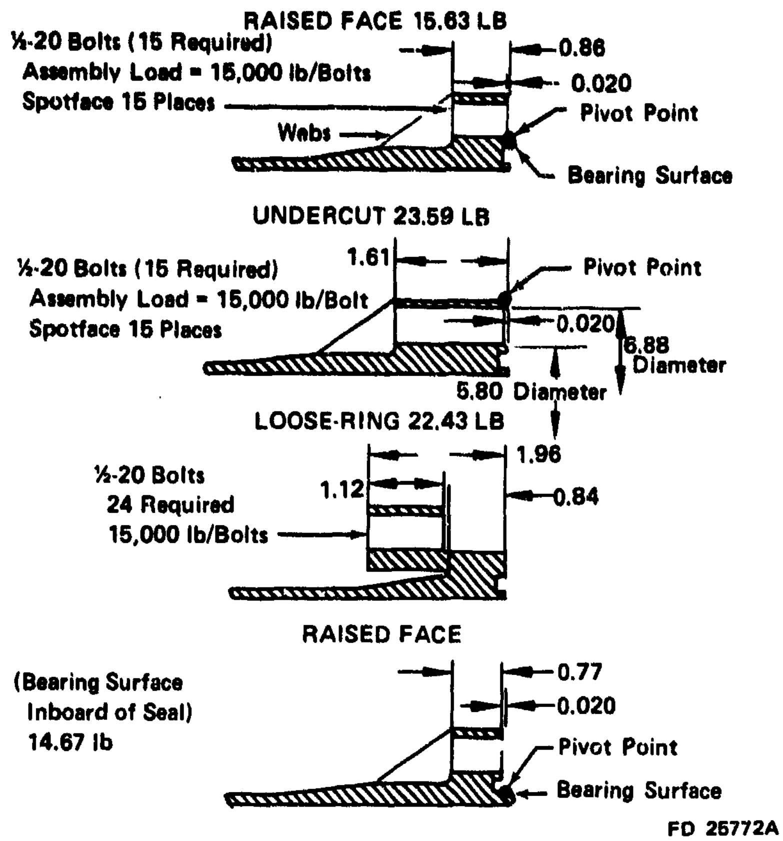

(U) Figure 540. Static Seal Rig 0.002 inch Deflection Flanges

(U) The trade-off between the number of bolts and webs on the backface of the flange was also considered. It was found that for a standard cantilever flange with seal point deflection of less than 0.0013 inch, it was more economical from a weight standpoint to use more bolts and no webs as shown in figure 541. Webs are shown to be more beneficial above a 0.0013-inch deflection because the stiffness of the webs and flange hubs are more nearly equal.

(U) A flange deflection compensation study showed that several schemes are feasible for flange deflections up to 0.020 inch. However, this deflection capability usually comes at the expense of a larger seal envelope and/or additional fabrication or maintenance problems.

(U) The three types of deflection compensation schemes shown in figure 542 were analyzed. The deflection compensation capabilities were determined not only for those that could be contained in the small face seal envelope, but also for the general case of larger envelopes.

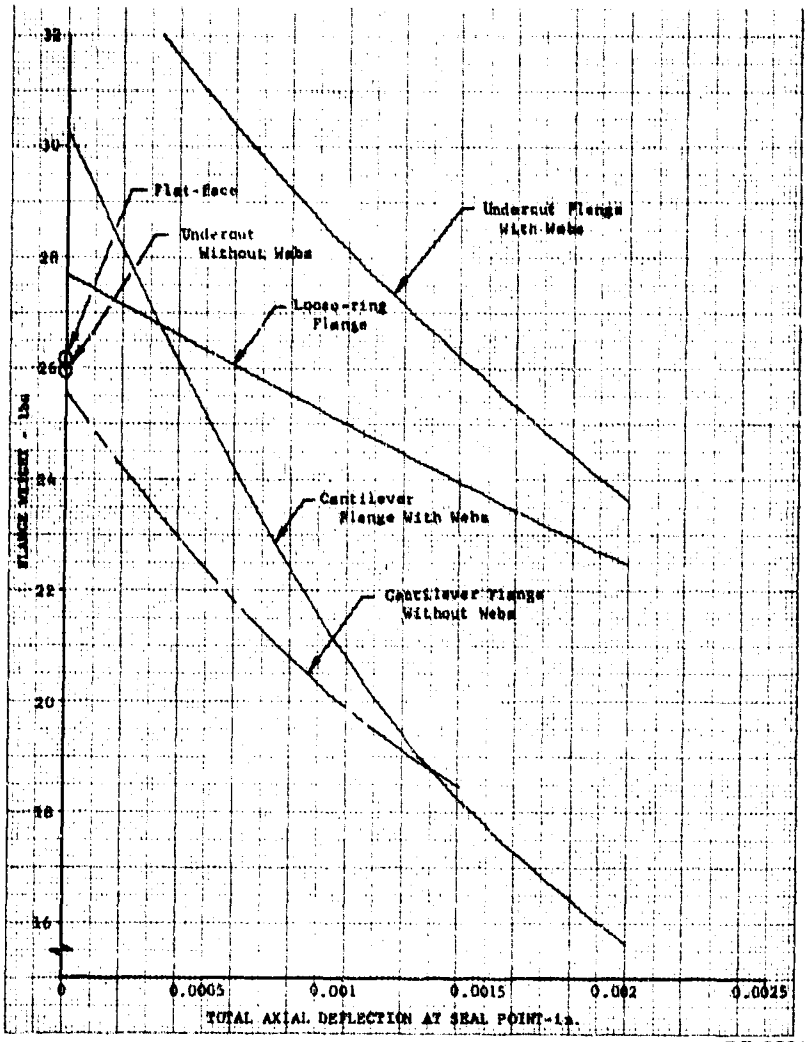

(U) Figure 541. Static Seal Rig Flange Weight vs Seal Point Deflection

(U) Static seals investigated were divided into two general classifications:

Face Seals: Those seals having sealing surfaces that are perpendicular to the bore of the joint and whose initial seating stress is obtained by axial compression or deformation of the seal as the joint is assembled.

Radial Seals: Those seals having sealing surfaces that are parallel to bore of the joint and whose initial seating stress is obtained by a radial compression or deformation of the seal as the joint is assembled.

(U) A number of cryogenic seals were investigated (see table LXXII). Many were rejected on the basis of excessive size and other obvious deficiencies.

(U) For comparison purposes, both the face-type and radial-type seals were divided into three subgroups:

Low deflection capability - 0 to 0.003 inch
Intermediate deflection capability - 0.003 to 0.010 inch
High deflection capability - above 0.010 inch.

(U) Seal deflection capability is the ability of the seal to adjust to distortion or dimensional changes of flange faces upon which the seal seats, without an excessive loss of seating contact stress. This deflection capability can be considered in both the axial and radial directions. However, due to the assumed deflection characteristics of the joint flanges, radial deflection characteristics become less critical than axial deflection capability.

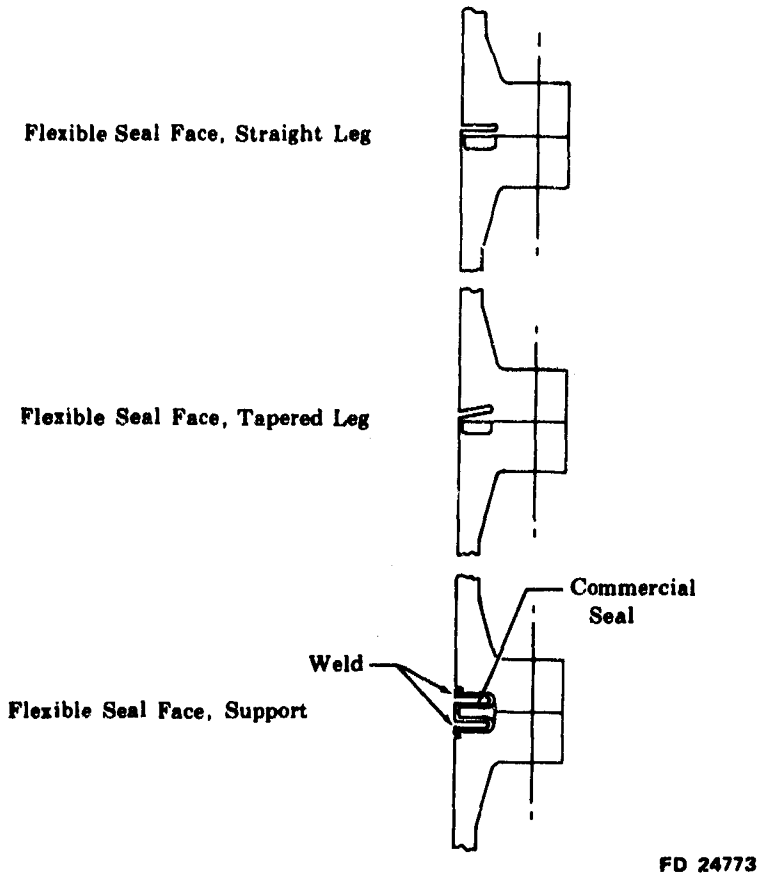

(U) Figure 542. Static Seal Rig Deflection Compensation Schemes

(U) Table LXXII. Applicable Commercial Seals

Size Category	Common Name	Manufacturer	Cross Section	Gland Dimension Width(in.)	Gland Dimension Depth(in.)	Seal Material	Vendor Recommended Seal Coating	Maximum Axial Deflection Capability	Remarks
Low Deflection Capability (Group A)	"V" Seal	Parker Seal Co.		0.166	0.110	Inconel-X750	Teflon TFE	0.002	
	Metal "O" Ring	United Aircraft Products Co.		0.154	0.095	AISI 321	Teflon TFE	0.002	
	"C" Ring	Pressure Science Incorporated		0.119	0.116	Inconel-X750	Indium	0.002	
	Bi-Metal Gasket	Del Mfg. Co.		0.096	0.100	Inconel-X750	Teflon TFE	0.002	
	Apex Seal	Servotronics, Inc.		0.170	0.106	Inconel-X750	Lead	0.002	
	Omega Seal	Servotronics, Inc.		0.170	0.106	Inconel-X750	Lead	0.002	
Intermediate Deflection Capability (Group B)	"E" Ring	Pressure Science Incorporated		0.127	0.120	Inconel-X750	Indium	0.006	Has High Axial Defl. Cap. for Small Profile Seal
	K-Seal	Harrison Mfg.		0.235	0.125	Inconel-X750	Teflon TFE or Nickel-Lead	0.010	
	Naflex Seal	Navan Inc.		0.293	0.175	Inconel 718	Teflon TFE	0.003	
	Dryerseal	W.S. Shamban & Co.		0.488	0.210	Inconel or SST	None - Is Teflon Filled	N.A.	Maximum Operating Temperature is 500°F
	Spring Gasket	Donaldson Co., Inc.		0.194	0.107	Inconel X	Silver	N.A.	
	Servoflex	The DSD Company		N.A.	N.A.	Inconel X	None	N.A.	Low Axial Defl. Capability. Slender Profile
	Lo-Load Seal	The Advanced Products Co.		0.165	0.088	Inconel 718	Indium Over Lead	0.005	Low Installation Load Required - 25 lb in.
Radial Seals (Group C)	Robbin Seal	Battelle Memorial Institute		N.A.	N.A.	Inconel 718	None	Per Seal Design	
	Radial "C" Ring	Pressure Science Incorporated		0.127	0.125	AISI 304	Indium	Per Flange Geometry	0.002 Maximum Radial Defl.
	Conoseal	Aeroquip Corp.		0.462	0.335	AISI 321	None	Per Flange Geometry	Vendor Quotes 0.040 Maximum Axial Deflection
	Bal-Seal	Bal-Seal Engr. Co.		0.127	0.197	Teflon TFE	None	Per Flange Geometry	8 RMS Gland Finish Req'd Maximum Temperature = 250°F
	Nuco Seal	National Utilities Corp.		N.A.	N.A.	A-286	N.A.	Per Flange Geometry	Info Requested from Vendor Not Received 10-10-68

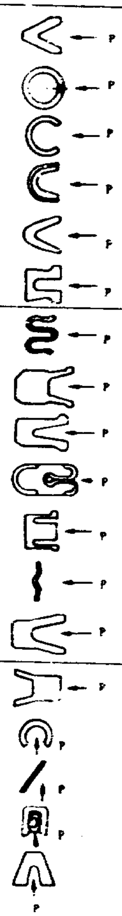

N.A. - Not Available

A. ENGINE MOCKUP

SECTION VI
DEMONSTRATOR ENGINE MOCKUP AND PLUMBING

A. ENGINE MOCKUP

1. Introduction

(U) The engine mockup serves as a tool to integrate all engine components into a compact and easily maintainable engine package. The mock-up and its components were used to: (1) verify design compatibility and individual fitting locations with respect to the total engine package (2) determine engine plumbing lines initial routing and line coordinates (used for inputs into tube stress analysis deck) (3) determine critical clearances and optimum component locations where interferences exist (4) verify envelopes of vendor supplied components (5) select location of engine required instrumentation, and (6) verify that all components were located within the required envelopes. The power package envelope (preburner and pumps) is 66.4 in. in diameter, and the remaining components (from the main burner injector to the end of the primary nozzle must be within the 45.6 in. inside diameter of the two-position nozzle because the two-position nozzle retracts over these components for sea level operation as shown in figures 543 through 545.

2. Description of Engine Configuration

(U) The transition case serves as the primary integrating component and provides the main support structure between the thrust chamber assembly and the gimbal mount pad. It also provides for the compact mount and support of the preburner, main turbopumps and main burner assemblies. The fuel and oxidizer low-speed inducers are located between the fuel turbopump and preburner injector and the oxidizer turbopump and preburner injector, respectively. Both inducers are mounted to the transition case through an adjustable system with attach points located at the top and bottom of the transition case. The main burner injector is mounted between the transition case and main combustion chamber. The actuator attach brackets (two located 90 degrees apart) are mounted on the main combustion chamber through a four legged structure, each leg being welded to the main combustion chamber as shown in figure 546. The primary nozzle attaches to the main combustion chamber and provides the lower support for the jackscrews on which the two-position nozzle is mounted. The upper supports for the jackscrews are attached to the transition case. Engine plumbing and the control system constitute the other engine components required to complete the engine package. Figures 543 through 550 show the engineering mockup with the major components listed above shown.

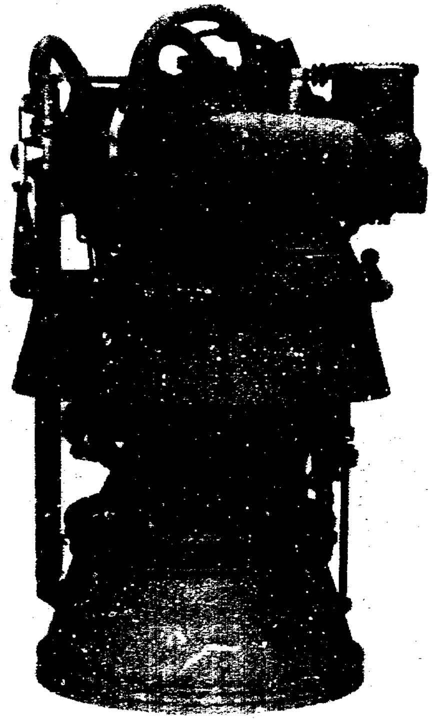

FE 92409

(U) Figure 543. Engineering Mockup, Two-Position Nozzle Retracted - 12 Inch Section Only (Sheet 1)

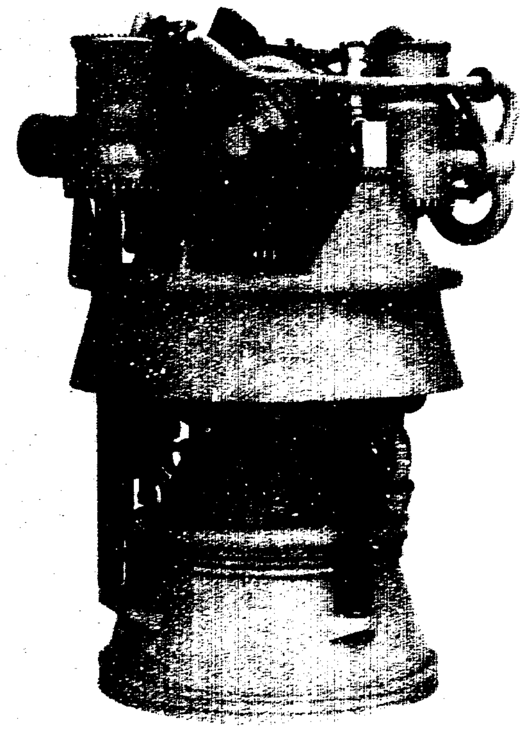

FE 92414

(U) Figure 544. Engineering Mockup, Two-Position Nozzle Retracted - 12 Inch Section Only (Sheet 2)

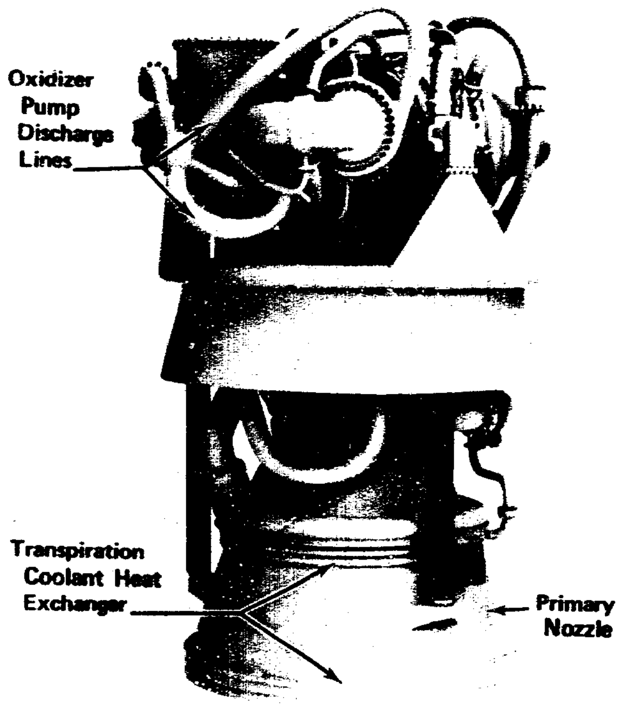

FD 34591

(U) Figure 545. Engineering Mockup, Two-Position Nozzle Retracted - 12 Inch Section Only (Sheet 3)

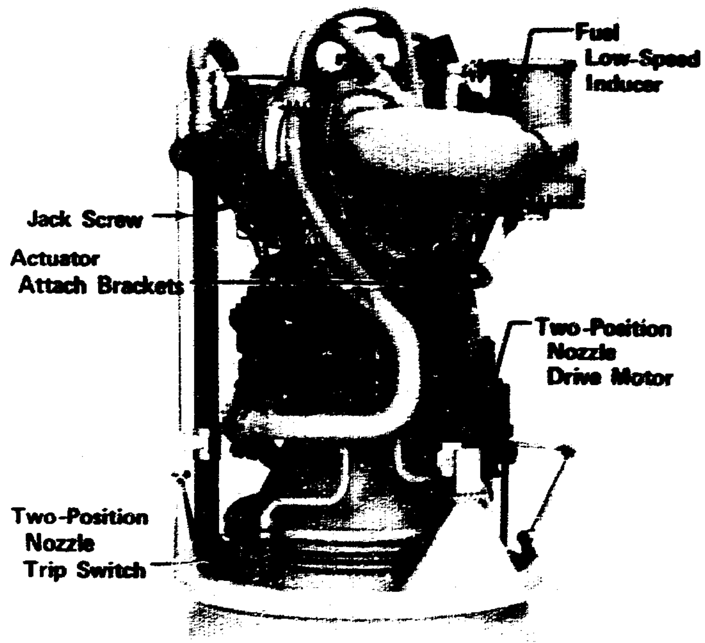

FD 34592

(U) Figure 546. Engineering Mockup (Sheet 4)

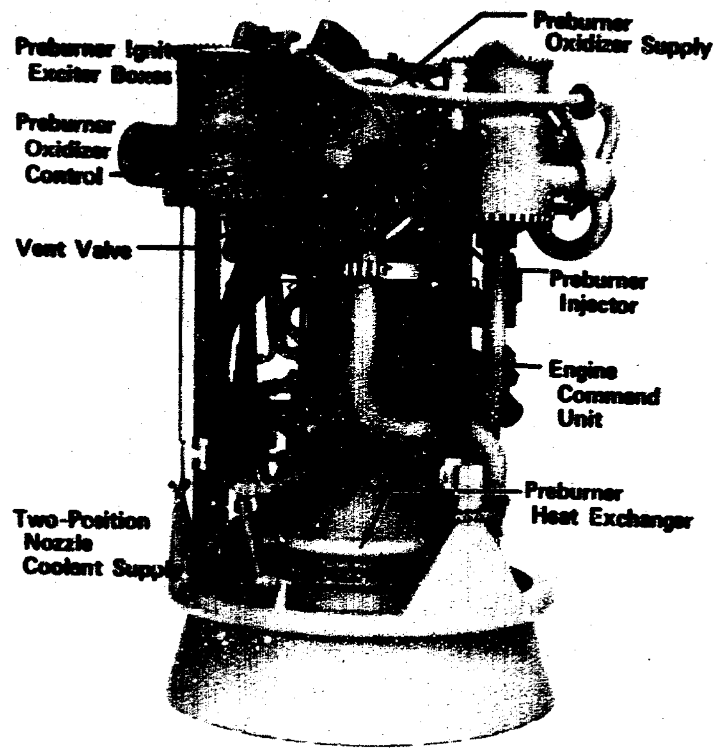

(U) Figure 547. Engineering Mockup (Sheet 5)

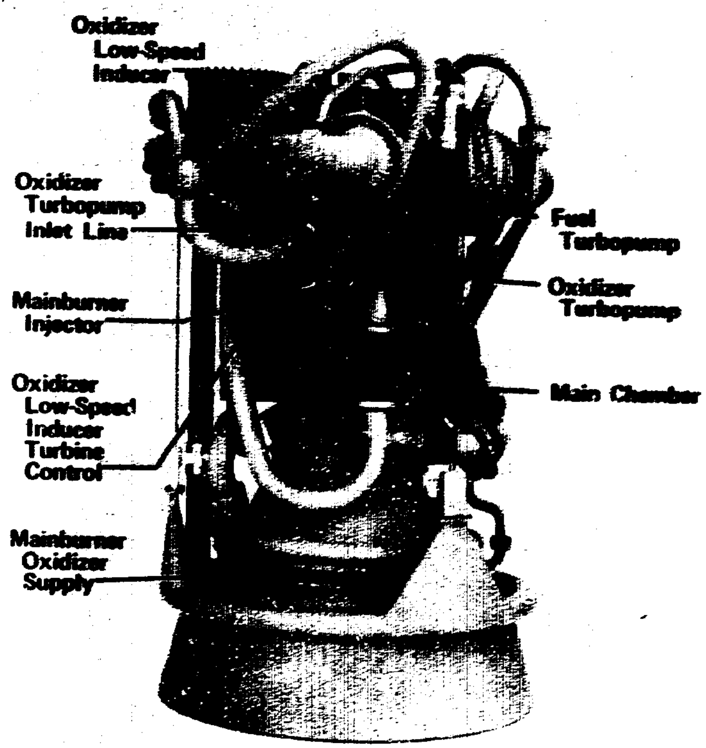

(U) Figure 548. Engineering Mockup (Sheet 6)

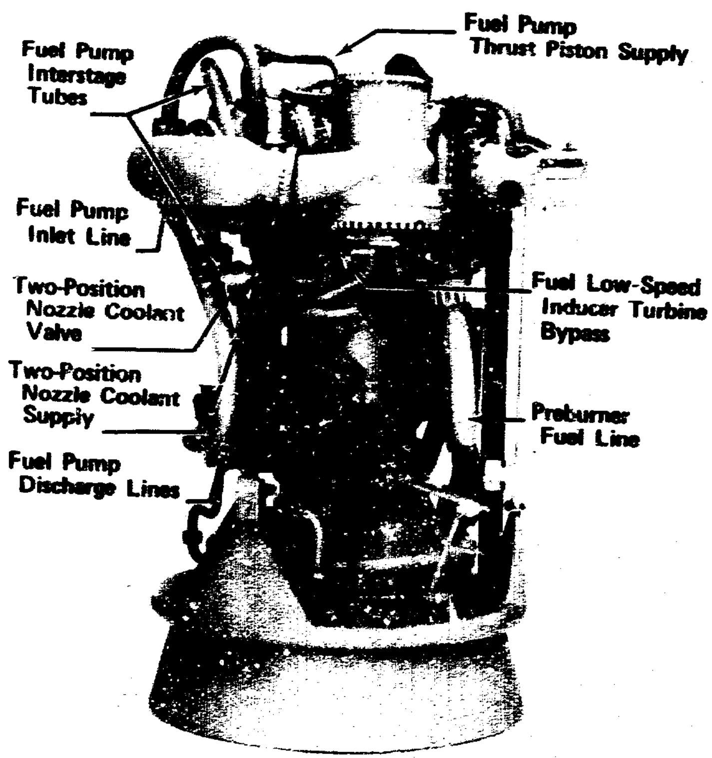

(U) Figure 549. Engineering Mockup (Sheet 7)

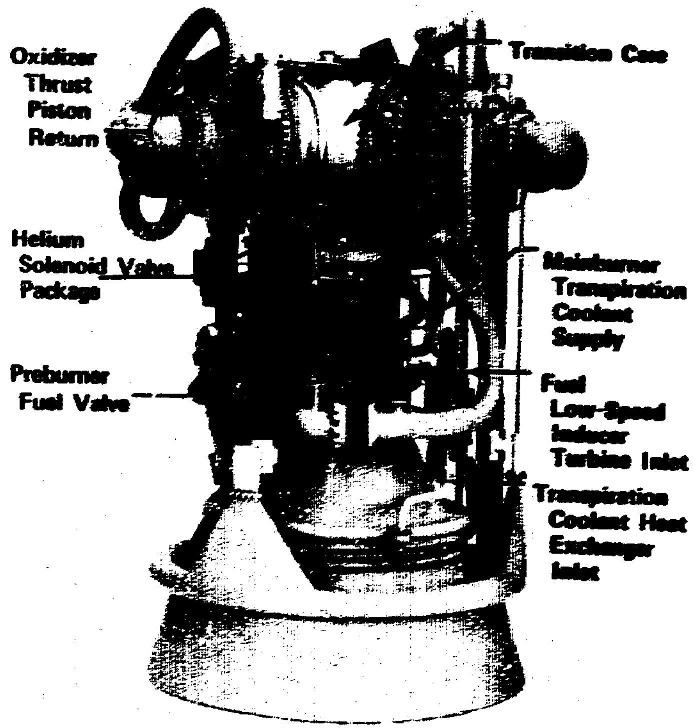

(U) Figure 550. Engineering Mockup (Sheet 8)

3. Component Design

(U) Mockup components have been used extensively during the layout design phase of most of the engine components. When component designs progressed to the point that the external configuration was defined, a mockup part was fabricated and installed. The component would then be judged for general appearances, interference with other components, optimum location of external fittings, and accessibility for maintenance. The results of the above evaluation were incorporated into the actual component design, often requiring a compromise of conflicting requirements. When the design was completed and the layout approved, the mockup component was then revised to reflect the true design. The general ground rule of 0.5-inch clearance between all components was used.

4. Engine Plumbing Design

(U) Plumbing lines must meet several requirements in keeping with the overall engine goals which are as follows: (1) minimum number of flange joints to reduce engine weight and overboard leakage, (2) orientation of flanges and tubing connections must accommodate convenient engine assembly and maintenance, (3) anticipate pipe to engine tolerance conditions and avoid routings that would impose excessive strain or loads on either the high pressure pipes or the components to which they are attached, and (4) route all lines in banks to achieve support in bracketing to the engine and ensure aesthetic appeal in the final appearance of the engine. All requirements are tailored to the overall goals of providing a lightweight, compact, easily maintainable engine. To accomplish this task, the plumbing design took place in the following stages: (1) general hydrodynamic requirements were determined, (2) rough line sizes and wall thickness were determined, (3) mockup line was fabricated and installed in a semi-finished condition, (4) preliminary tube stress analysis was performed on the mockup line configuration, (5) line configuration and routing were optimized, (6) layout design and updated tube stress analysis were completed, and (7) an updated mockup line was fabricated. This proved to be the most effective procedure for the plumbing design. Figures 545, 547, 548, 549, and 550 show the engine plumbing configuration.

5. Primary Component Locations

(U) An optimized location of all components is of prime importance because clearance is very critical for this compact engine configuration. Preliminary models of major components coupled with extensive design studies were used to establish the prime angles of the transition case which, in turn, located both main turbopumps and the preburner injector. All other component locations were selected to be compatible with the final 120-degree angles chosen for major component mounting on the transition case using 0.50 inch clearance as a general rule for fixed engine components.

6. **Envelope Definition of Vendor-Supplied Components**

(U) Mockups of vendor furnished components were incorporated for the purpose of envelope configuration definition. The igniter exciter box is a good example of this because the final configuration selected must be installed and be interchangeable between four separate locations. This mockup configuration was supplied to the vendors as the maximum allowable envelope. The two-position nozzle coolant solenoid valve is another example of this function. The valve size and porting were established to be compatible with other components. For the engine command unit and helium solenoid valve package, the required volumes were specified by the vendors, and the optimum configurations (considering all other components integrated into the engine package) were determined. This process involved a continuing interchange of information, but eventually a compatible configuration was obtained. The configuration of the engine command unit is still considered very preliminary. Figures 547, 549, and 550 show these components.

7. **Engine Instrumentation**

(U) All engine instrumentation (excluding rig test type instrumentation) is mounted on the mockup components to verify planned clearances and ensure ready accessibility on the engine. Engine command unit sense lines will be installed when defined.

8. **Two-Position Nozzle**

(U) A translating two-position nozzle and actuation system was fabricated and installed on the mockup for the purpose of: (1) verifying that all components and plumbing lines were within the envelope traversed by the two-position nozzle, (2) locate jackscrews, and (3) verify the functional operation of the movable coolant system. A 12-inch section of the two-position nozzle was used to accomplish this task. Figures 543 through 545 show the engine with the two-position nozzle retracted, and figures 546 through 550 show the two-position nozzle partially extended.

9. **General**

(U) The components constructed for the mockup maintain structures and brackets consistent with the actual engine hardware (except for materials). The general rule of ±0.030-inch tolerance for mockup parts was maintained, except where more critical tolerances were required; such as flange locations on the transition case. All mockup engine components have been fabricated and installed. Only minor changes are expected to refine the engine configuration or to improve accessibility for maintenance.

B. PLUMBING

B. PLUMBING

1. Introduction

(C) The problem of designing high pressure (up to 6000 psi) plumbing was resolved by: (1) avoiding the use of hot (turbine gas temperature) external lines, and (2) selecting Inconel 718 (AMS 5663) high strength tube material not only for lowest weight, but to ensure tube walls thin enough to realize a useful amount of tube flexibility with reasonable tube lengths. The engine transition case houses the only hot line on the engine, and consists of an unrestrained Y-duct connecting the preburner outlet with the main turbine inlets. Gas leakage at these slip joints is strictly internal, and the adverse thermal and pressure growth effects normally associated with external plumbing are completely avoided.

2. Design Philosophy and Criteria

(U) The realization that the large diameter, heavy wall plumbing used on the engine could produce high flange loads, pipe moments and excessive reaction loads on major engine components has required that each line be analyzed structurally. To ensure design consistency, a comprehensive set of ground rules and special analytical computer routines were established. These design guides control: (1) final flanged joint dimensions, (2) bolt size and quantity, (3) bolt assembly preloads and lowest predicted bolt load during operation, (4) minimum allowable tube wall thickness, and (5) an external pipe moment factor.

(U) Flange designs are accomplished by application of the analytical methods defined in Appendix I. The routine presented generates a practical low-weight cantilever, or raised face, flange that ensures the flange deflection at the gasket contact point not to exceed a specified value under maximum bolt preloading at 120% of maximum operating pressure (this deflection, per flange pair, is 0.002 inch for metal O-rings).

(U) Any flange analysis must be preceded by a bolt load determination study as outlined in Appendix I. The various design rules presented establish the minimum bolt preload value to specify at engine assembly. A 20% spread between minimum and maximum preload has been established and verified through test programs at FRDC.

(U) The coupling criteria rules generate the following equation that graphically describes the various bolt load factors that constitute the total specified minimum preload:

$$F_B = \frac{PA}{N} + \frac{F_{seal}}{N} + F_T + F_{Rotation} + F_{Moment}$$

The terms in the equation are:

F_B = Minimum load per bolt required at assembly

P = Maximum engine cycle pressure

A = Area enclosed by gasket contact diameter

F_{seal} = Total seal preload at 350 lb per inch of circumference

N = Number of bolts in bolt circle

F_T = Load lost per bolt caused by temperature lag (if any)

$F_{Rotation}$ = Load reduction per bolt caused by flange rotation at 120% of maximum cycle pressure (as determined from flange deflection computer analyses)

F_{Moment} = Bolt preload required to provide external pipe moment capability.

(U) In the above equation definitions, external moment is related to bolt preload by the basic equation:

$$F_{Moment} = \frac{2\ M}{R\ N}$$

where:

R is the bolt circle radius

N is the number of bolts

M is the external pipe moment in lb-inches, selected by overall considerations of tube section "moment of inertia" and tube routing limitations, or expressed simply as a percentage of blowoff load using about 30% as a general rule.

(U) The tube wall thickness determination was accomplished by calculating a minimum allowable wall based on setting the maximum hoop stress at 0.2% yield stress at operating temperature and 150% of maximum operating pressure, unless other considerations cause the tube to be designed with more stress margin. This establishes a minimum wall thickness specification allowed in any tube bend. The nominal tube wall thickness is established by increasing this minimum wall value by a factor of 30% to allow for thinning during fabrication. The remaining tube design criteria include the use of Inconel 718 (AMS 5663) welded and drawn tubing, for all sizes down to 0.375 inch outside diameter. For 0.3125 and 0.250 inch diameter tubing, AISI 347 (AMS 5512) material is used as seamless tubing stock.

(U) All tube assemblies greater than 1.000 inch outside diameter were analyzed in detail to establish the end loads and moments imposed by end point deflections that will occur because of component tolerances and additional strains that are caused by thermal and high pressure effects.

(U) The initial structural analysis involved the use of a computer program that was generated for use with low pressure tubes. Hand calculations showed that this program produced inconsistent results. A general structures program was then refined for specific tube deflection problems and is now used successfully to predict tube stress, reaction end loads and moments at the end flanges. Essential analytical assumptions are: (1) tubes are elastic with true circular cross sections (assured by high pressure) even in bends, and (2) that calculated loads and moments should be reduced to 90% values to account for the end supports not being completely rigid, which the program assumes. The program handles any single flowpath tube routing including bends which are solved as a series of straight sections. Analysis results are presented for each major line configuration.

(U) Tube routing configurations were established on the engine mockup, within specified envelope restraints in conjunction with interim analyses of initial designs. The selected configurations are shown in the Engine Mockup figures 546 through 550, and in the plumbing roadmap shown in figure 568.

(U) For initial plumbing designs, the practice of custom machining certain large high pressure lines was an acceptable design approach. This avoided overweight and relatively complex shapes that would otherwise be required to limit plumbing loads. Another ground rule that was established as a guide to routing selection was to limit the computed pipe moments at the flanges to not exceed 75% of the theoretical moment required to actually separate a given flange on a 100% maximum cycle pressure loading basis.

(U) The scheduling of major engine component designs has precluded any idealized dimensioning system or tolerancing to favor plumbing of the engine. Eventually, many refinements are possible to reduce the need for special pipe-to-engine mating at the engine assembly level.

3. Preburner Fuel Line

(C) This line supplies high pressure hydrogen from the exit of the regeneratively cooled section of the primary nozzle to the preburner injector. The maximum cycle pressure is 5123 psia and the flow rate is approximately 76.5 lb/sec at design point. The hydrogen temperature at this point in the system is 177°R. The configuration is shown in figure 551. At this juncture the pipe inside diameter is 3.800 inches and this size is maintained for about 40 inches. A transition section then occurs to reduce the flowpath to 3.000 inches to match the inlet to the preburner injector.

(C) The predicted pressure loss at the maximum flow is 21 psi and this compares favorably with the 25 psi loss allowed by the engine performance design table. At this flow condition the maximum fluid velocities are 280 ft/sec in the larger section and 450 ft/sec at the injector end.

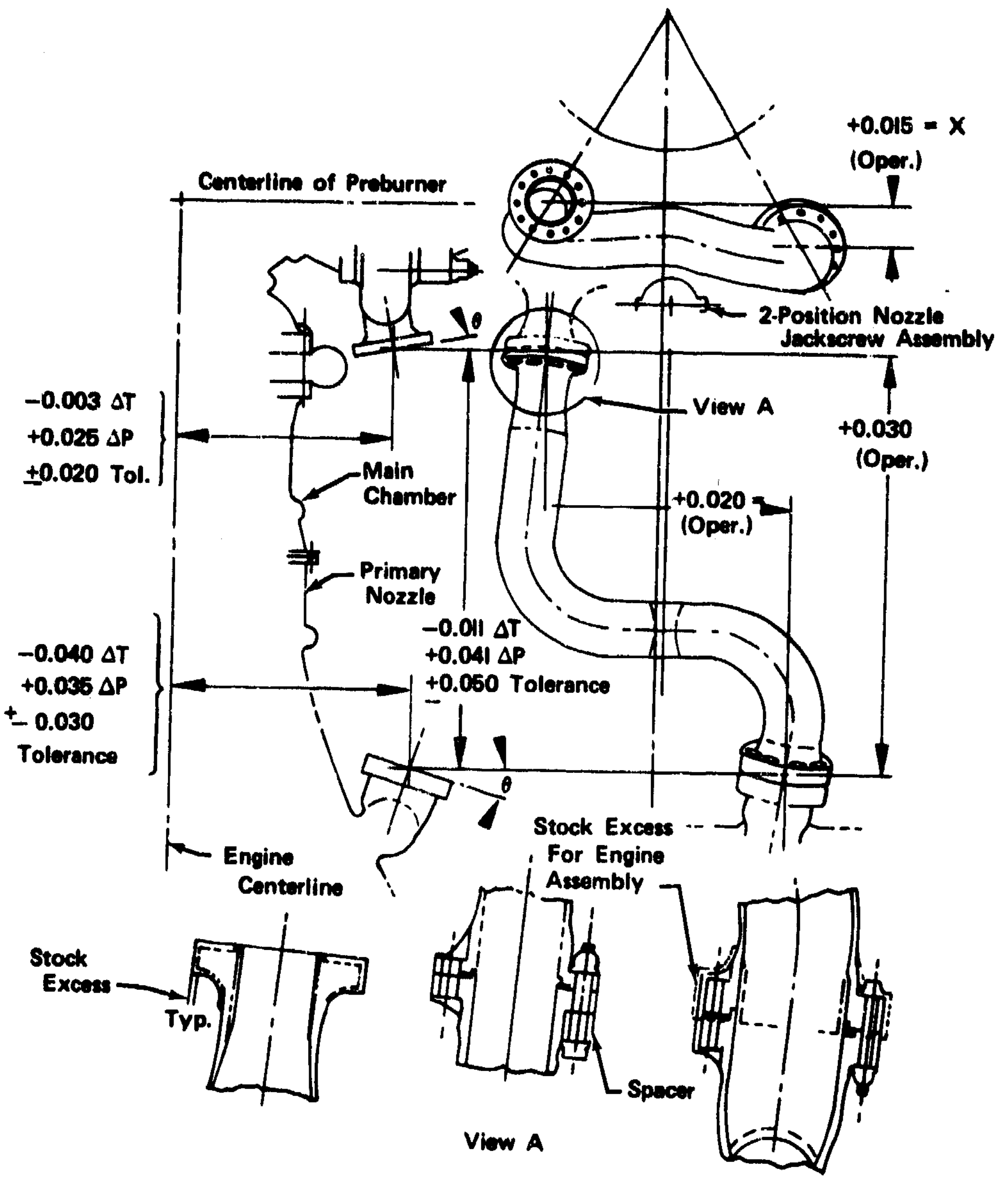

(U) Figure 551. Preburner Fuel Line

(U) Because this tube is not precooled prior to engine starting, a rapid change in metal temperature is expected in combination with maximum operating pressure, within a few seconds after engine start. The tube design allows for only 100°R differential between the flange material and the attaching bolts. There is at present no available experimental correlation with this 100°R value. Theoretically, this temperature difference value could be more than double under engine specification conditions. Therefore, it is advisable to moderate initial test conditions to avoid excessive loss of bolt preload until the effects of severe thermal transients can be fully evaluated.

(U) A general Z-type of configuration tube routing was selected to: (1) facilitiate assembly of this extremely stiff tube, (2) provide a workable level of flexure to compensate for engine thermals and pressure distortions, and (3) avoid an extreme expansion loop design that would increase weight and fluid pressure drop.

(U) The tolerances shown in figure 551 were determined from detail drawings of the preburner injector, transition case, main chamber and primary nozzle. The other ΔT and ΔP dimensions shown represent the summation of the calculated dimensional changes that occur between the mating pipe flanges. Values were computed on a steady-state basis.

(U) Prior to analyzing the tube, the wall thicknesses were calculated. A minimum thickness of 0.100 inches is required as a limit in the bend of the 3.800 I.D. section to: (1) meet the 150% pressure criteria rule and (2) to allow for only 90% yield strength properties of the welded and drawn Inconel 718 (AMS 5663) tube material. This large 4.000-inch diameter tube prevents the fabrication vendor from providing more than 20% area reduction during drawing. The standard percentage is 50% minimum, but in this case the wall (before bending) is 0.140 inches and the vendor's machinery does not have the required capacity. The wall thickness after drawing allows for an assumed 30% thinning expected in the bends.

(U) The reduced yield strength represents metallurgical concern for the welded seam where filler metal is being permitted and 50% drawing is lacking. The specific meaning of this 90% factor can be stated as follows: After solution and precipitation heat-treatment, yield and ultimate strength through the weld shall not be less than 90% of parent metal in the same tube, and elongation not less than 50% of parent metal. Planned tests of available tube specimens may show that the 90% factor is too conservative.

(U) A high pressure pipe computer program was used to establish the relationship between pipe flange moments and end point linear and angular deflections. The results of this structural analysis are plotted in figure 552, including the 10% reduction of computed moments to account for the estimated spring rates of the adjacent engine structure. The curves indicate that angular mismatch is much more critical than a linear misfit between the tube and engine. The analysis also shows that for any misfit condition, larger moments tend to occur at the preburner flange than at the nozzle end.

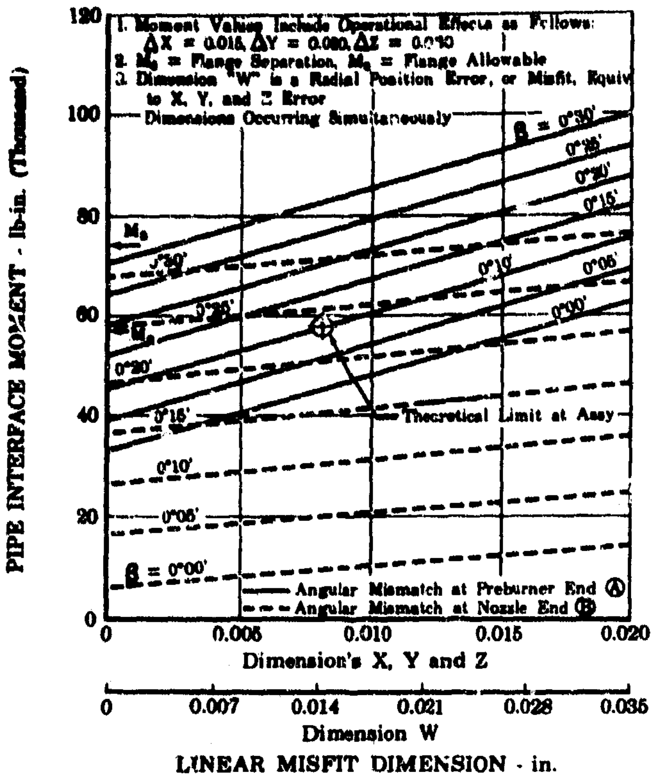

(U) Figure 552. Preburner Fuel Line Interface Moment vs Linear and Angular Mismatch Dimensions

(U) Referring to figure 552, the dimensions X, Y, and Z are equal linear misfits in all three planes simultaneously, while the term W is an equivalent radial mismatch dimension. This term was selected to simplify the problem of defining the engine misfit limitations that must be used in the sense of engine assembly instructions. The alternative would be a very complex assortment of dimensional limits involving various combinations of X, Y, or Z - plane misfits.

(U) This tube analysis also disclosed that an angular mismatch in the radial direction toward the engine centerline (θ angles in figure 552) is almost three times more critical than α angles in the plane 90 degrees away. However, to avoid assembly instruction complexity, an equivalent resultant angle (See β angles in figure 552) is used. Thus, the overall allowable mismatch in the simplest possible terms is: "a radial (linear) tolerance of 0.015 inch plus an angle of 0 degrees 15 minutes in any direction, at either end of the tube."

(U) The allowable moment acting at each flange was selected to be equal to 75% of the theoretical moment required to separate the flange during a thermal transient, at 100% of maximum cycle pressure. These moment values are 74,300 lb-in. and 57,000 lb-in., respectively, and are the same for each flanged joint. Increasing the minimum bolt tensile loads to 12,060 lb for the nozzle end and 14,580 lb for the preburner end provided the required moment capability. Presented in table LXXIII below is a summary of the essential design features and loading conditions for each flange.

(U) Table LXXIII. Flange Design Summary

Flange or Bolt Design Factor	Preburner Flange	Nozzle Flange
No. and Size of Bolt	(12) 9/16-18	(15) 1/2-20
Assembly Bolt Load Minimum lb	14580	12060
Assembly Bolt Load Minimum lb	18200	15100
Gasket Preload lb	3300	4800
100% Pressure Load lb	50600	77500
* 100% Pressure, Bolt Load lb	4210	5160
* Gasket, Bolt Load Factor lb	280	320
100°F T, Bolt Load Factor lb	3150	2450
Flange Rotation, Bolt Load Factor lb	1670	570
* Pipe Ext. Moment, Bolt Load Factor lb	5270	3560
Summation of all 5 Factors	14580	12060
Δ Minimum Oper. Bolt Load, lb	9760	9040
** Flange Preload K-Factor	2.25	1.69
*** Flange Contact Stress, 120% Press.	85000	55200
Flange Assy Contract Stress, Zero Press.	175000	67000
Flange Amb. Yield Strength	150000	60000
Flange Separation Moment, lb-in.	74300	74300
Flange Allowable Moment, lb-in.	57000	57000

CONFIDENTIAL

Δ This load equals sum of loads designated by (*)

** This number is the ratio of =

$$\frac{\text{Pressure Bolt Load + Moment Bolt Load}}{\text{Pressure Bolt Load}}$$

*** This is the average compressive stress at the flange interface, at 120% of maximum cycle pressure.

(U) The use of a spacer at the preburner joint was necessary to trade off bolt bending for the needed tensile load.

(U) The data in the foregoing table show marked differences in the "flange preload K-factor" between the two flanges of this tube. The 2.25 valve is larger because this flange has a small bolt circle and fewer bolts, but must carry the same pipe moment as the larger nozzle end. This K-factor corresponds to the 1.5 minimum preload bolt factor specified in Appendix I "Coupling Design." The 2.25 valve consists of a new operating preload equal to 100% blowoff pressure loading, plus 125% additional for external pipe moment allowance. The corresponding factor for the nozzle end is only 69% for pipe moment. If the general 150% total pressure area ground rule had been used in this design, the separation moment at the preburner would be only 31,700 lb-in., or about 40% of the predicted requirement.

(U) The specified maximum assembly bolt preloads do not cause the seal point flange deflection to exceed 0.002 inches at the 120% pressure condition according to the analysis performed with high pressure flange computer program. However, the average compressive stress at the interface under the maximum bolt load, and with no internal pressure, exceeds the (tensile) 0.2% yield stress at room temperature by 16.7% for the preburner flange and 11.7% for the nozzle flange.

(U) The final design for flight configuration of this tube should consider the following:

1. Resize the preburner flange inside diameter to more nearly match the nozzle. Flanges will then have needed geometric similarity and higher pipe moment capability, and the use of spacers will be avoided.

2. Restrict all significant linear and angular tolerances that adversely affect the potential interchangeability between this tube and the engine.

3. The bolt preload penalty is large to account for the 100° thermal load relaxation (see previous table) during transients. Experimental confirmation is very desirable to avoid either a preload deficiency if the ΔT lag is underestimated, or an overweight flanged coupling design if ground rules are too conservative.

(U) Areas requiring additional investigation, analysis, or testing are as follows:

1. Cantilever flange seal leakage at maximum pressure in conjunction with large external pipe moments.

2. Variations in tube wall thickness and out-of-roundness imposed by manufacturing limitations which are not yet well defined by fabrication vendors. (Calculated pipe wall stresses, flange moments and reaction loads while pressurized could vary widely from assumed conditions, i.e., true circular tube, with 30% thickness variation between straights and bends.

3. The true effects of thermal bolt load relaxation, and cantilever, flange rotation, on seal leakage rates.

4. The effects of actual spring rates of the adjacent engine components on the magnitude of moments generated at each flanged joint.

5. The correlation between the predicted computer program pipe moments and experimental valves.

6. The present analysis is based on static conditions and engine vibratory modes have not been evaluated beyond a simple natural frequency of the tube.

4. Fuel Pump Discharge Lines

(C) The main fuel pump design features two second-stage diffuser outlets that are merged together at a Y-section downstream. The combined flowpath curves around the aft end of the main burner chamber, passes through the preburner fuel valve, and enters the primary nozzle inlet manifold. The routing most suitable to the engine creates unequal geometry pipe segments upstream of the Y-fitting. It is, therefore, expedient to introduce an orifice plate within the shorter segment to balance the individual diffuser flows. (The design temperature pressure and flow rate are 139°R, 5610 psia and 99.5 lb/sec respectively.) The calculated pressure loss between the pump and the fuel valve is 68 psi, which is 9 psi more than engine cycle specifications, but lowering this loss to 55 psi (or 4 psi below the cycle point) would cause a 34% flow mismatch, and this condition is unacceptable.

(U) The tap-off outlet for supplying high pressure fuel to the thrust pistons of the main fuel pump and the fuel low-speed inducer is located in the longer upper segment to assist in balancing the diffuser flows. A second tap-off is located in the main pipe just upstream of the fuel valve. An overboard vent valve mounts directly on this boss. Because fuel passes through this outlet, only prior to the pumping mode of engine operation, its presence has no effect on pump performance.

(U) The design configuration is illustrated in figure 553. Upstream of the Y-fitting the two pipe segments have 1.970 inches inside diameters, and downstream the inside diameter is 3.030 inches to match the preburner fuel valve. The selected routing maintains a low profile in relation to the gimbal, and is located well inside the 22.80 inch radial envelope for clearance with the two-position nozzle. Only two flanged joints upstream of the tube exit end are employed in the engine configuration shown. (Rig pump housings, which were designed with mechanical joints at both diffuser outlets, can be altered for engine usage to accomplish design compatibility with this engine plumbing.)

(U) The pipe components are made of Inconel 718 (AMS 5663) material, with the tube sections formed from welded and drawn stock. Wall thickness in straight sections is based on 30% thinning in bends. Each diffuser outlet pipe is therefore approximately 2.120 inches outside diameter with a nominal wall of 0.105 inch which allows 0.073 inch minimum thickness in bends. The section downstream of the Y-fitting is 3.350 inches maximum with a nominal wall of 0.157 inch before bending, and the minimum allowable wall is then 0.110 inch.

(C) The pipe flanges are designed in accordance with the coupling criteria previously explained by the example presented for the preburner fuel line. Bolt preloads of 7200-8800 lb for the diffuser pipe joint, 6900-8300 lb for the lower diffuser outlet flange, and 12,900-15,000 lb for the outlet flange are specified to ensure a 40% margin against flange separation. The tube routing analysis established allowable flange moments of 18,600 lb-in. for the 2.120-inch sections and 43,000 lb-in. at the outlet flange that mates with the preburner fuel valve. Flange thicknesses were determined by high pressure flange design computer program based on a standard seal point deflection of 0.002 inches maximum at 120% cycle pressure, or 6780 psi. Each flanged joint is designed to accommodate a number of potential seal designs.

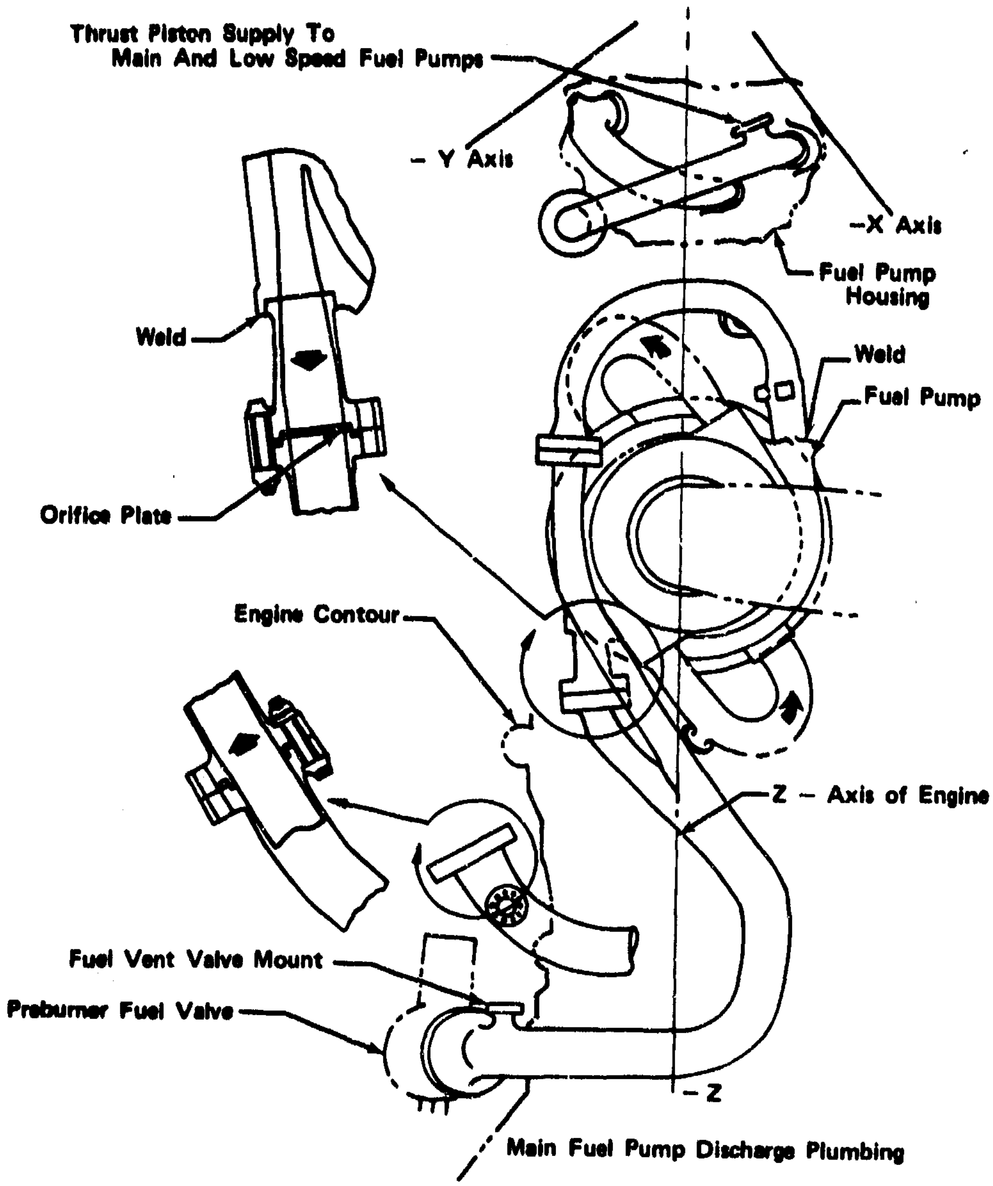

(U) Figure 553. Main Fuel Pump Discharge Plumbing

(U) The large outlet flange that mates with the preburner fuel valve contains tapped holes for engagement of the twelve 0.5625-18 studs that pass through the valve housing and mating flange on the primary nozzle. (Locknuts are secured to the opposite ends of the studs.) The intimate contact at these threaded holes ensures effective thermal conduction to pre-cool the studs before high pressure loading is imposed. This design thus avoids any significant loss of bolt preload caused by thermal lag relative to the valve housing.

(U) This pipe system is pre-soaked before starting, and is pre-cooled additionally by overboard hydrogen venting, prior to engine ignition. A heat transfer analysis shows that the initial assembly preload will fluctuate upwards as much as 3400 lb per bolt until the valve housing is exposed to the operating fuel flows. After thermal stabilization, the specified bolt loads are expected to increase only 130 lb each.

(U) The problem of mating this tube assembly to the engine with prevailing engine component tolerances had precluded designing for part interchangeability. All relevant tolerances were evaluated on the fuel pump, transition case, main chamber and primary nozzle. Results show that maximum variation of engine end points for tube mating could be X of ±0.056 inch, Y of ±0.056 inch also, and a Z value of ±0.075 inch. These axes are shown in figure 547.

(C) The analysis of the same engine components to determine dimensional movement of the tube mating point (taken at the fuel valve end) caused by thermals and high pressure effects indicate an acceptable condition. That is, the tube configuration and external moment capacity of the flanges are adequate to handle the calculated results. The calculated dimensional values for combined ΔT and ΔP effects, at 100% engine thrust and mixture ratio of 5:1 condition, are: $X = \pm 0.030$ inch, $Y = \pm 0.037$ inch, and $Z = \pm 0.095$ inches. The plus value means that the engine end points move apart when the engine is operating steady-state. The tube-to-engine assembly requirements that can be permitted in conjunction with these operational conditions are: Custom machining of the valve end of the tube assembly shall be performed as required to limit the total misfit to 0.015 inch in any direction and 0 degrees 10 minutes of angle in any direction.

5. Oxidizer Pump Discharge Lines

(U) The oxidizer pump discharge lines are part of a welded assembly consisting of the oxidizer pump volute housing, two diffuser sections, and both discharge lines which are joined at a spherical housing referred to as the "collector." The collector is located at the turbine inlet of the oxidizer low speed inducer and serves as a manifold to receive the flow of oxidizer from the pump and to direct a portion of the pump discharge flow to the preburner injector and the supply for the pump thrust piston. The general arrangement of this assembly is shown in figure 554.

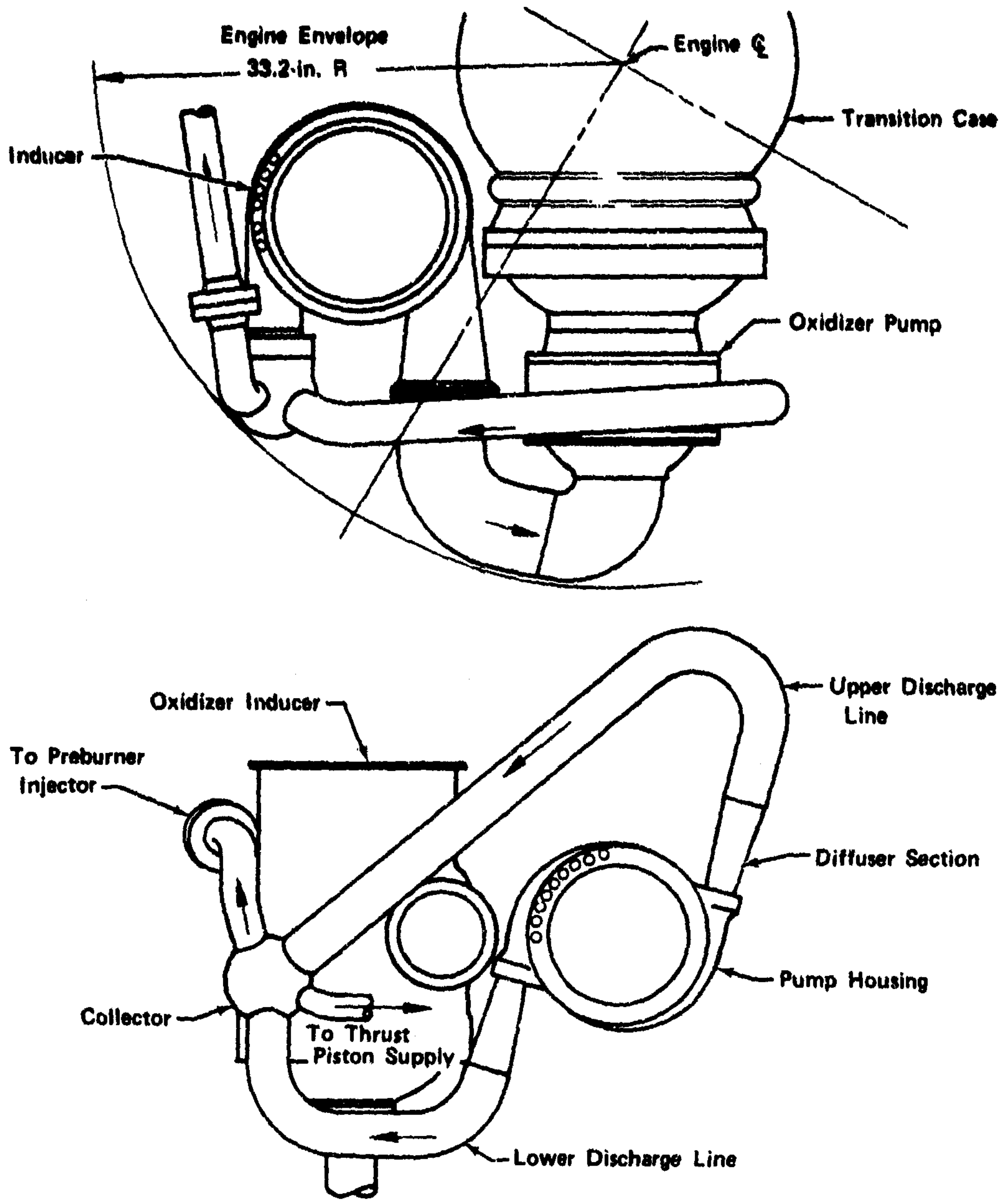

(U) Figure 554. General Arrangement of Oxidizer Pump Discharge Lines With Oxidizer Low-Speed Inducer

(C) Design conditions for the lines were as follows:

(C) Maximum Operating Pressure - 6000 psia
Operating Temperature - 244°R

(C) Maximum Flow Rate - 408 lb/sec
(Maximum flow does not occur at maximum pressure.)

(U) Design structural criteria is specified in Appendix I. The decision to use a welded assembly rather than bolted flange joints for the discharge lines was made on the basis of the weight saving which could be realized. The welded joints eliminated four flanged joints for a saving of approximately 20 pounds. Two flange joints are still required however, these being at the collector inducer interface and near the collector to connect with the preburner oxidizer supply line.

(U) The high pressure flanges were designed using the criteria of Appendix I with the analysis of the design being made by the high pressure flange computer program.

(U) The flange used on the collector housing is not considered as an ordinary cantilever flange. The half of the flange located on the inducer is a typical flange and is designed by using the basic criteria of Appendix I. The flange was designed with 0.001 inch deflection of the seal face at 1.2 maximum cycle pressure. The mating half of this flange joint is an integral part of the collector housing. This flange was designed using the "line of Action" concept where effort is made to have the resultant forces act through the centroid of the flange in order to reduce or eliminate the moments which tend to roll the flange increasing the deflection of the sealing surfaces. The engine envelope radius of 33.2 inches, as shown in figure 554, limited the length of the flange and diameter of the collector. Because of this envelope restriction it is necessary to use stud bolts rather than conventional bolts in this flange. The structural analysis of the spherical section of the collector and the flange portion was made by using the finite element structures program. Design stresses of this structure were limited to 85% of the 0.2% yield strength.

(U) The minimum bolt loads were determined from the criteria of Appendix I using the following procedure:

Minimum bolt load = 1.5 x blow-off load
+ seal load + thermal lag
+ bolt load relaxation due to flange rotation
+ bolt load due to external moments.

(U) A summary of the bolt loads and stresses are shown in table LXXIV. The effects of thermal lag were neglected in these bolt load calculations because of the cool down or soak conditions which occur before pressure is applied to the flange.

(U) Table LXXIV. Bolt Loads and Stress of Studs Used at Collector To LO_2 (Or Oxidizer) Inducer Flange

Bolt load due to:

Blow-off Load at 1.5 Operating Pressure	4810 lb
Seal Load	210 lb
Load Relaxation Due to Flange Rotation	334 lb
Load Due to External Moments	2130 lb
Total Axial Load	7484 lb

Bolt Tensile Stress Due to Axial Load	101,000 psi
Bolt Bending Stress Due to Flange Rotation	49,500 psi

$$\frac{\text{Tensile Stress}}{0.85 \times 0.2\% \text{ Yield Strength}} + \frac{\text{Bending Stress}}{1.3 \times 0.2\% \text{ Yield Strength}} \leqq 1.0$$

$$\frac{101,000}{0.85 \times 165,000} + \frac{49,500}{1.3 \times 165,000} = 0.717 + 0.232 = 0.949$$

Bolt Loads Based on Using 18 0.375-24 UNFJ Studs

(U) All high pressure tubing sections were sized using the basic design criteria of Appendix I with these additional requirements: thinning of tube in the bend areas is limited to 30% and stress levels are limited to 90% of the 0.2% yield stress at 150% of design pressure to account for reduced strength of welds in the welded and drawn tubing as discussed in the preburner fuel line section.

(U) The high pressure pipe analysis - Deck 6503 - was used to analyze the tubing and to determine the external moments required for the bolt load calculations. The inputs supplied to the program were the tolerances due to build up of the engine components, the displacements of the tube end points due to pressure and temperature changes and the angular mismatch of the components. The results of this analysis are tabulated in table LXXV.

(C) The analysis of the design is dependent upon the assumption that, at the time of assembly, the oxidizer inducer will be installed and adjusted at its mounting in order to avoid any mismatch of the collector and pump supply duct with the mating flanges on the inducer. It is also assumed that the inducer mounting will allow for the displacement of the end points due to the thermal effects during the cool down period. These features were included in the design of the oxidizer low speed inducer mount brackets; however slight redesign may be required to ensure that the desired movement is in the required direction.

(C) The calculated weight of the line and collector assembly is 43 pounds. The pressure drop is 25.4 psi as compared to a cycle pressure drop of 41 psi.

(U) Table LXXV. Tube Analysis Input and Results

Tolerance Due to Engine Build Up	X = ±0.025 Y = ±0.016 Z = ±0.029
Angular Mismatch	$\theta_{X,Y,Z}$ = ±0°30'
Displacements Due to ΔP & ΔT at Operating Conditions	X = -0.017 Y = -0.014 Z = -0.012
Resultant Moment at Diffuser End of Line	Upper Line 10,400 in. lb Lower Line 19,900 in. lb
Resultant Moment at Collector End of Line	Upper Line 49,000 in. lb Lower Line 45,300 in. lb
Resultant Moment at Collector/ Inducer Flange	42,200 in. lb

6. Preburner Oxidizer Supply Line

(C) The preburner oxidizer supply line directs liquid oxygen from the oxidizer pump discharge to the preburner oxidizer control valve. The tube size (2.125 O.D. x 0.100 wall thickness) was selected to match the inside diameter of the mating components. The line was designed for a maximum pressure of 5919 psia and a flow rate of 82 lb/sec. At the maximum pressure condition the operating temperature is 244°R and the pressure loss is 6.2 psi. See figure 555.

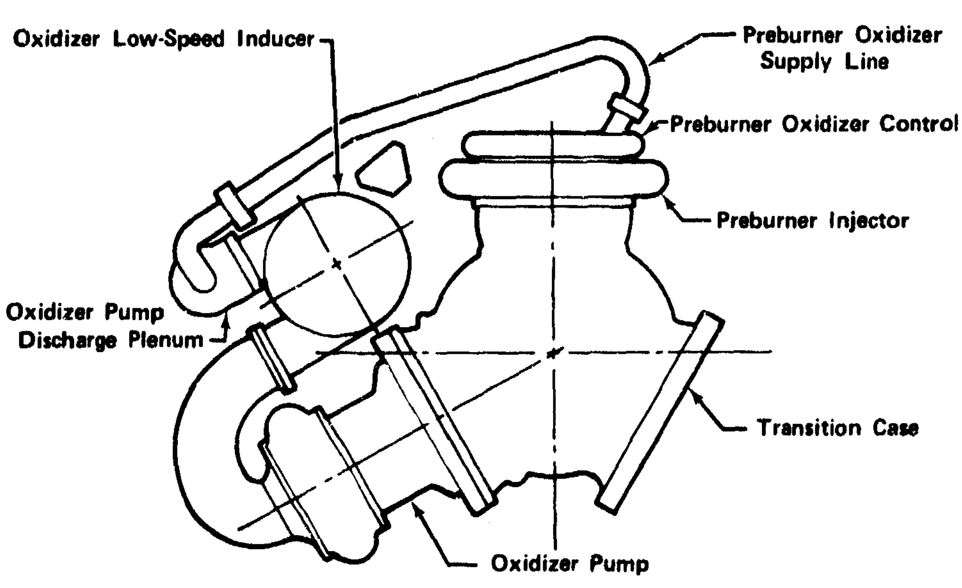

(U) Figure 555. Schematic of Engine Looking Aft

(U) Inconel 718 (AMS 5663) welded and drawn tubing was chosen for the line material because of its ductility at cryogenic condition, high strength and weldability. This material has an 0.2% yield strength of 166,000 psi at operating temperature. The minimum wall thickness of the tube is 0.065 inches (in the bends) and is based on a hoop stress limit equal to the 0.2% yield stress at 150% of the maximum operating pressure with allowance for a 90% weld efficiency. The minimum stock tube wall thickness of 0.095 inches allows for a 30% reduction in wall thickness at the bends during fabrication. The minimum bend radius is 1.7 times the nominal tube O.D.

(U) The flanges at each end of the line are identical and are designed to mate with existing component flanges. These flanges were designed by the high pressure flange computer program. The total line weight (including bolts and nuts for both flanges) is 22.9 pounds.

(U) The high pressure pipe computer program was used to determine the flange and pipe loadings resulting from pipe end point displacements. These displacements result from angular and linear tolerances and the thermal (ΔT) and pressure (ΔP) effects at operating condition on both the line and the engine components. The ΔP and ΔT effects at cooldown were examined and determined to be less than at operating conditions.

(U) The total tolerance stackup, thermal (ΔT) and pressure (ΔP) induced displacements are tabulated in table LXXVI along with the resulting flange moments. The maximum flange moment load is 19,750 lb-in. The allowable moment is limited by the tube structure limits rather than the flange separating moment capacity (as with all previous lines). The tube stress is within the allowable limit as specified in Appendix I.

(U) Table LXXVI. Total Tolerance Stackup

Tolerances due to buildup	X = ±0.059 in. Y = ±0.069 in. Z = ±0.050 in.
Angular Tolerance	0°37.4' (0.0108 in./in.)
ΔT and ΔP Displacements	X = -0.0236 in. Y = -0.0763 in. Z = +0.0 in.
Resulting Flange Moments:	
At Oxidizer Pump Discharge Plenum	19,750 in.-lb
At P/B Oxidizer Control Inlet	10,350 in.-lb

7. **Main Burner Oxidizer Line**

(C) The high pressure line that conducts liquid oxygen from the oxidizer low-speed inducer turbine discharge to the main burner operates at a maximum cycle pressure of 4800 psi and flows approximately 370 lb/sec at design point. The calculated pressure drop of 26.0 psi is compatible with theoretical cycle requirements. The oxidizer temperature at this point in the system is 244°R. The line is filled prior to engine starting because the downstream end mates with the main oxidizer (shut-off) valve as shown in figure 556. Near the tube exit there is a flange boss for mounting an overboard vent valve (the same valve design as the one that mounts on the main fuel pump discharge line). Oxidizer is vented overboard at this point to pre-cool the oxidizer system prior to engine ignition.

(C) The 2.850 inches inside diameter of this main oxidizer line is matched to the exit diameter of the hydraulic turbine located inside the low-speed inducer assembly. The wall is sized to 150% cycle pressure (or 7200 psi) at 0.2% yield strength in Inconel 718 (AMS 5663) welded and drawn tube material. The same 90% properties allowance is used here as described for the preburner fuel line. The nominal wall thickness is 0.117 inches and with a 30% wall thinning factor assumed, the minimum wall is 0.082 inch allowable in accordance with the design ground rules.

(U) The flange designs reflect complete analysis using the cantilever flange computer program. Flange thickness was set by the criterion of 0.002 inch total deflection for the mating pair with a metal O-ring the assumed gasket. Then the flange was further analyzed to be certain that deflection with alternative seals did not exceed 0.002 inch per flange set. The computer results are presented in table LXXVII.

(U) Flange rotation, bolt load loss is accounted for, but there is no thermal load loss because this tube is pre-cooled before operating high pressures exist. The specified minimum bolt preload is high enough to maintain at least 150% of fluid blow-off load at maximum cycle pressure after flange rotation.

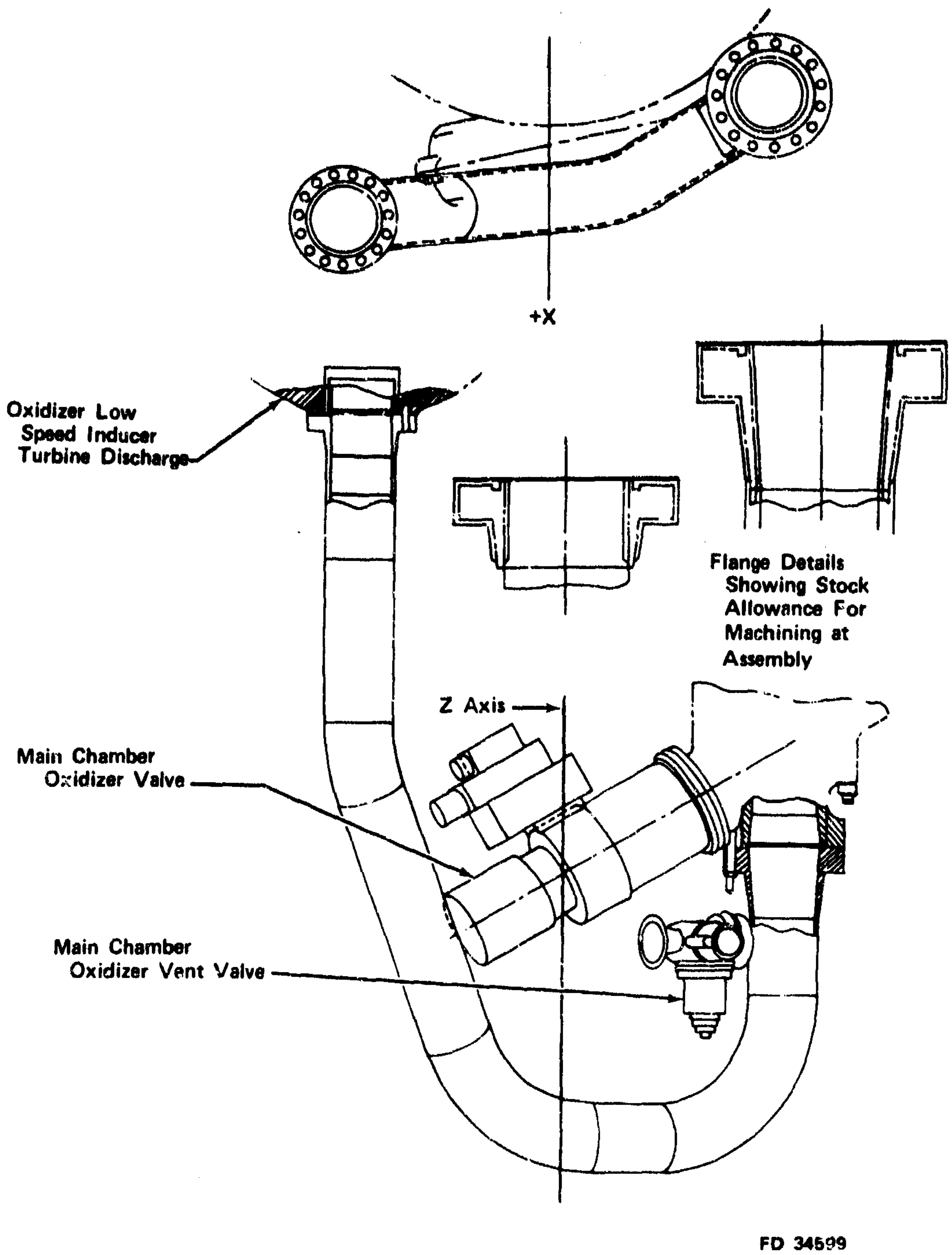

(U) Figure 556. Main Burner Oxidizer Supply

(U) Table LXXVII. Computer Design Results

	Inlet	Outlet
Flange Thickness (t_F)	0.769 in.	1.094 in.
Dia. Bolt Circle	4.071 in.	4.760 in.
Dia. Bolt	0.375 in.	0.375 in.
No. of Bolts	15	15
Inside Dia.	2.850 in.	3.280 in.
Flange Deflection per Side	0.0001	0.0001
Dia. at Seal Point	3.062 in.	3.500 in.
Assy. Bolt Load - Min.	5580 lb/bolt	6210 lb/bolt
Assy. Bolt Load - Max.	6700 lb/bolt	7450 lb/bolt
Max. Bolt Tensile Stress	74,000 psi	82,400 psi
Max. Bolt Bending Stress	35,050 psi	33,200 psi

(U) The standard routine of analyzing engine component tolerances ($X = \pm 0.36$, $Y = \pm 0.031$, $Z = \pm 0.023$) and thermal and pressure effects, on end point displacements was completed. Results are, that the ΔT and ΔP effects produce the following values: $X = -0.010$ inch, $Y = +0.049$ inch and $Z = +0.017$ inches. This tube design is basically limited by the bolted flange between the main injector and the main chamber oxidizer valve (which was sized to valve downstream pressure for low weight). That particular flange can support 14,500 lb-in. of external moment at 100% cycle pressure, with a 25% margin to flange separation. The oxidizer line design, therefore, must be custom machined to within 0.005 inch in the Z-direction and 0.010 inch in both the X and Y directions (see figure 556). Angular mismatch of zero degrees 10 minutes is permissible in addition. With these restrictions imposed, the calculated moment predicted at the injector flange is 13,300 lb-in.

(U) The moment produced at the tube inlet flange under the same conditions is 21,200 lb-in. which is 75% of the theoretical separation moment. The flanged joint at the outlet end of the tube (where it mates with main oxidizer valve) has a similar moment capability. The tube at this end also has a divergent section to match the inside diameter of the oxidizer valve.

(U) Inconel 718 (AMS 5663) studs and locknuts are used at each tube flange joint to assure thermal compatibility and light weight. Both stresses listed in table LXXVII reflect the prevailing bolt design criteria defined by the equation:

$$\frac{\text{Tensile Stress}}{0.85 \times 0.2\% \text{ Yield Strength}} + \frac{\text{Heading Stress}}{1.3 \times 0.2\% \text{ Yield Strength}} = 1$$

8. Fuel Turbopump Inlet Line

(C) Figure 557 illustrates the fuel inlet line, which consists of a flanged circular straight section that attaches to the fuel low-speed inducer flange, a circular-to-elliptical transition, an elliptical section that is contoured to match the 66.4 in. diameter engine envelope, and a final curved elbow of complex shape. (The design temperature, pressure, and flow rate is 47°R, 117 psia, and 90 lb/sec, respectively. This exit portion contains a series of splitter vanes to achieve a uniform velocity profile with low flow loss, and avoid possible cavitation. These vanes are designed per the S.A.E. Aerospace Applied Thermodynamics Manual and the method adapted to liquid flow in circular pipes. The elbow and turning vane concept has been evaluated in testing performed by Pratt & Whitney Aircraft and reported in Section C of AFRPL TR-69-3.

(C) The elliptical main section was dictated by available space to the engine outer envelope. The duct had to clear the two-position nozzle jackscrew mechanism at the inside contour as well. The pipe section was designed with vertical structural member located at the tube centerline. The web thickness was determined by the internal pressure (174 psi max) that tends to deform the ellipse into a circular section. The selected design is the lightest weight found in the space available.

(U) The duct material is Inconel 718 (AMS 5663) to achieve high stress to weight ratio, and weldability. The end flanges are of different thicknesses because of the different mating materials and the requirement to maintain the 0.002 inch seal point deflection criteria. The fuel inducer flange material is AMS 4924 titanium alloy with a modulus of 17.25×10^6 psi at -300°F. However, the modulus of the nickel alloy tube is 31.0×10^6 psi and this tends to reduce the thickness on the duct side because of the higher modulus. A more significant cause for the thickness difference is the thin wall adjacent to the flange of the fuel low-speed inducer outlet which tends to expand and rotate the flange.

(U) The fuel line applies only 4500 lb-in. of moment to the fuel turbopump inlet housing, which produces only 1200 psi stress in the pump housing. Part of this stress is the result of a 3-g transverse (engine) acceleration requirement. However, the critical cause of housing stress relates to the possible vertical Z-axis mismatch between the fuel inlet pipe and the low-speed inducer. A total misfit of 0.025 inch is allowable here in order to limit torsional stress on the turbopump housing which has a yield stress of 30,000 psi. The vertical mismatch limitation will be controlled by adjusting the inducer support structure with custom-machined spacers.

(U) Pipe stresses generated in the pipe caused by the 0.025 in. are 7500 psi shear stress and 14,900 psi in bending. The respective allowables for the Inconel 718 (AMS 5663) material at room temperature are 85,000 psi and 150,000 psi.

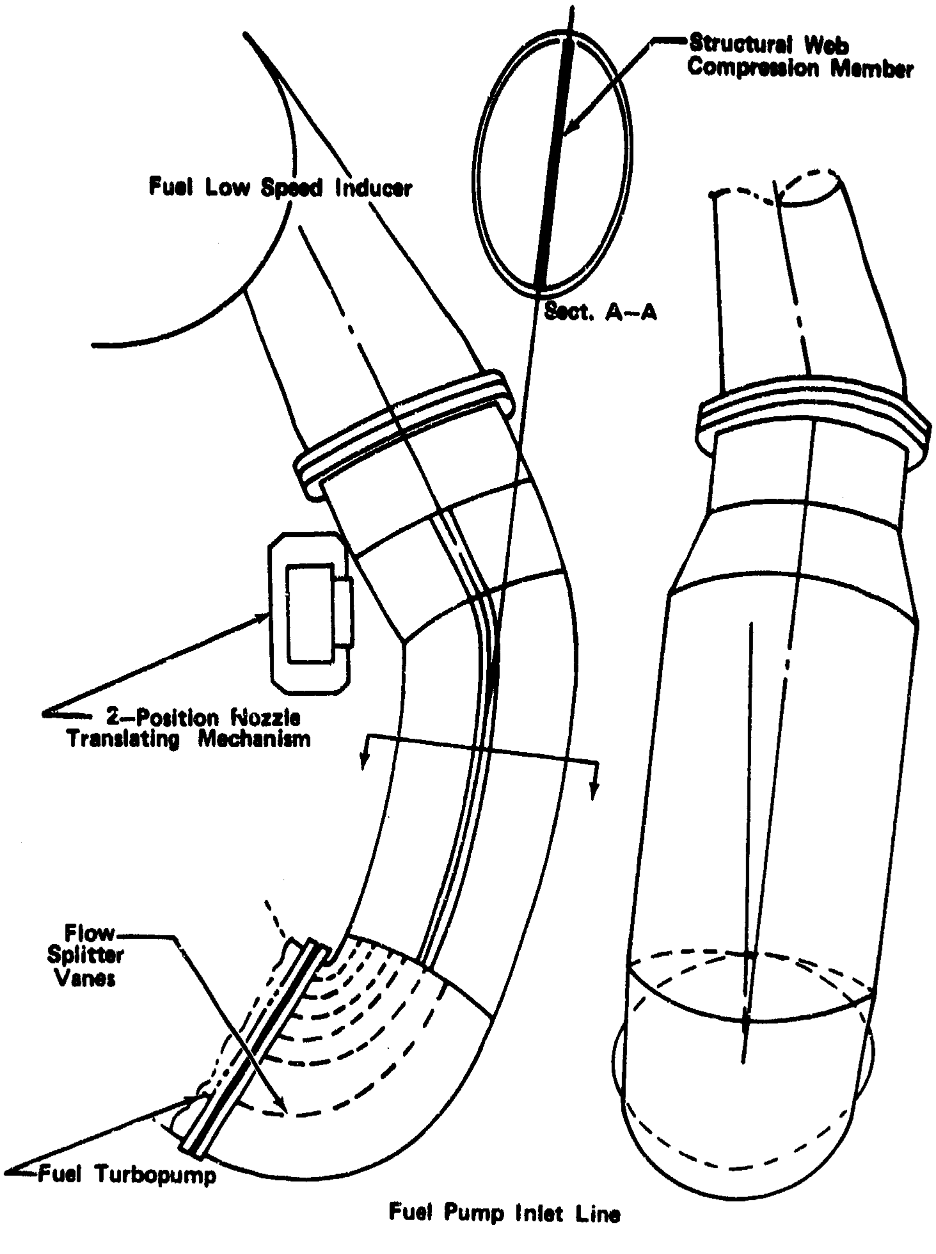

(U) Figure 557. Fuel Pump Inlet Line

(U) The mount system design of the low-speed inducer provides free travel in the X and Y directions of 0.200 inch and 0.760 inch, respectively. Calculations show that the fuel inlet pipe will contract 0.017 inch in the X-direction and 0.047 inch in Y, because of thermal and pressure effects in relation to the fuel turbopump. No significant reaction loads are created, however, because the inducer assembly is free to move in the resultant direction indicated.

9. Oxidizer Turbopump Inlet Line

(U) The inlet pipe to the oxidizer turbopump shown in figure 558 differs from the fuel pump design previously described in several ways. Both serve the same basic function of conducting low-speed inducer discharge flow to the inlet of the main pumps with minimum velocity distortion, low pressure loss, and no cavitation. The oxidizer side incorporates the special feature of a circular manifold for injecting various recirculation or return flows back into the main pump inlet with minimum flow disturbance. Both ducts have flow splitters, but the oxidizer design incorporates these vanes over a large portion of total length, primarily because of the inherent requirement to turn the flow through a total angle of 180 degrees. This design condition is dictated by engine envelope restraints.

(C) The distinctive mechanical feature of the oxidizer inlet duct is that it is made integral with the oxidizer turbopump inlet housing. The pipe structure is fabricated from Inconel 625 sheet and bar stock and welded to the inlet pump housing. The design temperature, pressure, and flow rate is 204°R, 267 psia, and 619 lb/sec, respectively. See Section IV-J for a discussion of alternate materials considered and all other relevant mechanical features, stresses, engine assembly mating requirements and test experience factors.

10. Fuel Low-Speed Inducer, Turbine Supply Line

(C) The subject tube assembly flows 55 pounds per second hydrogen at 408°R and 5121 psi operating pressure at design point. The flow is conducted from the primary nozzle (transpiration coolant heat exchanger section) forward to the turbine inlet on the fuel low-speed inducer. See figure 559. Two tap-off tee fittings are incorporated into this line to (1) supply fuel coolant to the engine transition case, and (2) provide a turbine bypass flowpath connection (see the Engine Plumbing Roadmap Diagram, figure 568 for the physical arrangement).

(U) The general routing of this relatively long tube was optimized on the mockup with specific attention to the engine envelope, the 0.500 in. minimum clearance to other components, and adequate expansion loops to achieve flexibility. The flowrate dictated a 1.500-inch outside diameter tube and the maximum cycle pressure at 150% set the wall thickness minimum for bends at 0.041 inches. With a 30% thinning allowance assumed, the nominal wall is 0.062 to 0.072 inches. Flanges are welded to each end of the Inconel 718 (AMS 5663) welded and drawn tube, and two tee fittings are welded into the assembly. Each tee has an integral, externally threaded boss similar to the MS 27850 through MS 27855 stain-steel configuration, except for dimensional changes that conform to the Inconel 718 alternate series.

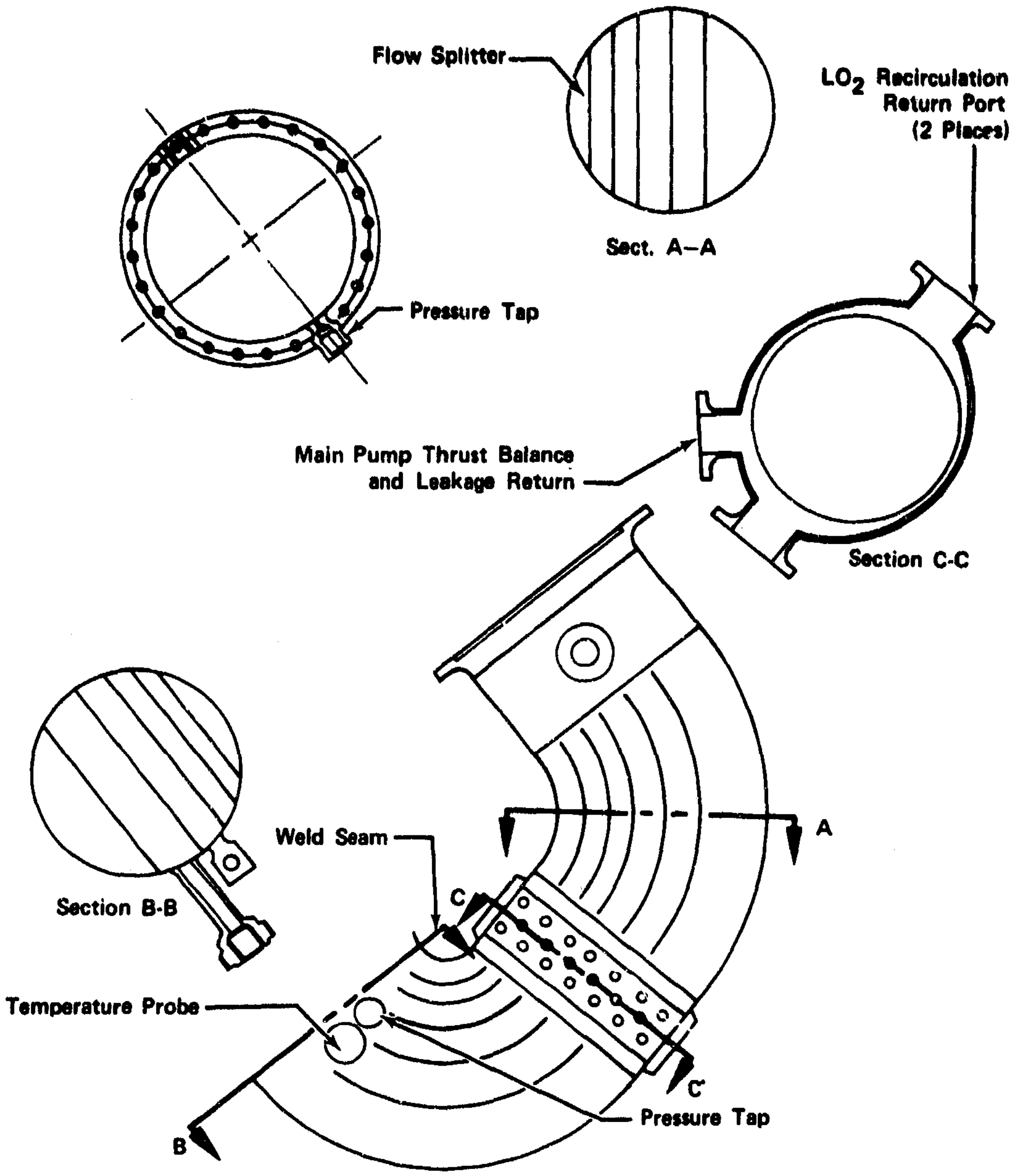

(U) Figure 558. Oxidizer Low-Speed Inducer-to-Oxidizer Turbopump

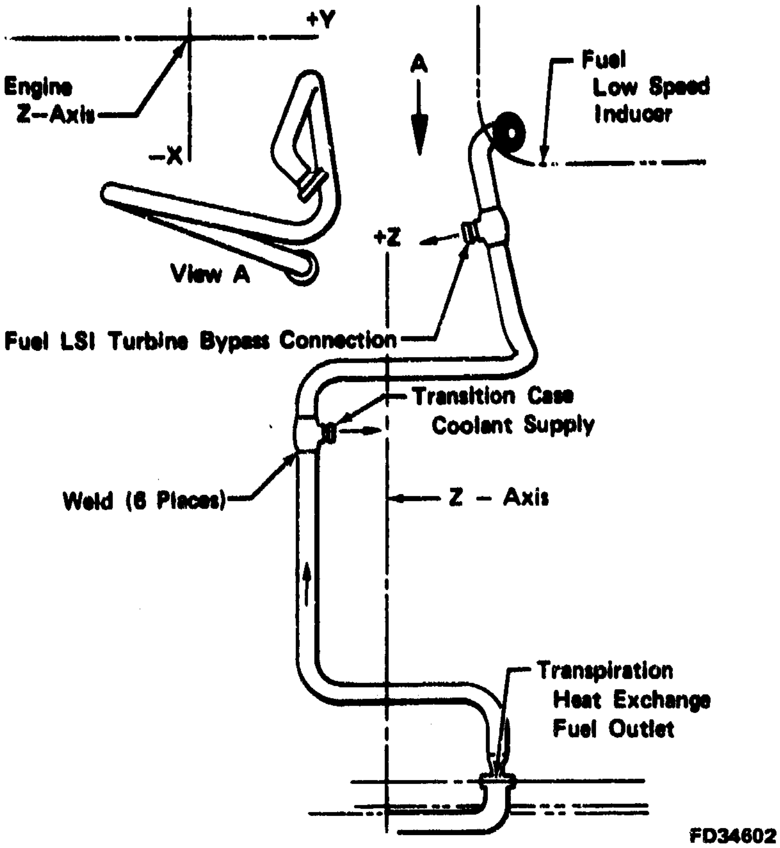

(U) Figure 559. Fuel Low-Speed Inducer Turbine Drive Fuel Supply

(U) The flange at the nozzle end is a mirror image of the flange design on the primary nozzle, which is made of Inconel 625 material. This solution is valid because the modulus of each mating material is nearly the same. Equal flange deflections of 0.001 inch each are thereby assured, and flange stresses are well within the yield stresses. The flange at the opposite end mates with a flush boss on the fuel low-speed inducer and was sized by the flange design computer program according to the general criteria. The moment capability of each flange based on the regular tube coupling ground rules is 2770 lb-in. for the nozzle end and 4490 lb-in. at the inducer interface.

(U) Following the established tube routing analysis, the mating flange end point motions caused by operating thermals and pressure effects were calculated from known dimensions and predicted metal temperatures. Results are as follows in engine coordinates: X = ±0.008 inch, Y = ±0.033 inch, and Z = ±0.043 inch. These values were used as input deflections in the tube analysis program, along with required dimensional tube coordinate information. Overall tolerances for the engine mating were evaluated and the estimated value of 0.100 inch in the X,Y, and Z direction was considered a realistic conclusion. When 0 degree 30 minutes angular misfits in two planes were also added to the above displacements, the final computed flange moments were 1035 lb-in. at the nozzle and 1575 lb-in. at the inducer flange. Because these values are well below the flange allowables, no custom fitting of the tube at engine is specified.

11. Primary Nozzle Fuel Supply Line

(U) Opening the preburner fuel valve permits hydrogen to flow from a side port in the valve housing through the subject tube to the transpiration coolant heat exchanger section of the primary nozzle. Figure 560 illustrates this relationship. Bolted flanges are incorporated at each end of the tube, and a special orifice is provided at the nozzle interface to flow balance the fuel system with no external power accessory installed. Near the valve end there is an integral tee fitting to supply coolant flow to the oxidizer pump rear bearing and fuel to each of the igniter assemblies.

(U) The outlet boss on the fuel valve mates with a 1.000-inch outside diameter tube with an 0.049 inch wall. This valve housing and the tube assembly are designed with Inconel 718 materials. The tube flange is designed like its mate on the valve. The same material is used for the eight, 0.250-28 studs employed. The bend at the tube inlet end has a 1.500-inch mean radius. This tight bend is necessary to achieve adequate clearance to the nozzle.

(U) The nozzle flange is sized to 1.250 outside diameter and the material is Inconel 625. A mating flange of similar geometry was designed for this end of the tube. Both flanges are the cantilever type and each is designed to accommodate a number of alternate seals.

(U) The 1.250 diameter tube size is used for most of the overall tube length to maintain pressure drop below 21 psi for cycle compatibility. The computer tube analysis however, shows the need to custom fit this tube to the engine. Operating pressure effects are negligible, and thermals are small: X = -0.007 inch, Y = 0.001 inch, and Z = -0.020 inch. However, the estimated overall tolerances that could reach 0.050 inches in any direction are significant. When a zero degrees 30 minutes angular mismatch is included, the tube analysis results are: 2200 lb-in. generated at the nozzle joint (the flange capacity is 2250 lb-in.), and 2300 lb-in. at the fuel valve flange. The capacity of this flange is only 1385 lb-inches. Therefore, it is necessary to restrict the strain imposed on this tube at engine assembly to avoid flange separation. Preliminary values of allowable mismatch are 0.030 inch in any direction together with zero degrees 15 minutes in any plane, and 0.100 inch of surplus stock is provided at the larger nozzle-end flange for the necessary custom machining.

12. Main Chamber Coolant Supply Line

(U) Fuel coolant to the main chamber is supplied from the discharge of the fuel low-speed inducer turbine. A 1.500-inch outside diameter tube is required to maintain the pressure drop below 18 psi. A minimum wall of 0.028 inch is needed in the bends to meet the 150% pressure criteria at 0.2% yield strength. Inconel 718 (AMS 5663) material is used for flanges and tube, which can be seamless in this size. The nominal wall thickness in the straight portions is to be 0.040-0.048 in. to allow for 30% thinning.

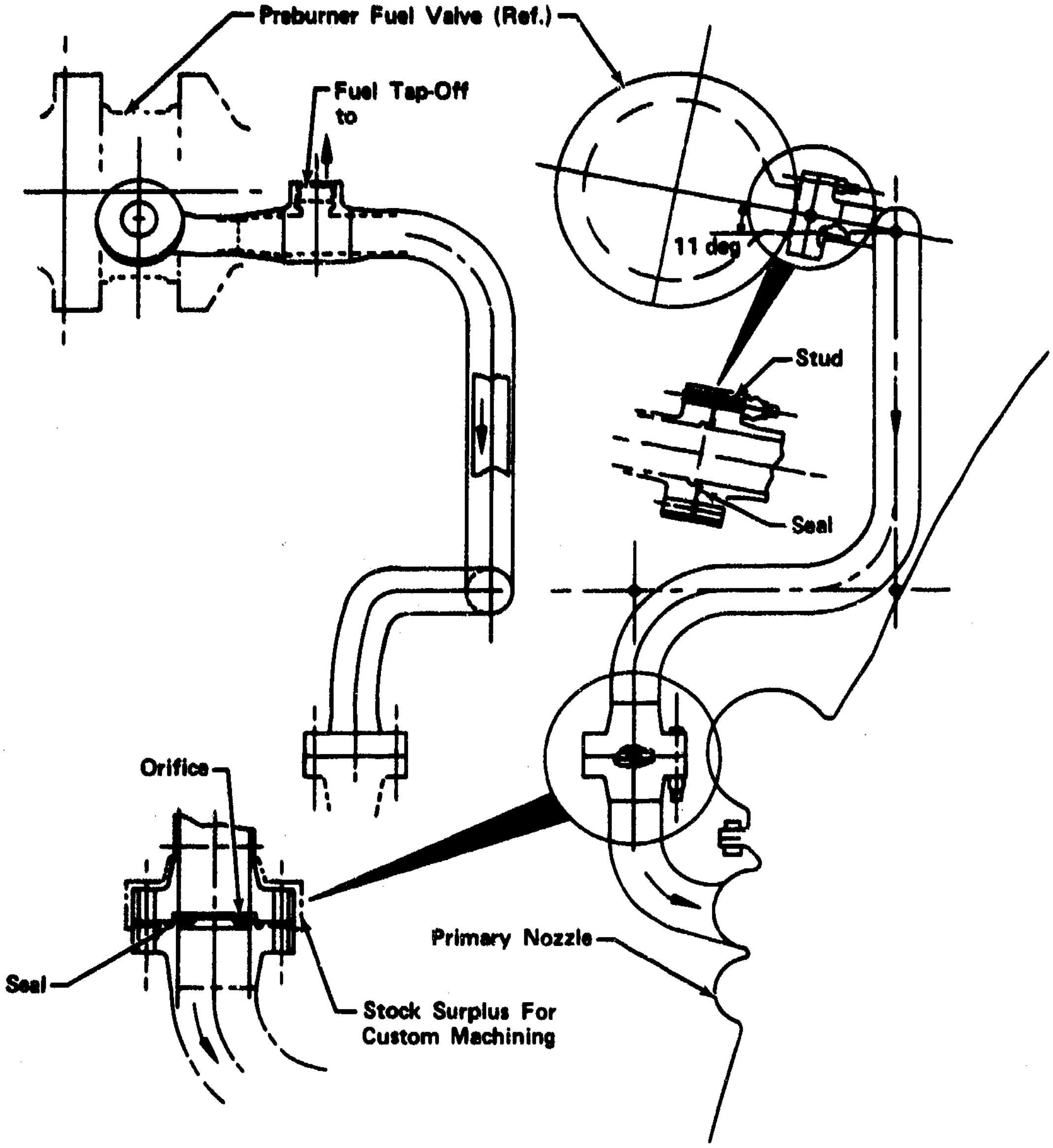

(U) Figure 560. Primary Nozzle Fuel Supply Line

(U) As shown in figure 561, the upper flange incorporates a 90° outlet tee for a 0.750 inch drive turbine bypass tube. The other end of this bypass line is shown in figure 559. The boss is machined integral on the adjacent flange due to space limitations. Both flange designs are identical to the existing flange design on the combustion chamber. The moment capacity of these flanges is calculated to be 2600 lb-in. and the thickness is set by 0.002-inch total deflection, per the standard.

(U) Results of the routine calculation for tube end-point deflections caused by pressure and thermals are X = -0.018 inch, Y = -0.039 inch, and Z = +0.028 inch, for the upper end in relation to the chamber end. Engine tolerance stock-up results are approximately as follows: X = ±0.049 inch, Y = ±0.048 inch, and Z = ±0.044 inch. Angular mismatch of zero degrees 30 minutes was assumed for the analysis. These values were used to input the high pressure tube analysis program and results are: The moment produced at the joint with the combustion chamber is 3195 lb-in., while the mement at the inducer end is only 785 lb-inches. The joint at the inducer can easily accommodate the predicted moment, but the other joint would be seriously overloaded from pipe moment without custom fitting at installation. A tentative assembly requirement is specified as follows: end point mismatch must not exceed 0.040 in. in any direction, and flange planes cannot be out of plane more than zero degrees 30 minutes in any direction.

13. Small Line Connector and Seal Selection

a. Battelle Bobbin Seal

(C) The initial selection effort consisted of a literature search to determine the availability of flight weight commercial connectors rated for XLR129 requirements (up to 6000 psi operating pressure). This investigation resulted in the selection of the AFRPL Bobbin Seal connectors developed by Battelle Memorial Institute for the Air Force Rocket Propulsion Laboratory for additional study and testing.

(U) The existing AFRPL Bobbin Seal connectors were type 347 SST (MS 27850 through 27855) rated for 4000 psi working pressure and 6000 psi proof pressure. The reported leakage rate for these connectors is well below the 10^{-4} standard cc per second required.

(U) Battelle Memorial Institute was contacted to up-rate their 347 SST connector design to the program requirements and the operating conditions and structural limits were supplied by Pratt & Whitney Aircraft. These specifications included the nominal tube OD wall thickness, tube material, operating temperature and pressure, externally applied moments and fatigue limits.

(U) Because the connectors are joined to the tubes by a butt weld, material selection was the first requirement. Inconel 718 (AMS 5663) was selected for both the tubing and fittings because of its high strength and weldability.

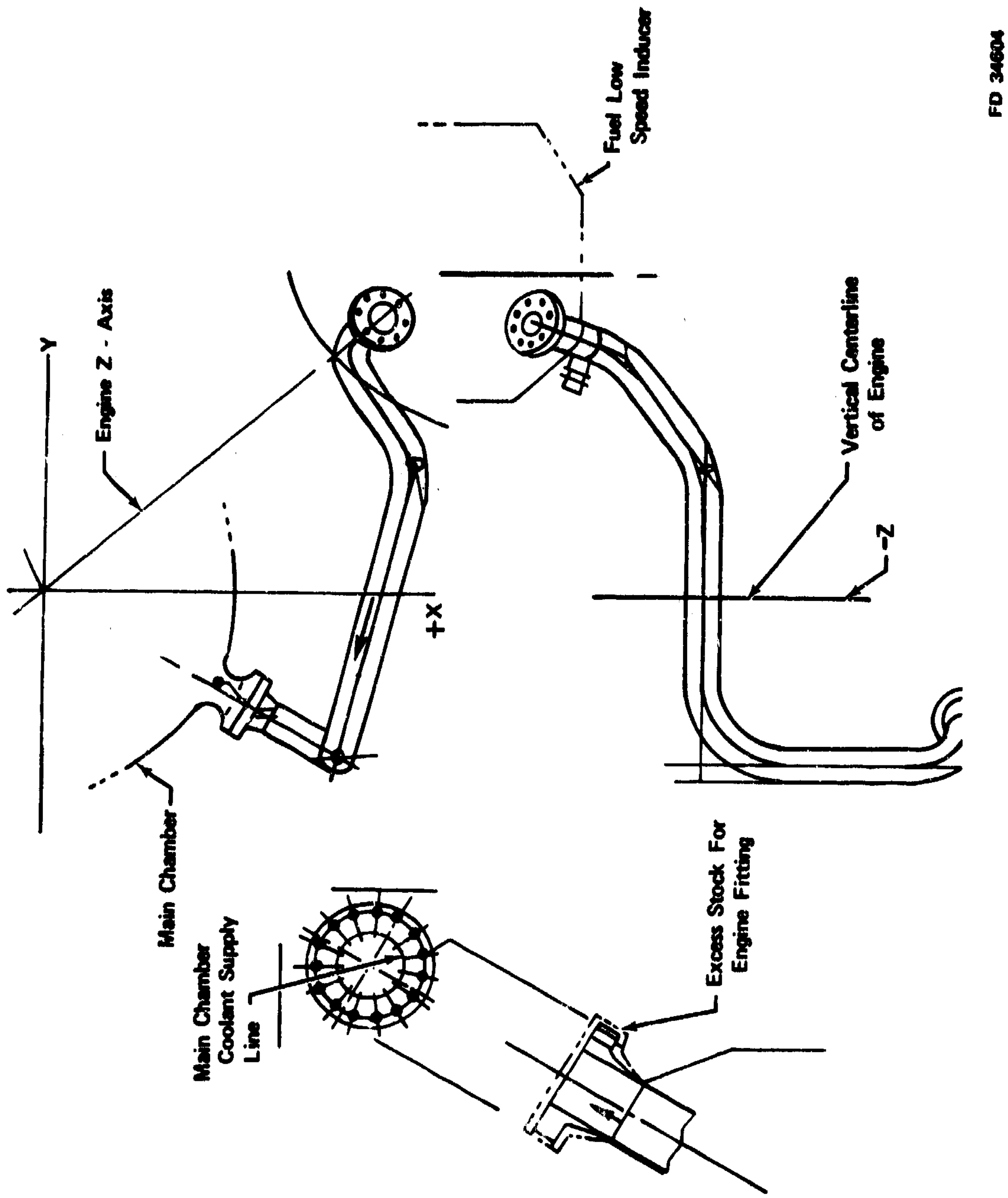

(U) Figure 561. Main Chamber Coolant Supply Line

(U) The structure limit for both the tubes and the fittings is that proof pressures (1.5 times operating pressure) must not produce stresses in excess of the 0.2% yield strength and that stresses at operating pressure must not exceed 0.85% of the 0.2% yield strength (See Appendix I). The tubing wall thicknesses were sized by selecting the thinnest (Pratt & Whitney Aircraft) standard wall in which the hoop stress in the minimum wall produced by the minimum bend radius (equal to twice the nominal tube OD) would not exceed the allowable stress.

(C) The specified allowable tube bending moment produces the maximum allowable combined stress in the tube wall when applied to a tube pressurized to 6000 psi (working pressure). When combined with working pressure stresses, the vibratory stresses specified yield a life of 10^7 cycles (See Appendix I, Goodman Diagram for material used).

(C) Using these specifications, Battelle Memorial Institute produced a computer designed Inconel 718 (AMS 5663) connector rated for 6000 psi for 3/8-inch to 1-inch nominal diameter tubes. In addition to the design effort, several seals of the 3/8-inch and 1-inch sizes were machined and tested to ensure that adequate contact stresses on the seal surfaces would be present. (Appendix II) figure 562 shows the Battelle seal and a connector assembly. Figure 563 shows the sequence of steps for assembly of the Battelle bobbin seal.

(U) These designs consist of the two Inconel 718 (AMS 5663) flanges which are butt welded to the tube ends and subsequently fully heat treated. The coupling nut is also fully heat-treated Inconel 718 (AMS 5663). Battelle specified an annealed Inconel 718 seal with soft nickel plating on the sealing surfaces (Appendix II).

(U) An investigation of the plating requirements revealed a hardness specification (150 Knoop) to be produced by a 1500°F vacuum anneal. This plating annealing process is not compatible with the annealed Inconel 718 seal material because precipitation hardening of annealed Inconel 718 will commence at approximately 1000°F. After consulting with Battelle Memorial Institute, silver plate (AMS 2410) was substituted for nickel plating.

(U) The 347 SST AFRPL couplings designed by Battelle (MS 27850 through 27855) are designed to be butt welded to tubes whose wall thickness is specified by the ASA Code for Pressure Piping (see ref. 1). These wall thicknesses are greater than those required by present XLR129 design limits (hoop stress limited). The same situation exists with the Inconel 718 couplings designed by Battelle. A weld mismatch between the coupling flange and the tube was eliminated by requiring that the coupling ID match that of the tube and by adding a transition taper to the coupling flange at the weld joint.

(U) Silver plate (AMS 2410) has been added to the coupling flange thread as an anti-seize agent. Torque limits were recalculated using coefficients of friction for silver-plated threads to produce the same maximum seal compressive stress used by Battelle. The minimum seal load will be less than Battelle's value because the actual minimum coefficient of friction (f = 0.11 based on test experience) will be approximately one-half the maximum value rather than the constant coefficient (f = 0.20) used in Battelle's calculations.

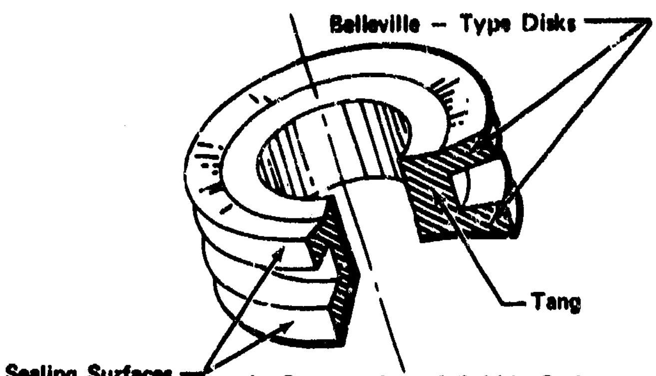

b. Construction of Bobbin Seal

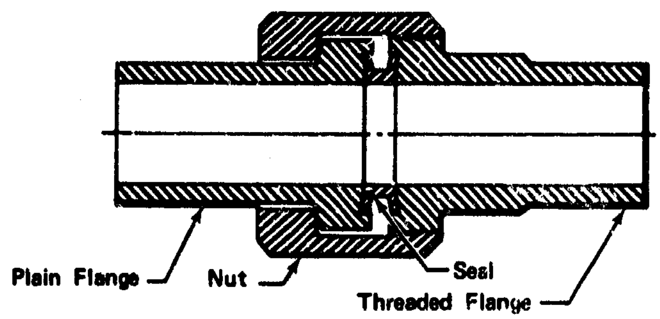

a. Connector Assembly

FD 34605

(U) Figure 562. Connector and Seal

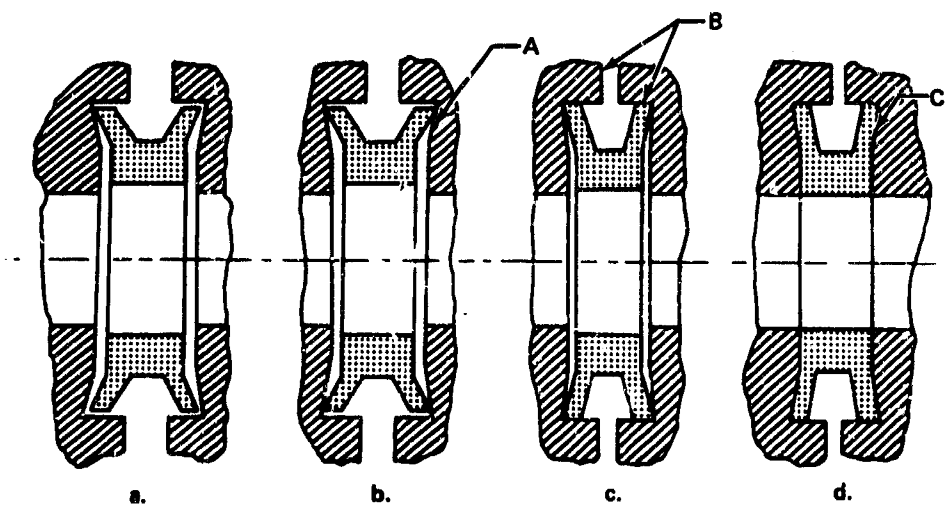

FD 34606

(U) Figure 563. Bobbin Seal Assembly

b. Boss Connectors

(C) The need for a 6000 psi tube to housing boss connector capable of meeting leakage requirements resulted in the adaptation of the AFRPL Bobbin Seal and portions of the tube connector to fulfill this requirement. Two designs have evolved, one consists of a semi-permanently installed connector which adapts the boss to the line (see figure 564) and the other design in which the flange on the end of the tube is mated directly with the boss (see figure 565). Both designs use the same boss and also the same bobbin seal as the high pressure line connector. Because the thread size is the same on both the line connector nut and the boss connector, the torque limits are the same. (See figure 566).

(U) The first design (the boss connector) will be used during the development program to determine if the second design can be incorporated later realizing a significant weight reduction. The advantages of the boss connector include those of any tube to boss adapter, protection of boss threads and seal surfaces during frequent plumbing installation and removal, and in this case, it eliminates the blind installation of the bobbin seal in the field. Its disadvantages are its protruding length, which may increase tube installation difficulties in confined spaces, and also the requirement for two seals for a single tube to boss connection.

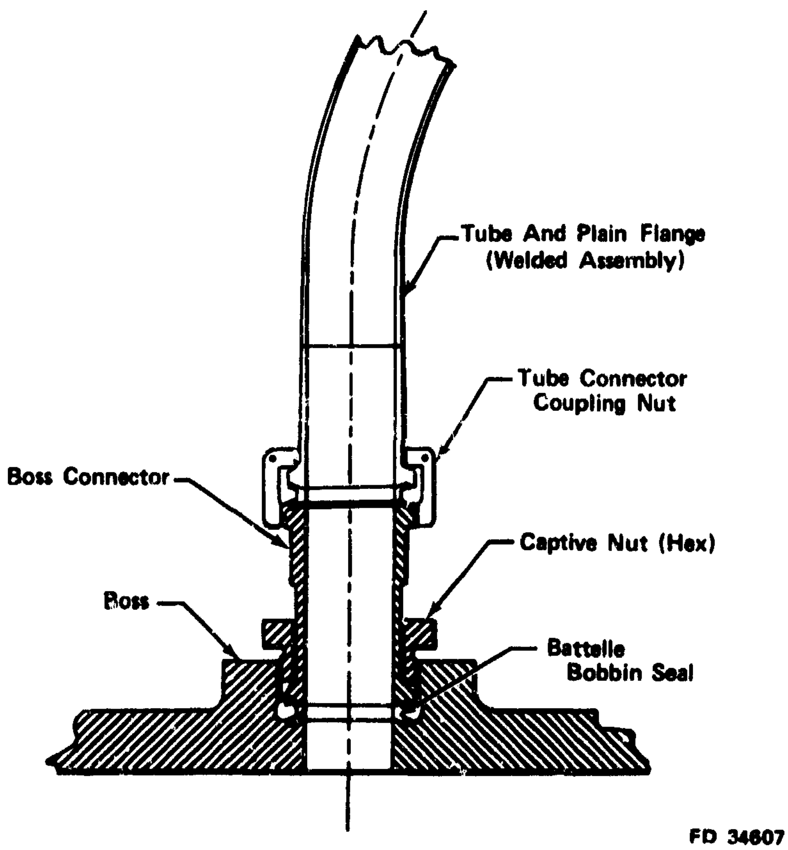

(U) Figure 564. Inconel 718 High Pressure Boss Connector

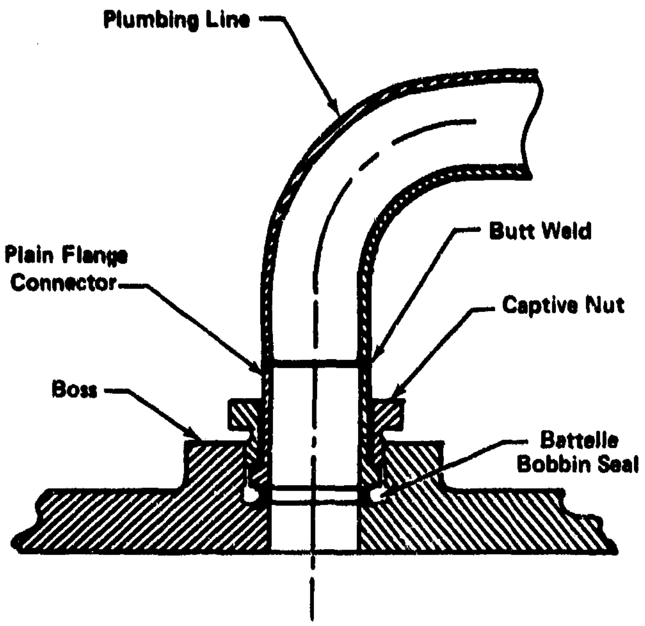

FD 34608

(U) Figure 565. Alternative Boss Connector Design

(U) The second design eliminates one seal, minimizes weight and reduces the required installation space. The primary disadvantages are possible installation difficulties resulting from the tube deflection required to position the tube end in the boss and blind installation of the bobbin seal in the bottom of the boss recess under less than ideal assembly conditions.

(U) The flight engine design will probably include both types of boss connections with the boss connector (first design shown in figure 564) used only where large tube deflections are required to assemble the tube to the boss or where blind assembly of the seal is difficult.

c. Miscellaneous Elbows, Tees and Fittings

(U) Presently, none of these connectors have been designed but no difficulties are expected in the various combinations of the fitting ends required to form the required joints. Sketches of the required fittings are shown in figure 567. Tables LXXVIII, LXXIX, and LXXX list all engine small lines and presents functional information about the line and its design. Tables LXXVIII, LXXIX, and LXXX also contain key letters that will provide identification of each line on the engine plumbing road map figure 568.

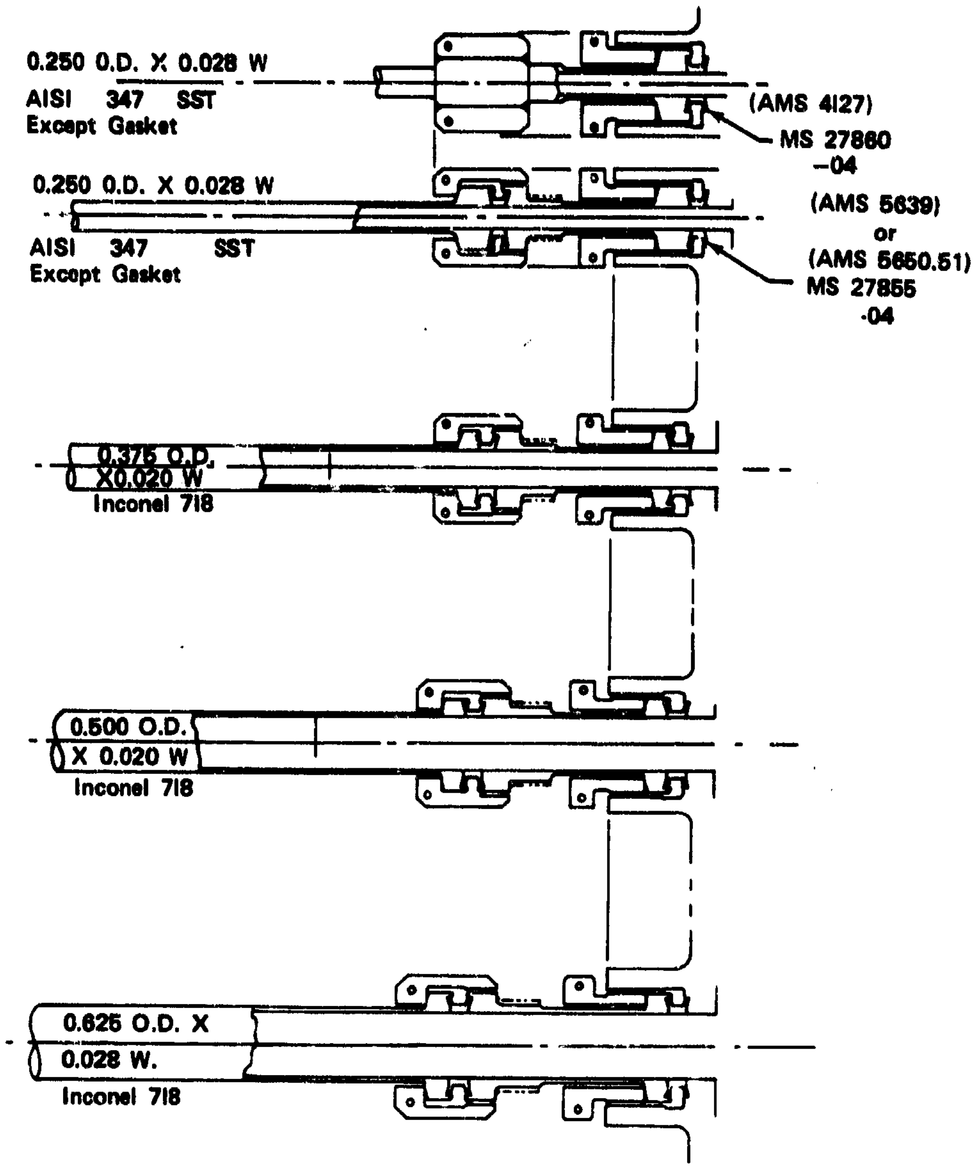

(U) Figure 566. Line Connectors and Bosses

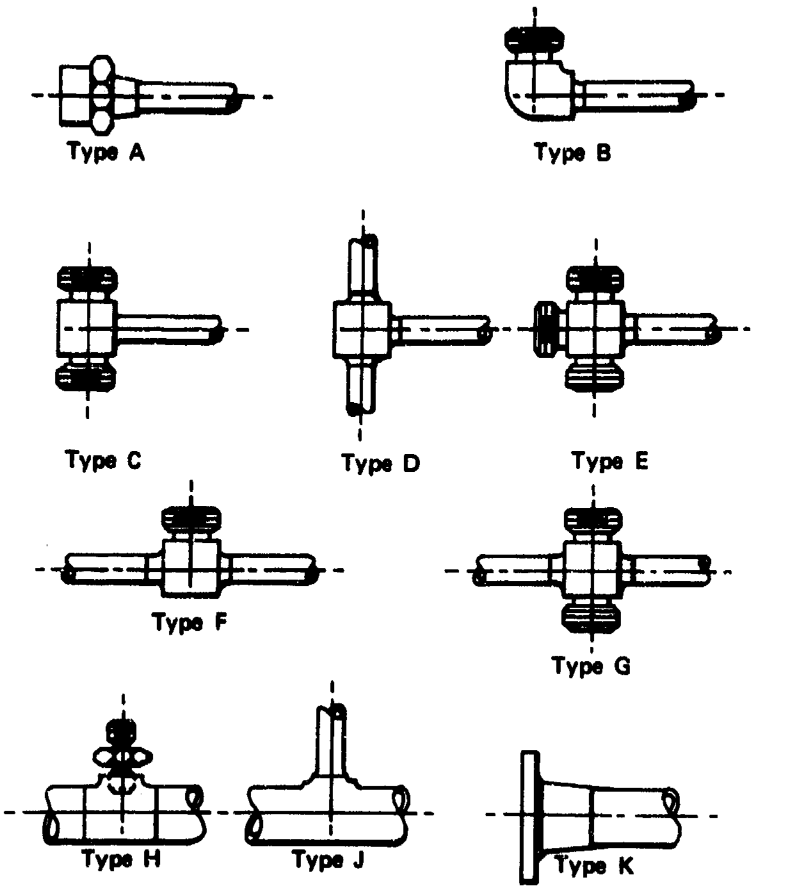

(U) Figure 567. Tube Fittings

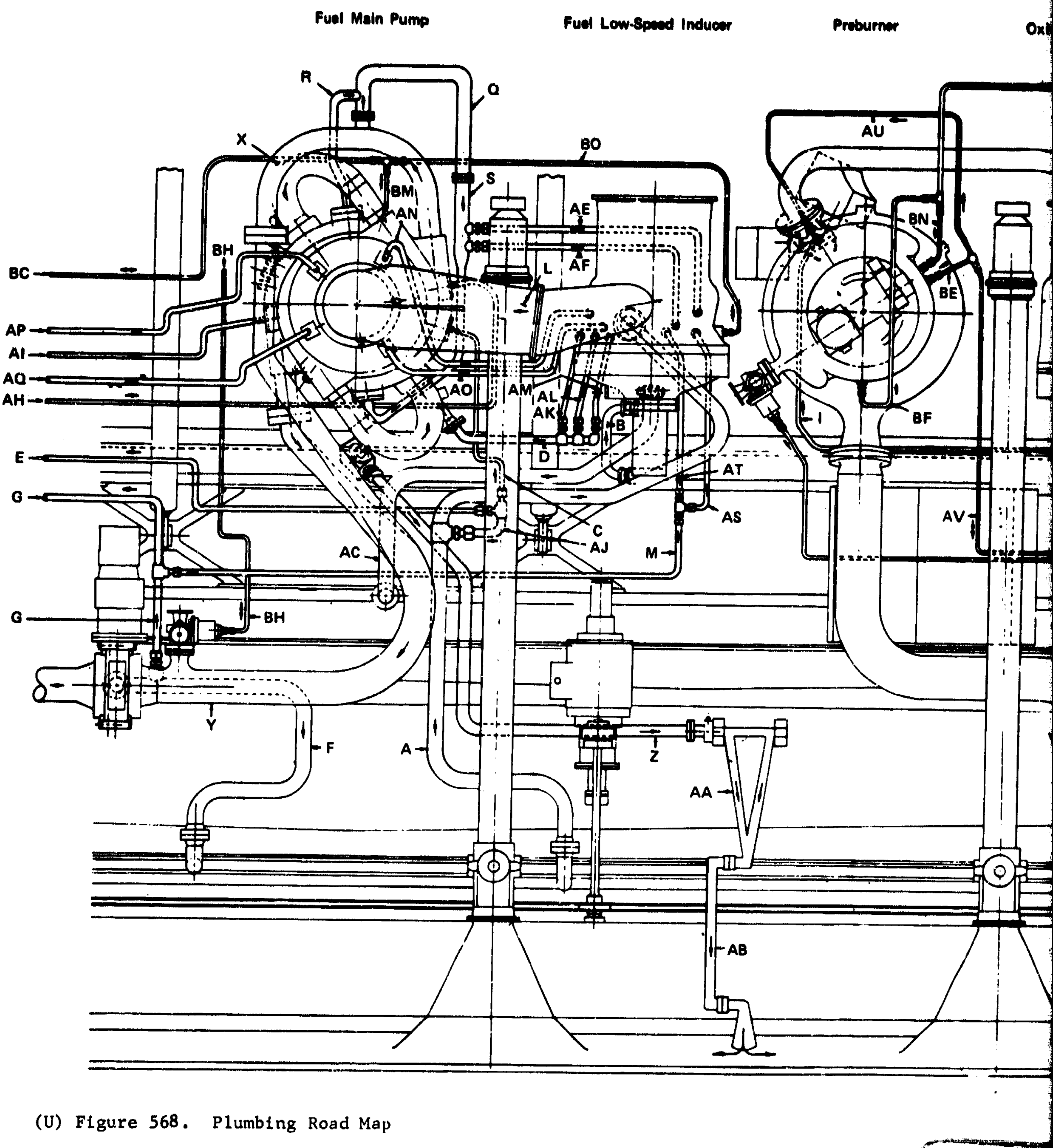

(U) Figure 568. Plumbing Road Map

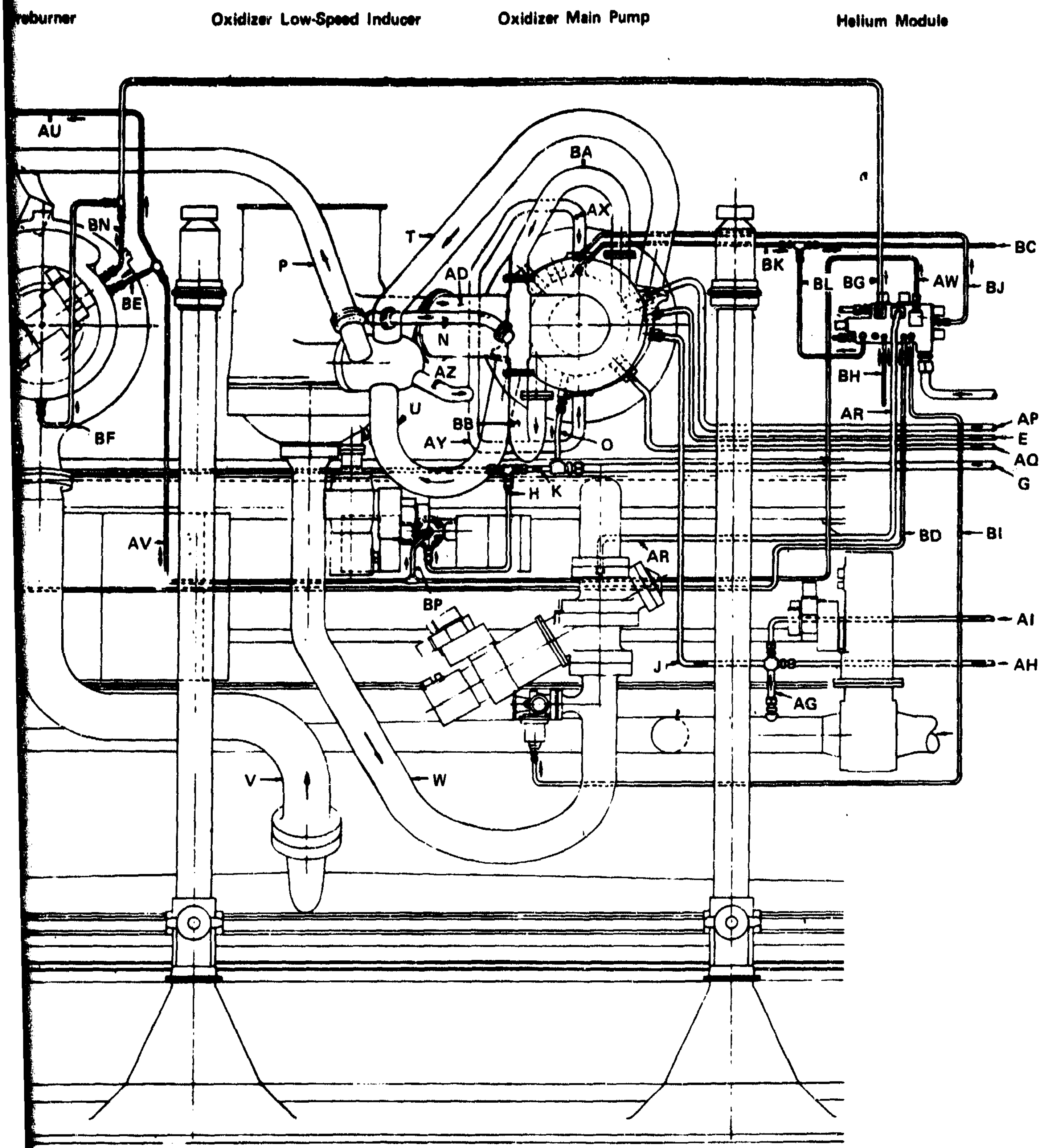
reburner
Oxidizer Low-Speed Inducer
Oxidizer Main Pump
Helium Module
AU
BN
BE
BF
AV
P
T
BA
AX
AD
N
AZ
U
BB
AY
O
H
K
BP
AR
V
W
J
BK
BL
BG
AW
BJ
BC
BH
AR
AP
E
AQ
G
BD
BI
AI
AH
AG

FD 34611

(U) Table LXXVIII. Fuel Small Lines Summary

*	Description	Tube Size (in.)	End Fitting	Tube Material
Q	Main Fuel Pump and Fuel LSI Thrust Piston Supply (See Note 1)	1.500 OD 0.049 Wall 20.0 Long	K Inlet J Inline K Exit	Inconel 718 (AMS 5663)
S	Fuel LSI Thrust Piston Main Supply and Fuel Pump	1.500 OD Wall 10.0 Long	K Inlet 2 H Inlines	Inconel 718
	Thrust Piston Supply No. 2 (See Note 2)	0.875 OD 0.33 Wall 30.0 Long	K Exit	Inconel 718
Z	Two-Position Nozzle Coolant Supply (Valve to Translation Linkage)	1.000 OD 0.035 Wall 43.0 Long	K Inlet K Exit	Inconel 718
R	Main Fuel Pump Thrust Piston Supply No. 1	0.875 OD 0.035 Wall 12.0 Long	J Inlet K Exit	Inconel 718
B	Fuel LSI Turbine By-Pass	0.750 OD 0.028 Wall 8.0 Long	A Inlet A Exit	Inconel 718
D	Fuel LSI Thrust Piston Discharge Collector	0.750 OD 0.028 Wall 15.0 Long	B Inlet 2 F Inlines K Exit	Inconel 718
AJ	Transition Case Liner Coolant Main	0.750 OD 0.028 Wall	A Inlet C Exit	Inconel 718

Notes:

(1) Includes Welded on Branch to F/P Thrust Piston Supply #1

(2) 21.50 OD Sect. Includes Two Type H Tap-Offs then Reduces to 0.875 OD to F/P Thrust Piston #2 Supply.

*Road Map Reference Letter

(U) Table LXXVIII. Fuel Small Lines Summary (Continued)

*	Description	Tube Size (in.)	End Fitting	Tube Material
G	Igniter Fuel Supply and Bearing Coolant Supply for Fuel LSI and Oxidizer LSI	0.625 OD 0.028 Wall 50.0 Long	A Inlet F Inline A Exit	Inconel 718
AG	Main Fuel Pump and Main Oxidizer Pump Turbine Coolant Supply	0.625 OD 0.028 Wall 20.0 Long	A Inlet E Exit	Inconel 718
M	Fuel LSI Rear Bearing Coolant Main Supply	0.500 OD 0.020 Wall 46.0 Long	A Inlet A Exit	Inconel 718
AE	Fuel LSI Thrust Piston Supply No. 1	0.500 OD 0.020 Wall 5.0 Long	A Inlet A Exit	Inconel 718
AF	Fuel LSI Thrust Piston Supply No. 2	0.500 OD 0.020 Wall 12.0 Long	A Inlet A Exit	Inconel 718
AN	Fuel LSI Front Bearing Coolant Drain No. 1	0.500 OD 0.020 Wall 42.0 Long	A Inlet A Exit	Inconel 718
AO	Fuel LSI Front Bearing Coolant Drain No. 2	0.500 OD 0.020 Wall 35.0 Long	A Inlet A Exit	Inconel 718
K	Igniter Fuel Main Supply	0.500 OD 0.020 Wall 4.0 Long	F Inlet A Exit	Inconel 718
AP	Main Oxidizer Pump Rear Bearing Coolant Drain No. 1	0.500 OD 0.020 Wall 65.0 Long	A Inlet A Exit	Inconel 718

Notes:

(3) Includes Welded in Line "O" at Inlet.

*Road Map Reference Letter

(U) Table LXXVIII. Fuel Small Lines Summary (Continued)

*	Description	Tube Size	End Fitting	Tube Material
AQ	Main Oxidizer Pump Rear Bearing Coolant Drain No. 2	0.500 OD 0.020 Wall 55.0 Long	A Inlet A Exit	Inconel 718
C	Transition Case Liner Coolant Supply No. 1 (Via Main Fuel Pump)	0.375 OD 0.020 Wall 25.0 Long	A Inlet A Exit	Inconel 718
E	Transition Case Liner Coolant Supply No. 2 (Via Main Oxidizer Pump)	0.375 OD 0.020 Wall 55.0 Long	A Inlet A Exit	Inconel 718
J	Main Oxidizer Pump Turbine Coolant Supply	0.375 OD 0.020 Wall 24.0 Long	A Inlet A Exit	Inconel 718
AS	Fuel LSI Rear Bearing Coolant Supply No. 1	0.375 OD 0.020 Wall 4.0 Long	A Inlet A Exit	Inconel 718
AT	Fuel LSI Rear Bearing Coolant Supply No. 2	0.375 OD 0.020 Wall 12.0 Long	A Inlet A Exit	Inconel 718
O	Main Oxidizer Pump Rear Bearing Coolant Supply	0.375 OD 0.020 Wall 6.0 Long	F Inlet A Exit	Inconel 718
AH	Main Fuel Pump Turbine and Duct Coolant Supply No.1	0.375 OD 0.020 Wall 44.0 Long	A Inlet A Exit	Inconel 718
AI	Main Fuel Pump Turbine and Duct Coolant Supply No. 2	0.375 OD 0.020 Wall 35.0 Long	A Inlet A Exit	Inconel 718
AK	Fuel LSI Thrust Piston Drain No. 1	0.375 OD 0.020 Wall 15.0 Long	A Inlet A Exit	

*Road Map Reference Letter

(U) Table LXXVIII. Fuel Small Lines Summary (Continued)

*	Description	Tube Size (in.)	End Fitting	Tube Material
AL	Fuel LSI Thrust Piston Drain No. 2	0.375 OD 0.020 Wall 16.0 Long	A Inlet A Exit	Inconel 718
AM	Fuel LSI Thrust Piston Drain No. 3	0.375 OD 0.020 Wall 20.0 Long	A Inlet A Exit	Inconel 718
H	Main Combustion Chamber Igniter Fuel Supply	0.312 OD 0.035 Wall 12.0 Long	A Inlet A Exit	(AMS 5512)
I	Preburner Igniter Fuel Supply	0.317 OD 0.035 Wall 45.0 Long	C Inlet A Exit	AISI 347

* Road Map Reference Letter

(U) Table LXXIX. Oxidizer Small Lines Summary

*	Description	Tube Size (in.)	End Fitting	Tube Material
AZ	Main Oxidizer Pump Thrust Piston Main Supply (See Note 1)	1.500 OD Wall 13.0 Long	Welded, Both Ends	Inconel 718 (AMS 5663)
BA	Main Oxidizer Pump Thrust Piston Discharge No. 1	1.500 OD 0.035 Wall 22.0 Long	K Inlet K Exit	Inconel 718
BB	Main Oxidizer Pump Thrust Piston Discharge No. 2	1.500 OD 0.035 Wall 16.0 Long	K Inlet K Exit	Inconel 718
N	Oxidizer LSI Thrust Piston Discharge	1.062 OD 0.035 Wall 28.0 Long	K Inlet K Exit	Inconel 718
AX	Main Oxidizer Pump Thrust Piston Supply No. 1 (See Note 1)	1.000 OD 0.035 Wall 30.0 Long	Welded, Both Ends	Inconel 718
AY	Main Oxidizer Pump Thrust Piston Supply No. 2 (See Note 1)	1.000 OD 0.035 Wall 12.0 Long	Welded, Both Ends	Inconel 718
AU	Preburner Igniter Oxidizer Supply	0.250 OD 0.028 Wall 12.0 Long	F Inlet A Exit	AISI 347 (AMS 5512)
AV	Main Combustion Chamber Igniter Oxidizer Supply (See Note 2)	0.250 OD 0.028 Wall 32.0 Long	A Inlet A Exit	AISI 347
BE	Igniter Oxidizer Main Supply (See Note 2)	0.250 OD 0.028 Wall 16.0 Long	A Inlet F Exit	AISI 347

Notes:

(1) This Line is an Integral Part of MOP Discharge Plumbing
(2) This Line is also Used as Preburner Primary He Purge

*Road Map Reference Letter

(U) Table LXXX. Helium Small Lincs Summary

*	Description	Tube Size (in.)	End Fitting	Tube Material
AR	Main Combustion Chamber Purge Supply	0.375 OD 0.020 Wall 40.0 Long	A Inlet A Exit	Inconel 718 (AMS 5663)
BG	Preburner Secondary Purge Main Supply	0.375 OD 0.020 Wall 40.0 Long	A Inlet F Exit	Inconel 718
AW	Preburner Primary Purge Supply (To Cross Fitting)	0.250 OD 0.028 Wall 28.0 Long	A Inlet D Exit	AISI 347 (AMS 5512)
BC	Main Fuel Pump and Fuel LSI Lift-Off Seal Signal	0.250 OD 0.028 Wall 34.0 Long	A Inlet A Exit	AISI 347
BD	Preburner Oxidizer Vent Valve Signal	0.250 OD 0.028 Wall 56.0 Long	A Inlet A Exit	AISI 347
BF	Preburner Secondary Purge Supply No. 2	0.250 OD 0.028 Wall 16.0 Long	F Inlet A Exit	AISI 347
BH	Preburner Fuel Vent Valve Signal	0.250 OD 0.028 Wall 40.0 Long	A Inlet A Exit	AISI 347
BI	Main Combustion Chamber Oxidizer Vent Valve Signal	0.250 OD 0.028 Wall 50.0 Long	A Inlet A Exit	AISI 347
BJ	Main Oxidizer Pump Helium Dam Supply	0.250 OD 0.028 Wall 38.0 Long	A Inlet A Exit	AISI 347
BK	Main Oxidizer Pump Lift-Off Seal Signal	0.250 OD 0.028 Wall 20.0 Long	A Inlet A Exit	AISI 347
BL	Main Fuel Pump and Fuel LSI Lift-Off Seal Main Signal	0.250 OD 0.028 Wall 7.0 Long	A Inlet Exit	AISI 347

*Road Map Reference Letter

(U) Table LXXX. Helium Small Lines Summary (Continued)

*	Description	Tube Size (in.)	End Fitting	Tube Material
BM	Main Fuel Pump Lift-Off Seal Signal	0.250 OD 0.028 Wall 8.0 Long	A Inlet A Exit	AISI 347 (AMS 5512)
BN	Preburner Secondary Purge Supply No. 1	0.250 OD 0.028 Wall 18.0 Long	A Inlet A Exit	AISI 347
BO	Fuel LSI Lift-Off Seal Signal	0.250 OD 0.028 Wall 40.0 Long	A Inlet A Exit	AISI 347

*Road Map Reference Letter

d. Helium and Low Pressure Lines

(U) At the present time, all lines less than 3/8-inch nominal tube size are to be fabricated from 347 SST tubing with AFRPL connectors (MS 27850 through 28855).

14. Summary

(U) Although additional engine plumbing design itterations may be necessary, sufficient work has been completed to indicate that the design goals can be achieved within the weight goal of 310 pounds. Estimated plumbing weight is 295 lb. Custom fitting of flanges can be eliminated with only minor redesign of component flanges (increase flange thickness with bolt load); this redesign can be accomplished with approximately 15 lb weight increase. Figure 568 is a plumbing road map showing each engine line and its end points.

APPENDIXES

APPENDIX I
DESIGN STRUCTURAL CRITERIA

(U) This appendix is proprietary to Pratt & Whitney Aircraft Division of United Aircraft Corporation. This appendix will be provided to Government Agencies upon request.

APPENDIX II
INCONEL 718 THREADED CONNECTORS FOR A 6000-PSI FLUID SYSTEM

A. INTRODUCTION

(C) In a Request for Quotation dated March 27, 1969, the Florida Research and Development Center of Pratt & Whitney Aircraft requested the design of Inconel 718 threaded connectors for a 6000-psi cryogenic system. The connectors were to be similar to the AFRPL connectors developed by Battelle-Columbus for the Rocket Propulsion Laboratory at Edwards Air Force Base. The design information was to be presented in a form similar to Military Standards MS27851 - MS27855 inclusive.

(U) In a letter dated April 11, 1969, Battelle-Columbus proposed to develop the necessary designs through the selective use of a computerized design procedure developed for the AFRPL connector. The design work was to be accompanied by the fabrication and load testing of typical seals to verify a satisfactory seal performance. This report summarizes the program activities and presents the resulting design information.

B. SUMMARY

(U) The material selected for the nut, the threaded flange, and the plain flange was fully heat-treated Inconel 718. The material selected for the seal was annealed Inconel 718. Load tests performed on 3/8-inch and 1-inch seals showed that the seals deformed properly and that satisfactory radial and axial seal loads were obtained. The computer design procedure (Program UNDSGN) was used to develop the connector designs given in Appendix III. It is believed that connectors made in accordance with these designs will meet the specific performance requirements.

C. PROGRAM ACTIVITIES

(C) The connector requirements specified by Pratt & Whitney Aircraft were as follows:

<u>Pressure</u>

Operating	6000 psig
Proof	9000 psig

<u>Temperature</u>

Lower limit	-320°F
Upper limit	160°F

<u>Other Requirements</u>

Leakage rate	10^{-5} sccs GN_2 at -320°F
Fatigue stress for 10^7 cycles	40,000 (approximately)

Minimum Weight

Tube OD, in.	Nom. Wall Thickness, in.	Max Moment, lb-in.
3/8	0.020	108
1/2	0.020	495
9/16	0.020	601
5/8	0.028	1091
3/4	0.028	1517
7/8	0.035	2650
1.0	0.035	3335

1. Seal Design

(U) The design of seals for the Inconel 718 connectors required the selection of a seal material, the extrapolation of dimensions from previous design work, and the load testing of typical seals. The sealing principle and other aspects of the Bobbin seal (the type of seal used in the AFRPL connectors) are discussed in detail in References 1 and 2.

(U) Based on experience with materials such as aluminum, René 41, etc., it has been found that the seal material should have the following characteristics: (1) be softer than the flange material, (2) be compatible with the flange material from a corrosion standpoint, (3) have a similar coefficient of thermal expansion, and (4) have a ductility of at least 18 to 20 percent. A review of mechanical properties of annealed Inconel 718 in References 3 and 4 showed that this material would be suitable for the seals. The selected annealing temperature was 1750°F for 2 hours, air cooled.

(U) Seals similar in size to those required for the Inconel 718 connectors were established in an earlier research program for aluminum, stainless steel, and René 41. These dimensions were further tested in another program[2]. The extrapolation of these dimensions consisted essentially of maintaining similar disk dimensions and adjusting the seal tang dimensions to provide adequate radial loading without increasing the size of the connector structures.

(U) The seals designed for a 3/8-inch tube size and a 1-inch tube size were selected as typical, and six seals of each size were machined. Each seal was assembled with one disk in a flange cavity and one disk in a strain-gaged load ring. Figure 569 shows the axial load trace obtained from the tensile machine and associated strain readings obtained from the load ring for a 3/8-inch seal. Table LXXXI shows the load test results for all the seals tested. The calculated radial load is based on formulae established in Reference 2. The seals deformed properly without exception and the loads were judged to be adequate from experience.

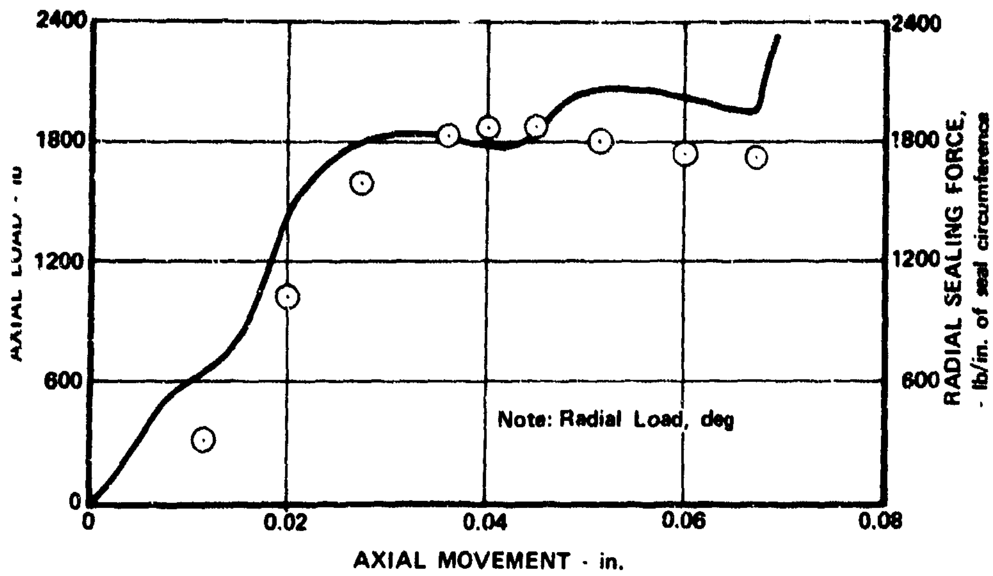

(U) Figure 569. Axial Load Trace and Radial Load Increments for 3/8-Inch Annealed Inconel 718 Seal (Specimen No. 1)

(U) Table LXXXI. Load Test Results for 3/8- and 1-in. Seals Machined from Annealed Inconel 718

Nominal Tubing Size, in.	Specimen	Maximum Axial Load, lb	Max Load per Inch of Seal Circumference, lb/in. Axial	Radial	Calculated Radial Load, lb/in. Sy = 80,000 psi
3/8	1	2000	1070	1670	1480
3/8	2	1980	1055	1580	1480
3/8	3	2220	1175	1630	1480
3/8	4	2100	1120	1650	1480
3/8	5	1980	1055	1550	1480
3/8	6	1860	1000	1600	1480
1.0	1	4440	1150	1420	1190
1.0	2	4620	1190	1370	1190
1.0	3	4440	1150	1300	1190
1.0	4	4200	1080	1250	1190
1.0	5	4200	1080	1250	1190
1.0	6	4020	1035	1255	1190

2. Fitting Design

(U) Besides the Bobbin seal, an AFRPL connector consists of three other elements: a nut, a threaded flange, and a plain flange. The procedure for designing these elements is presented in Reference 1. For each nominal tube size a connector tube-wall thickness was computed and was found to be bigger than the wall thickness specified by Pratt & Whitney Aircraft*. Rather than change the connector design procedure, the tube inside diameter was made equal to the tube inside diameter required by Pratt & Whitney Aircraft. It was mutually agreed that Pratt & Whitney Aircraft would modify the drawings for the required tubing weld joint.

(U) Program UNDSGN provides 15 possible connector designs for each tube size. The lightest weight connector design was selected as the final design for all tube sizes. UNDSGN also establishes the upper and lower assembly torques for each size. These values are included in Appendix III. Since the torque value for the 1-inch nominal tube size is high because of the high system pressure, special tightening techniques may be needed to assemble that size.

3. Drawings and Specifications

(U) Appendix III lists the dimensions for all of the elements of the threaded connectors for the tube sizes required by Pratt & Whitney Aircraft. These drawings are similar to MS27851 - MS27855.

D. REFERENCES

1. "Development of AFRPL Threaded Fittings for Rocket Fluid Systems," TDR No. AFRPL-TR-65-162, November 1965.

2. "Development of AFRPL Flanged Connectors for Rocket Fluid Systems," TDR No. AFRPL-TR-69-97, July 1969.

3. "Nickel Base Alloys - Alloy 718," Processes and Properties Handbook, DMIC, Battelle Memorial Institute, Columbus, Ohio.

4. "Inconel 718," Technical Bulletin T-39, Huntington Alloy Products Division.

*Larger factor of safety on hoop stress used by program.

APPENDIX III
FINAL DESIGNS FOR INCONEL THREADED FITTINGS

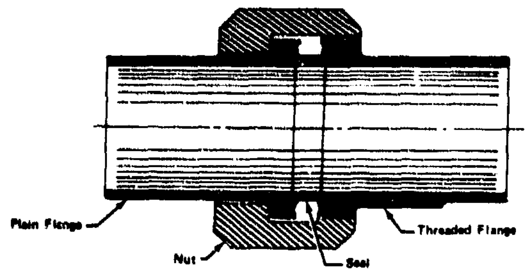

Nominal Tube OD	Wrench Torque for Tightening Fittings, lb-in. Minimum	Maximum
3/8	375	425
1/2	640	725
9/16	805	910
5/8	990	1120
3/4	1515	1710
7/8	2190	2470
1	3150	3540

(C) Figure 570. Fittings, Installation Torque 6000 psi

FD 33405

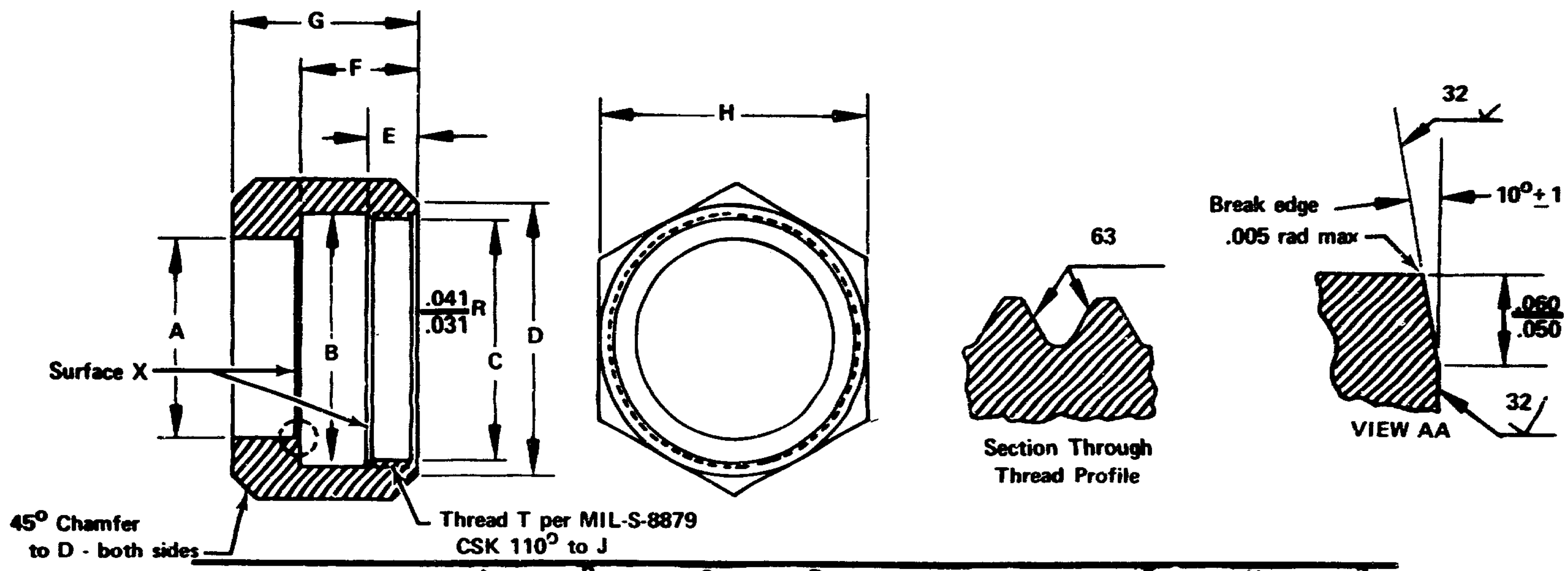

Nominal Tube OD	Thread-T UNJEF-3B	A DIA +.004 -.000	B DIA +.003 -.000	C DIA +.004 -.000	D DIA ±.010	E +.004 -.000	F +.004 -.000	G +.000 -.005	H +.001 -.002	J DIA
3/8	3/4-20	0.445	0.752	0.702	0.795	0.250	0.543	0.729	0.813	0.750
1/2	7/8-20	0.586	0.877	0.827	0.920	0.250	0.556	0.778	0.938	0.875
9/16	15/16-20	0.649	0.940	0.889	0.983	0.250	0.565	0.801	1.000	0.938
5/8	1-20	0.695	1.002	0.952	1.045	0.250	0.573	0.826	1.063	1.000
3/4	1-1/8-18	0.834	1.127	1.071	1.170	0.278	0.656	0.946	1.188	1.125
7/8	1-1/4-18	0.959	1.252	1.196	1.295	0.278	0.655	0.979	1.313	1.250
1	1-3/8-18	1.098	1.447	1.321	1.483	0.278	0.643	1.017	1.500	1.365

1. Thread PD shall be square to surfaces X within .005 FIR and concentric with hex and diameter B within .005 FIR.
2. Flange chamfer (View AA) shall be square to thread PD within .005 FIR.
3. Dimensions are to sharp corners unless otherwise specified.
4. Break sharp edges .003 - .005 unless otherwise specified.
5. Dimensions in inches. Unless otherwise specified, tolerances, linear dimensions ± .010, angular dimensions ± 5°.

(U) Figure 571. Nut, Inconel 718, Fully Heat Treated

FD 33403

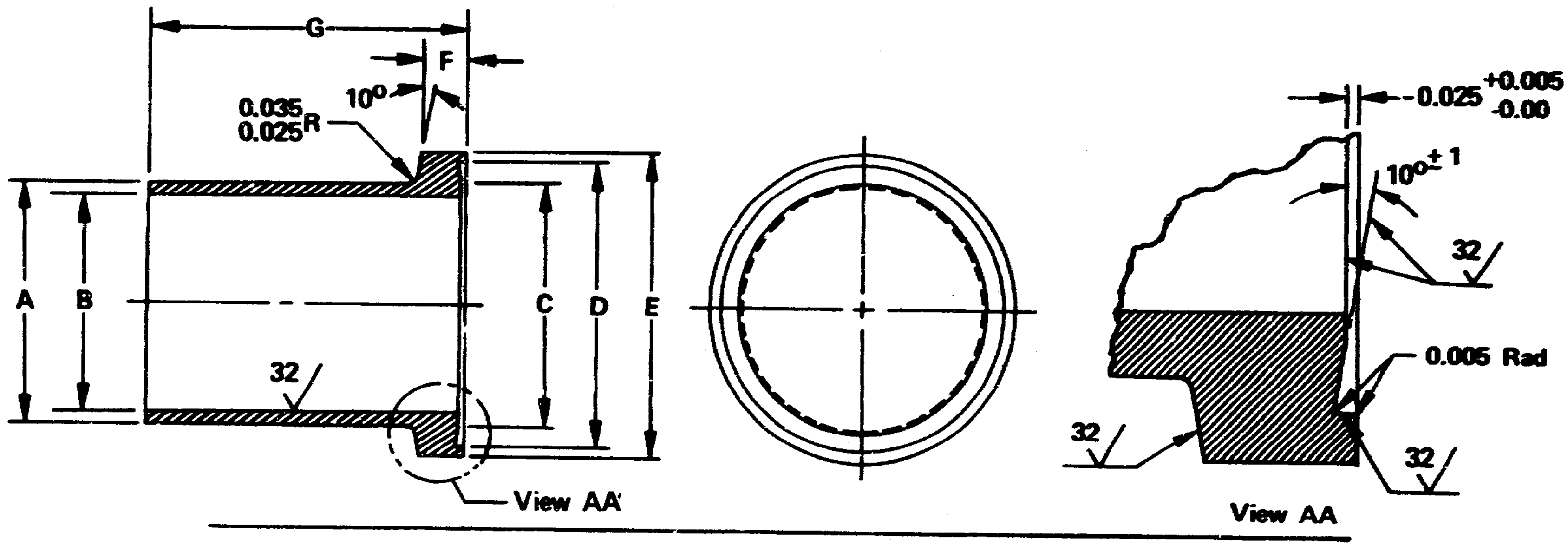

Nominal Tube OD	A DIA +0.000 -0.002	B DIA +0.002 -0.000	C DIA +0.000 -0.004	D DIA +0.002 -0.000	E DIA +0.000 - 0.002	F +0.005 - 0.000	G ±0.010
3/8	0.377	0.333	0.410	0.598	0.678	0.173	1.250
1/2	0.518	0.458	0.549	0.737	0.809	0.186	1.250
9/16	0.581	0.521	0.611	0.799	0.871	0.195	1.250
5/8	0.627	0.567	0.674	0.862	0.934	0.202	1.250
3/4	0.766	0.692	0.789	0.977	1.049	0.209	1.375
7/8	0.891	0.803	0.914	1.102	1.174	0.208	1.375
1	1.030	0.928	1.049	1.237	1.309	0.197	1.375

1. All diameters shall be concentric within 0.005 FIR.
2. Dimensions are to sharp corners unless otherwise specified.
3. Break sharp edges 0.003 - 0.005 unless otherwise specified.
4. Dimensions in inches. Unless otherwise specified, tolerances, linear dimensions ± 0.010, angular dimensions ±5°.

(U) Figure 572. Plain Flange, Inconel 718, Fully Heat Treated

FD 33406

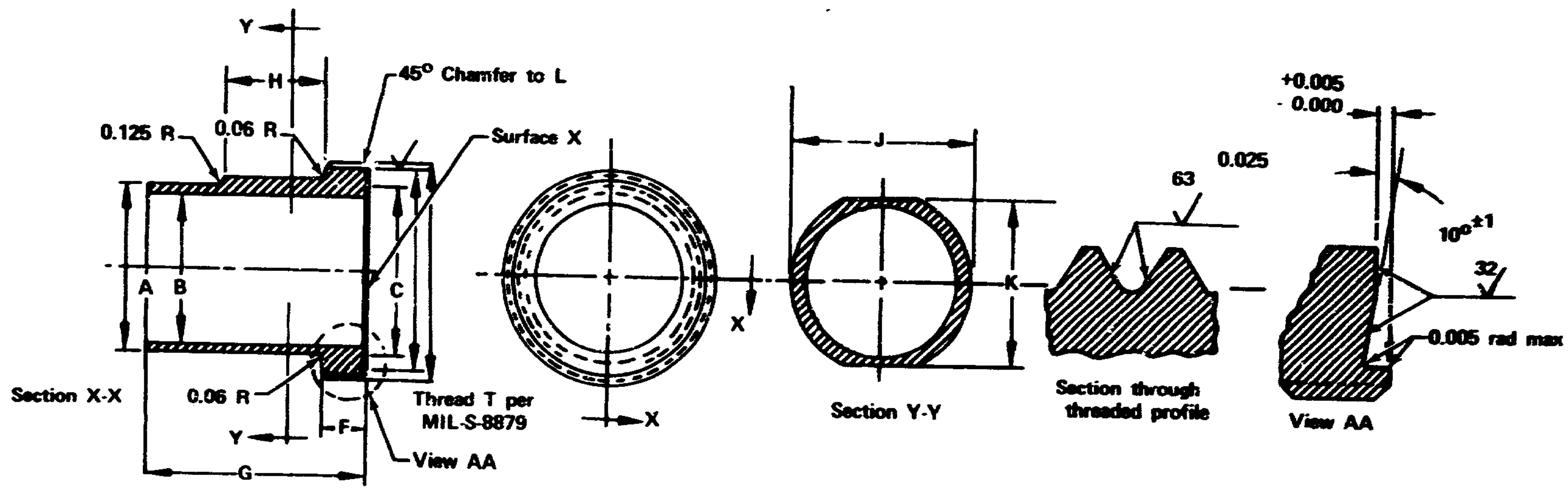

Nominal Tube OD	Thread T UNJEF-3A	A DIA +.000 -.002	B DIA +.002 -.000	C DIA +.000 -.004	D DIA +.002 -.000	E DIA +.002 -.000	F +.005 -.000	G ±.010	H ±.031	J DIA +.010 -.000	K +.000 -.002	L DIA
3/8	3/4-20	0.377	0.333	0.410	0.598	0.748	0.250	1.250	0.319	0.506	0.438	0.715
1/2	7/8-20	0.518	0.458	0.549	0.737	0.873	0.250	1.250	0.389	0.668	0.579	0.840
9/16	15/16-20	0.581	0.521	0.611	0.799	0.936	0.250	1.250	0.421	0.740	0.641	0.903
5/8	1-20	0.627	0.567	0.674	0.862	0.998	0.250	1.250	0.444	0.794	0.688	0.965
3/4	1-1/8-18	0.766	0.692	0.789	0.977	1.123	0.278	1.375	0.513	0.954	0.827	1.087
7/8	1-1/4-18	0.891	0.803	0.914	1.102	1.248	0.278	1.375	0.576	1.096	0.952	1.211
1	1-3/8-18	1.030	0.928	1.049	1.237	1.373	0.278	1.375	0.646	1.260	1.091	1.336

1. Thread PD shall be square to surfaces X within .005 FIR and concentric with diameter D within .005 FIR.
2. Dimensions are to sharp corners unless otherwise specified.
3. Break sharp edges .003-.005 unless otherwise specified.
4. Dimensions in inches. Unless otherwise specified, tolerances, linear dimensions ± .010, angular dimensions ±5°.

(U) Figure 573. Threaded Flange, Inconel 718, Fully Heat Treated

FD 33404

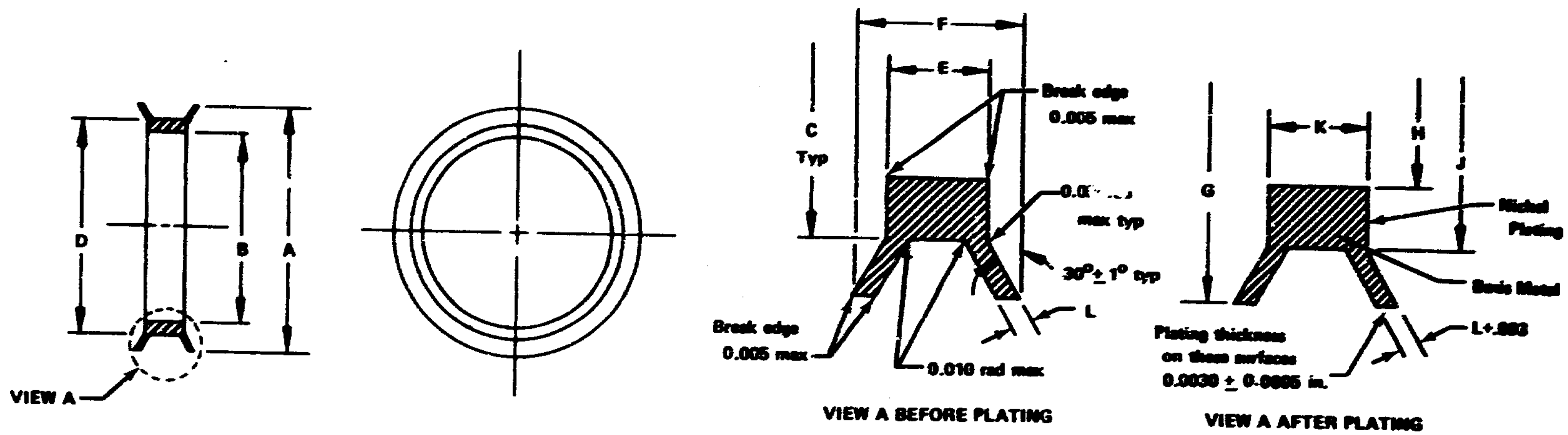

Nominal Tube OD	A DIA +.000 -.002	B DIA +.002 -.000	C DIA +.010 -.000	D DIA +.000 -.005	E ±.004	F REF	G DIA +.001 -.003	H DIA +.002 -.000	J DIA +.000 -.005	K ±.004	L ±.002
3/8	0.580	0.347	0.420	0.423	0.150	0.248	0.586	0.343	0.427	0.154	0.027
1/2	0.729	0.472	0.559	0.562	0.150	0.248	0.735	0.468	0.566	0.154	0.027
9/16	0.791	0.534	0.621	0.624	0.150	0.248	0.797	0.530	0.628	0.154	0.027
5/8	0.854	0.581	0.684	0.687	0.150	0.248	0.860	0.577	0.691	0.154	0.027
3/4	0.969	0.706	0.799	0.802	0.200	0.298	0.975	0.702	0.806	0.204	0.030
7/8	1.094	0.817	0.924	0.927	0.200	0.298	1.100	0.813	0.931	0.204	0.030
1	1.229	0.942	1.059	1.062	0.200	0.293	1.235	0.938	1.066	0.204	0.030

1. All diameters shall be concentric within .002 FIR.
2. Dimensions are to sharp corners unless otherwise specified.
3. Break sharp edges .003 - .005 unless otherwise specified.
4. Dimensions in inches. Unless otherwise specified, tolerances, linear dimensions ±.010, angular dimensions ±5°.
5. Surface roughness: AS 291. Unless otherwise specified, surfaces to be 32 microinches (AA).

(U) Figure 574. Seal, Annealed, Inconel 718

FD 33007

UNCLASSIFIED

Security Classification

DOCUMENT CONTROL DATA - R & D

(Security classification of title, body of abstract and indexing annotation must be entered when the overall report is classified)

1. ORIGINATING ACTIVITY (Corporate author) Pratt & Whitney Aircraft Division of United Aircraft Corporation Florida Research and Development Center	2a. REPORT SECURITY CLASSIFICATION Confidential UNCLASSIFIED 2b. GROUP 4

3. REPORT TITLE

Air Force Reusable Rocket Engine Program XLR129-P-1 Demonstrator Engine Design

4. DESCRIPTIVE NOTES (Type of report and inclusive dates)

Design Milestone Report, 6 November 1967 to 1 December 1969

5. AUTHOR(S) (First name, middle initial, last name)

Atherton, Robert R.

6. REPORT DATE	7a. TOTAL NO. OF PAGES	7b. NO. OF REFS
May 1970	719	

8a. CONTRACT OR GRANT NO. F04611-68-C-0002	9a. ORIGINATOR'S REPORT NUMBER(S) PWA FR-3337
b. PROJECT NO. 57 x 3600 2894703	
c. P63681C 634084F	9b. OTHER REPORT NO(S) (Any other numbers that may be assigned this report)
d. S669800	

10. DISTRIBUTION STATEMENT In addition to security requirements which must be met this document is subject to special export controls and each transmittal to foreign governments or foreign materials may be made only with prior approval of AFRPL (RPOR/STINFO) Edwards, California 93523

11. SUPPLEMENTARY NOTES	12. SPONSORING MILITARY ACTIVITY
	AFFTC Procurement Division (FTMKR-2) Edwards AFB, California 93523

13. ABSTRACT

(U) This report describes the design of the XLR129-P-1 Demonstrator Rocket Engine and its principal components. The program is being conducted by Pratt & Whitney Aircraft under Air Force Sponsorship at the Florida Research and Development Center. Design of all components, the second of five program phases, has been completed. Included in the report is the design approach, mechanical description, and operating characteristics for each component. The engine is designed to operate with liquid oxygen and liquid hydrogen propellants, uses the staged combustion cycle, incorporates variable thrust, and variable mixture ratio capability. The XLR129-P-1 engine, having a high area ratio nozzle, is designed to be reusable as in aircraft engine practice, and provides 250,000 pounds thrust in vacuum. The program started 6 November 1967, and is planned for 54 months. The major program objectives include: (1) design of the components and engine system with a series of component tests to support the design effort, (2) development of the components to qualify them for engine use and to demonstrate the life of life-limited sub-components, and (3) a series of engine tests to demonstrate operational capabilities.

DD FORM 1 NOV 65 1473

UNCLASSIFIED

Security Classification

UNCLASSIFIED

Security Classification

14. KEY WORDS	LINK A		LINK B		LINK C	
	ROLE	WT	ROLE	WT	ROLE	WT
Air Force Reusable Rocket Engine Program						
XLR129-P-1 Demonstrator Engine Design						
Pratt & Whitney Aircraft						
Component Design						
Preburner Injector						
Transition Case						
Main Burner Injector						
Main Burner Chamber						
Primary Nozzle						
Two Position Nozzle						
Translating Mechanism						
Low Speed Inducers						
Fuel Turbopump						
Oxidizer Turbopump						
Control System						
Engine System Description and Performance						
Demonstrator Engine Plumbing and Mockup						

UNCLASSIFIED

Security Classification